A comparison of single vision aspheric spectacle lenses for aphakia

by

Colin William Fowler

Submitted for the degree

of

Doctor of Philosophy

The University of Aston in Birmingham

March 1985

A comparison of single vision aspheric spectacle lenses for aphakia

by

Colin William Fowler

Submitted for the degree

of

Doctor of Philosophy

1985

Aspheric lenses have become the devices of choice for the spectacle correction of aphakia, particularly when made of plastic material. However, they are often supplied with very little information concerning their design, and hence the first part of this thesis is concerned with reviewing the published design concepts behind these lenses. Secondly, instruments are described which have been developed for the measurement of surface topography and optical characteristics of these lenses, together with the results of measurements of a series of lenses. Finally some measurements are described of subjective response to some lenses, including an experimental design for which a novel method of manufacture has been developed.

Key Words: spectacle lens, aspheric, aphakia, lens manufacture

To the memory of

A.C.F.

List of contents

PART 2

PART 3

PART 4

Figures		Page
1.1	Field loss in positive power lens	18
1.2	Spherical aberration and coma	22
1.3	Tangential and Sagittal meridians	25
1.4	Oblique astigmatism	27
1.5	Tangential image	29
1.6	Sagittal image	33
1.7	Ray tracing procedure	36
1.8	Tscherning's ellipses	38
1.9	Astigmatic image shells	41
1.10	Distortion calculation	44
2.1	Conic surface	48
2.2	Normal and tangent to conic surface	51
2.3	Oblique astigmatism	56
2.4	Mean Oblique Power	56
2.5	Distortion	56
2.6	von Rohr design, oblique astigmatism	62
2.7	von Rohr design, distortion	62
3.1	Davis and Fernald lens, Mean Oblique Power	77
3.2	Bechtold lens, oblique astigmatism	82
3.3	Bechtold lens, distortion	85
4.1	Welsh Four Drop Curves, after Renier	94
4.2	Frieder lens curves, after Frieder	97
5.1	Conventional lenticulars	103
5.2	Blended aspheric lenticular	105

Tables

Acknowledgements

I would like to thank the following for their help with this work:

Professor G F A Harding, my supervisor, for his continual help and encouragement.

Arthur Bennett, who during many conversations proved a tremendous source of inspiration and information.

The British Technology Group, for financial support for the work described in Part 3.

Sola Optical (UK) Ltd, for assistance with the manufacture of lenses, as well as providing a number of sample lenses of their own manufacture.

Norville Optical Company Ltd, for surfacing semi-finished lenses, as well as providing sample lenses.

The following Companies also supplied lenses:

American Optical
British American Optical Ltd
London Williamson Ltd
Essilor Ltd
Sealite Ltd

Communications Media Unit, Aston University, for taking the photographs.

Mrs Paula Sliwinski for her quick and efficient typing of this thesis.

Finally to Carolyn, Philip and Claire, for their encouragement and putting up with the neglect.

PART 1

CHAPTER 1

INTRODUCTION

This design of a spectacle lens to be worn by an aphalic patient is a challenging venture. The removal of a cataractous crystalline lens changes the overall power of the eye, rendering a previously emmetropic eye around 12 Dioptres hypermetropic. The fact that this change happens suddenly, and often to a person who is elderly, means that any imperfections in the spectacle lens will be immediately noticed. Some wearers will adapt to any design of spectacle lens, however bad, if their visual acuity was very poor before the operation. But the aim should be to provide a spectacle lens that will provide the easiest transition from the phakic to aphakic state.

Recent years have seen an expansion in the types of lens available for the correction of aphakia, particularly those using one aspheric surface. Often these lenses are simply sold as 'aspheric', with little information supplied on the purpose of the design.

The aims of this work were:-

1. A comparison of published aspheric lens designs.
2. Development of equipment for the measurement of aspheric curves on physical lenses.
3. Measurement of the curves of a series of commercially produced lenses, and compare not only different lenses, but also differences between published designs and the resulting lens.

As a result of aims 1-3, it became apparent that certain trends in aspheric design were taking place, and therefore further work was carried out on a comparison between a new type of lens, not commercially available, and two existing designs. This required the development of a lens manufacturing method, and also a means of subjectively assessing optical distortion.

1.1 The problems of aspheric lens design

The most obvious change that the new aphakic will notice is the increased magnification of the visual world. This is approximately 23% in the case of the emmetrope (Bennett 1969), and results in disorientation and poor hand-eye coordination. This effect is caused by the fact that the lens inside the eye has been replaced by one outside, usually positioned around 10mm. from the cornea. The magnification is considerably reduced in the case of contact lenses, and is effectively eliminated with intra ocular implant lenses, surgically fitted in practically the same place as the original crystalline lens. It is possible to design a lens system to be mounted in the spectacle plane that will give a low magnification effect (von Rohr and Boegehold, 1934). However such systems have a poor cosmetic appearance and poor optical performance off axis. One consequence of the large amount of magnification induced by an aphakic spectacle lens is to make binocular vision difficult in the monocular aphakic. For such individuals, a contact lens or implant would offer a better chance of maintaining binocular vision.

Another disturbing effect of aphakic spectacle lenses is the

very small field of view with conventional spherical lens designs. In Figure 1.1 an eye rotates about an assumed centre of rotation C. The limiting ray through each edge of the spectacle lens is (1), but around the edge of the lens, a ray (2) will be seen in direct (blurred vision. The hatched areas indicates the zone that cannot be seen by the eye without moving the spectacle lens with a head movement. The diagram shows only one section through the centre of the lens, the complete patern of field loss being an annulus. The greater the power of the lens at its edge, the larger will be the angle between rays (1) and (2), and hence the area of field loss. In low power hypermetropic lenses, this field loss will be hardly noticed, but the aphakic will be very aware of this phenomenon. This effect can be reduced by the use of certain types of aspheric lens surface, though not without the penalty of reduced peripheral power in the lens.

1.2 Lens aberrations

Although the effects of magnification and field loss have been considered by the designers of aphakic spectacle lenses, the main efforts have been in attacking other problems, namely lens aberrations. In Figure 1.1 the ideal situation would be for the lens performance to be the same for all angles of view. But the most likely situation in a single lens is that vision through the edge of the lens will be worse than through the centre. It is convenient to divide aberrations up in the following manner (Bennett, 1973):

Figure 1.1

Loss of field in positive power spectacle lens caused by angular deviation of marginal ray through lens (1) compared with direct vision past lens (2), the eye rotating about a point C.

Field of view

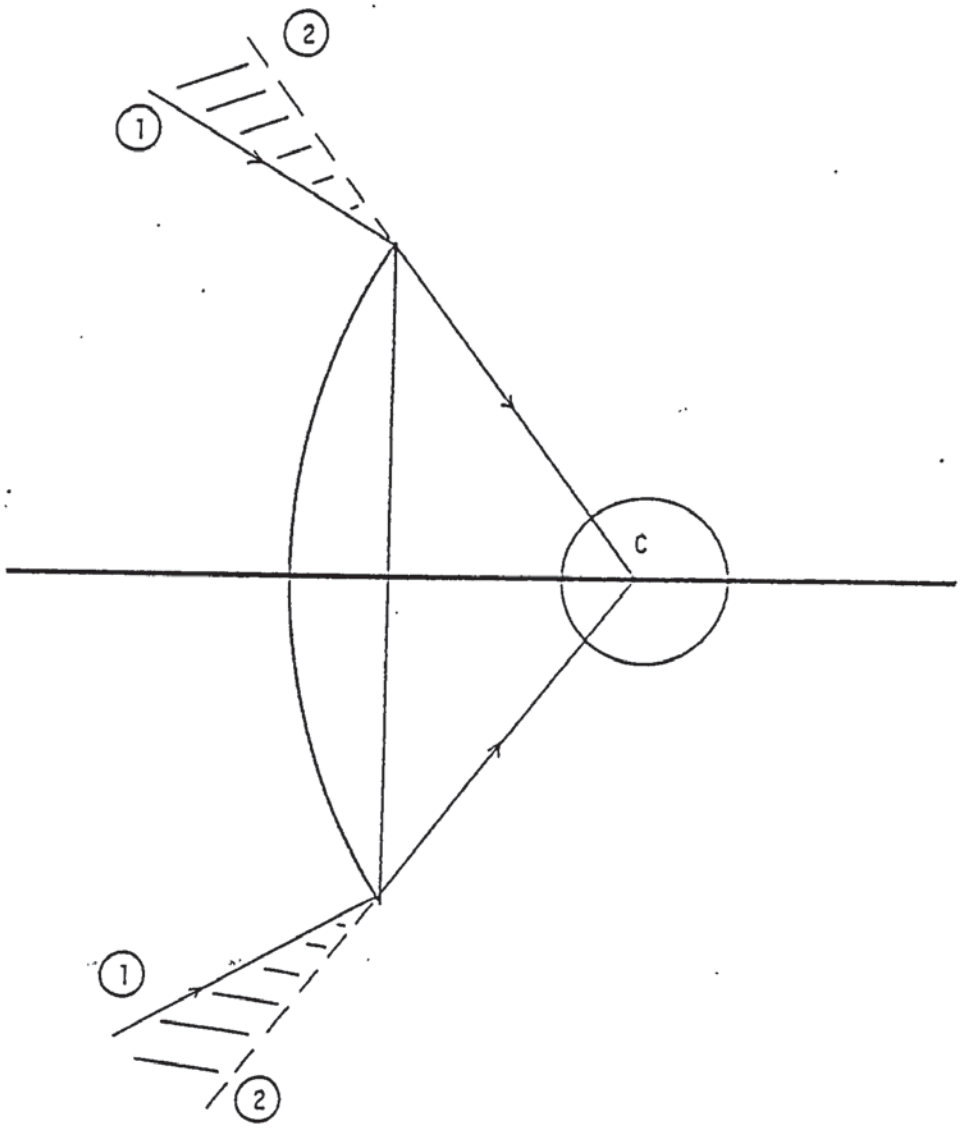

Axial	Spherical	Oblique	Coma
	Chromatic		Transverse chromatic
			Distortion
			Curvature
			Oblique astigmatism

Although all of these aberrations affect spectacle lenses, just as they do any other lens, they are not all of equal importance.

1.2.1 Chromatic Aberration

Chromatic aberration occurs because the refractive index of lens materials varies with the wavelength of light. This is described by the constringence (V_d) of the material, where the refractive index of the blue (n_C') and red (n_F'), ends of the spectrum are compared with the refractive index for yellow light (n_d) at 587.56nm (BS 3062, 1970). Thus:-

$$V = \frac{n_d - 1}{n_F' - n_C'} \qquad - I\ (1)$$

A high number for 'V' is desirable, ophthalmic crown class (the commonest lens material) having a value of 58. An approximate value for axial chromatic aberration can be found from the expression

$$A.C.A. = F/V_d \quad (D) \qquad - I\ (2)$$

where F is the power of the lens. Axial chromatic aberration thus depends primarily on the 'V' of the lens material, for a given power. For a 'V' of 60 and a lens power of +10 D, this will give axial chromatic aberration of 1/6 D. Fortunately, the eye exhibits considerable chromatic aberration, which will mask

the amount produced by the spectacle lens. But if a lens material with a lower 'V' is used, the chromatic aberration will be increased. For example, polycarbonate plastic with a V_d of 30 will give 1/3 D of chromatic aberration.

A similar situation exists with transverse chromatic aberration, except that the aberration varies with the distance from the optical centre of the lens 'y'. A first approximation to transverse chromatic aberration (based on Prentice's rule) is:-

$$\text{T.C.A. (in Prism Dioptres)} = F\ (D)\ /V_d\ .\ y\ (cm) \quad - I\ (3)$$

In a practical situation, 'F' will not be constant as 'y' varies, particularly in aspheric lenses where 'F' decreases towards the edge of the lens, thus reducing the T.C.A.

Transverse chromatic aberration has two effects. In low degrees it causes increased blurring of peripheral light rays compared with monochromatic light, and in extreme cases there will be noticeable coloured fringes on bright contours.

1.2.2 Spherical aberration and coma

Both of these aberrations are conventionally ignored in ophthalmic lens design. The philosophy of this being that these are aberrations of large aperture optical systems, whereas the ophthalmic lens/human eye system is small aperture, because of the small pupil size of the human eye. In Figure 1.2 a) rays near the edge of the lens are focused nearer to the lens than paraxial rays, giving rise to spherical aberration. In the ideal

Figure 1.2

a) Spherical aberration in a positive power lens, where wide angle rays focus nearer the lens than paraxial rays, which pass through the second principal focus (F')

b) Coma of a single positive power lens with a wide aperture, where different zones of the lens have different focal lengths, giving an asymmetric blurred patch around a point focus.

Spherical Aberration

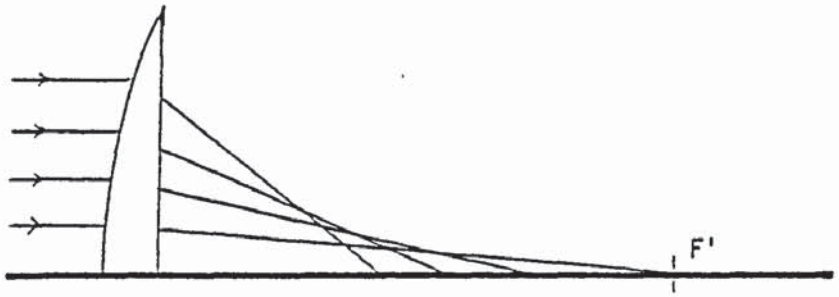

Coma

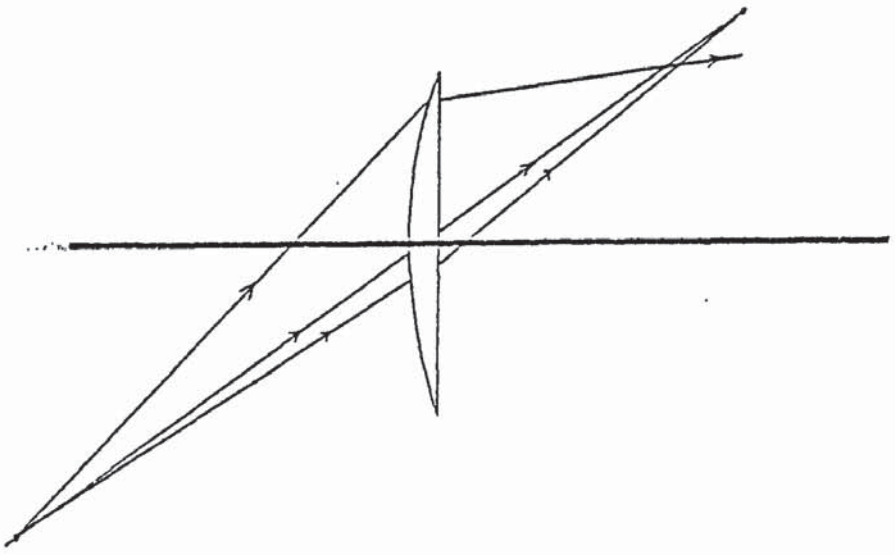

lens, all rays from a distant object would pass through F', the second principal focus. Figure 1.2.b) illustrates coma, an aberration of obliquely incident rays. In a similar manner to spherical aberration, different zones of the lens focus the light at different points.

1.2.3 Oblique astigmatism and image curvature

An obliquely incident ray to a lens or lens system with oblique astigmatism will give an astigmatic image for a point object. In a spectacle lens this is because the tangential meridian (T) of the lens (see Figure 1.3) is more powerful in the periphery than the sagittal meridian. This causes an astigmatic image with the tangential image closer to the lens than the sagittal (Figure 1.4).

1.2.3.1 Calculation of oblique astigmatism (After Emsley, 1956)

The astigmatism induced by oblique incidence at a spherical refracting surface can be calculated for a spherical refracting surface in a method analagous to that used for paraxial refraction. Hence rather than considering a finite sized incident ray bundle, a very small group of rays is considered, of negligble diameter.

In Figure 1.5, a chief ray TO is obliquely incident towards a spherical refracting surface, radius 'r', the incident refractive index being n and the refracting medium (the denser) being n'. Consider a very close ray, in a tangential section, UM. This will have angles of incidence and refraction I+dI and I'+dI', as

Figure 1.3

Tangential sections (T) through the optical centre of lens seen in plan view, with Sagittal sections (S) perpendicular to the Tangential.

Tangential and Sagittal Meridians

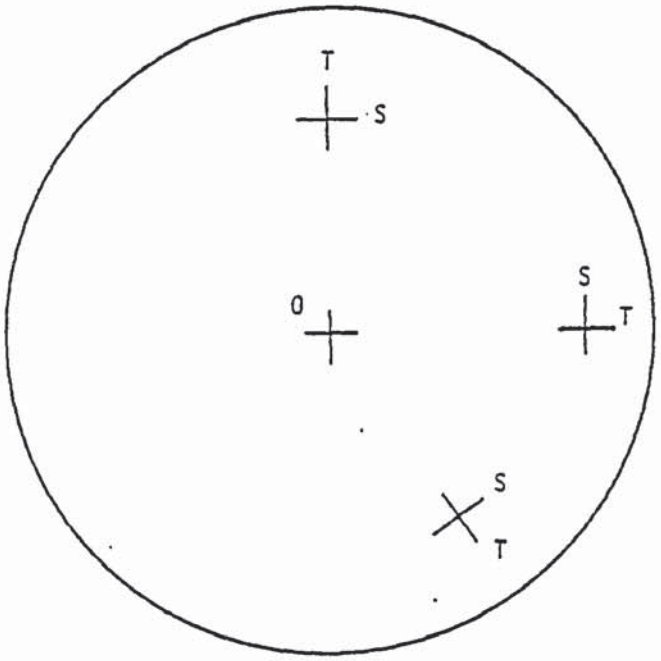

Figure 1.4

Schematic representation of oblique astigmatism through a spectacle lens, with paraxial focus at F'. Light is obliquely incident through the lens, passing through the centre of rotation of the eye at an angle U'_2, and forming a Tangential image at T', and a Sagittal image at S'.

Oblique Astigmatism

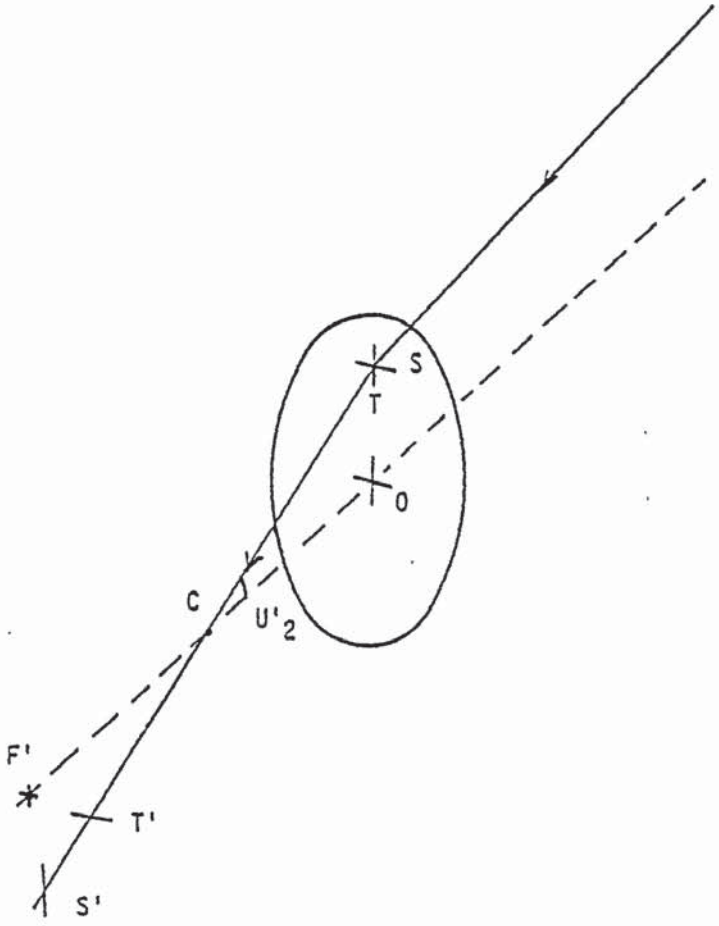

Figure 1.5

Proof of formula used for the calculation of the position of the Tangential image position (q't) when a narrow beam of light is obliquely incident at a spherical refracting surface.
(After Emsley, 1956)

Tangential Image

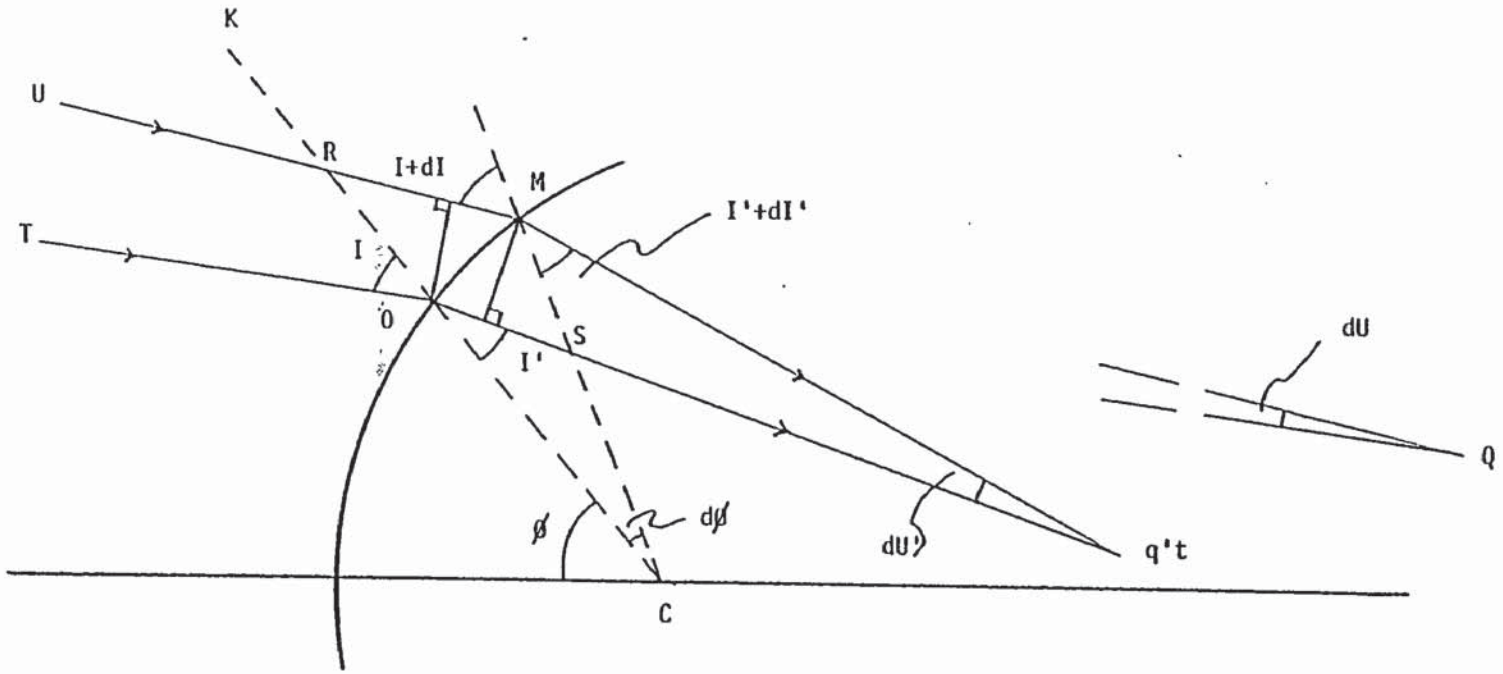

opposed to I and I' for the chief ray.

From the geometry of the figure:

KRU = I+dI-dØ = I-dU

CSq't = I'+dI'+dU' = I'+dØ

Thus dI = dØ - dU and dI' = dØ - dU'

If we call the arc length OM dx, then

$$dU = \frac{dx.CosI}{t} \quad \text{and} \quad dU' = \frac{dx.CosI'}{t'}$$

$$\text{also } d\emptyset = \frac{dx}{r}$$

where the values t and t' are the tangential object and image distances respectively.

By substitution,

$$dI = \frac{dx}{r} - \frac{dx.CosI}{t} = dx\left(\frac{1}{r} - \frac{CosI}{t}\right)$$

$$\text{Also } dI' = \frac{dx}{r} - \frac{dx.CosI}{t'} = dx\left(\frac{1}{r} - \frac{CosI'}{t'}\right)$$

$$\text{Then } \frac{dI}{dI'} = \frac{\frac{1}{r} - \frac{CosI}{t}}{\frac{1}{r} - \frac{CosI'}{t'}}$$

From Snell's law, n.SinI = n'.SinI'

and n.Sin(I+dI) = n'.Sin(I'+dI')

Since the incremental angles dI and dI' are very small,

Sin dI=I and Sin dI'=I' and Cos dI = Cos dI' = 1

Thus, by expansion, n.CosI.dI = n'.CosI'.dI'

$$\text{Then } \frac{dI}{dI'} = \frac{n'.CosI'}{n.CosI} = \frac{\frac{1}{r} - \frac{CosI}{t}}{\frac{1}{r} - \frac{CosI'}{t'}}$$

more usually written as:

$$\frac{n'.Cos^2I'}{t'} - \frac{n.Cos^2I}{t} = \frac{n'.CosI' - n.CosI}{r} \qquad - I\ (4)$$

This gives the tangential image distance (t'), but it is also necessary to find the position of the sagittal image (s'). In Figure 1.6, a sagittal section through a spherical refracting surface is shown. By Young's construction, the sagittal image will be positioned on the refracted ray where this is cut by the auxiliary axis through the centre of curvature of the refracting surface (C) and the object (Q).

If the distance OQ in the figure is taken as s and Oq's as s', then since:

Area of OQC = Area Oq'sC + OQq's

and OC = r

$$\tfrac{1}{2}rs.\mathrm{Sin}I = \tfrac{1}{2}rs'.\mathrm{Sin}I' + \tfrac{1}{2}ss'.\mathrm{Sin}(I - I')$$

$$\frac{\mathrm{Sin}I}{s'} - \frac{\mathrm{Sin}I'}{s} = \frac{1}{r}.\mathrm{Sin}(I - I')$$

Multiply all through by $\frac{n'}{\mathrm{Sin}\,I}$

$$\frac{n'}{s'} - \frac{n'.\mathrm{Sin}I'}{\mathrm{Sin}I.s} = \frac{n'}{\mathrm{Sin}I}(\mathrm{Sin}I.\mathrm{Cos}I' - \mathrm{Cos}I.\mathrm{Sin}I').\frac{1}{r}$$

or by simplifying

$$\frac{n'}{s'} - \frac{n}{s} = \frac{n'.\mathrm{Cos}I' - n.\mathrm{Cos}I}{r} \qquad \ldots (5)$$

For a point object, s = t, and for a distant object,

$$\frac{n}{s} = \frac{n}{t} = 0$$

These equations apply only to one surface of a lens. For a complete lens, oblique astigmatism is conventionally calculated by tracing a ray backwards from the centre of rotation of the eye,

Figure 1.6

Proof of formula used for the calculation of the position of the Sagittal image position (q's) when a narrow beam of light is obliquely incident at a spherical refracting surface.
(After Emsley, 1956)

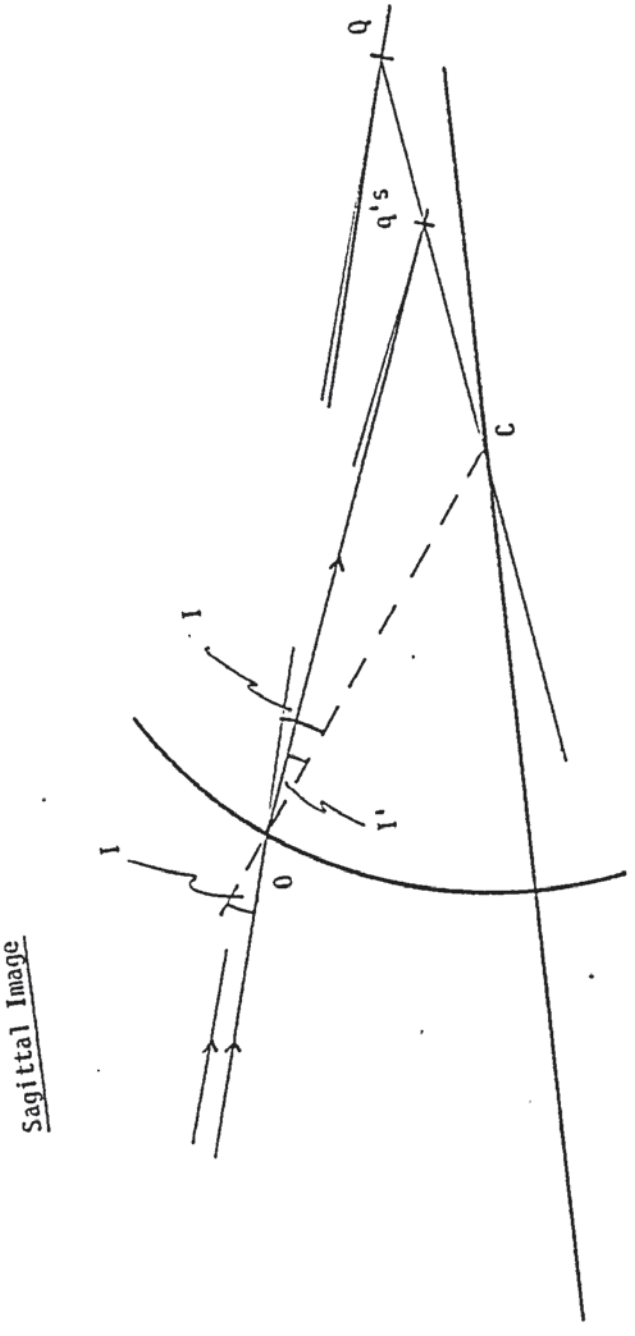

Sagittal Image

at an assumed angle of eye rotation (Figure 1.7). From this, the angle of incidence and refraction can be calculated at each surface, and if a distant object is assumed, the calculated reciprocal sagittal and tangential focal lengths become the sagittal and tangential oblique vertex sphere powers, once due allowance has been made for the distance from the rear surface of the lens to the vertex sphere. These equations are extensions of the paraxial lens equations, and only consider a very small bundle of light. An even simpler approach is to consider the lens as being 'thin', ignoring the centre thickness 't', and consider only angles where 'third order' approximations can be made. Then astigmatism free lenses can be calculated from the quadratic (Bennett, 1973):-

$$((n+2)F_1^2 - ((n+z)F+2(n^2-1)(Z+L))\ F_1+n(F+(n-1)Z)^2 - (n-2)$$

$$(n^2-1)FL+2(n-1)(n^2-1)ZL) = 0 \qquad \text{- I (6)}$$

For distance vision, the incidence vergence is zero, and hence the terms involving 'L' disappear.

If the results are plotted graphically, then this gives a construction known as Tscherning's ellipse. In Figure 1.8, two ellipses are plotted for distance vision, using lens materials with a refractive index of 1.523 and 1.701. From the point of view of the present discussion, the most interesting fact is that the use of a higher refractive index material extends the range of negative powers that can be made free from oblique astigmatism, but it does not extend the positive power range at all, the upper limit staying at approximately +7 D. Thus although the majority of negative power lenses can be supplied in a form free from

Figure 1.7

Ray tracing procedure through lens of finite thickness (t), with light passing through the centre of rotation of the eye (C) at an angle U'_2.

Ray Tracing Procedure

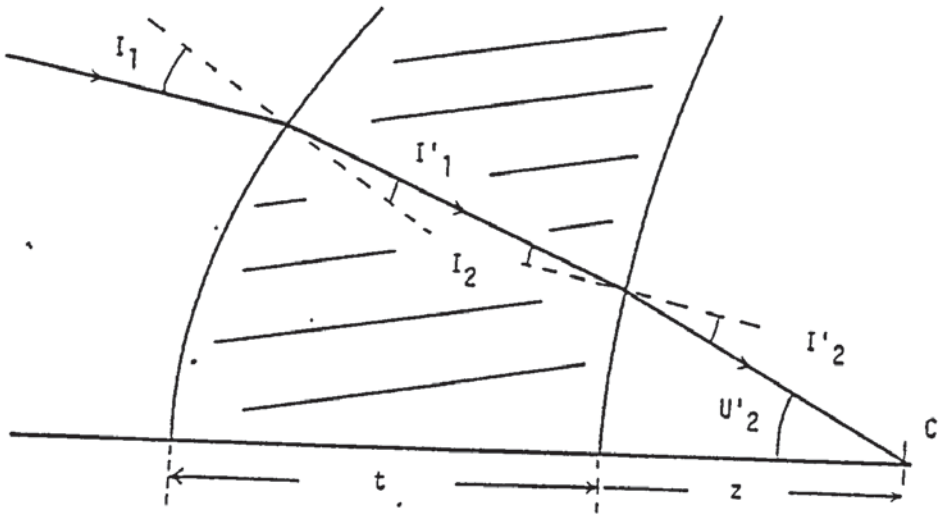

Figure 1.8

Tscherning's ellipses, showing the lens forms free of oblique astigmatism for two lens materials. The effect of lens thickness is ignored, light is assumed to be only shallowly oblique, and the fixation distance is infinity.

Ellipses are plotted from equation I(6), where F_1 is the front surface power, F the power of the lens, Z the dioptric distance to the centre of rotation.

Tscherning's Ellipses

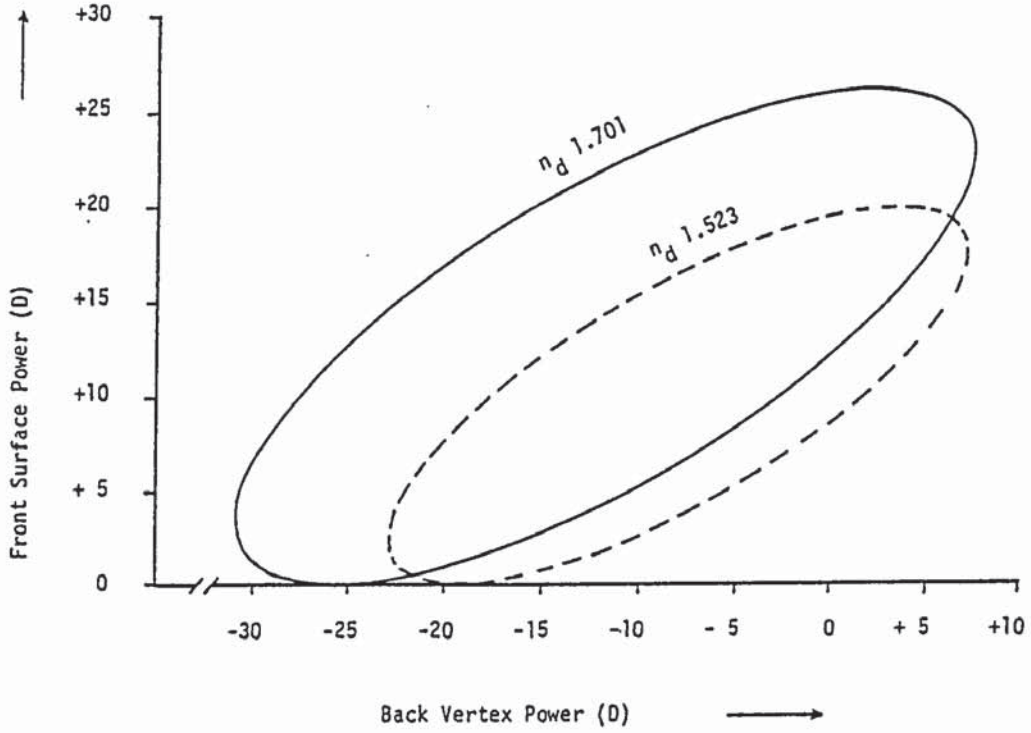

oblique astigmatism (Fowler, 1978) the aphakic power range (+10 to 16 D) cannot. These comments apply to spherical surface lenses only, as the use of aspheric surfaces enables astigmatism free lenses to be designed, because the tangential and sagittal radii in the periphery of the surface are unequal.

The effects of oblique astigmatism on the spectacle lens are shown diagrammatically in Figure 1.9. Two image lines are produced, the sagittal and tangential, rather than a point image. As the eye rotates about its centre of rotation, the positions of these lines form a locus of points. The ideal situation would be to collapse these loci to a single image plane (astigmatism free) coincident with the locus of the far point, the far point sphere. Unfortunately this is usually not possible in the aphakic power range. The choices available to the lens designer are either:

a) Eliminate oblique astigmatism, but accept a residual power error between the image plane and the far point sphere,

or b) Accept some residual oblique astigmatism, but place the locus of points corresponding to the mean of the tangential and sagittal powers (the mean oblique powers) coincident with the far point sphere.

The power error in a) above is the curvature error. Curvature is desirable in ophthalmic lenses, unlike most other lenses, as the far point locus is on a curved surface. The problem is in trying to curve the image plane to match the far point sphere.

Figure 1.9

Astigmatic image shells, being the loci of the far point of the eye and the tangential and sagittal image points formed as the eye rotates. In a similar manner, the vertex sphere is the locus of the back vertex of the spectacle lens.

Astigmatic image shells

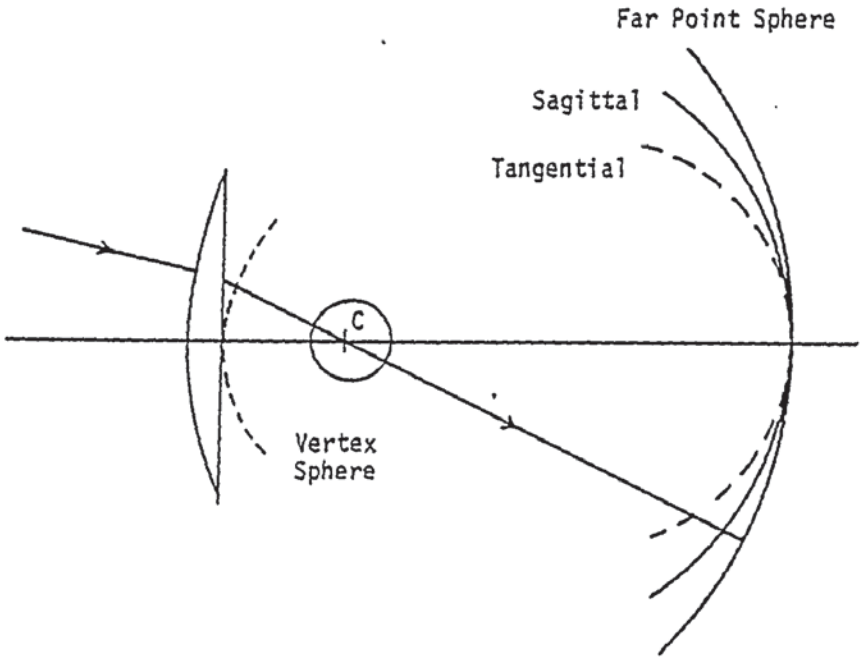

1.2.4 Distortion

An image can be in focus, in the correct plane, but still be defective if it is distorted into the wrong shape. Distortion can be considered as an error in magnification across the lens. In Figure 1.10 if a ray of light that passes through the lens makes an angle of U'_2 with the axis, and the ray of light incident to the lens makes an angle of U_1, then for the lens to be distortion free, the ratio $\text{Tan}U'_2/\text{Tan}\ U_1$ should be a constant. Distortion can be eliminated in spectacle lenses, but using spherical surface lenses, very steep base curves are required. Again, aspheric curves can be used to reduce distortion, since as the power varies across the surface, so does the angular magnification.

1.3 The use of aspheric surfaces in aphakic lenses

From the above discussion it can be seen that aspheric surface lenses can be used for the control of a number of important aberrations. However, aphakic spectacle lens design is still a compromise, whether or not aspheric surfaces are used. It is normal practice to use just one aspheric curve (the front in most cases), the other surface being worked spherical or toroidal as demanded by the prescription. Even using the most sophisticated single aspheric curve, it is not possible to completely remove all lens aberrations, particularly when cosmetic considerations are taken into account as well.

There is an infinite variety of lens curves that could be used

Figure 1.10

Angles used for the calculation of rotary distortion. U'_2 is the angle formed at the centre of rotation by the incident ray to the eye, and U_1 is the angle between the incident ray to the lens and the axis.

Distortion Calculation

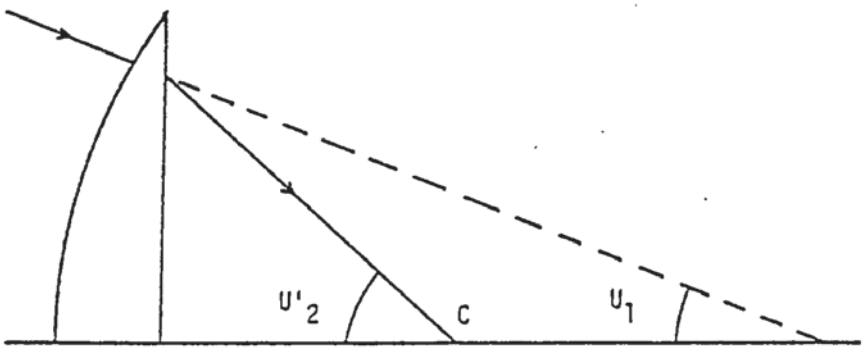

for the aspheric surface of a spectacle lens. But those in practical use can be considered as belonging to one of four groups.

CHAPTER 2

Conic Section Lenses

This type of lens surface is produced by rotating a conic section about an axis. The section normally used for the front surface of aphakic lenses is an ellipse, although other sections could be used. The use of hyperbolic curves has been suggested (Jalie, 1980) for use on lenses outside the aphakic prescription range, in order to reduce the thickness and weight of lenses, without adversely affecting the optical properties.

From the theoretical point of view, conic section lenses are straightforward to deal with mathematically, particularly if the approach of Baker (1943) is used

2.1 Equation of a conic surface

The definition of a conic surface is the locus of a point which moves so that there is a constant ratio between its distance from a fixed point (the focus) and a fixed straight line (the directrix). This ratio is known as the eccentricity. From this definition, a standard equation can be developed (Bennett, 1968) to describe the curve.

In Figure 2.1, a conic curve (in this case an ellipse) has DD' as the directrix and S as the focus. Hence from the above definition,

$$\frac{PS}{PN} = \frac{QS}{QM} = \frac{RS}{RL} = \text{eccentricity}(e)$$

Figure 2.1

A conic surface, having points P,Q,R on the surface, and a line through OT being the axis of symmetry. DD' is the directrix to the surface, and S the focus.

If the vertex of the curve on the axis of symmetry (O) is taken as the origin of a rectilinear coordinate system, then by definition:

$$e = \frac{OS}{OE} = \frac{PS}{PN}$$

If the distance OS = f, and the coordinates of point P are (x,y), then in triangle PST

$$PT^2 + ST^2 = PS^2 = e^2PN^2$$

since $ST = x - f$ and $PN = OE + OT = (f/e + x)$,

this equation can be rewritten as:

$$y^2 + (x - f)^2 = e^2((f/e) + x)^2$$

or $$y^2 = 2f(1 + e)x - (1 - e^2)x^2 \qquad - II\ (1)$$

For optical use, it is essential to know the power at the vertex of the curve (O). In Figure 2.2, a point P is considered very close to the axis, here exaggerated. PH is a tangent to the curve, and PG the normal. Hence angle PHO(θ) is found from:

$$\theta = \frac{dy}{dx} = \frac{2f(1 + e) - 2(1 - e^2)x}{2y}$$

The complementary angle $\emptyset = \frac{dx}{dy}$

The distance OG is the paraxial radius of curvature, and since the coordinates of P (x,y) are very small

$$r = y/\emptyset = y.\frac{dy}{dx}$$

$$= f(1 + e) - (1 - e^2)x$$

$$= f(1 + e) \qquad - II(2)$$

If this is substituted in the general equation of a conic

Conic Surface

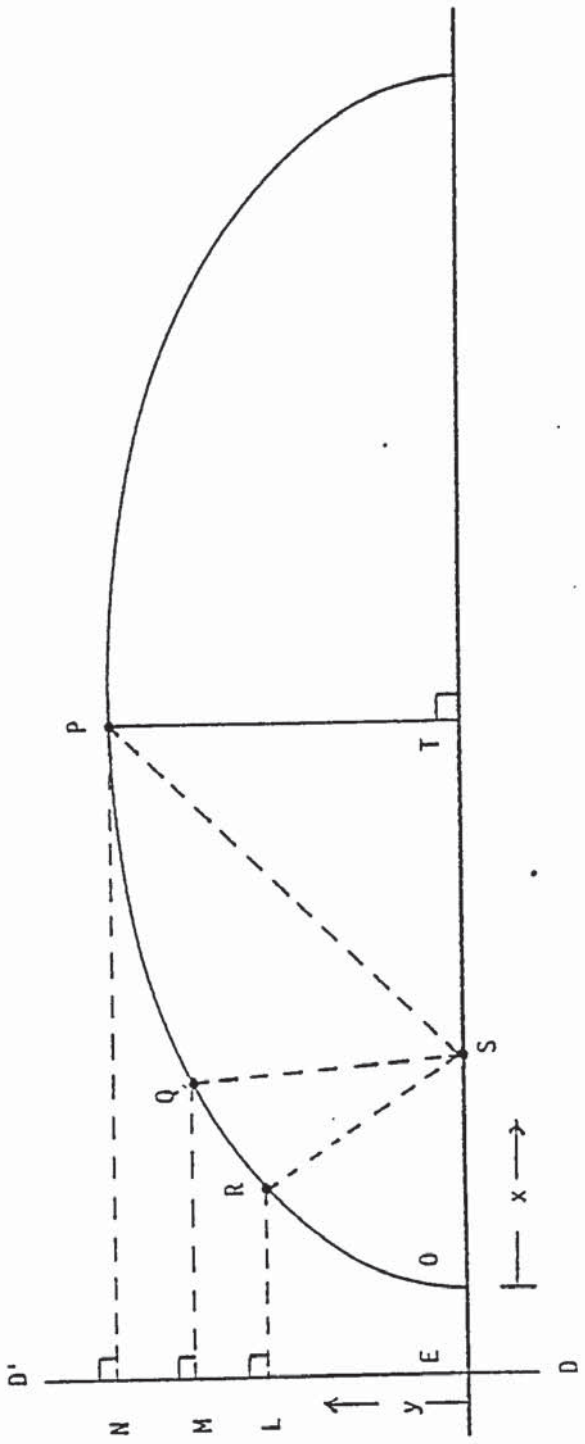

Figure 2.2

Conic surface, with normal at point P being PG and tangent PH. The sagittal radius is given by PG and the tangential by PV.

Conic Surface

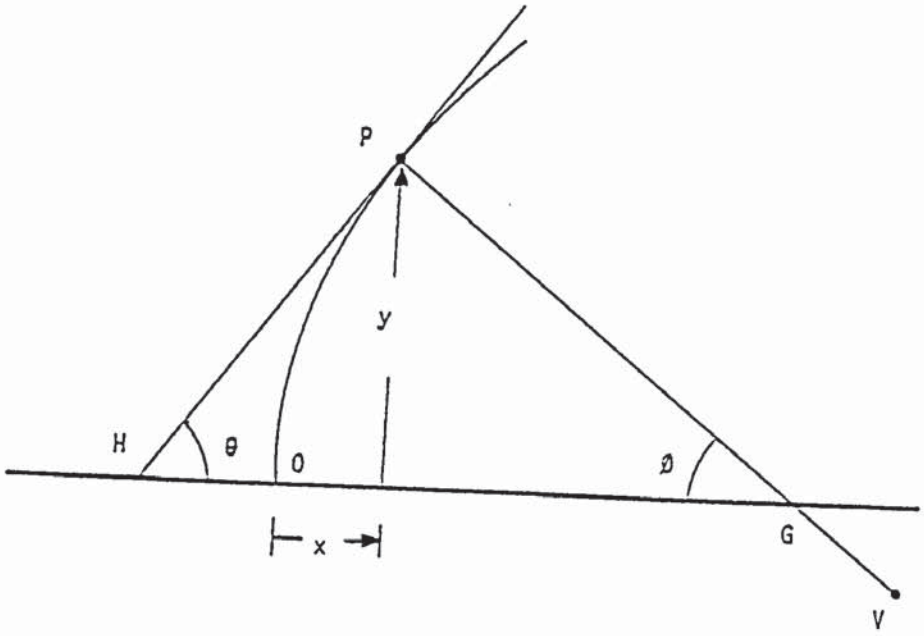

found earlier, and $p = 1 - e^2$, then

$$\underline{y^2 = 2rx - px^2} \qquad \text{- II(2)}$$

Equation II(2) will give the surface coordinates of any conic, where the curve type is described by the parameter 'p', such that:-

$p = 1$	Spherical
$p = 0$	Paraboliдd
$1 > p > 0$	Ellipsoid (prolate)
$p < 0$	Hyperboloid

The property of aspheric surface that makes them useful for controlling lens aberrations is their difference in sagittal and tangential curves at points away from the axis of symmetry, unlike a spherical surface. Hence for ray tracing, these radii of curvature need to be calculated.

The centre of curvature of a sagittal section is the intersection of the normal at any point with the axis of symmetry. Hence in Figure 2.2, for point P, G is the centre of curvature, and PG the radius of curvature. Differentiating equation II(2) gives

$$\frac{dy}{dx} = \frac{r - px}{y}$$

$$\text{and } \text{Tan } \emptyset = \frac{dx}{dy} = \frac{y}{r - px}$$

$$\text{also } \text{Tan } \emptyset = \frac{y}{TG}$$

$$\text{thus } TG = r - px$$

If the sagittal radius of curvature is denoted by r_s, then since:

$$PG^2 = PT^2 + TG^2$$

$$r_s^2 = y^2 + (r - px)^2$$

this can be expanded to:-

$$r_s^2 = y^2 + r^2 - 2rpx + p^2x^2$$

or

$$r_s^2 = r^2 + y^2 - p(2rx - px^2)$$

Substituting the right side of II(2) for the value in brackets

$$r_s^2 = r^2 + y^2 - py^2$$

$$r_s = (r^2 + (1 - p)y^2)^{\frac{1}{2}} \qquad - \text{II(3)}$$

The tangential radius of curvature (r_t) for any curve is related to the first and second differentials to the curve (Bennett, 1968) by

$$r_t = \frac{(1 + (\frac{dy}{dx})^2)^{3/2}}{\frac{d^2y}{dx^2}}$$

since $\frac{dy}{dx} = \frac{r - px}{y}$ then $\frac{d^2y}{dx^2} = \frac{-r^2}{y^3}$

or by substitution,

$$r_t = \frac{r_s^3}{r^2} \qquad - \text{II(4)}$$

Note that in the special case of a spherical surface, where p=1, the sagittal and tangential radii both reduce to 'r', the paraxial value, as would be expected. Thus these equations can be used in a general purpose computing scheme for use on spherical as well as conic surface lenses, as shown in Appendix I.

2.2 Examples of the effects of using a conic lens surface

In order to illustrate the effects of using a front conic surface on a high power hypermetropic lens, ray tracing was carried out through a hypothetical lens, with the following characteristics:

Back Vertex Power	:	+14.00 DS
Thickness	:	8.00 mm
Index (n_d)	:	1.498
'z' distance	:	27.00 mm

Using a looping program, the rear surface power of the lens was varied from -1.00 to -6.00 D, and at the same time various conics from spherical (p = 1) to parabolic (p = 0) were used for the front surface. The results of these calculations are shown graphically, in terms of the theoretical aberrations, in Figures 2.3 to 2.5.

In order to simplify the comparison, the aberrations are only shown for one oblique angle (U') of 30 degrees. Figure 2.3 illustrates the oblique astigmatism and gives the expected result that it is not possible to design a lens using spherical curves (p_1 = 1) and obtain zero oblique astigmatism. As the front surface is made flatter in the periphery and eventually reaches parabolic (p_1 = 0), combinations of Back Surface Power and front surface asphericity are reached which correct the astigmatism, and then over correct it. If correction of oblique astigmatism was the only aim, there would thus be a number of options open. However, there are other aberrations to be considered, and also the cosmetic aspect. A shallower rear surface will tend to make a

Figure 2.3

Theoretical oblique astigmatism values for a series of front surface conic lenses.

Figure 2.4

Theoretical Mean Oblique Power values for a series of front surface conic lenses.

Figure 2.5

Theoretical distortion values for a series of front surface conic lenses.

In all cases, B.V.P. +14.00 DS, axial lens thickness 8 mm, centre of rotation 27 mm from lens, lens index 1.498, eye rotation angle 30 degrees, distant object.

Conic front surface lenses

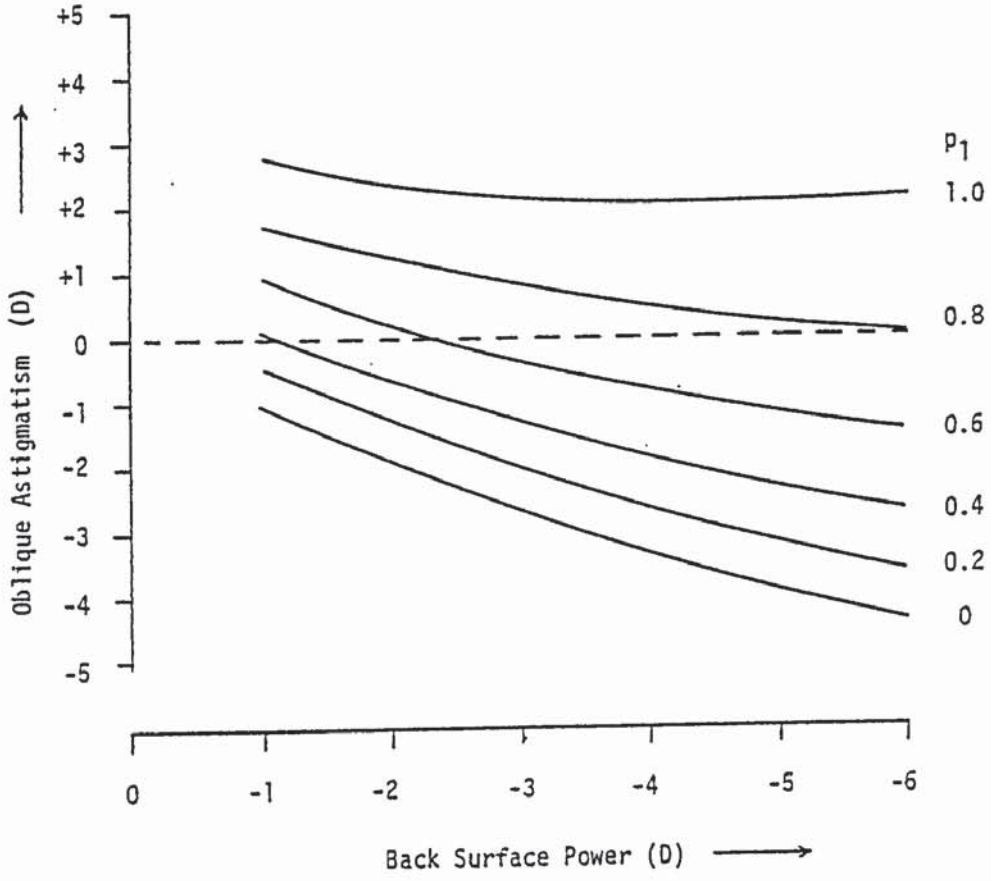

Conic front surface lenses

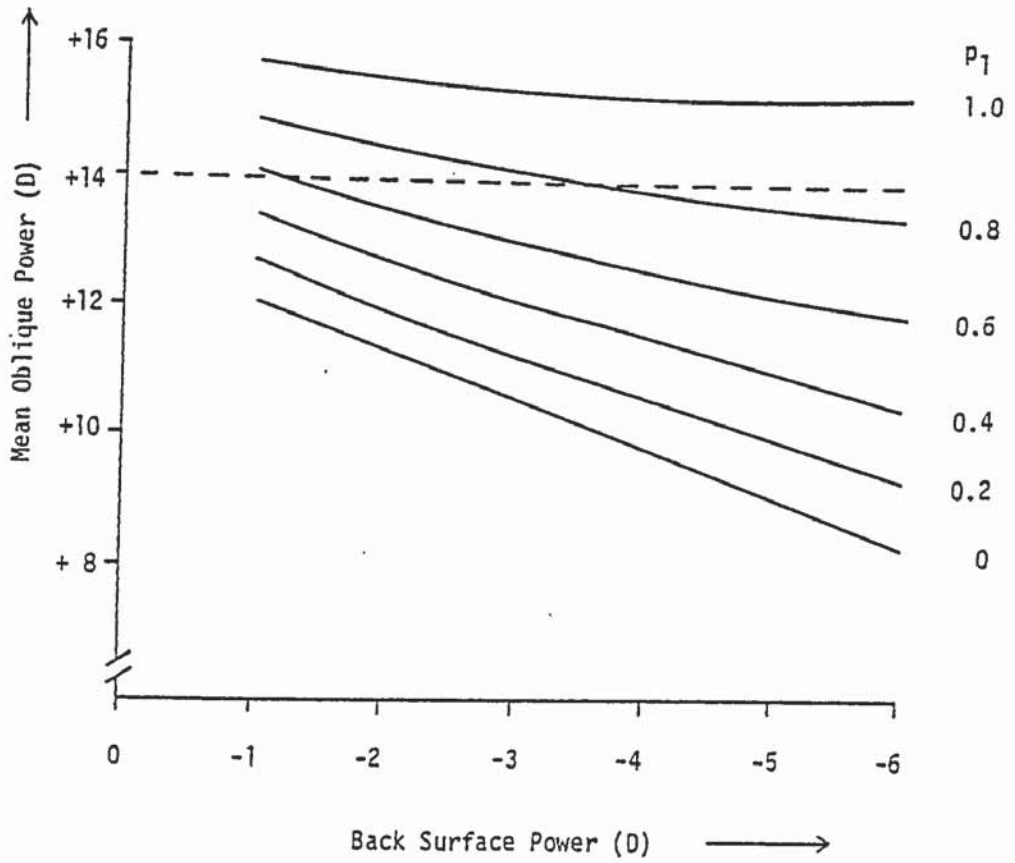

Conic front surface lenses

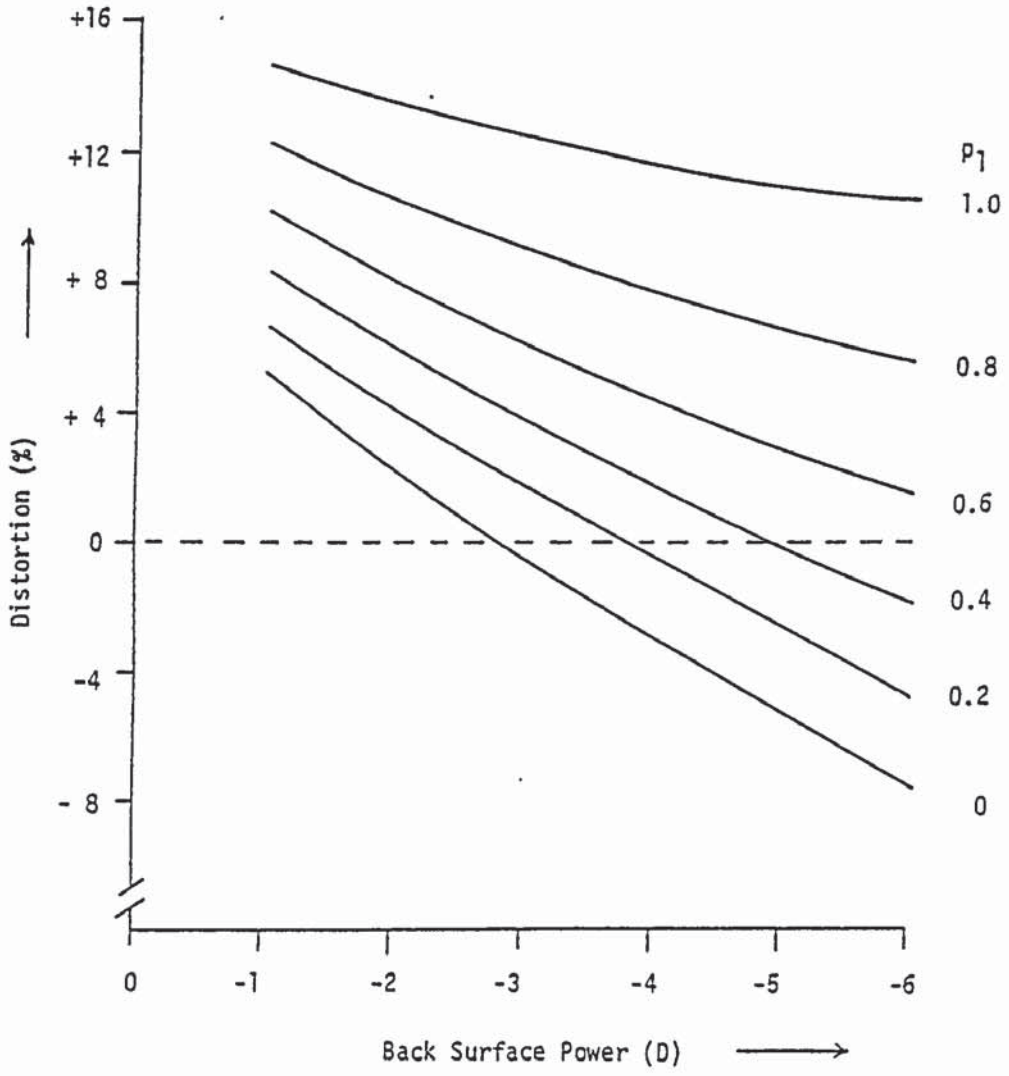

lens appear less bulbous to the onlooker. Thus in recent years manufacturers have used surface powers in the range -1.00 D to -2.00 D, whereas at one time it was common to use powers between -3.00 D and -4.00 D.

In the ideal lens, there would be no mean oblique power error in the lens at this angle of rotation, so that the mean oblique power would be +14.00 D, the same as the back vertex power. From Figure 2.4 it can be seen that this can be achieved by a p_1 value of 0.8 combined with a rear surface of -3.00 D. Again, the steeper aspherics correct this defect better than those nearer the parabolic form.

Figure 2.5 illustrates the effects of lens form on distortion, and shows that flatter forms are required for its correction than the other two aberrations already mentioned. For example, a parabolic front surface (p_1 =0) with a rear surface of -2.75 would be a suitable combination. Recently, Smith and Atchison (1983a, 1983b) and Atchison (1984) have produced modified Tscherning's ellipses to show the third order lens forms free from oblique astigmatism using conic surfaces.

2.3 von Rohr design

The first commercially available design using an aspheric surface was the Zeiss 'Katral'. An aspheric spectacle lens design, for both high positive and high negative prescriptions, was patented by von Rohr for Carl Zeiss (von Rohr, 1909). This used very steep lens surfaces, the positive power lens quoted as an example in

the patent having the following characteristics:

Equivalent Power :	+13.80 DS
F_2 :	-18.714 D
n :	1.655
t :	5.0 mm

The lens is unusual by modern standards in having the rear surface aspheric, undoubtedly due to the existing expertise at Carl Zeiss for the aspherisation of concave surfaces (Abbe, 1900a, 1900b). Details of the lens design are not given, except that the surface used is steeper than the equivalent spherical surface, and also that at a diameter of 34 mm there is a difference of 0.25 mm between the aspheric and its equivalent sphere. However, from the performance data, some deductions can be made. For an object at 1/3 metre from the lens, the sagittal and tangential focal lengths (in mm.) are given as:

Object angle	s'	t'
0	86.66	86.66
10.596	88.27	87.19
16.123	91.36	93.78

From ray tracing data it would appear that an object angle of 10.596 degrees is approximately equivalent to an eye rotation of 20 degrees, and an object angle of 16.123 degrees is approximately equivalent to an eye rotation of 30 degrees. Hence the above table is equivalent to:

Figure 2.6 and 2.7

Effect of varying rear surface conic asphericity of plus lens in British Patent 15,533 on oblique astigmatism (2.6) and distortion (2.7)

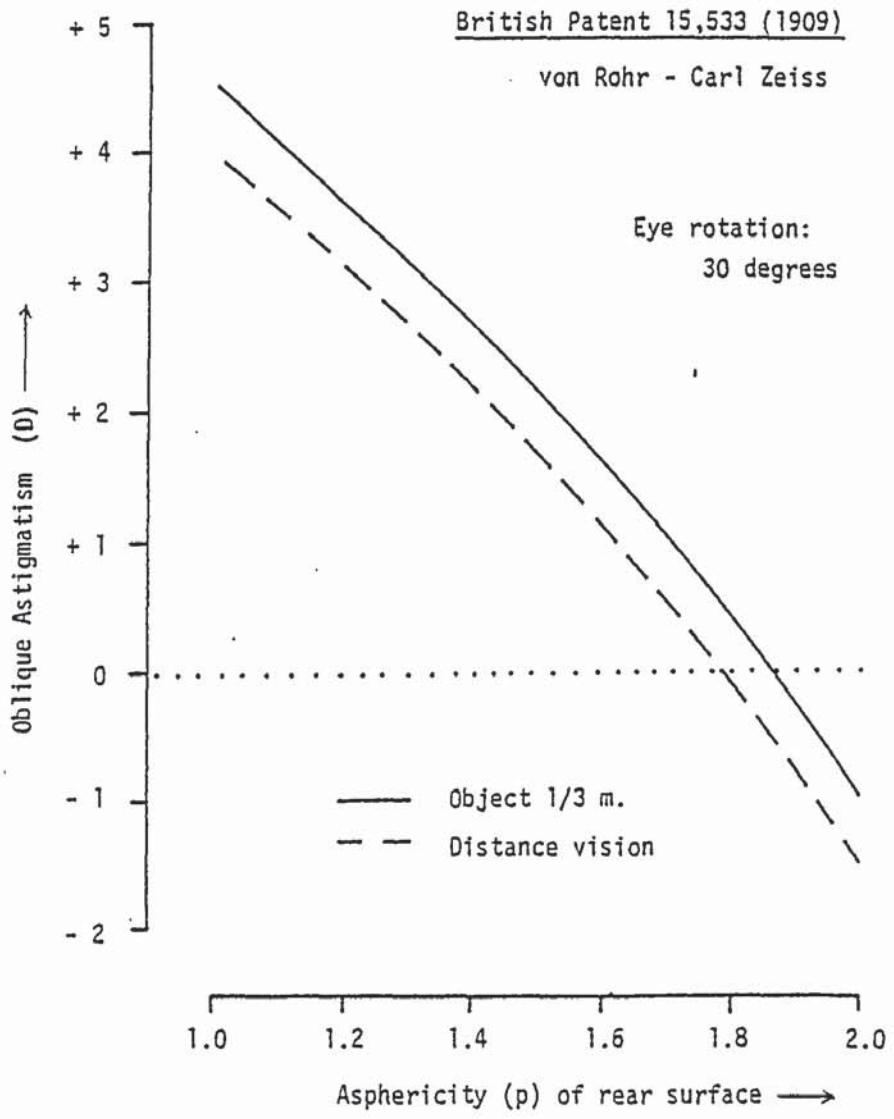
British Patent 15,533 (1909)
von Rohr - Carl Zeiss
Eye rotation:
30 degrees
+ 5
+ 4
+ 3
+ 2
+ 1
0
- 1
- 2
Oblique Astigmatism (D) ⟶
Object 1/3 m.
Distance vision
1.0
1.2
1.4
1.6
1.8
2.0
Asphericity (p) of rear surface ⟶

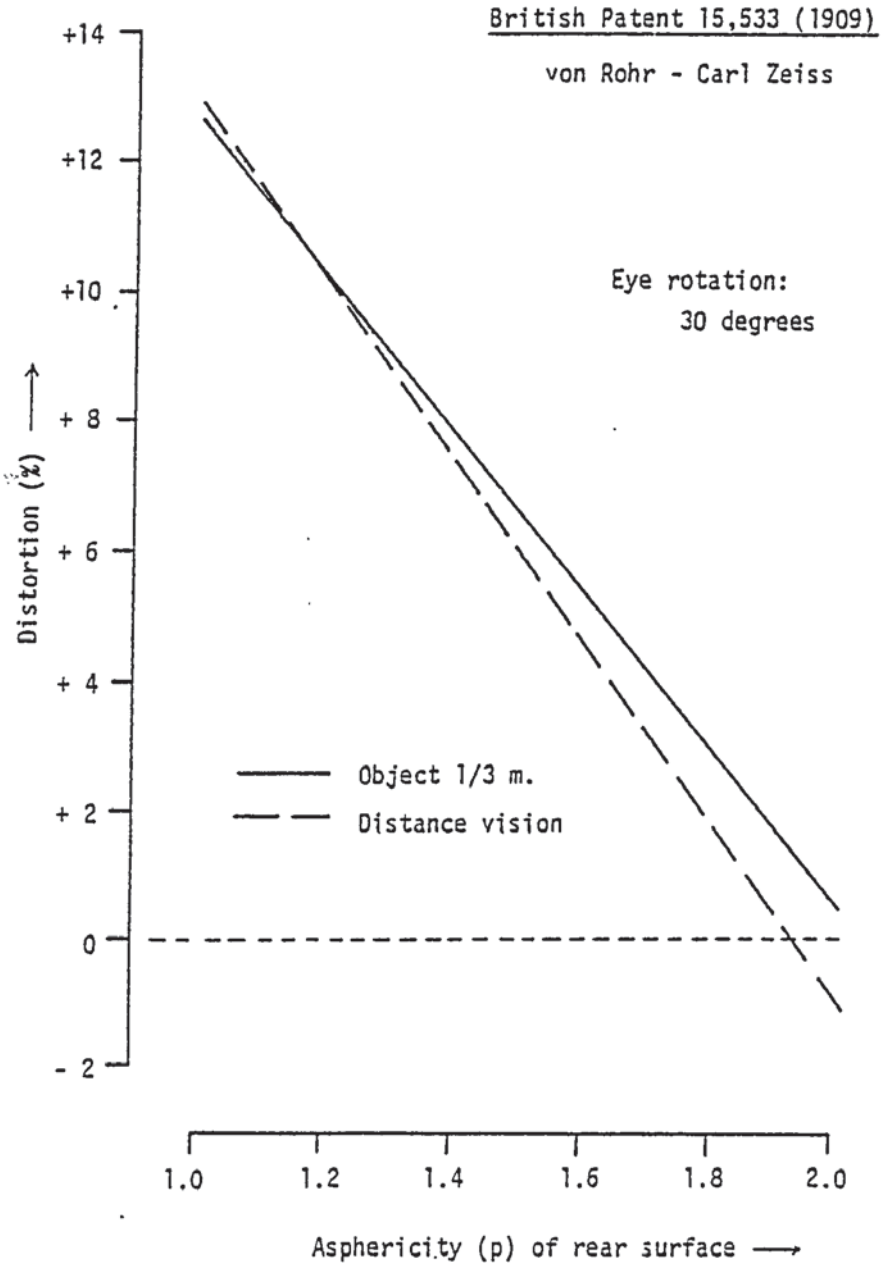
British Patent 15,533 (1909)
von Rohr - Carl Zeiss
Eye rotation:
30 degrees
+14
+12
+10
+ 8
+ 6
+ 4
+ 2
0
- 2
Distortion (%)
Object 1/3 m.
Distance vision
1.0
1.2
1.4
1.6
1.8
2.0
Asphericity (p) of rear surface

Eye rotation	S'(D)	T'(D)	Astigmatism
20	+11.33	+11.47	+0.14
30	+10.95	+10.66	-0.29

If we assume that the rear surface of the lens is made with a conic surface, then Figures 2.6 and 2.7 show the relationship between aspherics of varying 'p' (steeper than spherical) and astigmatism, and 'p' plotted against distortion, for both distance and near vision. A rear surface 'p' of 1.9 would appear to fit the aberration data quoted very well, although from the departure of the lens curve from spherical, the value of 'p' should be 1.7.

It is particularly noteworthy that apart from exhibiting very little oblique astigmatism, the lens is virtually distortion free. However, according to Henker (1924), the commercial 'Katral' lens used a much flatter form, thus considerably reducing the correction of distortion.

2.4 Volk lens

A lens disign for an aspheric spectacle lens for the correction of aphakia was produced by Volk (1958, 1961), with a conic section front surface. This design is interesting as a method of lens manufacture was also patented (Volk, 1966a 1966b).

There is no specific detail given of the precise conic section used, except for a table of sag differentials in the 1961 paper (see Table 2.1). It is stated that the lenses were designed to be manufactured in ophthalmic crown glass (n=1.523), thus by substituting this index for the base curve power, a table of 'p'

Table 2.1

Sag Differentials, Volk lenses

Base Curve (D)	Lens Diameter (mm)						
	38	40	42	44	46	48	50
11	0	0	.1	.2	.2	.2	.2
12	0	0	.1	.2	.2	.2	.2
13	0	0	.2	.2	.2	.2	.3
14	0	0	.2	.2	.2	.2	.4
15	.1	.1	.2	.2	.3	.3	.5
16	.1	.2	.4	.5	.7	.7	.9
17	.3	.4	.7	.8	1.1	1.1	1.4
18	.3	.4	.7	.9	1.2	1.2	1.7
19	.4	.5	.9	1.2	1.5	1.5	2.3
20	.6	.8	1.3	1.7	2.5	2.5	3.7

(Sag differentials from sphere, mm.)

Table 2.2

Table of 'p' values calculated from Volk (1961) data

Base Curve (D)	Lens Diameter (mm)						
	38	40	42	44	46	48	50
11	1	1	.63	.70	.49	.59	.66
12	1	1	.73	.78	.63	.70	.76
13	1	1	.80	.66	.73	.78	.73
14	1	1	.85	.75	.80	.84	.74
15	.81	.85	.88	.81	.85	.82	.76
16	.85	.76	.82	.70	.71	.67	.66
17	.63	.61	.62	.58	.63	.60	.60
18	.71	.70	.72	.69	.70	.69	.66
19	.69	.71	.69	.70	.70	.73	.69
20	.62	.62	.69	.66	.69	.67	.68

values used could be calculated (Table 2.2). It is likely that all the bases were designed to have a similar 'p' value, the differences shown in Table 2.2 arising from rounding errors in the original data, Table 2.1. This lens series was designed to cover a prescription range of +7.50 to +24.00 D, with an optimum rear surface power of -3.00 D. The stated aim of the design was to give a wider field of good visual acuity than could be achieved with a spherical surface lens.

2.5 Essel Lens

A very interesting lens, which has unfortunately recently gone out of production, is the Essel 'Atoral'. This lens is unusual in having an aspheric toric surface, and was described in two patents (Societe des Lunetiers, 1968, 1970). Although the principal appears to have been used mainly for varifocal lenses, single vision lenses also were made. These are of interest because they have an aspheric rear surface. One problem with this type of lens is that having a spherical fornt surface does nothing to improve the cosmetic aspects of the lens, and also restricts the maximum diameter that can be manufactured.

CHAPTER 3

Aspheric lenses with polynomial surface curve

From the discussion Chapter 2, it will be apparent that although conic surface lenses enable considerable control of aberrations to be achieved, the resultant lens design is still a compromise.

In an attempt to reduce these compromises, lenses having a front surface described by a polynomial equation have been used. The aspirations of this type of lens are summarised quite well in the following advertisement for an Armorlite aspheric lens:

> "In aphakic lenses - to correct marginal astigmatism above, choose an ellipse:
>
> $$x = \frac{y^2/r}{1 + (1 - (y/r)^2(1 + A))^{\frac{1}{2}}}$$
>
> To correct all aberrations maximally, use a higher order aspheric:
>
> $$x = \frac{y^2/r}{1 + (1 - (y/r)^2(1 + A))^{\frac{1}{2}}} + By^4 + Cy^6 \text{ "}$$

The first equation quoted here is a rearrangement of the conic equation (with p = 1 + A):

$$y^2 = 2rx - px^2 \qquad - - - \text{III(1)}$$

solved for 'x'. Hence the second equation in this quotation is a conic section with the addition of additional terms y4 and y6.

3.1 The designs of Davis

The use of such a surface was demonstrated by Davis and Clotar (1956). The form of surface equation used for the front of the lens was:

$$x = ay^2 + by^4 + cy^6 \qquad \text{- - III(2)}$$

where $a = 1/(2r)$ - - III(3)

'r' representing the paraxial radius of curvature. Davis and Clotar give an example of a +12.00DS lens made with this type of design. This lens had the following characteristics:

Rear surface radius	176.66 mm
Front paraxial radius	36.55 mm
centre thickness	4.60 mm

If used with a glass of refractive index 1.530, this gives a rear surface power of - 3.00 D. The aspheric coefficients used were:

a	1.3679×10^{-2}
b	3.8942×10^{-6}
c	-3.7126×10^{-9}

The relationship between 'a' and the front surface paraxial radius is the same as would be expected from equation III (3). Surprisingly, the lens values quoted do not give a finished lens BVP of +12.00DS for an index of 1.530, or for any other commonly used value. Thus the rear surface power was modified to -3.162 D to give the correct value.

Using these figures, a ray trace was carried out through this lens design, for distance vision. The program used was TRACE 4

(Appendix II). No value of 'z' was given by David and Clotar, so the figure of 27mm was assumed. The calculated aberration figures are shown in Table 3.1. These appear to correlate well with the figure of Davis and Clotar, which are only given in graphical form.

The ray trace illustrates the stated design objectives, which were to give zero astigmatism and power error at one wide angle of view (25 degrees), with a reasonable performance at smaller angles. This is naturally still a compromise as can be seen in Table 3.1. Although the astigmatic error at 25 degrees is only −0.031 D, with a Mean Oblique Error (MOE) of -0.043D, the astigmatism and power errors increase rapidly above this angle. At smaller angles, the tangential power error reaches a maximum at 15 degrees of +0.500 D.

This would probably have been a very acceptable lens design in practice, but it was never produced commercially. Davis (1959) described the philosophy of a design that was later patented (Davis and Fernald, 1965) and produced commercially as the American Optical aspheric lenticular. With this lens, the design concepts were slightly different to those described by Davis and Clotar. It was felt that the most important feature of any design was to keep the tangential power as near constant as possible, rather than the complete elimination of astigmatism. This had been decided after photographic studies, which showed that with the aphakic range of spectacle lens powers, transverse chromatic aberration was also reduced. The practical limits set were for eye rotations up to 30 degrees a maximum tangential error of

Table 3.1

Calculated aberration values for +12.00DS lens

(Davis and Clotar, 1956)

Eye Rotation (Degrees)	S' (D) v	T' (D) v	M.O.P.(D)	Distortion
5	+12.024	+12.093	+12.059	0.353
10	+12.067	+12.308	+12.187	1.334
15	+12.105	+12.500	+12.302	2.868
20	+12.091	+12.459	+12.275	4.817
25	+11.973	+11.942	+11.957	6.985
30	+11.696	+10.725	+11.210	9.151

BVP +12.00DS

F_2 -3.162D

t 4.60 mm

n_d 1.53

z 27.00 mm

Distance vision

+0.50D, and a sagittal error maximum of -0.75D.

In order to cover a range of prescriptions with BVPs of +7.00D to +16.00D, Davis and Fernald (1965) designed ten separate base curves. This was done to try and keep the lens performance at an optimum level for all powers. The lens series was designed with a rear surface power of -3.50D for spherical prescriptions. This had been found to be the value that gave a minimum change in performance for various lens to eye fitting distances.

Of particular interest is the No.14 blank, as a lens of this value was available for measurement (Chapter 9). The patent does not give the equation of the lens surface and aspheric coefficients, but the rectilinear coordinates of the aspheric surface are quoted. Using a curve fitting programe (Appendix III), the coordinates for blank No.14 were fitted to a modified conic equation of the form:

$$x = \frac{y^2/r}{1 + (1 - p(y/r)^2)^{\frac{1}{2}}} + Ay^4 + By^6 \quad - - \text{III(4)}$$

Using the stated value for front surface paraxial radius (r), the following aspheric coefficients were calculated

P	-1.366×10^{-3}
A	3.298×10^{-6}
B	2.339×10^{-9}
r	30.796 mm

A surfacing chart is given in the patent, but this does not give the correct lens power by calculation. Davis (1981) has stated that the thicknesses given in the patent for finished lenses are incorrect, and has supplied the correct values. A ray trace was carried out through the lens, using the above aspheric coefficients. The results are shown in Table 3.2, and illustrate the lens design philosophy. This tangential error increases as the eye rotates, up to a maximum error of +0.227D. The sagittal error also increases with eye rotation, but at a faster rate, giving a maximum error of -0.478D. However, the maximum MOE is only -0.125D, a very small value.

Recently, Davis (1981) has described the aspheric coefficients actually used for this lens. These are:

P	0
A	3.279×10^{-6}
B	2.3716×10^{-9}

If a ray trace is carried out through a lens with these values for the front surface coefficients, then the maximum error from the value found in Table 3.2 is 0.007D, a very small difference.

Table 3.2

Calculated aberration values for +14.00DS lens

(Davis and Fernald, 1965)

Eye Rotation (Degrees)	S' (D) v	T' (D) v	M.O.P.(D)	Distortion (%)
5	+13.984	+13.994	+13.989	0.192
10	+13.937	+13.984	+13.960	0.784
15	+13.863	+13.993	+13.928	1.824
20	+13.767	+14.042	+13.905	3.382
25	+13.655	+14.132	+13.893	5.553
30	+13.522	+14.227	+13.875	8.448

BVP	+14.00DS
F_2	-3.50 D
t	8.04 mm
n_d	1.4925
z	23.25 mm

Aspheric coefficients derived by curve fitting data given in patent

Table 3.3

Comparison of surface coordinates for various conics with coordinates from Davis and Fernald (1965)

Blank No.14 Assume r = 30.796 mm

p	2	6	10	14	18
					y mm
0.75	0.0649	0.5887	1.6570	3.3161	5.6490
0.77	0.0649	0.5888	1.6579	3.3200	5.6610
0.79	0.0649	0.5889	1.6588	3.3239	5.6732
0.81	0.0649	0.5890	1.6598	3.3278	5.6855
0.83	0.0650	0.5891	1.6607	3.3318	5.6979
0.85	0.0650	0.5892	1.6616	3.3357	5.7104
					x mm

Davis and Fernald patent values:

0.0650	0.5888	1.6587	3.3260	5.6853

Figure 3.1

Comparison of Mean Oblique Power values calculated from curve fit of data in Davis and Fernald (1965) with conic front surfaces. Data points (circles) from Table 3.2.

Davis and Fernald Lens

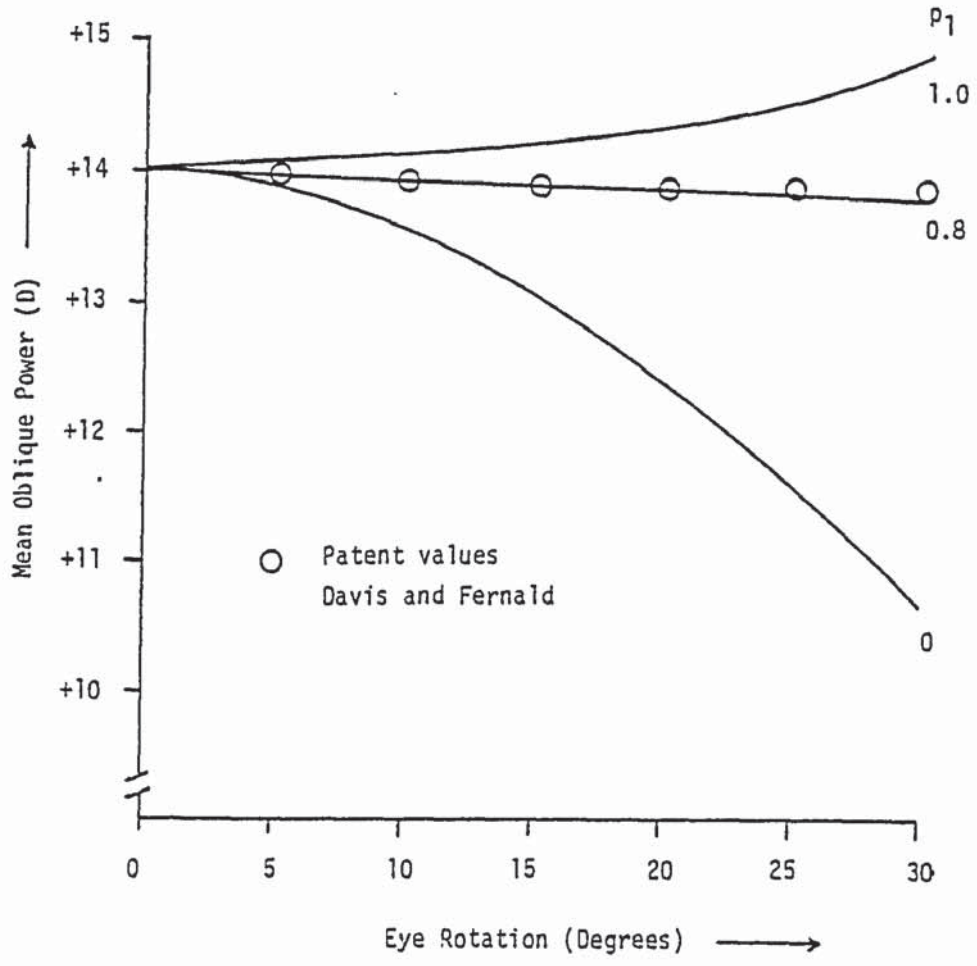

The obvious question to be asked of this type of lens design is this: does the increased complexity compared with a conic surface make for much better performance? The most straight-forward comparison to make is between the surface coordinates quoted in the patent and the coordinates of a family of conics. This is done in Table 3.3 for the No.14 blank. Quite clearly, the surface co-ordinates in the patent fall within a narrow band of equivalent conics. The similarity to a conic surface is even more dramatic when the optics are compared, at least up to a thirty degree eye rotation. In Figure 3.1 the Mean Oblique Power value for various conics are compared with the values in Table 3.2. It will be apparent that a lens with a conic front surface having a 'p' in the region of 0.8 will have very similar properties. This is confirmed if one inspects the astigmatism and distortion values as well.

3.2 Bechtold Lens

There is another well - documented polynomial surface lens, this being the lens designed by Bechtold (1973) for the Itek Corporation. This design is interesting as it uses a rather different type of polynomial power series to describe the surface. The lens is also different from the Davis and Fernald design in being a full aperture lens, rather than a 40mm aperture lenticular. The advantages claimed in the patent for this lens are:

1. Good visual acuity up to 30 degrees off axis
2. Reduced distortion compared with other designs

3. Tangential and sagittal errors equal and opposite at 20 degrees, with zero tangential error at 30 degrees.

4. Insensitivity to fitting distance and base curve variations.

5. Bifocal segment is near circular.

This last claim refers to the fact that bifocal segments on aspheric surfaces are often distorted to non-circular shapes.

The equation of the surface is quoted as:

$$x = a/(by^2 + 1) + cy^2 + dy^4 - a \qquad - - - \text{III(5)}$$

Aspheric coefficients are given for 8 different base curves, covering a finished lens power range of +7.00 D to +19.00 D. For comparison purposes, the 16.43 base curve was studied. Aberration values are quoted for this blank assuming it to be finished to a BVP of +14.50 D. Assuming the quoted thickness of 7.8mm and refractive index of 1.4975, this would require a rear surface power of - 3.468 D. The aspheric coefficients for this blank are given as:

a	+2.197
b	+0.001
c	-0.0143155
d	-6.035×10^{-6}

The calculated aberration figures for distance vision are given in the patent as:

Angle (Degrees)	Tangential (D)	Sagittal (D)
10	+ 0.06	- 0.04
15	+ 0.13	- 0.09
20	+ 0.20	- 0.16
25	+ 0.20	- 0.27
30	0.00	- 0.43

These figures illustrate the aims of the design in claim 3. above.

Does this design represent any improvement over the earlier Davis and Fernald lens? Can the surface equation be approximated by any other power series? The surface co-ordinates for the 16.43 blank (produced from equation III(5)) were fitted using POLYFIT 3 (Appendix III) to an equation of the type shown in III(4). This gave the following aspheric coefficients:

P	-2.6808×10^{-3}
A	3.945×10^{-6}
B	1.296×10^{-9}

If these values are substituted into TRACE 4, assuming a BVP of +14.500, rear surface power of -3.468D, centre thickness of 7.8mm, refractive inded of 1.4975, and a 'z' value of 27mm, then aberration values for distance vision are as shown in Figure 3.2.

It should be noted that the rear surface power was calculated in order to give the correct BVP as shown in the patent, and that the value for 'z' is an assumed figure, as none is given.

Figure 3.2

Calculated values of tangential and sagittal power, based on ray trace through curve fitted to points derived from Bechtold (1973) equation, compared with aberration values given in the patent.

Bechtold Lens

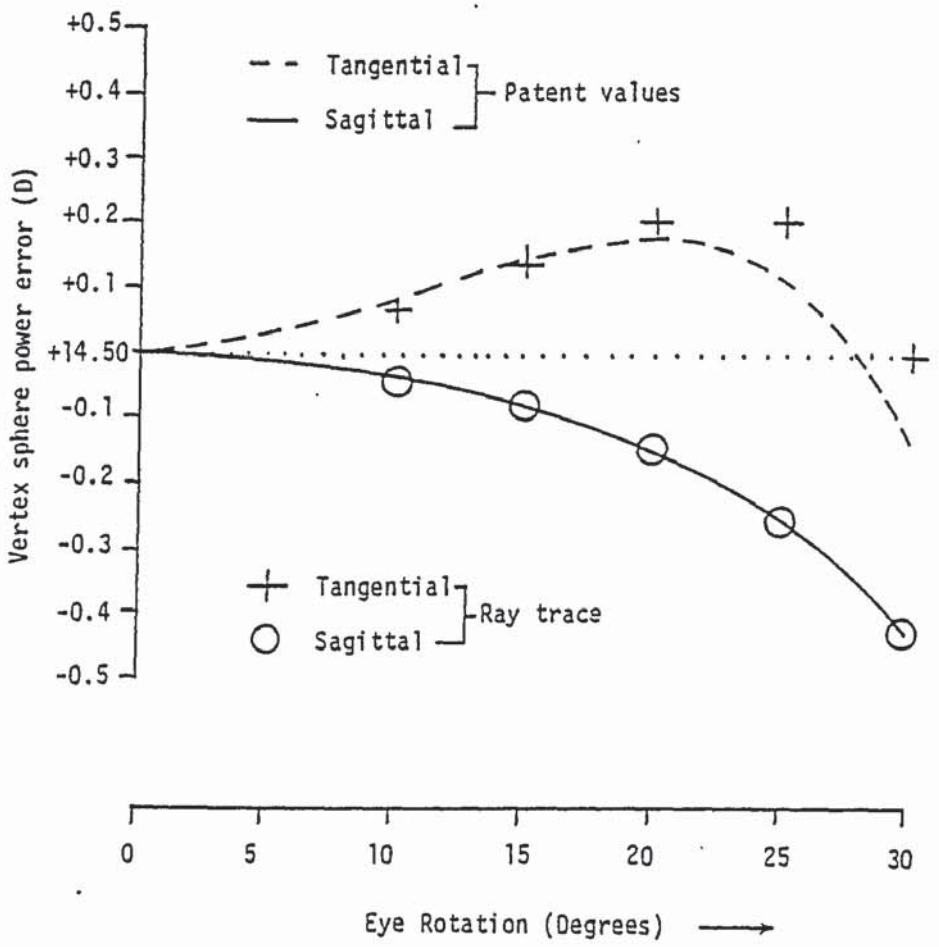

From Figure 3.2 it will be apparent that the surface found by curve fitting gives a reasonable optical equivalent to the Bechtold design, thus the use of this form of equation does not give much advantage from the astigmatism and curvature viewpoint, at least up to 30 degrees.

It is specifically claimed with this lens that the distortion is better than with other designs. No values are given in the patent, so the distortion values were taken from the curve - fitting surface and compared with a family of front surface conic lenses. The results are plotted in Figure 3.3, and show that up to 30 degrees, the distortion is similar to a conic surface lens with a front surface 'p' of just over 0.8.

From the calculations on these designs it would appear that their advantages over conic surface lenses is minimal. There may be more advantage at very wide angles, but this is not claimed in the literature.

Indeed, Davis (1973) has described the differences between polynomial lenses and ones with a conic (ellipsoidal) surface as 'trivial'. He states that the main reason for the use of such a surface for the American Optical lenticular was computing convenience.

Figure 3.3

Calculated distortion, based on ray trace through curve fitted to points derived from Bechtold (1973) equation, compared with distortion from same lenses with conic front surface.

Calculated distortion of Bechtold lens

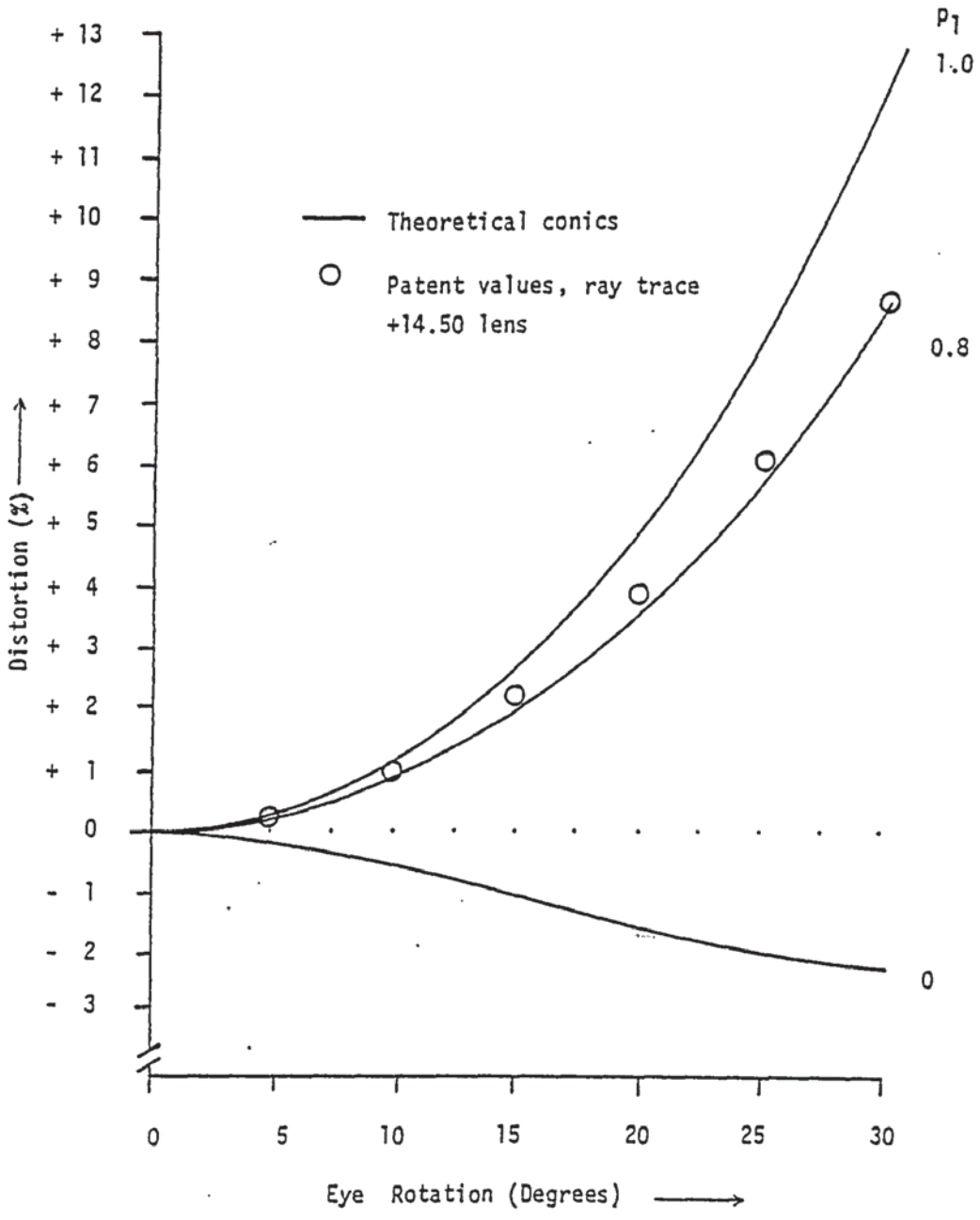

3.3 Jeffree Lens

A lens designed by Jeffree (1963) used on aspheric curve on the rear surface only. This lens was designed to be manufactured in polymethyl methacrylate plastic, and has an aspheric curve described by the equation:-

$$Qx^2 + By^4 + y^2 - 2Rx = 0 \qquad \text{- III(6)}$$

where (x,y) are the coordinates of a section through the optical centre, (R) is the paraxial radius of curvature, and (Q,B) are the aspheric coefficients. For a + 14 Dioptre lens, the values of the radius and aspheric coefficients are given as:-

R: 3.712 cm

Q: 2.00

B: 0.0223

No details of lens aberrations are given in the patent. As the surface equation was not in a form convenient for ray - tracing, a curve fitting program was used to fit the surface coordinates to a curve of the form:-

$$x = cy^2/(1+(1-(K+1)c^2y^2)^{\frac{1}{2}}) + Ay^4 + By^6 \qquad \text{- III(7)}$$

The resulting aspheric coefficients are shown in Table 3.4. This lens was never produced in more than prototype form, and would have suffered from two mechnical problems. First, the use of a spherical front surface would have given a very bulbous design, unattractive cosmetically, and also very limited in diameters in which it could be manufactured, except in lenticular form. Following on from this, the second problem would be that

any cylindrical correction would have to be incorporated into this steep front surface.

3.4 Katz Lens

In a design study, Katz (1982) used the ACCOS V lens design package in order to try and produce various lenses with minimum oblique astigmatism, mean oblique error and distortion. In order to achieve this, Katz used two aspheric surfaces, which are described by equations of the form:

$$x = cy^2/(1+(1-(K+1)c^2y^2)^{\frac{1}{2}}) + Ay^4 + By^6 + Cy^8 + Dy^{10} \quad - \text{III(8)}$$

where (x,y) are the surface coordinates of a section through the optical centre, (c) is the paraxial curvature, and (K,A,B,C,D) are aspheric coefficients. If (A,B,C,D) are zero, then the surface is a conic section of revolution. The details of the +14 Dioptre lens designed by Katz are shown in Table 3.4.

It is interesting to compare this design of lens by Katz with earlier lenses, designed with the same ideal. Like the Jeffree lens, this design study of Katz was intended for a restricted diameter of 40mm, and would therefore have to be manufactured in lenticular form for use in modern frames. The lens of von Rohr (1909) discussed in Chapter 2 was also designed to give low distortion and power errors, at a diameter of 34 mm. For comparison purposes, the von Rohr lens was adjusted to have a B.V.P of +14.00 DS, though the rear surface asphericity was kept at $p_2 = 1.9$, equivalent to a 'K' value of 0.9 in equation III(7), as $p = (K + 1)$. The resulting lens details are given in Table 3.4.

Table 3.4

Aspheric lens parameters

	von Rohr*	Jeffree*	Katz
B.V.P.(D)	+14.00	+14.00	+14.00
t(mm)	5.00	6.00	9.20
F_2 (D)	-18.714	-13.227	-5.100
n	1.655	1.491	1.523
K_1	0	0	-3.66537E + 01
A_1	0	0	-3.64926E - 06
B_1	0	0	-2.91705E - 09
C_1	0	0	-5.56478E - 12
D_1	0	0	-3.34229E - 14
K_2	0.9	-9.4457600E -01	-1.56764E - 01
A_2	0	7.1448974E - 6	-1.84671E - 06
B_2	0	1.0754103E - 8	-7.99216E - 09
C_2	0	0	-1.46071E - 11
D_2	0	0	6.64155E - 15

* Derived values

The calculated aberrations of the designs from von Rohr, Katz and Jeffree are given in Table 3.5. In each case the lens was assummed to be placed 27 mm from the centre of rotation of the eye, and TRACE 4 was used for calculation, with an incident ray bundle diameter of 3.0 mm. These are slightly different conditions to that given by Katz, who used a 3.0 mm pupil. It will be apparent that all three lenses are virtually distortion free, the maximum value being less than 1.0% for eye rotations up to 30 degrees from the axis. The oblique astigmatism is also well controlled, particularly in the Jeffree lens. Unfortunately, the Mean Oblique Error reaches much higher values in all the lenses, which would give rise to some blurring of vision for wide angles of view. Thus despite the use of a more sophisticated design, Katz was unable to improve on the optical performance of the earlier, single aspheric surfaces, designs. Where the Katz design does score is in lens appearance, as this design requires a rear surface power of only -5.10 D paraxially, whereas von Rohr and Katz required -18.71 and -13.23 D respectively, and hence the Katz design would be 'flatter' and better looking. But against this, the use of two aspheric surfaces would make the incorporation of a cylindrical correction difficult, and increase the cost of the finished product.

Table 3.5

Calculated Lens Aberrations

		von Rohr	Jeffree	Katz
5 Degrees				
Astigmatism	(D)	-0.003	+0.008	-0.104
M.O.E	(D)	-0.007	+0.009	-0.132
Distortion	(%)	+0.082	+0.106	-0.191
10 Degrees				
Astigmatism	(D)	-0.011	+0.137	-0.355
M.O.E	(D)	-0.084	-0.044	-0.466
Distortion	(%)	+0.231	+0.270	-0.506
15 Degrees				
Astigmatism	(D)	-0.055	-0.045	-0.620
M.O.E	(D)	-0.234	-0.187	-0.902
Distortion	(%)	+0.463	+0.448	-0.807
20 Degrees				
Astigmatism	(D)	-0.174	-0.210	-0.761
M.O.E	(D)	-0.488	-0.461	-1.320
Distortion	(%)	+0.718	+0.526	-0.833
25 Degrees				
Astigmatism	(D)	-0.437	-0.420	-0.731
M.O.E	(D)	-0.898	-0.849	-1.655
Distortion	(%)	+0.925	+0.430	-0.366
30 Degrees				
Astigmatism	(D)	-0.940	-0.413	-0.314
M.O.E	(D)	-1.537	-1.201	-1.767
Distortion	(%)	+0.971	+0.226	+0.833

CHAPTER 4

'Drop' type aspheric lenses

All the lenses manufactured commercially that we have so far considered have had one common purpose: to give as wide a field of good visual acuity as possible. The disadvantage of this type of approach is that although the distortion through the edge of the lens is reduced compared with a spherical surface lens, there is still an appreciable amount present. From Figure 2.5 it will be apparent that distortion free lenses can be manufactured, but that correction of oblique astigmatism and curvature has to be compromised, unless very steep curves are used.

4.1 The Welsh Four Drop

A lens design specifically aimed at reducing distortion was described by Welsh (1978). This design is completely different to those described so far in that the front surface of the lens is not given by a mathematical equation. The central 24 - 30mm (depending on the blank curve) is spherical, blending into an aspheric, peripheral curve. This peripheral area is apparently formed by blending a number of spherical zones of gradually decreasing power (Watkins, cited by Atchison and Smith, 1980). Thus it is not possible to quantify the surface topography in a detailed manner, and Welsh's patent gives very little quantitative information. The central spherical zone can have a front surface power of +12, +14 or +16 D, and the power at the edge of the lens drops to a value of +3.25 to +7.50 D. In particular, the +12

blank is claimed to have an edge power of +7.00 D. The ideal rate of drop is claimed by Welsh to be 1/3D per mm across the lens starting at the edge of the spherical zone. Lenses of this type were originally marketed as 'Welsh Four Drop' lenses, but recently the name has been changed to 'Armorlite Multi Drop'.

The information given in the Welsh patent is slightly contradicted by Renier (1977), who gives a diagram of the front surface curves of the Welsh lens (Figure 4.1). Welsh was aware of this diagram, as he gave some editorial comments to the text.

The main performance claim for this lens is that peripheral distortion is reduced while the wearer is fixating straight ahead, and that the peripheral scotoma is reduced by 50%. Hence the wearer will have to turn his head to view peripheral objects clearly, due to the reduced power through the edge of the lens.

4.2 Signet Hyperaspheric and Sola Hi-Drop

Other lenses have been designed with a similar philosophy. Examples of these are the Signet Hyperaspheric, Sola Hi Drop, and the designs of Frieder. In general these designs have criticised the Welsh lens for having a constant rate of drop for each of the lens blanks. At the present time there are three CR39 drop lenses available commercially in the UK, with drop details as follows:

Figure 4.1

Front surface power zones of the Welsh Four Drop lens, redrawn from Renier (1977)

Front surface power zones of'Welsh Four Drop'

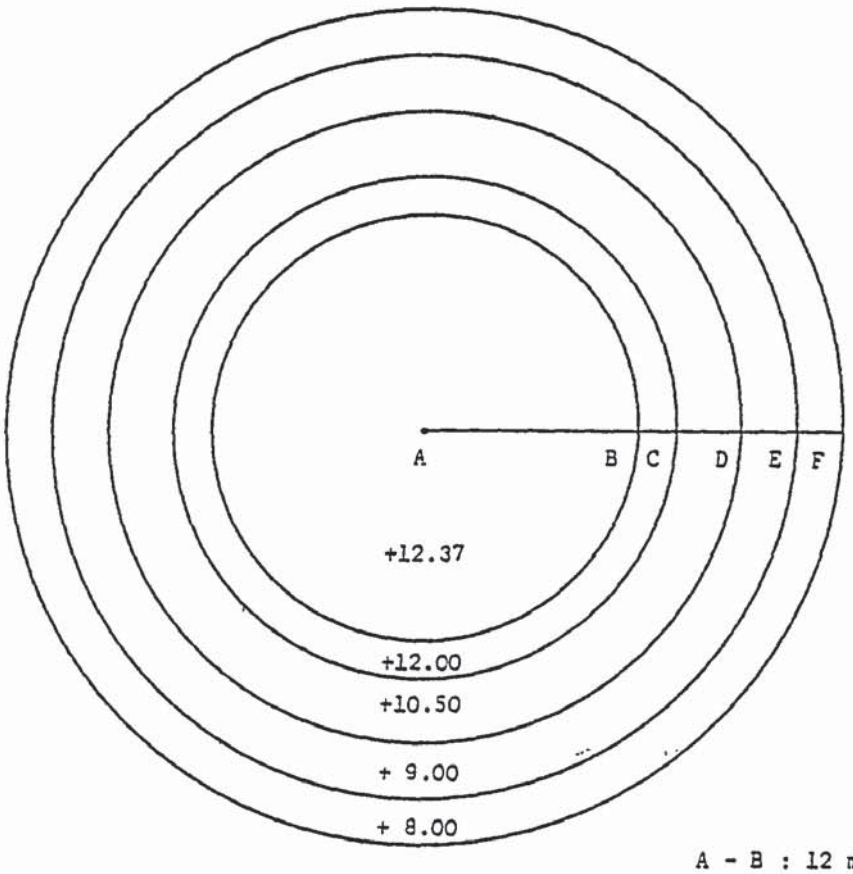

A - B : 12 mm
B - C : 3 mm
C - D : 5 mm
D - E : 5 mm
E - F : 4 mm

	Blank No.	Drop (D)
	12	4.00
Welsh Four Drop	14	4.00
	16	4.00
	12	2.50
Signet Hyperaspheric	13.50	3.25
	15	?
	12	2.50
	13.50	3.25
Sola Hi Drop	15	4.00
	16.50	?

This is the information given in the advertising literature by the manufacturers.

4.3 Frieder Lenses

Frieder (1980) describes two types of drop lens, the first is similar to the Welsh in having a central spherical zone, but the surrounding area has a greater rate of drop for the higher lens powers. This is shown in the following table:

Base Curve (D)	Drop (D/mm)	Central zone Diameter (mm)
+10.00	0.43	27
+12.00	0.45	26
+14.00	0.48	25
+16.00	0.51	23

Figure 4.2

Front surface power zones of one type of Frieder lens.

Redrawn from Frieder (1980)

Front surface power zones of Frieder lens

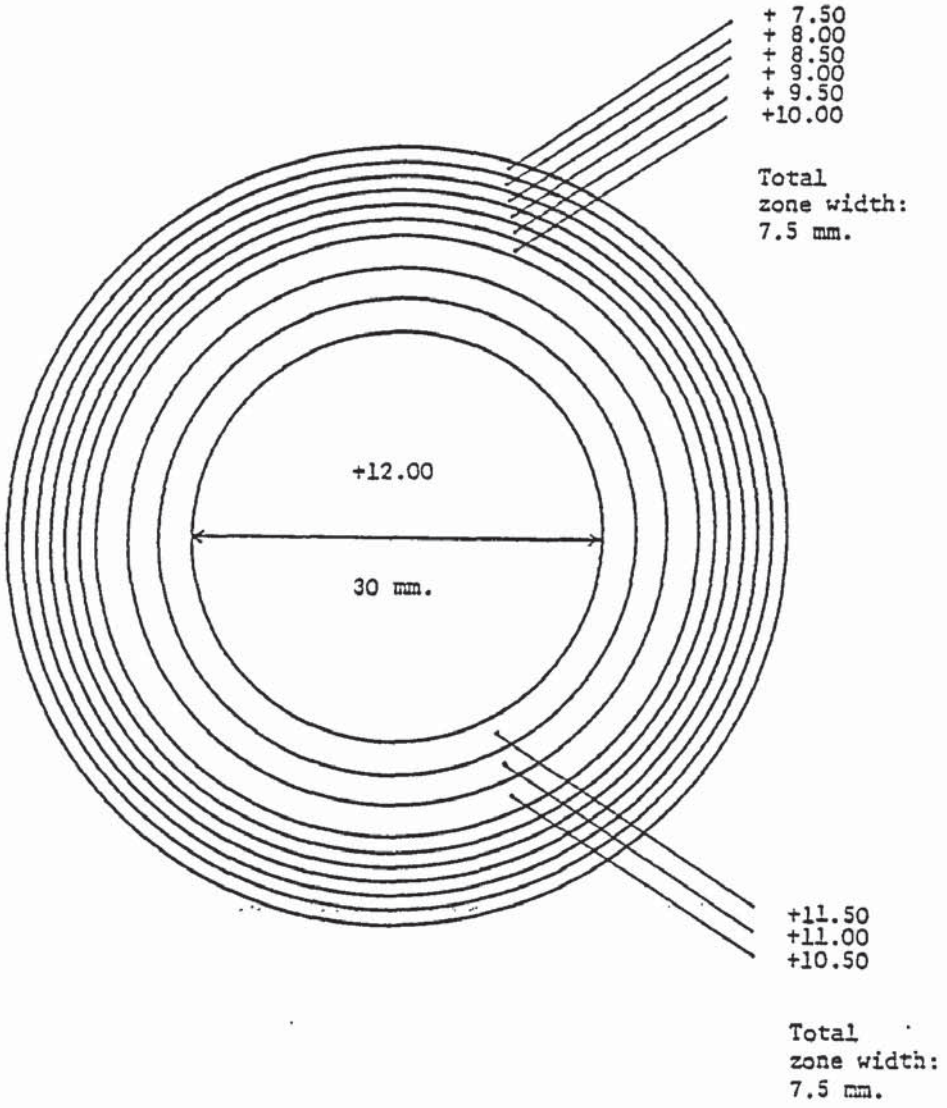

It is stated in the patent that this design of lens will also correct the tangential and sagittal powers at the edge of the lens.

The second design also has a spherical central zone, which is 30mm in diameter, but the aspheric area is subdivided into two different areas. Around the spherical zone is an intermediate are, 7.5mm across, made up of three concentric rings of power, each ½D less in power as you go towards the edge. This gives a drop rate of 0.2D/mm. Surrounding this intermediate zone is a peripheral area where the annular power drop is also at ½D per ring, but this time the width of each ring is only 1¼mm, hence the rate of drop is doubled to 0.4D/mm. This width of this area is again 7.5mm. Figure 4.2 is reproduced from the patent, and gives the powers for a +12.00D blank. Frieder describes the contour of the surface as 'roughly parabolic'.

Since there is little information as to the optical properties of drop lenses, reports of wearing trials are particularly useful for assessing their effectiveness. Michaels (1978) fitted 28 aphakics with four different types of spectacle lens in identical frames, then got them to wear the lenses for a week at a time in a random order. The lenses used were spherical, American Optical aspheric lenticular, Signet Hyperaspheric and Welsh Four Drop. As might be expected, the aspheric lenticular gave a wider field of good visual acuity than the other lenses, whereas the 'drop' lenses gave less ring scotoma, as measured on a bowl perimeter. At the end of the trial, the participants were asked which lens they preferred.

The answers were as follows:

No.	Percentage	Preferred lens
11	39.3	AO lenticular
8	28.6	Signet Hyperaspheric
7	25.0	Welsh Four Drop
2	7.1	None

The most clear cut result is that no individual preferred the spherical lens, and that the preference for the two types of 'drop' lenses was roughly equal. The population of aphakics used for the trial was very mixed, consisting of monocular and binocular patients of a wide variety of ages and length of time since operation. Michaels noted a tendency for the more recently operated to prefer the lenticular, whereas the long-standing aphakics preferred the 'drop' lenses.

In determining preference the patient would also consider other aspects besides the optics. For example, the lenticular would be by far the lightest lens, whereas the 'drop' lenses would have the best cosmetic appearance.

Thus 'drop' type lenses can be considered as attempts to produce aspheric lenses using spherical lens manufacturing techniques. The problem with objective assessment of their optics is that even if the precise surface curves are known which have been ground on to the lens, the effect of 'blending' is indeterminate.

It was this lack of precise information on these types of lenses that gave the stimulus to develop techniques for the measurement

of aspheric curves and off-axis aberrations, as described in later chapters.

CHAPTER 5

Blended aspheric lenticular lenses

An aspheric lenticular aphakic lens is thin, lightweight, but has an appearance that is not always acceptable. The usual aperture diameter is 40 - 42 mm, thus in a modern spectacle frame with a 50mm datum length of lens size, some of the surrounding carrier portion of the lens is going to be visible. To try and overcome this problem, a 45 x 40mm horizontal oval aperture lens has been developed, so that the aperture will practically fill the average frame. However, even small amounts of decentration will give a very poor cosmetic appearance. In Figure 5.1, the appearances of a round aperture lenticular (A), non-decentred oval aperture aspheric (B), and decentred oval (C) are compared. In the last case, the appearance will be worse due to the much thicker lens edge on the nasal side (N).

An obvious solution would be to blend the powered aperture into the surrounding carrier portion, thus making it less visible. This was done many years ago in the case of bifocal segments (Youngers seamless bifocal), in order to render the segment invisible. The use of blending appears to have been first considered by Davis (1959) for aphakic lenses. He rejected its use, however, in favour of a conventional lenticular for the American Optical design. At that time, frame sizes were much smaller than those currently fashionable. Hence the 40mm lenticular did not have too much cosmetic disadvantage.

Figure 5.1

Conventional lenticulars, showing (A) the poor appearance of a round aperture in a quadra lens shape, (B) the improved appearance from using an oval aperture aspheric lenticular, and (C) the large variation of edge thickness and poor appearance resulting from excessive decentration. (N indicates the nasal side)

Lenticulars

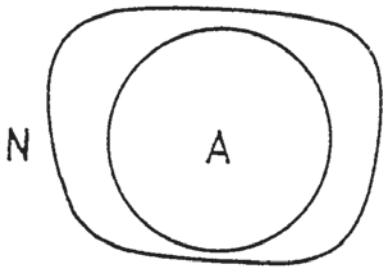

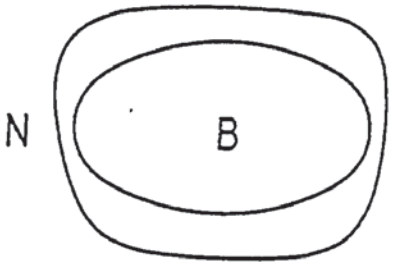

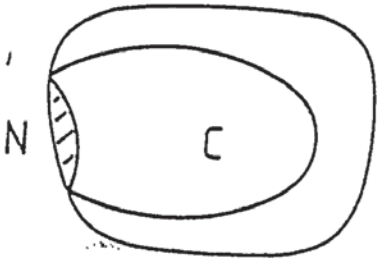

Figure 5.2

Blended aspheric lenticular, illustrating the area 'filled in' (dotted) to improve appearance compared with conventional lenticulars.

Blended Aspheric

Lenticular

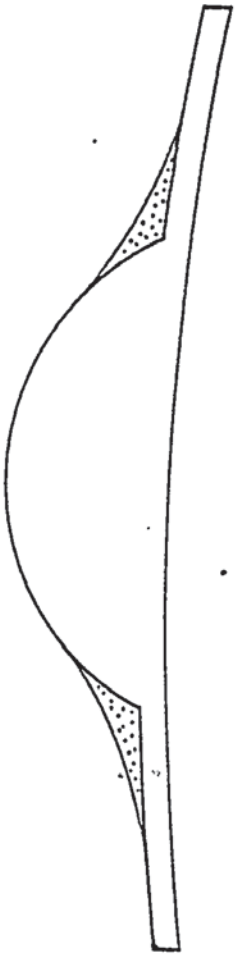

Figure 5.3

Parameters used in the calculation of aberrations of blended lenticulars.

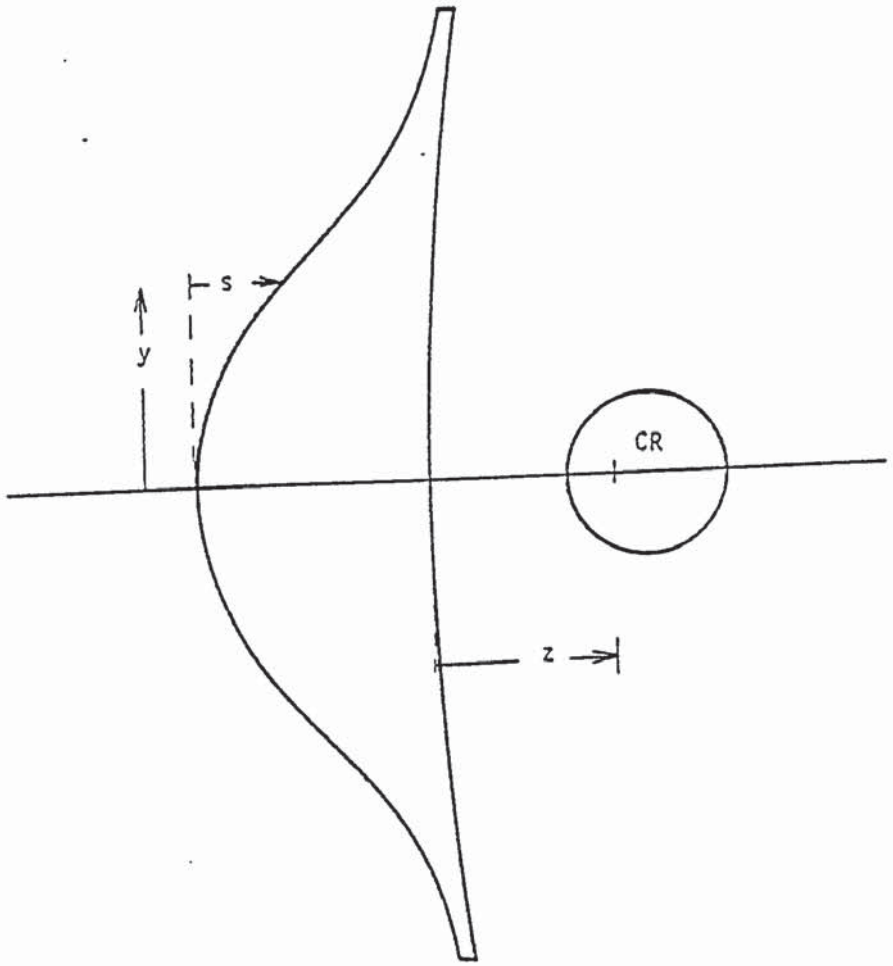
s
y
CR
z

Also, as Davis pointed out, because of the poor optics in the blending zone, a blended lenticular has to have a larger 'aperture' than a conventional lenticular in order to have a comparable field of view. This will make the blended lens thicker and heavier.

Despite the increased frame sizes now used, very few lenticulars have been developed with an aperture size of greater than 40mm. But several blended designs have been marketed.

5.1 American Optical 'Ful-Vue' lens

The American Optical lens has been described in detail, both in advertising literature (Whitney, 1980), and in a patent (Whitney, Reilly and Young, 1980). The front surface of the lens is stated to be a polynomial curve of the type:

$$s = \frac{Ry^2}{1+1(K+1)R^2y^2} + Ay^4 + By^6 + Cy^8 + Dy^{10} \qquad - V \quad (1)$$

where s and y are shown in Figure 5.3, R is the vertex curvature, and K,A,B,C,D are aspheric coefficients. The first term appears to contain a typographical error, as the more usual form of this equation is:

$$s = \frac{Ry^2}{1+(1-(K+1)R^2y^2)^{\frac{1}{2}}} + Ay^4 + By^6 + Cy^8 + Dy^{10} \qquad - V \quad (2)$$

A total of thirteen different base curves is used to cover the design prescription range. A table gives the aspheric coefficients for each base, and also a surfacing chart is given, assuming 1.530

Figure 5.4

Calculated power errors for American Optical Ful Vue, using TRACE 4, with aspheric coefficients derived from patent (Whitney, Reilly and Young, 1980), as shown in Table 5.1.

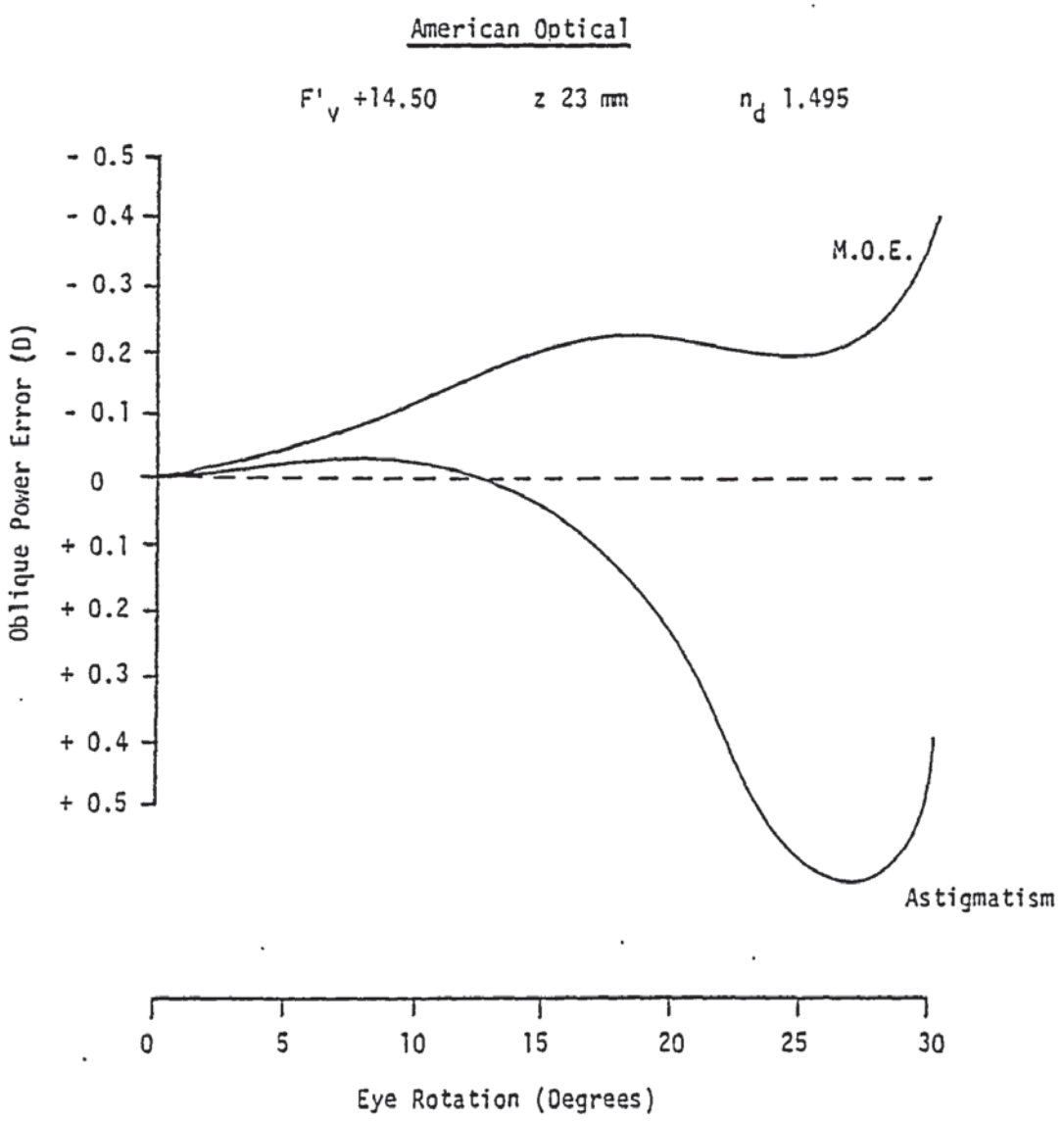
American Optical
F'v +14.50
z 23 mm
nd 1.495
- 0.5
- 0.4
- 0.3
- 0.2
- 0.1
0
+ 0.1
+ 0.2
+ 0.3
+ 0.4
+ 0.5
Oblique Power Error (D)
M.O.E.
Astigmatism
0
5
10
15
20
25
30
Eye Rotation (Degrees)

tools on a lens index of 1.495. The value of K is always -1, hence the above equation reduces to:

$$s = Ry^2/2 + Ay^4 + By^6 + Cy^8 + Dy^{10} \quad - \quad V(3)$$

This equation describes the front surface up to a diameter of 52 mm. It is stated that for larger diameters, the aspheric is blended into a spherical carrier curve. American Optical have produced a commercial lens to this design, the 'Ful-Vue', with a diameter of 66mm.

The optical design aim of this lens is given as a maximum of 0.25 D of Tangential power error for eye rotations up to 30 degrees from the axis, assuming a fitting distance (z) of 23 mm. The optical properties of an arbitrary lens from the series are shown in Figure 5.4, as derived from a theoretical ray trace. This agrees with the figures given in the patent, and shows that the oblique astigmatism does not exceed 0.63 D. However, if a longer fitting distance is used, then the picture changes for wide angles of view. In Figure 5.5 the ray trace has been repeated, except that a value for the fitting distance of 27 mm has been substituted. Note that at angles greater than 25 degrees the oblique astigmatism changes rapidly, going off the scale to a value of -1.60 D at 30 degrees. Hence this lens has a well defined central zone where the power is stabilised, outside of which the oblique astigmatism increases rapidly due to a sharp fall in Tangential power.

Figure 5.5

Calculated power errors for American Optical Ful-Vue, using TRACE 4, with aspheric coefficients derived from patent (Whitney, Reilly and Young, 1980), as shown in Table 5.1. Note that these conditions are identical to Figure 5.4 except that 'z' has been increased to 27 mm.

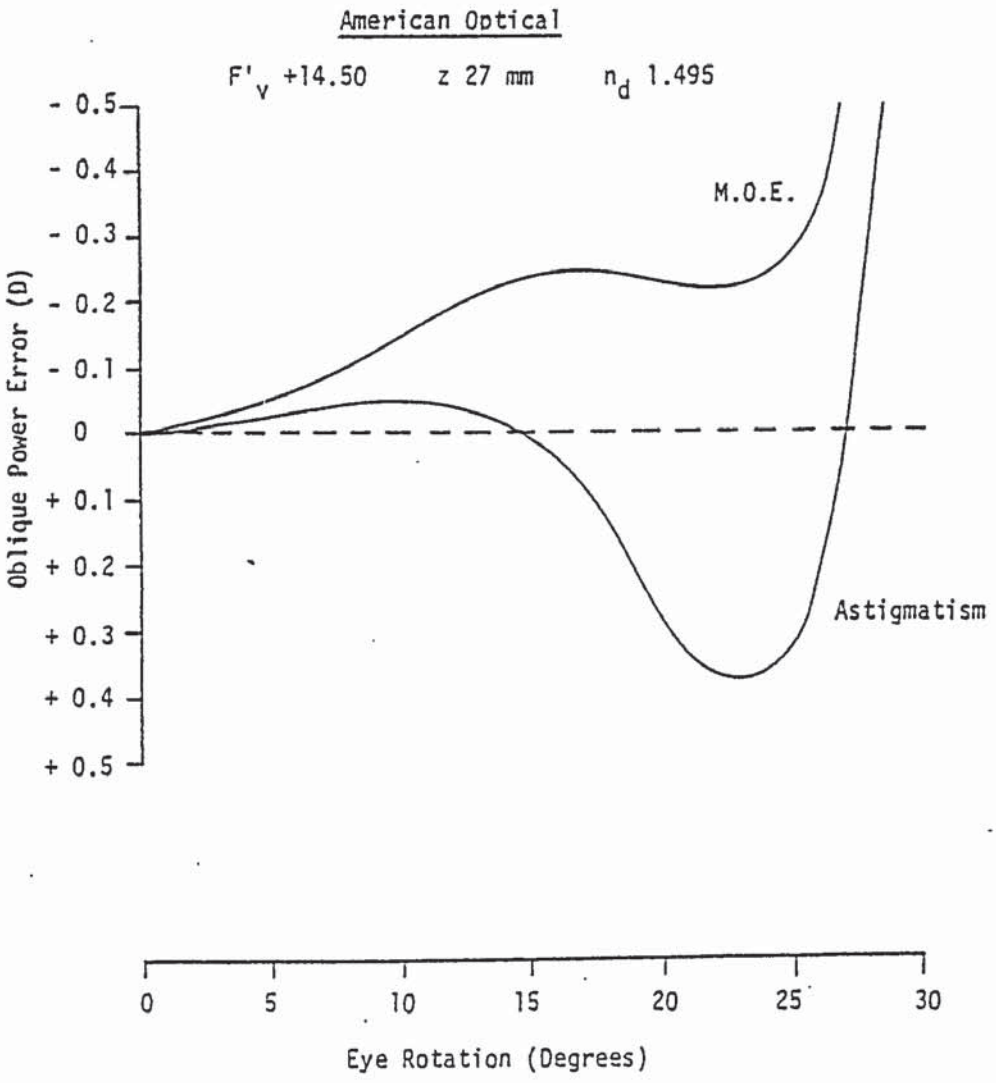
American Optical
F'v +14.50
z 27 mm
nd 1.495
- 0.5
- 0.4
- 0.3
- 0.2
- 0.1
0
+ 0.1
+ 0.2
+ 0.3
+ 0.4
+ 0.5
Oblique Power Error (D)
M.O.E.
Astigmatism
0
5
10
15
20
25
30
Eye Rotation (Degrees)

Table 5.1

Table of Lens Parameters

Lens Type	American Optical	Rodenstock (Type 1)	Rodenstock (Type 2)
Front Surface			
Vertex radius (mm)	34.057	34.269	34.269
K_1	- 1.00	- 0.398	-0.495
A_1	1.28124E-6	7E-6	9.6E-6
B_1	1.82120E-9	0	2.6E-7
C_1	8.38095E-12	0	1E-10
D_1	- 2.38066E-14	0	1E-12
Thickness (mm)	10.2	11.0	11.0
$F_2(D)$	-1.634	-1.768	-1.768

Back Vertex Power (F'_v) +14.50 DS

5.2 Rodenstock Lens

This is a well documented design (Guilino, Barth and Koeppen, 1983), with an aspheric front surface of the form:

$$s = \frac{Ry^2}{1+(1-(K+1)R^2y^2)^{\frac{1}{2}}} + Ay^3 + By^4 + Cy^5 + Dy^6 - V \quad (4)$$

This patent is unusual in that it supplies two different tables of aspheric coefficients, in order to make lenses of two different types of design. The first type is based on the criterion of optimum visual acuity, expressed in the patent as:

3 x visual acuity at 10 degrees + visual acuity at 25 degrees = maximum

The second type is based on the traditional concept of optimising power errors, such that:

Mean oblique error at 25 degrees + oblique astigmatism at 25 degrees = minimum

It is claimed that lenses up to + 22.00 D can be manufactured from the series of base curves given in the patent. It is interesting to note that although there are nine blanks given for each type of design, these do not cover the same range of vertex curvatures. For example the shortest vertex radius for the first type of lens is 31.53 mm, whereas it is 27.104 mm for the second. However, some vertex curvatures are duplicated in the two blank series, and in addition, some vertex curvatures are duplicated in the same series. Thus for a vertex radius of 44.76 mm, four different front surface designs are patented. It is stated that the purpose of this is to retain similar optical properties for

a range of rear surface curves.

The aberrations associated with the two designs are shown in Figures 5.6 and 5.7 for a power of + 14.50 DS. As a surfacing chart is not given in the patent, the values of lens thickness and vertex curvature were chosen from graphs given in a description of the commercial product associated with this patent, the 'Perfastar' lens (Koeppen and Barth, 1982). The differences between the two lens design concepts would appear to be small, and one wonders if they would be noticed by a wearer.

The aspheric curve described above is used for the central 42 mm of the lens only. Beyond this, the lens has a marked reduction in power, up to a diameter of 66 mm.

These two patents for blended lenticular lenses both describe designs that are trying to achieve the same purpose - provide a high plus spectacle lens with a large uncut diameter, good cosmetic appearance, low weight and acceptable optical performance.

Both patents assume that the lenses will be moulded from plastic material, and it is this capability of moulding complex curves that has made possible the use of lens designs which would be prohibitively expensive in glass material.

In comparing the optical properties, it will be noted that the American Optical design shows more oblique astigmatism and power error for a given fitting position. However, as shown in Figure 5.8 it does have less distortion in the central area than the

Figure 5.6

Calculated power errors of Rodenstock Perfastar, using a modified version of TRACE 4, the aspheric coefficients being derived from Guilino, Barth and Koeppen (1983) and shown in Table 5.1. Type 1 lens.

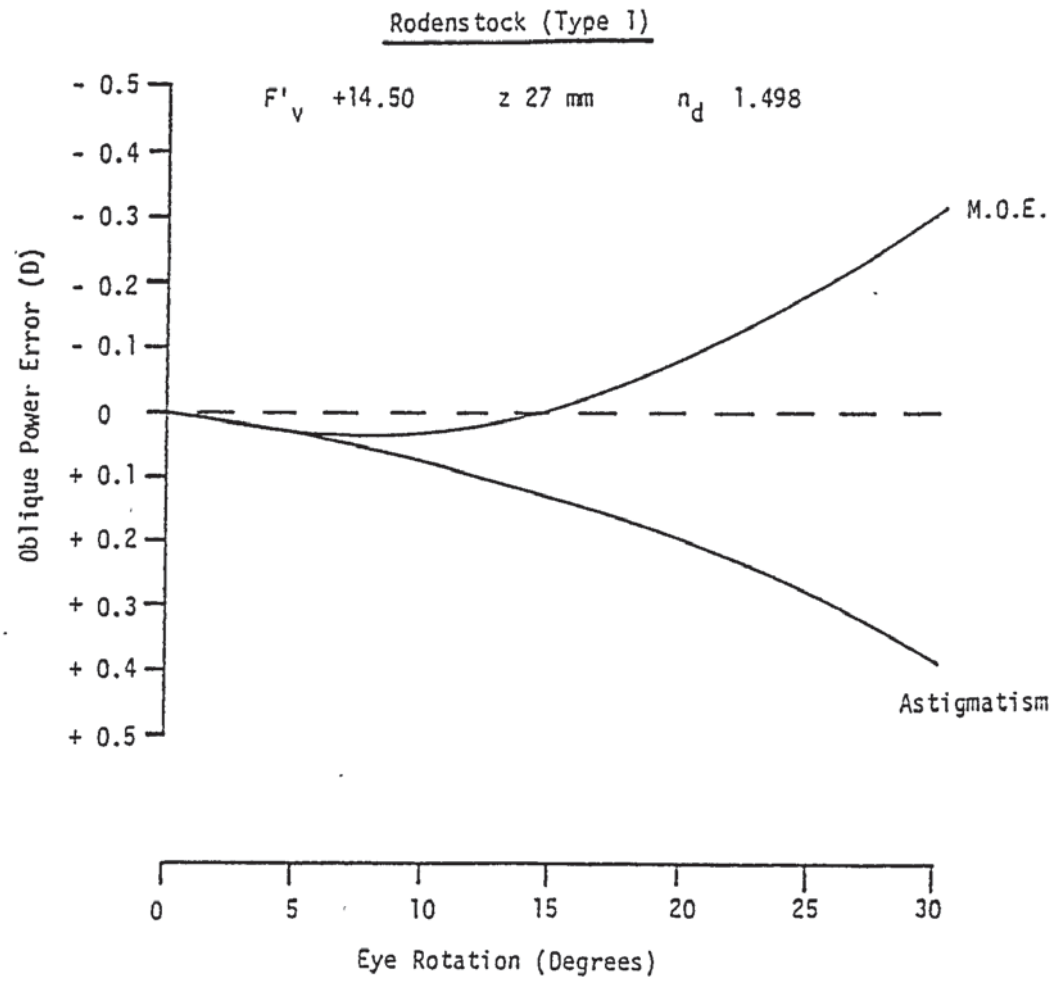
Rodenstock (Type 1)
F'v +14.50
z 27 mm
nd 1.498
M.O.E.
Astigmatism
Oblique Power Error (D)
- 0.5
- 0.4
- 0.3
- 0.2
- 0.1
0
+ 0.1
+ 0.2
+ 0.3
+ 0.4
+ 0.5
0
5
10
15
20
25
30
Eye Rotation (Degrees)

Figure 5.7

Calculated power errors of Rodenstock Perfastar, using a modified version of TRACE 4, the aspheric coefficients being derived from Guilino, Barth and Koeppen (1983) and shown in Table 5.1. Type 2 lens.

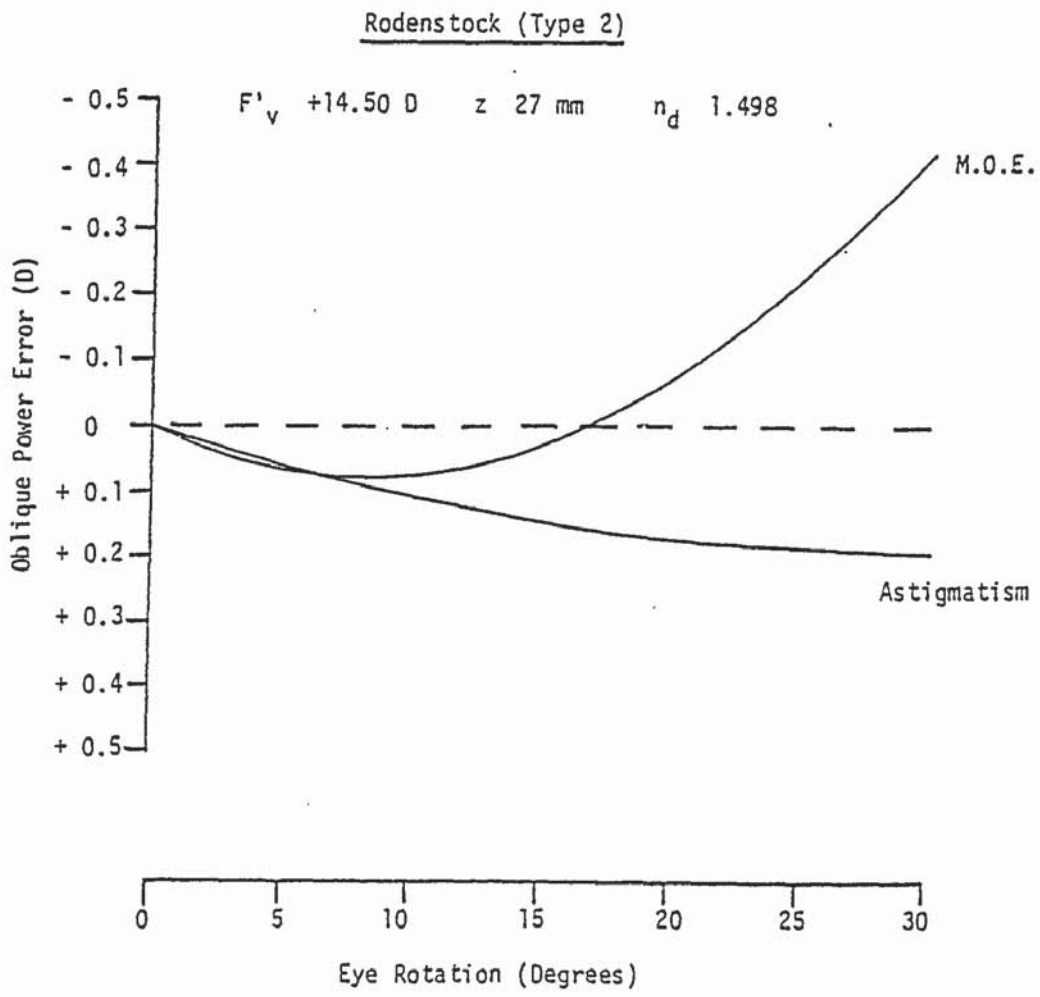
Rodenstock (Type 2)
F'v +14.50 D z 27 mm nd 1.498
M.O.E.
Astigmatism
Oblique Power Error (D)
- 0.5
- 0.4
- 0.3
- 0.2
- 0.1
0
+ 0.1
+ 0.2
+ 0.3
+ 0.4
+ 0.5
0
5
10
15
20
25
30
Eye Rotation (Degrees)

Figure 5.8

Calculated distortion for Rodenstock Perfastar (Type 2) and American Optical Ful-Vue, using aspheric coefficients shown in Table 5.1.

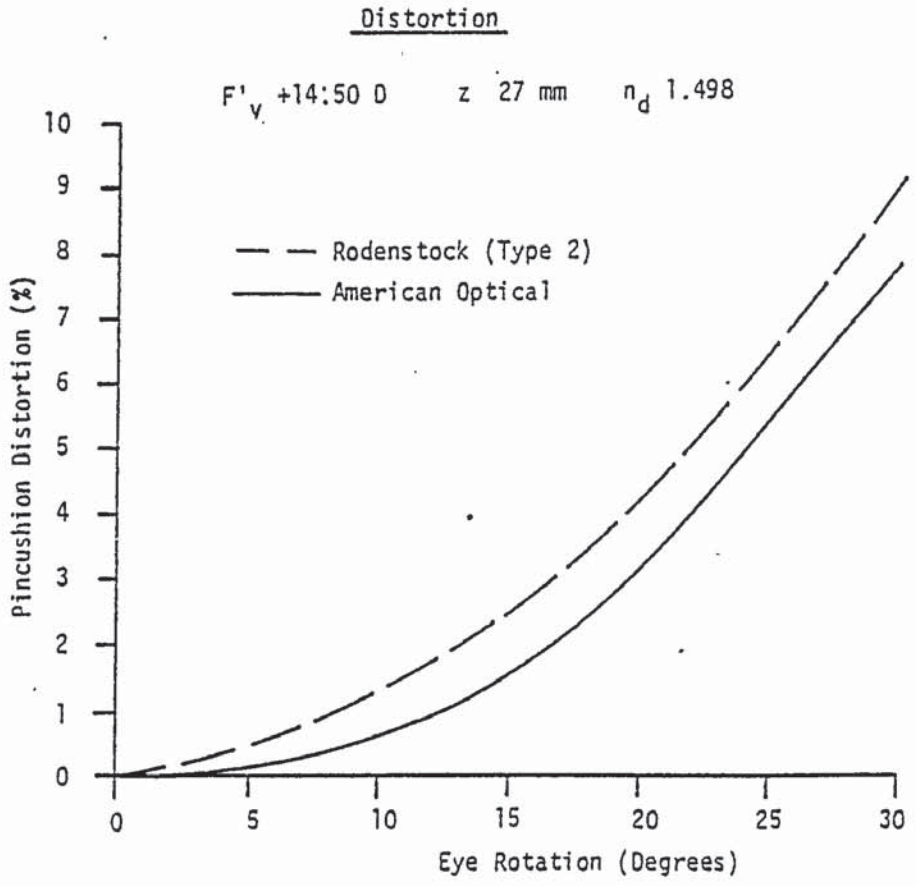
Distortion
F'v +14.50 D
z 27 mm
nd 1.498
Rodenstock (Type 2)
American Optical
Pincushion Distortion (%)
0
1
2
3
4
5
6
7
8
9
10
0
5
10
15
20
25
30
Eye Rotation (Degrees)

Rodenstock designs, due to the more rapid rate of power drop. All ophthalmic lens designs are compromises, and these two patents have taken slightly different approaches to the same problem.

American Optical repeated the trial of Michaels (1978), but with fewer patients, and with the Ful - Vue lens substituted for the aspheric lenticular (American Optical 1980). This showed the Ful-Vue lens superior in all respects to the Signet Hyperaspheric and the Welsh Four Drop. One is naturally, however, slightly suspicious of the objectivity of such an investigation.

5.3 Essilor Omega

By contrast, the information on the 'Omega' is somewhat limited, being confined to a technical brochure (Essilor 1981). The lens appears to be of a fairly simple design. It is claimed that the central 43 mm is ellipsoidal, with the same characteristics as the Essilor aspheric lenticular. The overall diameter is 67 mm, and the lens has the typical blended aspheric appearance of a concave tangential curve in the mid - periphery.

It is claimed that the lens has a clear field of vision of 'about 80 degrees'. It is also claimed that the ring scotoma effect is reduced because of the rapid decrease in power towards the edge of the lens.

CHAPTER 6

The measurement of surface curves

Having discussed the basic designs of aspheric spectacle lenses for aphakia, it is reasonable to ask whether these different surface curves can be measured on the lens itself. If this can be done accurately, an unknown lens can be classified into its basic type, and also, the accuracy of manufacture of a known type of lens can be assessed.

The problems in measurement are that it only takes a very small change in surface curve to cause a large change in optical performance. This is illustrated quite well if we consider a surface with a radius on axis of 30.2799 mm. At a distance of 20mm from the axis of symmetry, a spherical curve would have a sag of 7.55mm. The equivalent parabola would have a sag of 6.61mm. Many lenses are much less aspheric than this, so that the difference from a spherical lens will be even less.

It is quite simple to detect an aspheric curve on a qualitative basis, by using a Geneva lens measure. Figure 6.1 illustrates the use of such an instrument for this purpose. As the lens measure is slid along the surface of the lens, the power will reduce from the centre to the edge. A spherical lens surface would give a constant reading.

To obtain a quantitative assessment of a given surface, ideally one would measure the x-y surface co-ordinates, as this information can be easily correlated with the equation describing the surface.

Figure 6.1

Schematic example of Geneva lens measure being used to measure variation in power along a tangential section of an aspheric surface. A spherical surface would give a constant reading.

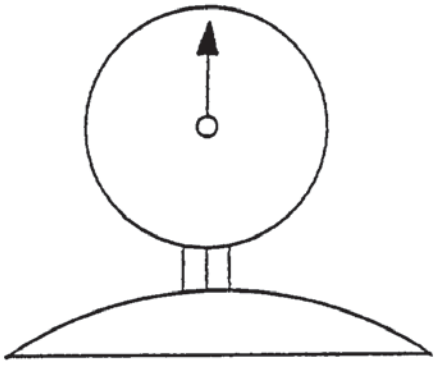

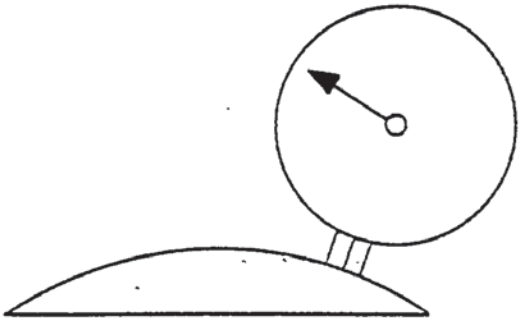

Various methods for doing this were considered, namely profile projection, surface reflection, and direct measurement by travelling microscope.

The attraction of profile projection is that a magnified image of a lens profile is produced, which should make for ease of accurate measurement. The main problem would appear to be that in order to obtain a profile through the axis of symmetry, the lens would have to be illuminated by a collimated light beam. This is not a problem with small lenses, and this method has been used quite successfully with contact lenses, but with an uncut spectacle lens, where the diameter is often in the order of 60-65mm, large diameter collimating lenses would be required.

The second method considered was a system whereby the angle of reflection of a small diameter beam of light, parallel to the axis of symmetry of the lens, was measured. This could then be used to find the surface co-ordinates, assuming that the distance of the beam of light from the optical centre of the lens was accurately known. Alternatively, a photograph could be taken of the reflections of a number of concentric illuminated rings. Measurements of the ratio of magnification of the rings would give an indication of lens profile.

The method that was finally used was the direct measurement of the lens surface with a travelling microscope, as this seemed to be the most straightforward approach. Because none of the commercially produced instruments available seemed suitable, an instrument was built especially for this purpose. The problem

with the commercial instruments was that the microscope could not traverse across a section through the optical centre of a large diameter lens.

A schematic diagram of the instrument is shown in Figure 6.2. The lens to be measured (1) rests on a transparent acrylic ('Perspex' - ICI Ltd.) baseplate. The microscope (2) is moved across the lens by turning the knob controlling a screwed rod (5). The lateral displacement ('y') is measured on a micrometer dial gauge (4), calibrated in 0.01mm steps. The sag of the lens surface ('x') is measured by focussing the microscope on the lens surface by moving it in the vertical direction. This movement is sensed by an electronic distance measuring unit (3), manufactured by ASL Ltd. The displacement is displayed as a voltage, which is linearly related to movement. Using suitable electronics, the manufacturers claim a resolution of 0.001mm. The lens is illuminated from beneath (6) in order to make the surface of the lens being measured more visible.

Originally, the apparatus did not use a microscope, but allowed the probe (3) to rest directly on the lens surface. This technique was abandoned as firm clamping of the lens was required, which was difficult to achieve without distorting or damaging the lens surface. In addition, the results were not repeatable to any useful degree of accuracy.

Figure 6.2

Section through travelling microscope built for the measurement of front surface aspheric curves of spectacle lenses.

Travelling Microscope

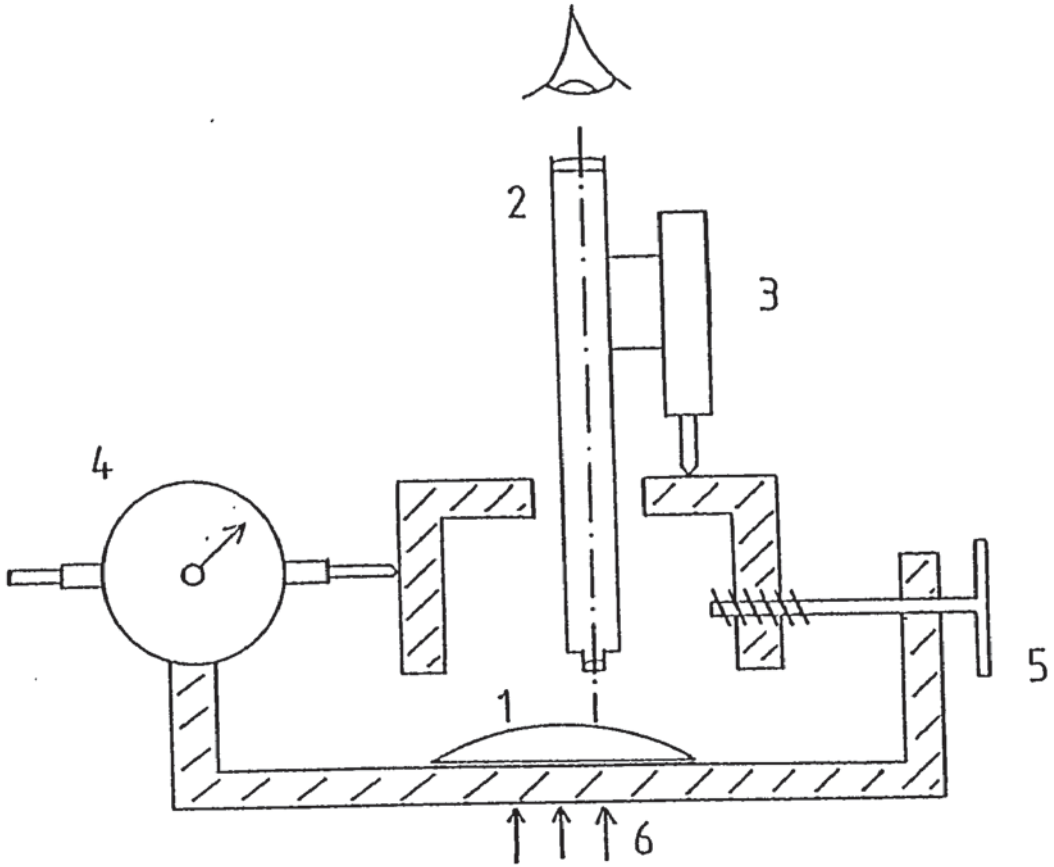

6.1 Procedure for surface measurement

1. Measure BVP with focimeter, centre thickness with micrometer dial guage, and rear surface sag with optical spherometer. Mark optical centre of the lens.

2. Make front surface of the lens semi-opaque with spirit-soluble felt tip marker.

3. Focus microscope on base plate, take five readings of initial voltage (V1). Then take four readings of voltage V2 when microscope is focused on calibration object of known thickness (Figure 6.3).

4. Place lens, front surface uppermost on baseplate, and locate the optical centre mark. This becomes the zero mark for the 'y' axis dial gauge. Read off V5. It will be assumed that for this, and all subsequent readings that four measurements are taken for later averaging purposes.

5. Take reading V3 and V4 at a distance of 15 mm. on either side of the optical centre. This is to assess if the lens is level.

6. Take series of voltage readings for various values of 'y'. Because of limitations in micrometer travel this is only carried out in one direction from the optical centre towards the edge of the lens.

Figure 6.3

Schematic diagram illustrating the measurements taken with the travelling microscope for calibration, and also to correct any tilt in the front surface.

Calibration of travelling microscope

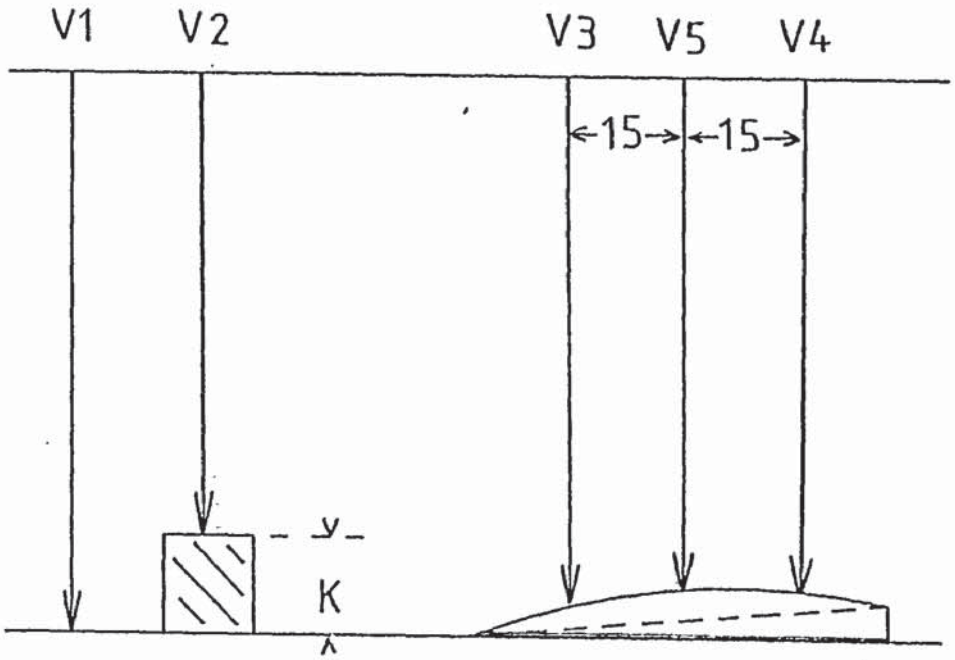

A computer program was used to interpret the data. The function of this program was to:

a) Averge the voltage readings at each point.

b) Calculate the paraxial front surface radius of the lens from the values of BVP, centre thickness, and rear surface power measured in 1.

c) Using the voltages V1-V5, calibrate the instrument, convert the voltage readings to millimetres, and apply a tilt correction factor, using the expression:

$$x_{(mm)} = (x_{(V)} - V5+(V3-V4)/30 \cdot y_{(mm)}) \cdot K/(V1-V2) \quad --VI(1)$$

where K is the thickness of the calibration object, in millimetres.

d) Compare the 'x' values for known increments of 'y' with a series of known conics, from p = +2 to -2. Find the best fit conic by finding the minimum sum of squares error score.

e) Plot results graphically.

f) List 'x' and 'y' co-ordinates, in millimetres.

The instrument was constructed predominantly from acrylic sheet, of half inch thickness. It was considered that this should provide adequate rigidity. However, with experience, it was found that excessive heat from the lamp (6) could warp the base plate. Thus precautions were taken to ensure that overheating did not occur.

The output from the electronic distance measuring unit (3) was taken to a signal conditioner, supplied with a stabilised voltage of $\pm$ 15 volts. This converted the variable capacitance of the transducer into a variable voltage, which was displayed on a digital voltmeter. This latter instrument had a built-in calibration source so that the calibration could be frequently checked.

6.2 Accuracy of measurement

The verification of accuracy was based on the fact that measurement and analysis of a spherical curve should give a spherical result. It is probably that any spherical refracting surface could be considered as aspheric if it was measured accurately enough. Here, the criteria was that a spherical surface of a well manufactured spectacle lens should be adequately spherical, particularly in glass. Thus a +6.00DS crown glass Zeiss Punktal lens was used for calibration.

Four separate sets of measurements were taken. The sag 'x' was measured at 10,15 and 20 mm from the optical centre of the lens. The 'x' co-ordinates for given 'y' values are shown in Table 6.1, together with the mean p_1 values, 0.95, would indicate an error in measurement of 0.01 mm at y = 20 mm. This assumes that the front surface of this lens is truly spherical, with p_1 of 1.00.

Also of interest is the variation in 'x' measurement between experiments. The values for the surface co-ordinates are used in determining the actual polynomial curve of some lenses, to

Table 6.1

Travelling microscope accuracy assessment

Experiment	y = 10	y = 15	y = 20	Mean p_1
A	1.050	2.356	4.220	1.04
B	1.052	2.345	4.189	0.86
C	1.027	2.348	4.203	0.91
D	1.053	2.352	4.213	1.00
Mean values:	1.046	2.350	4.206	0.95
		x values		

Zeiss Punktal	BVP	+ 6.06 DS
	F2	- 5.02 D
	t	6.30 mm
	n_d	1.523

check on the design reproduction. It is apparent that the variation in measurement is different for the values of 'y' indicated. For example, at y = 5 mm, the variation in 'x' about the mean is +0.007/ -0.019 mm, whereas at y = 15mm, the variation is +0.006/ -0.005 mm. This could have been caused by non-linearity in the 'y' direction dial gauge.

In retrospect it would probably have been possible to obtain greater accuracy by having ring gauges for determining 'y', with a known, fixed diameter. These could have been bored centrally to take a depth measuring device. Thus the accuracy would not have depended on two gauges, only one being used. However, this arrangement would have made the measurement of lenses with a front surface bifocal segment difficult.

CHAPTER 7

Measurement of oblique astigmatism with a modified focimeter

As a result of the importance placed on the reduction of oblique astigmatism (and curvature) by lens designers, it would obviously be useful if the oblique power errors could be readily measured in actual lenses. Instruments for measuring lens power (focimeters) are readily available, so it is an obvious step to modify such an instrument to measure oblique powers rather than paraxial powers as normal. This was done by Knoll (1953), who used the instrument to measure the performance of various designs of low and medium power lenses under various conditions. A similar, but more sophisticated, investigation was carried out by Morgan (1961). Washer (1955) produced a very sophisticated instrument at the U.S. National Bureau of Standards, to check on the performance of mass produced best form lenses. This instrument was not a modified focimeter, but was built from scratch to simulate the human eye/spectacle lens arrangement as closely as possible.

7.1 Apparatus

The apparatus used in this thesis is shown in Figure 7.1. The basis of the instrument is a Nikon focimeter. This instrument was chosen because, besides being a good quality instrument, it had an easily removable lens support, which made it ideal for modification.

The spectacle lens (1) is mounted on the focimeter (2) so that it can be rotated about a point on the axis of the instrument (4). The original position of the lens rest is at (5), so that when the angle of rotation, U'_2, is zero, the instrument reads the same vertex power as it did before modification. The distance from (4) to (5) is fixed at 27mm, a commonly assumed distance, from lens to centre of rotation of the eye, in ray tracing calculations. A Risley rotary prism (3) is used to neutralise the large amounts of prism induced by viewing through the edge of a high positive power lens. This could provide prism power of up to 30 Prism Dioptres. The purpose of having a removable lens support in the original design of the Nikon focimeter was to enable different stop diameters to be easily used on the instrument. Because the effect of the modifications was to give a very large aperture to the system, an aperture could be introduced at (4). Diameters of 2 and 5 mm were used. A protractor enabled the desired value of angle U'_2 to be set. A similar modification to a Nikon projection focimeter has been made by Simonet, Papineau and Gordon (1983). The modification described here was designed to be a minimal conversion of the instrument, with the option of returning it to its original form, and one obvious drawback of such a simple conversion is the use of the rotary prism. Morgan (1961) used a better system where the focimeter telescope was articulated so that it could be angled in the vertical direction, thus removing the requirement to use the prism.

The measurement procedure consists of first aligning the lens on the holder so that when U'_2 is zero, the optical centre of the lens is aligned with the axis of the instrument. Then the lens

Figure 7.1

Modifications to Nikon eyepiece focimeter to enable it to read oblique powers.

Modified Focimeter

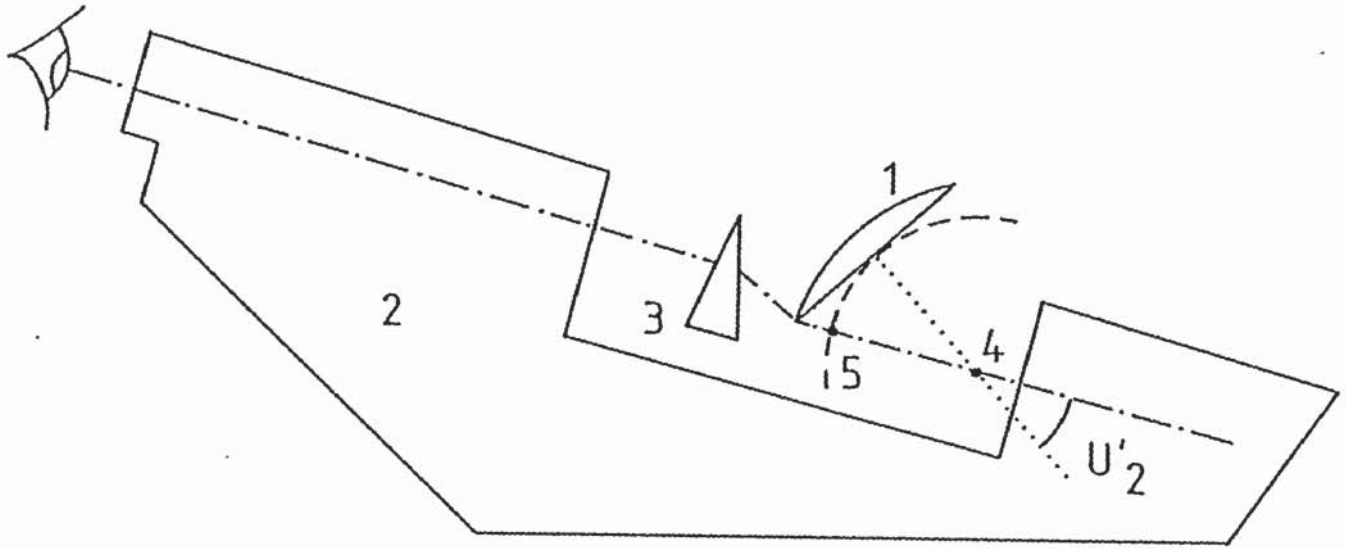

is set at predetermined values of U'_2 (normally in five degree intervals), and the oblique power is measured. The tangential power is measured by focusing on the horizontal focimeter image, and the sagittal power by focusing on the vertical image. The power of the rotary prism is altered to bring the target to the centre of the telescope field.

7.2 Accuracy of measurement

In order to assess this method of lens measurement, the same Zeiss 'Punktal' lens was used as described in Chapter 6. Four sets of measurements of oblique power errors were taken, and the results are shown in the accompanying table. The maximum variation in measurement about the mean values is 0.08 D. This would seem to be a satisfactory value. However, the powers in the tangential and sagittal meridians proved quite easy to measure with this particular lens. With the aphakic lenses of greater power, the measurements were not so easy to take.

The measurements taken have also to relate to the degree of asphericity of the front surface of the lens. This was assessed by comparing the measurements with the theoretically calculated values of oblique power errors that would arise from the use of a variety of aspheric front surfaces on the lens. Hence in Figure 7.2 the Mean Oblique Power measurements of the 'Punktal' lens are shown compared with expected values of front surface asphericity. As might be expected, the measured values are virtually identical with the theoretical value of $p_1 = 1$, indicating a spherical surface. This is a fairly crude analysis, and it is sometimes

Table 7.1

Sagittal and Tangential power measurements

Zeiss 'Punktal' + 6.06 DS

	5°	10°	15°	20°	25°	30°	Eye Rotation
A	+6.06	+6.00	+6.00	+5.90	+5.87	+5.80	
B	+6.06	+6.06	+5.90	+5.87	+5.87	+5.80	
C	+6.06	+6.06	+5.90	+5.87	+5.87	+5.80	Sagittal (D)
D	+6.06	+5.95	+5.87	+5.87	+5.87	+5.80	
	+6.06	+6.02	+5.92	+5.88	+5.87	+5.80	Mean

A	+6.06	+6.00	+6.12	+6.12	+5.00	+6.00	
B	+6.06	+6.06	+6.06	+6.06	+6.00	+5.90	
C	+6.06	+6.06	+6.06	+6.06	+6.00	+5.90	Tangential (D)
D	+6.06	+6.03	+6.03	+6.03	+6.01	+6.00	
	+6.06	+6.05	+6.07	+6.07	+6.00	+5.95	Mean
	+6.06	+6.03	+6.00	+5.98	+5.94	+5.88	Mean Oblique Power (D)

Figure 7.2

Calibration of modified focimeter, using +6.06 DS Zeiss Punktal glass lens with spherical surfaces. Ray trace comparison with lenses having varying conic value (p_1) for front surface.

Zeiss Punktal

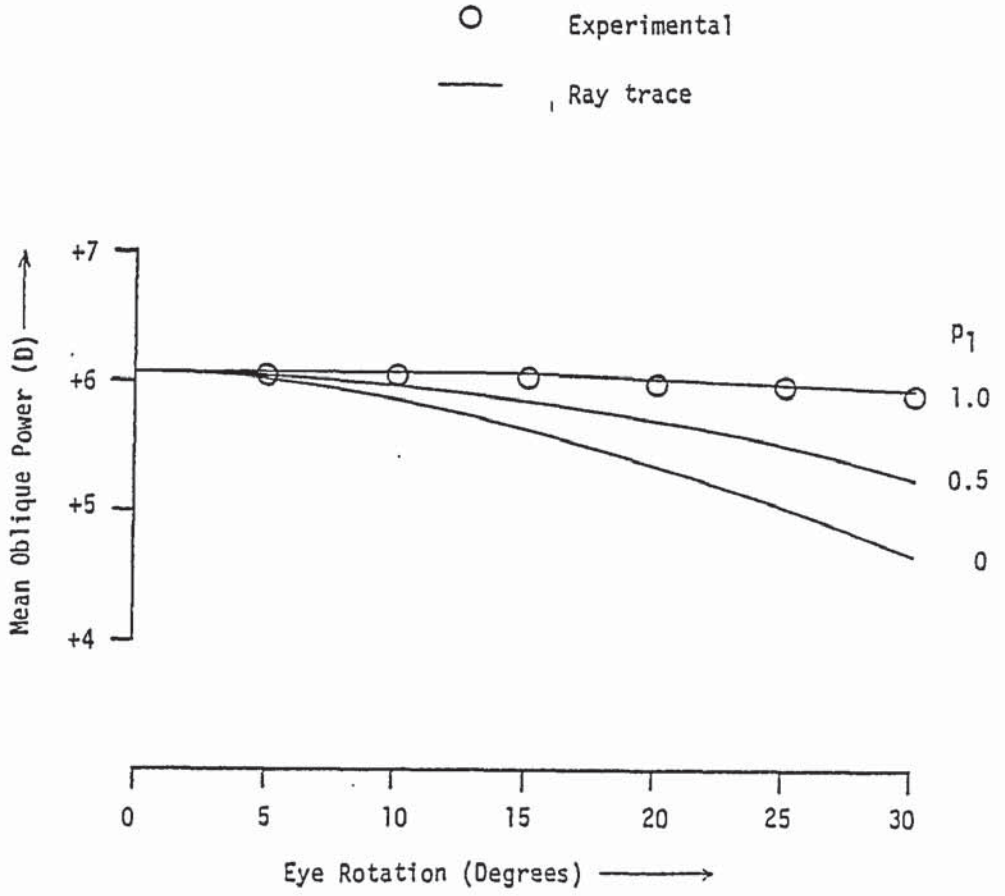

Figure 7.3

Calibration of modified focimeter, using +6.06 DS Zeiss Punktal lens with spherical surfaces. Practical measurements compared with ray trace.

Oblique Astigmatism, Zeiss Punktal, +6.06DS

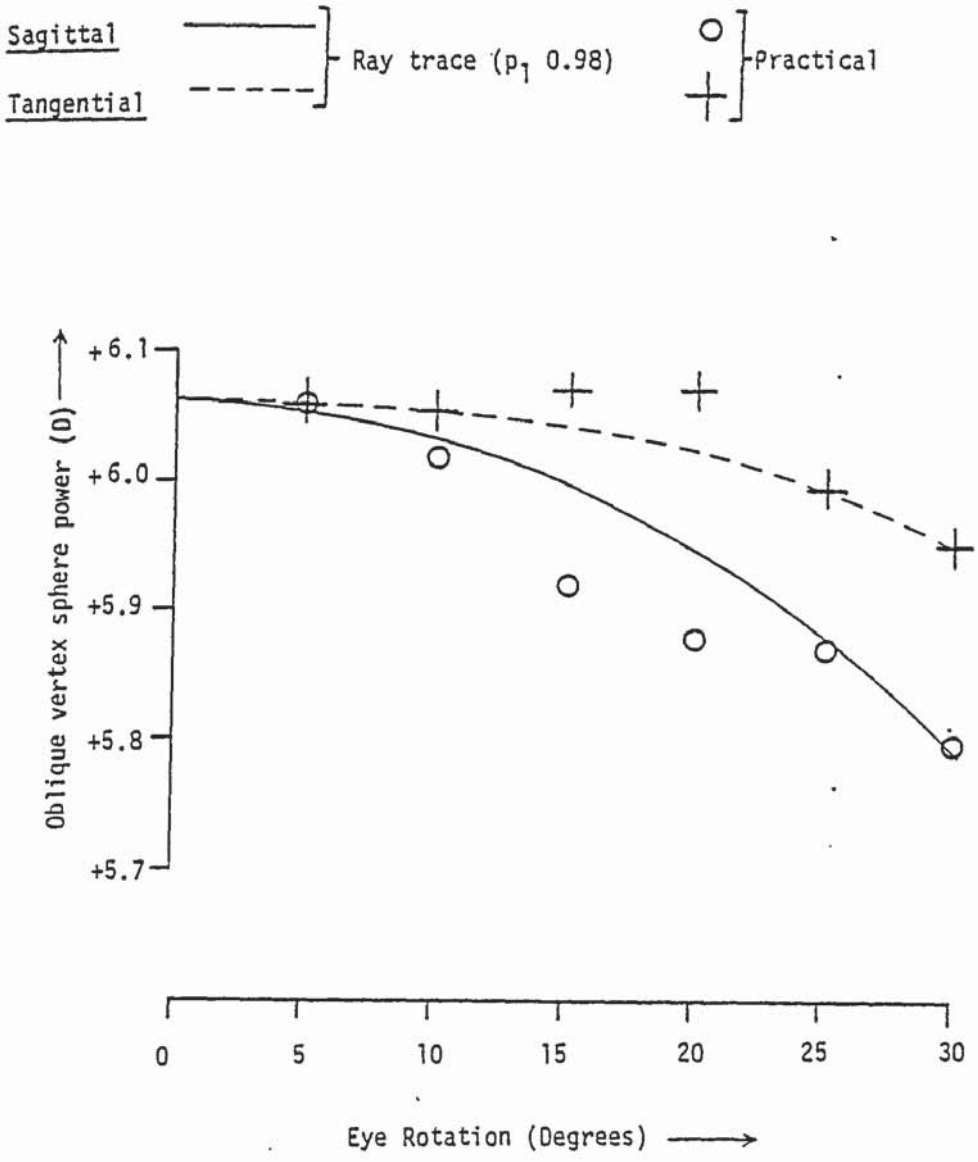

better to plot the individual sagittal and tangential measurements against the theoretical values. This has been done in Figure 7.3, with the lens power plotted on a more sensitive scale. This shows that $P_1 = 0.98$ is a reasonable approximation to the front surface.

CHAPTER 8

Measurement of optical distortion

Some modern lenses for the correction of aphakia, such as the 'drop' type lenses, make specific claims as regards a reduction in distortion. Unfortunately, numerical values are not given, so that a comparison cannot be made with other lenses. In general, numerical claims are not made by manufacturers or designers about any aspheric lens. This is probably due to a lack of agreement on the method of calculating distortion on a theoretical basis in the spectacle lenses. The main argument is on the position of the entrance pupil - should it be at the pupil plane of the eye (Fry 1977, Jalie 1972) or at the centre of rotation? This will obviously make a difference when considering distortion in the rotating eye compared with the fixed eye situation. In this discussion, the relative merits of different methods of calculation are not considered, as the comparative data is more important than trying to derive an absolute value.

The method of calculation used here was that described by Bennett (1973). In Chapter 1 of this thesis it was stated that a lens was distortion free if the ratio (W) of $\text{Tan } U'_2/\text{Tan}U_1$ was a constant for all angles U'_2. This ratio (W) is compared with the paraxial magnification of the centre of rotation to lens distance (z) produced by the lens. This magnification is computed from the shape factor and power factor product, using the expression:

$$w = \frac{1}{(1 - z.F'_v).(1 - t/n.F_1)} \qquad \text{- - VIII (1)}$$

From this, distortion is calculated, using the expression:

$$D = \frac{100(W - w)}{w} \quad (\%) \qquad - - \text{VIII(2)}$$

Thus to measure distortion in a lens on this basis, one has to be able to measure the angles U'_2 and U_1 accurately, at a known value of 'z'.

8.1 Apparatus

The apparatus used is shown schematically in Figure 8.1. It is a modified prism spectrometer. The spectacle lens (1) is mounted on an adjustable holder so that it can be positioned accurately at a given distance 'z' from the centre of rotation of the instrument (2). The table (3), on which the lens holder is mounted can be rotated to make any angle U'_2 with the collimator axis. Normally, of course, the collimator (4) produces parallel light. Here it was modified to produce divergent light at the rear surface of the lens by means of an auxillary lens system (5), so that parallel light would emerge from the front surface of the spectacle lens. This parallel light was viewed by the telescope (6). The light source (7) was a monochromatic sodium vapour lamp. By means of a protractor and vernier scale, reading to one minute of arc, the angular movements of the telescope and table about the centre of rotation could be measured.

Figure 8.1

Modified prism spectrometer for the measurement of rotating eye distortion of spectacle lenses.

Modified Spectrometer

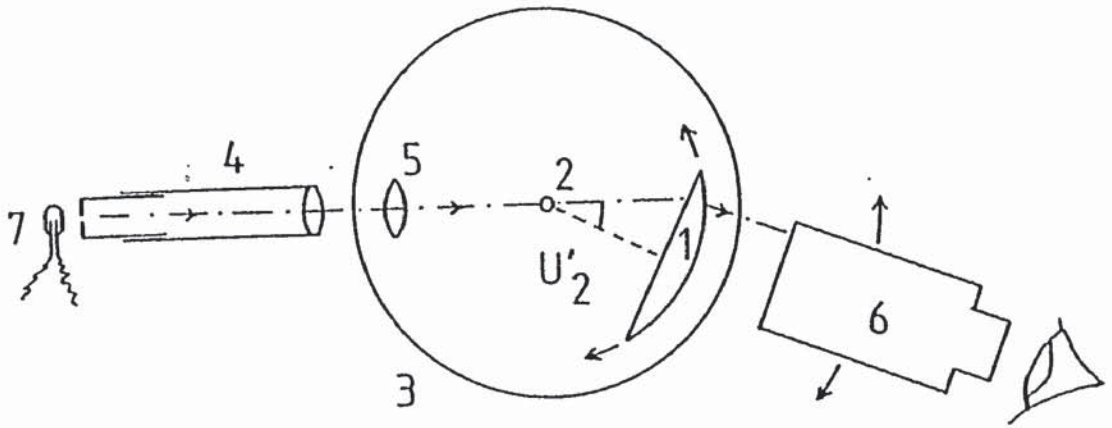

8.2 Measurement procedure

1. Align telescope with collimator azis.
2. Place lens on holder at correct 'z', with optical centre aligned with optical axis of the instrument.
3. Rotate lens holder about a given angle U'_2.
4. Rotate telescope to align with slit image. Read off angle (θ) of telescope rotation. Note that:

$$\theta = U'_2 - U_1$$

5. Measure BVP (F'_v), centre thickness (t), rear surface power. Asuming a value for refractive index (n), calculate the power of the front surface of the lens (F_1).
6. Calculate percentage distortion from expressions VIII(1) and VIII (2).

In order to align the telescope with the collimator, and then align optical centre of the lens (steps 1. and 2.), the system must be focused by adjusting the position of the lens system (5). In order to cancel out any alignment errors, measurements were made to the left and right of the optical centre and then averaged.

8.3 Accuracy of measurement

Examination of Table 8.1 shows the calculated distortion values for four experiments (A - D). The variation in percentage distortion is greater at low angles of eye rotation because the experimental error is large in relation to the angle being measured. As the angle

Table 8.1

Distortion, Zeiss Punktal +6.06 DS

Practical

	5	10	15	20	25	30	Eye Rotation
A (R)	+0.05	+0.33	+1.39	+2.29	+3.86	+5.76	
B (R)	+0.89	+0.55	+1.39	+2.40	+3.67	+5.68	
C (L)	+0.05	+0.75	+1.24	+2.18	+3.39	+5.26	Distortion (%)
D (L)	-0.36	+0.33	+1.09	+1.84	+3.48	+5.43	
	+0.16	+0.49	+1.28	+2.18	+3.60	+5.53	Mean

Ray trace

p_1	5	10	15	20	25	30	Eye Rotation
0.94	+0.13	+0.54	+1.22	+2.23	+3.60	+5.40	
0.96	+0.13	+0.54	+1.24	+2.26	+3.64	+5.46	
0.98	+0.14	+0.55	+1.25	+2.28	+3.68	+5.52	Distortion (%)
1.00	+0.14	+0.55	+1.26	+2.30	+3.72	+5.59	

Figure 8.2

Measured distortion for +6.06DS Zeiss Punktal, spherical surface glass spectacle lens, compared with ray trace values for two theoretical front surface conic lenses.

Distortion of Zeiss Punktal

B.V.P +6.06 DS

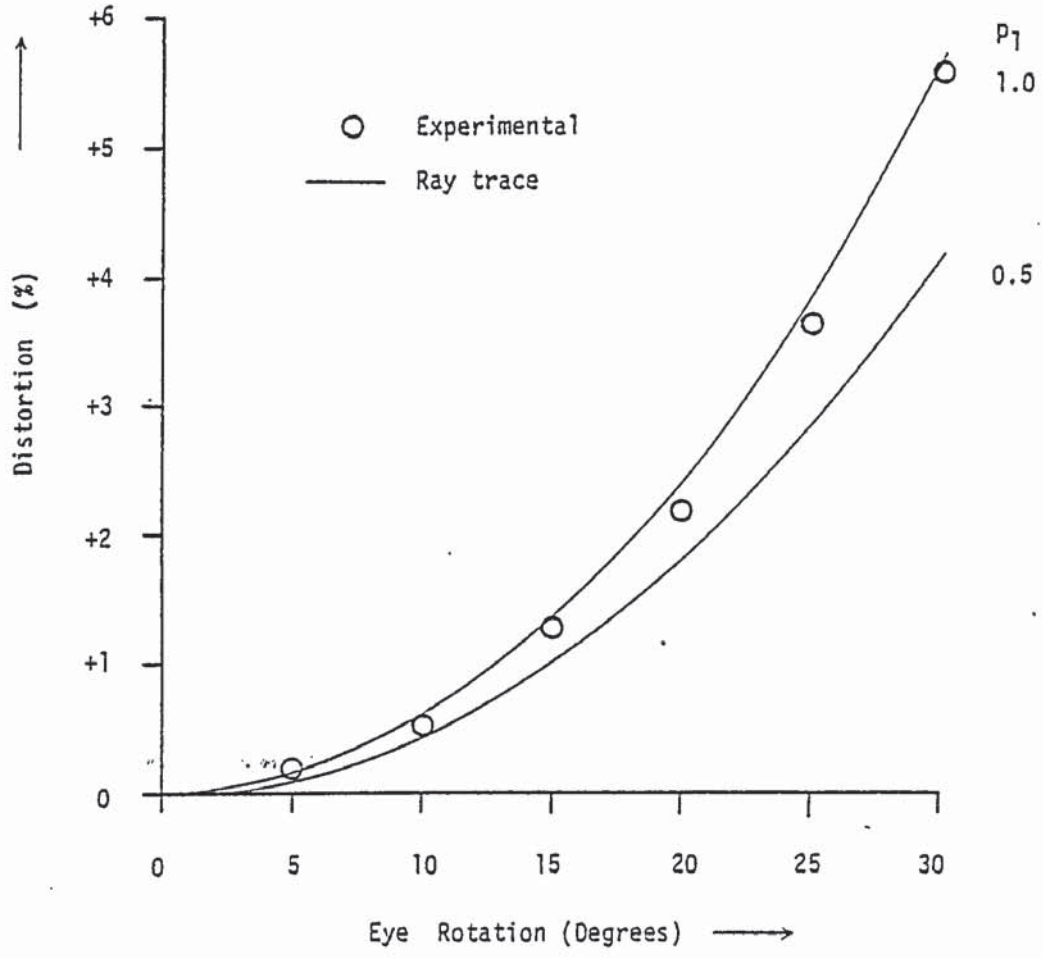

increases, the experimental error is less significant. For example, the differences in percentage distortion at 5 degrees of eye rotation are caused by a range of 3' of arc in angular measurement.

Also shown in the table are the expected values for distortion, derived from ray trace information. If these values are compared with the mean practival percentages, and a sum of absolute differences is calculated, then the best fitting value of p_1 is found to be 0.97.

8.4 Subjective Measurement of distortion

Objective measurements of distortion on spectacle lenses are only useful if they give some indication of the type of effects experienced by the lens wearer. In order to try and measure distortion effects subjectively, the apparatus shown schematically in Figure 8.3 was used. This consists of a vertical sheet of 'Perspex' plastic sheet, 2.5 mm thick, viewed from one edge. This is supported at each end, and can be adjusted by a screw thread at the centre to vary its curvature from zero to either convex or concave curves. The observer views the sheet at a given object angle relative to the otpical axis of the spectacle lens under test. The lens is worn in a spectacle frame and the object angle kept constant by the observer being located by a bite bar. The curve of the sheet can be set remotely by the observer, using a pulley, system connected to the adjusting screw.

Figure 8.3

Arrangement of apparatus used for the measurement of subjective distortion.

Distortion Measurement

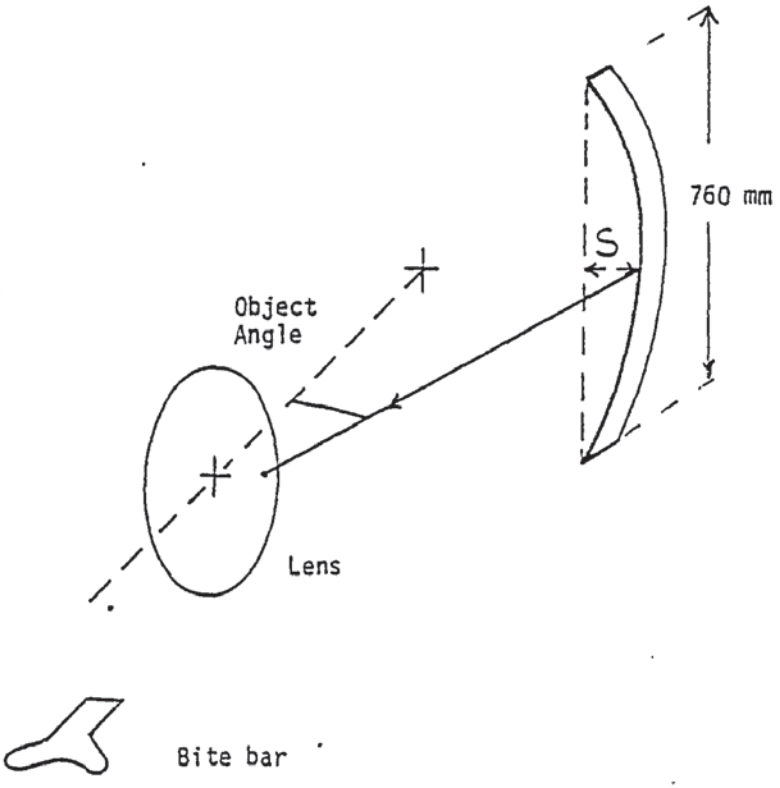

The target appears to the observer as a thin white line against a dark background. This background has an irregular border in order to remove reference verticals. The task of the observer is to set the line so that it appears to be straight. Readings are taken both to the left and right for a given object angle and then averaged, in order to cancel out any positioning errors of the spectacle lens. The sag 's' of the plastic sheet is measured by reading off the position of the central point against a fixed ruler.

8.4.1 Relation of subjective readings to ray trace

In Figure 8.4 the flexible strip is represented by the curved line BE, which represents the mid point to the top edge. This is viewed by a distorting lens to give a vertical straight line image, AD. The curve of the sheet is given by the sag to the mid point, 's', measured from the physically straight position, EC. If the distance of the lens to the object plant is OL, then the object angle is given by:

$$\theta = \mathrm{Tan}^{-1}(CO/OL)$$

If the sag set by the observer (s) fully corrects the distortion, then DA will be vertical, which can be represented by:

$$DO \cos\theta - AO = 0$$

Thus the distances DO and AO are required, which can be calculated from a ray trace, since if points B and E are considered as two object points, then the equivalent values of angle U_1 are:

$$\text{Tan}^{-1}\ (EO/OL) \qquad \text{(for E)}$$

$$\text{and}\ \ \text{Tan}^{-1}\ (BC+CO)/OL) \qquad \text{(for B)}$$

After refraction by the lens, the angle that the image makes at the centre of rotation (U'_2) is equivalent to:

$$\text{Tan}^{-1}\ (DO/OL) \qquad \text{(for D)}$$

$$\text{Tan}^{-1}\ (AO/OL) \qquad \text{(for A)}$$

One complication in the calculation is that although the known variable in the geometric ray trace is U_1 in each case, it is conventional to carry out reverse ray traces through a lens, so that all the rays pass through the centre of rotation. Thus the conventional input variable is U'_2, with U_1 being determined after tracing the ray through the two lens surfaces. This can be overcome by either using tables relating U_1 to U'_2 for a given set of conditions for a lens, or else by using an approximate value of U'_2 in a computer program that is modified by an error detection feedback loop to give the required value of U_1.

8.4.2 Calibration

This apparatus was tested for calibration purposes by making one experienced observer (CWF) artifically hypermetropic with a contact lens, and then using a +14.00 DS spectacle lens to correct this ametropia. As will be seen from Table 8.2, the experimental values for the sags on the instrument required to correct the perceived distortion were not as large as predicted from the ray trace through the lens.

Figure 8.4

Subjective distortion analysis, showing the curved strip (BE), and its undistorted image (DA)

Subjective Distortion Analysis

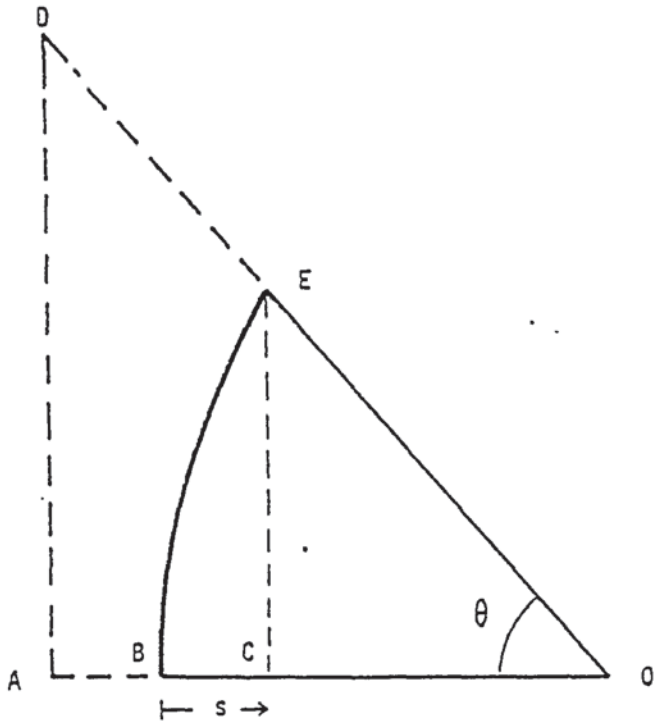

Table 8.2

Subjective distortion results for spherical surface lens (+14.00 DS) compared with anticipated values from ray trace

Object angle (Degree)	2.5	5.0	7.5	10.0
Mean experimental sag (mm)	1.1	1.6	2.5	4.0
Sag from ray trace (mm)	1.9	3.8	5.8	8.1

Object distance: 5350 mm

The apparatus used here for the subjective measurement of distortion is similar to that used in a number of studies which investigated perceptual adaptation. For example, Vernoy and Luria (1977) investigated the perception of distortion under water as seen through a diver's face mask, and found that sags of curves were only perceived to be 70% of the expected curvature from theoretical optical predictions. Unfortunately, it is not stated how these theoretical predictions were obtained. This adaptation occurred after only 15 minutes underwater experience, a similar time to which the spectacle lens was worn before measurements were taken in this experiment.

It is interesting to compare this experiment on the +14.00DS lens with the results from CWF wearing his habitual myopic spectacle correction. This is shown in Figure 8.5, and illustrates that in this case the practical and theoretical figures agree quite well. Similar results have been obtained on another myopic spectacle lens wearer.

Thus as a means for assessing the absolute value of distortion in an aphakic spectacle lens, this method of measurement is not a good predictor. However, as shown in Part 3, this method is useful for ranking lenses in order of their distortion properties.

Figure 8.5

Relationship of subjective distortion results for R eye of myopic observer (CWF) to expected values from ray trace (dotted line). Lens power -5.50 DS

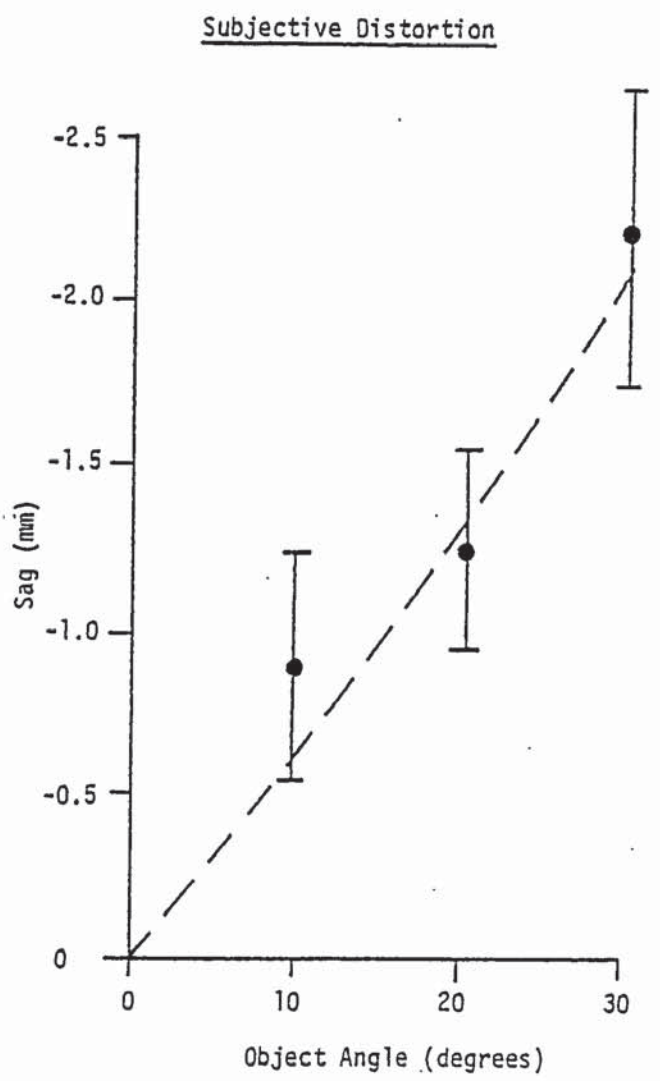
Subjective Distortion
-2.5
-2.0
-1.5
-1.0
-0.5
0
Sag (mm)
0
10
20
30
Object Angle (degrees)

PART TWO

CHAPTER 9

Results of lens measurements

9.1 CONIC SECTION LENSES

9.1.1 Combined Optical Industries Ltd aspheric lenticular

This lens was of particular interest as it was not a production item, but a prototype, kindly lent by its designer, Mr A G Bennett. The basic parameters of this lens are shown in Table 9.1 and from the refactive index it will be apparent that this lens is made from acrylic material, and not CR39 like the majority of other designs. This 65 mm uncut lens with a 40 mm aperture has a notably flexible feel, due to a combination of the type of material and the low centre thickness.

Measurement of the lens showed that the front surface was not a regular conic surface. Figure 9.1 and 9.2 show the oblique astigmatism and Mean Oblique Power of the lens, and show the spherical central zone, beyond which the lens becomes aspheric. It was known from the designer that the lens was intended to have a conic section front surface with a p_1 of 0.66, and there are obvious departures from this ideal, as is further shown by the results of the distortion measurement in Figure 9.3. In addition, the measurement of front surface coordinates by the travelling microscope yielded different results depending on the program used for interpretation. The normal least - squares program gave a p_1 of 0.5, whereas POLYFIT3 gave a value of 0.61. This is

Table 9.1

Lens Details

Len Type	BVP(D)	F2(D)	t(mm)	n	Uncut size(mm)
Conic Section:					
C.O.I.L.	+13.75	-3.78	7.35	1.491	65 (L)
Essel Atoral	+13.75	-3.33	10.20	1.498	52 *
Norville	+14.18	-2.63	9.20	1.498	67 (L)
Polynomial:					
American Optical	+14.06	-3.74	7.50	1.498	65 (L)
'Drop':					
Signet Hyperaspheric	+14.12	-1.79	12.20	1.498	60
Sola Hi Drop Armorlite	+14.00	-2.03	12.10	1.498	63 (P)
Multi Drop: (+)					
a) No.16 blank	+14.25	-2.83	10.40	1.498	60 (P)
b) No.14 blank	+14.00	-0.62	10.90	1.498	60 (P)
c) No.12 blank	+12.00	-0.24	8.25	1.498	60 (P)
Younger	+12.25	-5.02	6.50	1.701	55
Blended lenticular:					
A.O. Ful-Vue	+14.50	-1.77	10.75	1.498	66
Rodenstock Perfastsar	+14.00	-2.26	11.00	1.498	66
Essilor Omega	+13.80	-3.05	10.90	1.498	67
Hoya THI	+14.12	-7.18	5.70	1.806	55

Notes:- (L) Lenticular lens

(P) Lens has peripheral flange, useful diameter approximtely 4 mm less

* Rear surface aspheric

(+) This lens was originally known as the Welsh Four Drop. Both names are used in this thesis.

Figure 9.1, 9.2, 9.3

C.O.I.L. aspheric lenticular, showing oblique astigmatism measurements using the modified focimeter compared with lens design (9.1), and Mean Oblique Power measurements compared with lens design and theoretical spherical front surface (9.2). Figure 9.3 shows distortion measurements from the modified spectrometer, compared with the theoretical lens design and a front surface spherical lens. Lens parameters as in Table 9.1

Combined Optical Industries Ltd aspheric lenticular

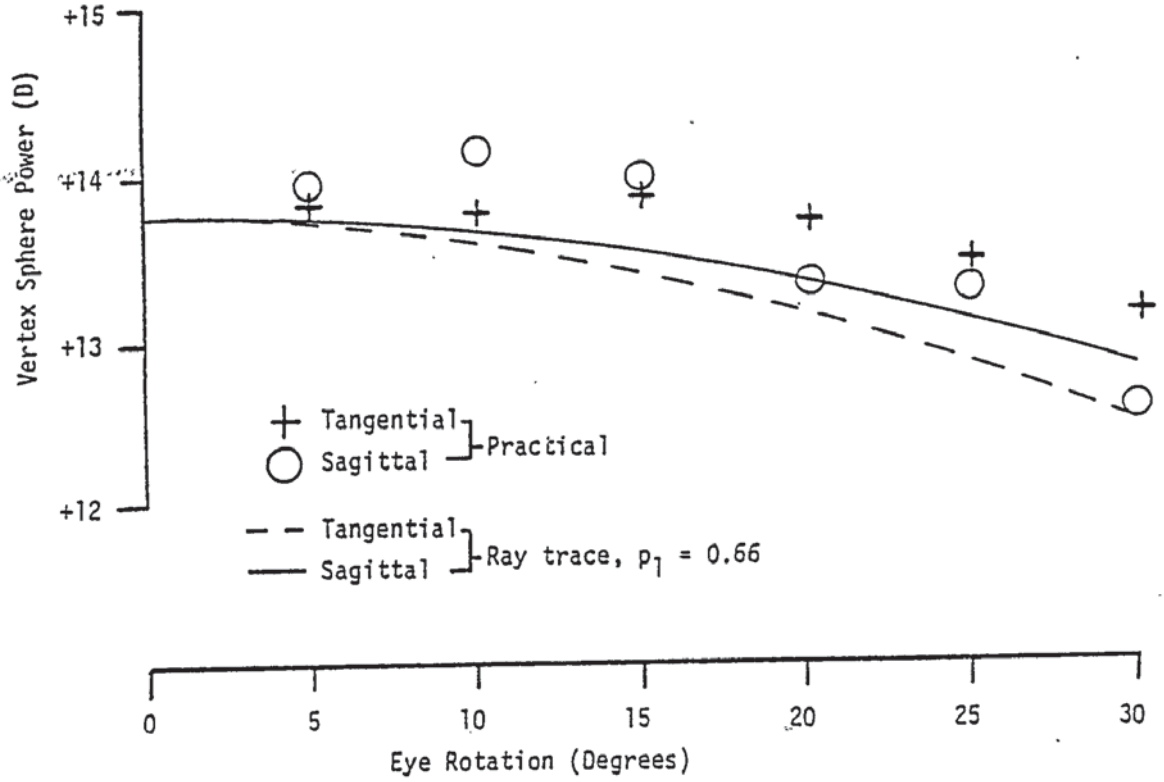

Combined Optical Industries Ltd aspheric lenticular

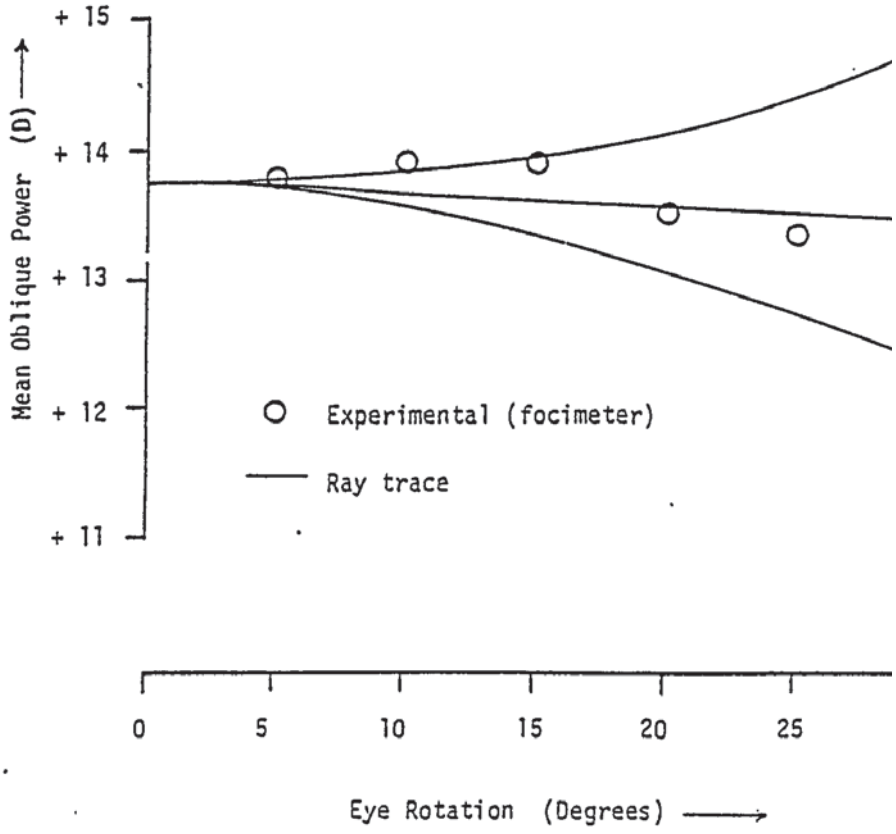

Combined Optical Industries Ltd aspheric lenticular

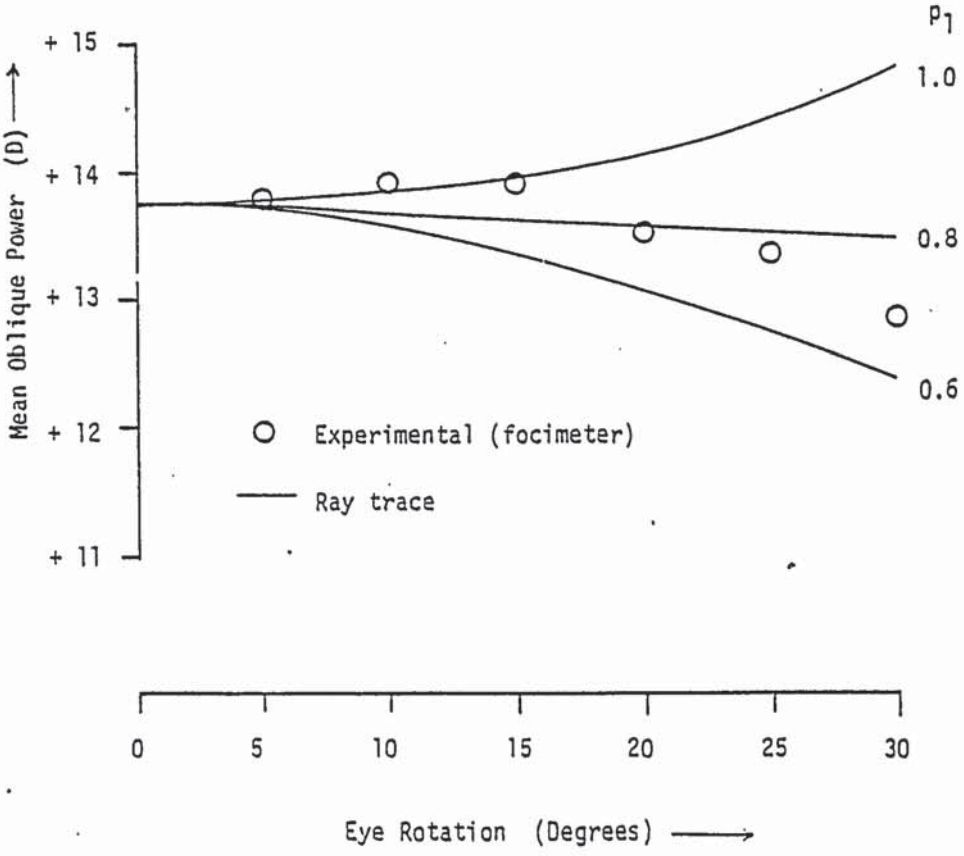

Combined Optical Industries Ltd aspheric lenticular

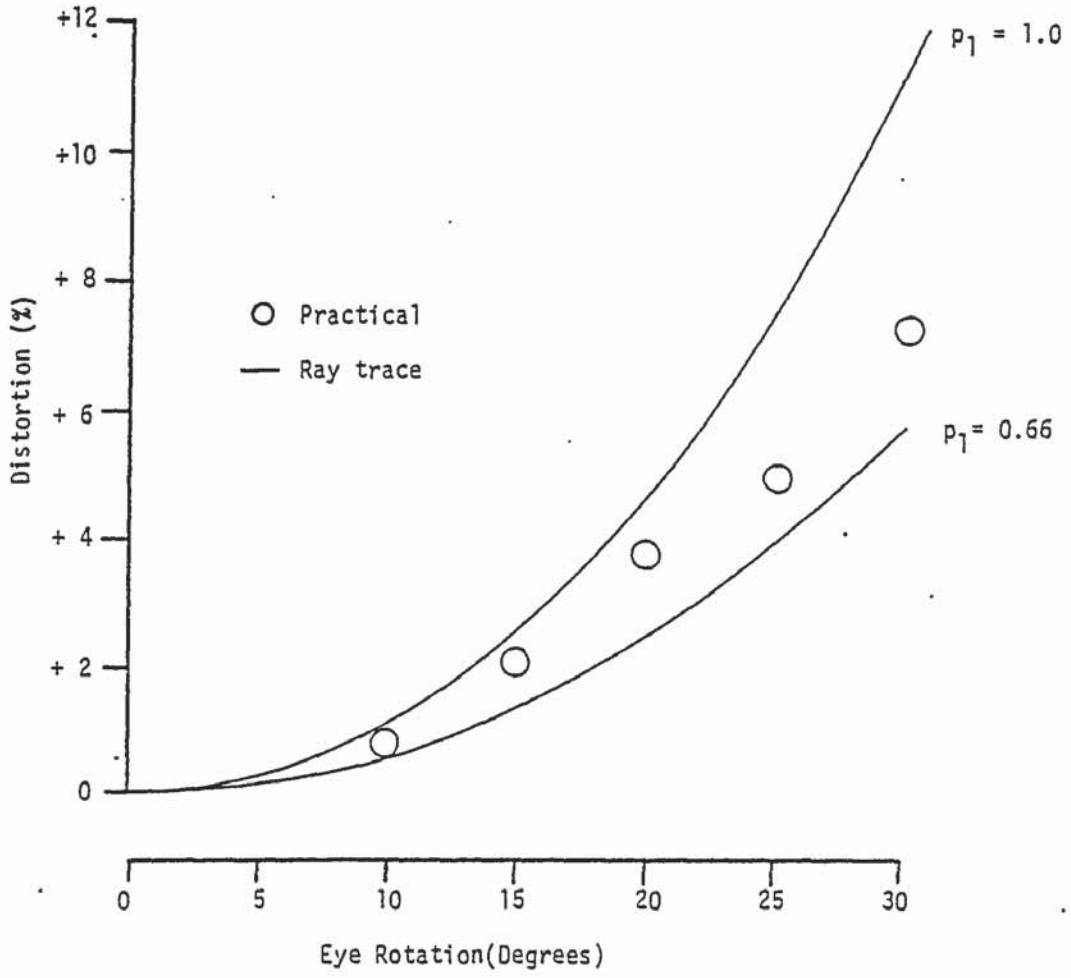

undoubtedly due to the different weighting that the two programs give to the measurement points. Furthermore, POLYFIT3 showed that a better fit could not be achieved by using a y^4 or y^6 polynomial.

Somewhat surprisingly it was found that the rear surface of the lens had an irregular curvature. In the optical zone of the central 40 mm the surface is spherical, but it rapidly flattens across the lenticular margin. This is undoubtedly due to deformation after release from the mould. The quantitative values were -3.775 D measured across the central 20 mm of the rear surface, and -3.594 D measured across 46 mm diameter. Paraxially, the front surface was found to be fairly close to the design, the measured value for the radius being 30.44 mm rather than the intended 30.34 mm.

9.1.2 Essel 'Atoral'

This is full aperture lens with an uncut diameter of 52 mm. It was until recently available both in single vision and varifocal ('Atoral Variplas') forms, but both types of lens have now been discontinued. Assessment of the lens surfaces using a lens measure shows that for the single vision lens the front surface is spherical, and the rear surface aspheric is form. Since the travelling microscope could not be used for aspheric concave surfaces, an indication of the rear surface asphericity was gained by use of two sag measurements. A lens measure with an outer leg separation of 21 mm gave a rear surface power, corrected to CR39 refractive index of -3.330 D., equivalent to a rear surface

Figure 9.4 and 9.5

Experimental values of oblique astigmatism on Essel Atoral as measured with the modified focimeter compared with an aspheric rear surface (p_2 16.598) and a spherical rear surface (9.4). Figure 9.5 shows a similar exercise on distortion, measured with the modified spectrometer. Lens details as in Table 9.1

Essel 'Atoral'

Front surface assumed to be spherical

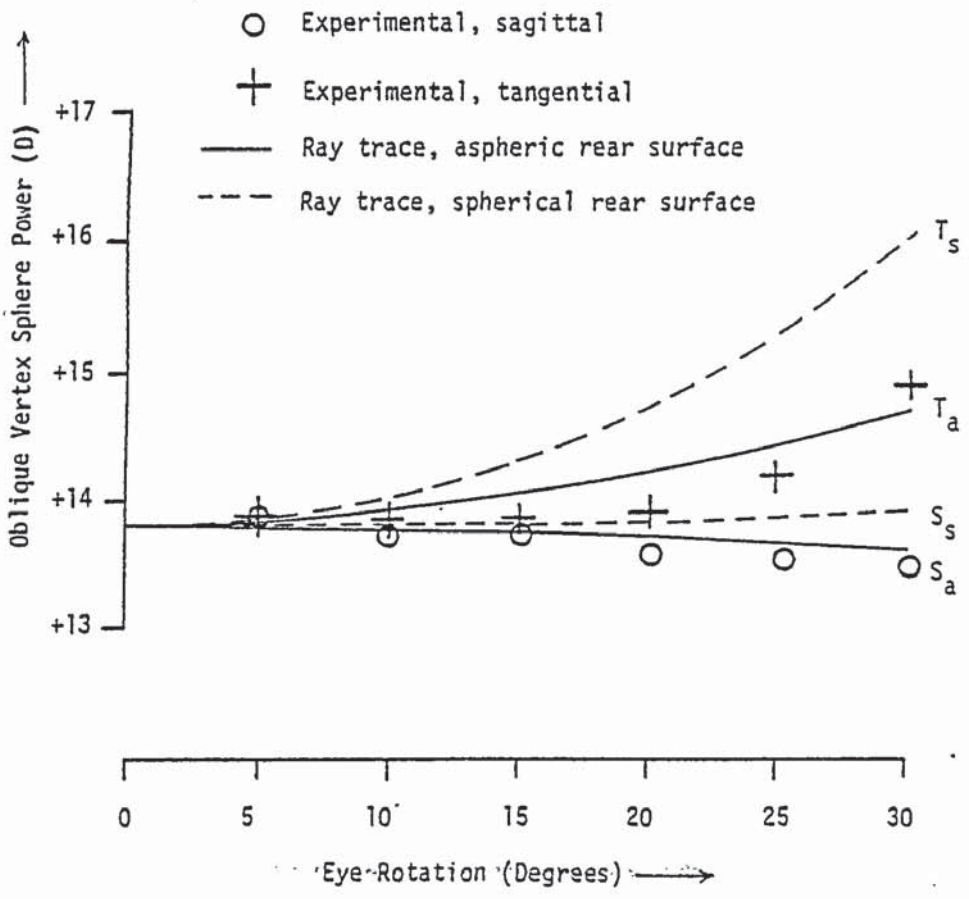

Essel 'Atoral'

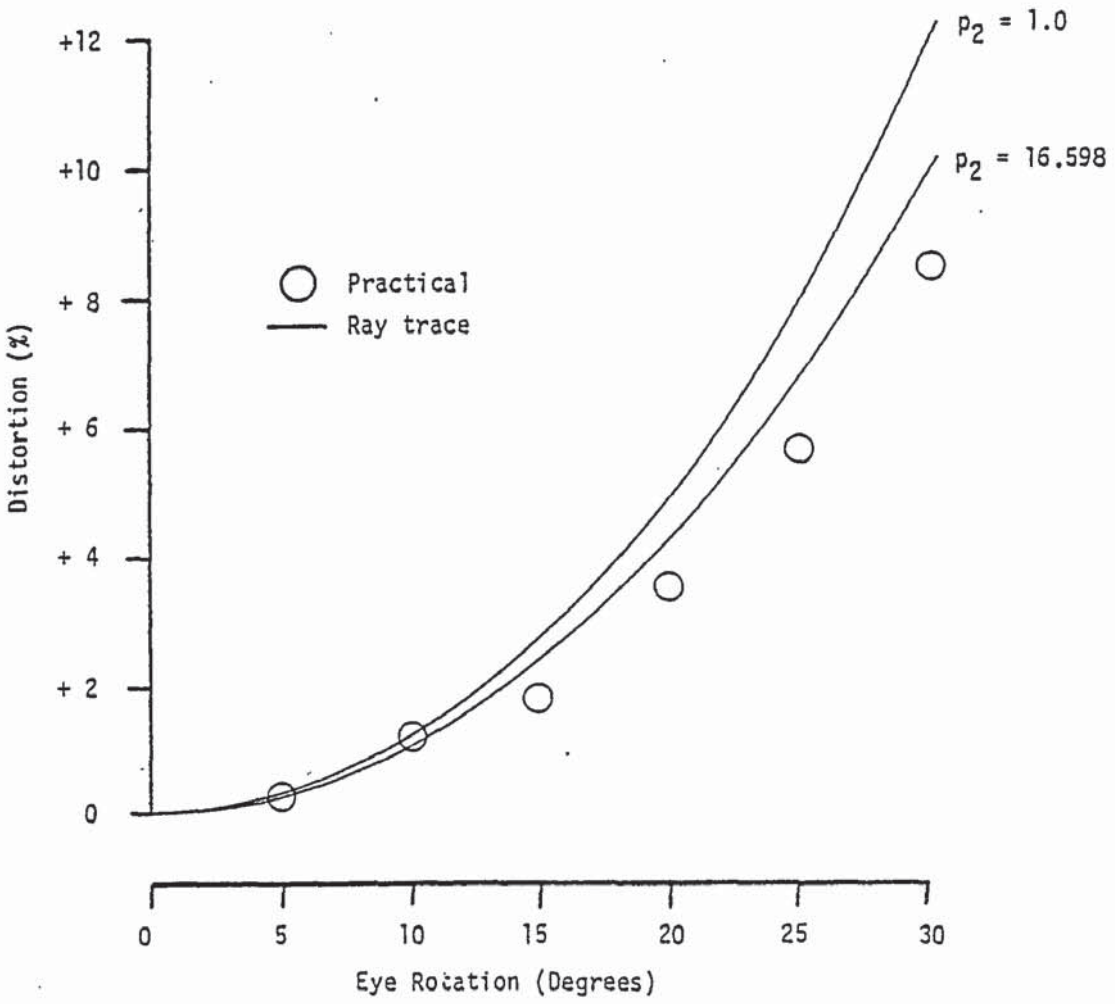

radius of 149.43 mm. The sag across a chord of 46 mm was also measured, using a spherometer, and this gave a value of 1.99 mm. Substitution of these values into the relationship:

$$p = \frac{2rx - y^2}{x^2} \qquad \text{-IX (1)}$$

gives a value of rear surface p (p_2) of 16.598. This indicates a surface which becomes steeper than spherical away from the centre, which is to be expected. The large value of p_2 is explained by the fact that relatively greater deformation of the shallow rear surface is required to give the same optical effect as deformation of the steeper front surface.

The oblique vertex sphere powers were measured on the modified focimeter, and the results are shown in Figure 9.4. The measured tangential and sagittal powers are shown compared with the expected values from a ray trace. Two conditions are shown, one assuming a spherical rear surface, the other a conic rear surface with a p_2 of 16.598. This shows that the two methods of assessment give a reasonable correlation. The effect of the rear surface in aspheric form is to reduce the oblique astigmatism (by one dioptre at 30 degrees), but also to reduce the curvature error. In addition, there is a small reduction in distortion, as shown in Figure 9.5 although here there is not a good agreement between the theoretical predictions and prectical measurement.

The lens has one major disadvantage compared with other aspheric designs, and that is the fact that the cosmetic appearance is no better than a normal spherical surface lens, and due to the rear surface, the overall diameter is severely limited.

9.1.3 Norville aspheric lenticular

This 42 mm aperture CR39 lenticular is sold under the above name but is is known to be a repackaged lens produced by Essilor.

Compared with the superficially similar COIL lenticular, this lens gave better results. Figure 9.6 shows a comparison of the Mean Oblique Power measurements with some conic ray traces with various front surfaces 'p' values, Figure 9.7 illustrates the distortion, and it will be seen that a p_1 of 0.7 fits the data quite well. This fit is not quite so good if the oblique astigmatism values are examined (Figure 9.8). Analysis of the travelling microscope results gave a p_1 of 0.66.

This is a good design for a lens of this power, since by ray tracing it was found that oblique astigmatism is less than 0.5 D, and the maximum tangential error is less than 0.25 D, for eye rotations up to 30 degrees.

Figure 9.6, 9.7, 9.8

Figure 9.6 and 9.7 show Mean Oblique Power as measured with the modified focimeter, and distortion as measured with the modified spectrometer compared with theoretical front surface conic lenses. Figure 9.8 illustrates the measured oblique astigmatism compared with the theoretical performance of a lens having a p_1 of 0.7. Lens parameters as in Table 9.1

Norville Aspheric Lenticular

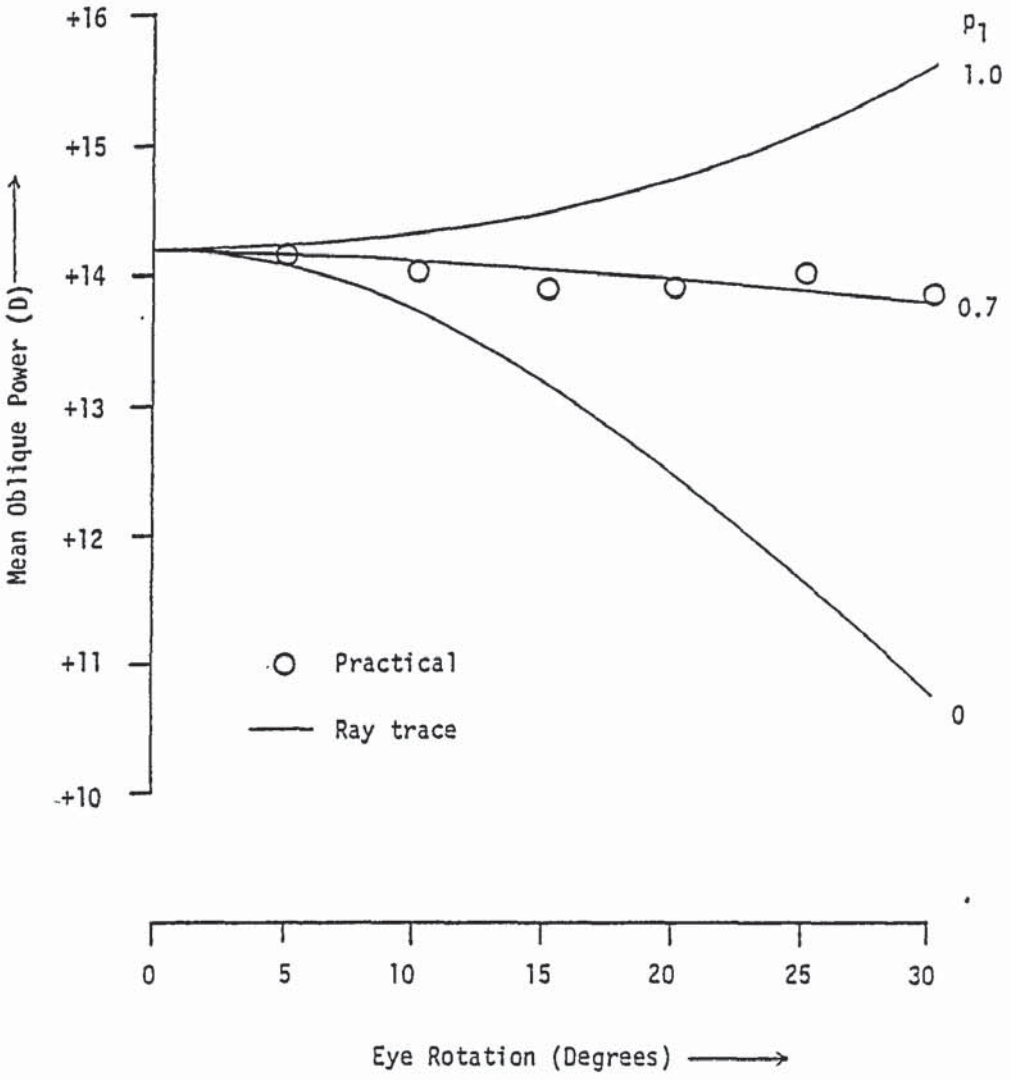

Norville aspheric lenticular

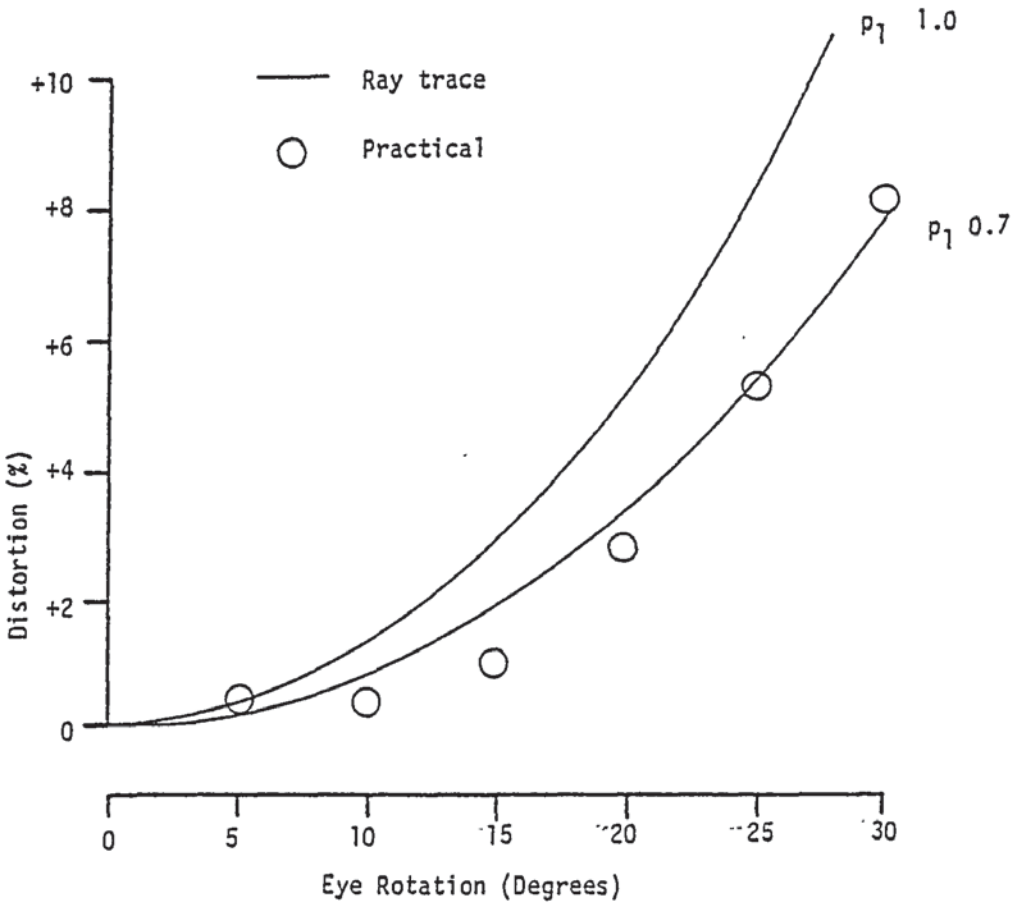

Norville aspheric lenticular

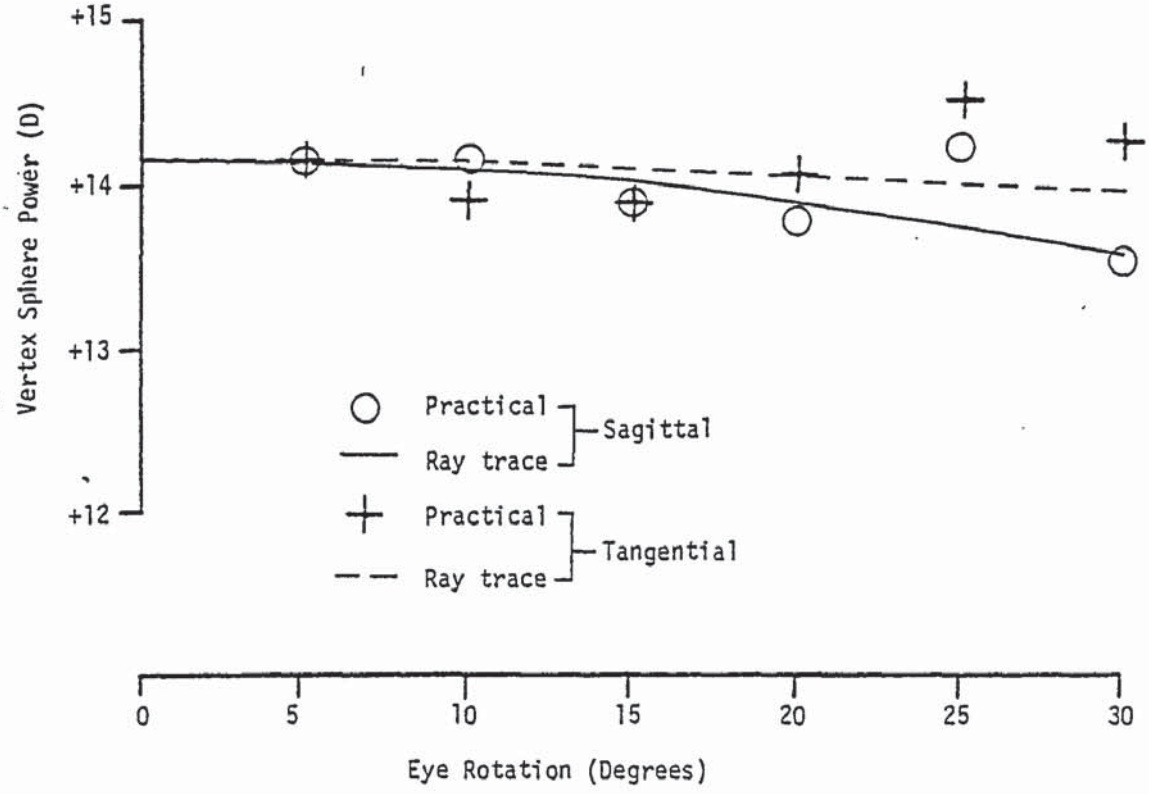

9.2 POLYNOMIAL SURFACE LENS

Only one type of lens was available for measurement in this group.

9.2.1 American Optical aspheric lenticular

As described in Chapter 3, the design of this lens is known in some detail. Thus the question to be answered here is: how well is the design reflected in the finished lens?

The two examples of this lens available for measurement could not be directly compared with the expected values from the patent because the measurement technique used different parameters, and also because the lenses were not made to the same rear surface curves, index or thickness. Davis and Fernald (1965) designed the lens for a 'z' of 23.25 mm, whereas the instrument used here for the measurement of oblique vertex sphere powers had a fixed arbitrary value of 'z' of 27 mm. The theoretically correct lens parameters are given in Table 3.2, and the lens measurements actually found are given in Table 9.1.

It should be mentioned that the index given in the patent (1.4925) is not a known value for any commonly used optical plastic. Thus the normal value for CR39 (1.498) was substituted as being the most likely actual index.

The first stage of measurement was to assess the surface co-ordinates of one example of this lens design. These values were then substituted into POLYFIT3, along with the calculated paraxial

radius of the front surface, in order to find the aspheric coefficients. The results of this exercise were as follows:

'x' (mm)	'y'
1.710	10
2.469	12
3.889	15
5.693	18

r : 30.476

Front surface aspheric coefficients

p 0.44

A -4.405×10^{-7}

B 6.074×10^{-9}

By ray tracing through the surface described by this equation, and also by measuring the oblique vertex sphere powers on the focimeter, comparable measurements could be made. The results of this are shown in Figure 9.9. These results were rather unexpected, as they show a lens performance completely different to that predicted by Davis and Fernald, which is shown in Figure 9.10. This latter graph was produced by fitting the co-ordinates from the patent with a curve from POLYFIT3, and then ray tracing through this. Figure 9.10 shows the very small tangential error of the design, and the fact that the oblique astigmatism is always less than 0.5 D. Compare this with the situation in Figure 9.9, where the lens shows a large tangential error, and over 2 D of astigmatism at 30 degrees. These results were shown to Davis, and his opinion was that this must have been a very poor example

Figure 9.9

Practical readings on American Optical aspheric lenticular taken with modified focimeter, compared with ray trace through curve with aspheric coefficients determined by curve fitting of travelling microscope coordinates. Other lens parameters as in Table 9.1

Front surface aspheric coefficients:

p 0.44

A -4.405×10^{-7}

B 6.074×10^{-9}

American Optical aspheric lenticular

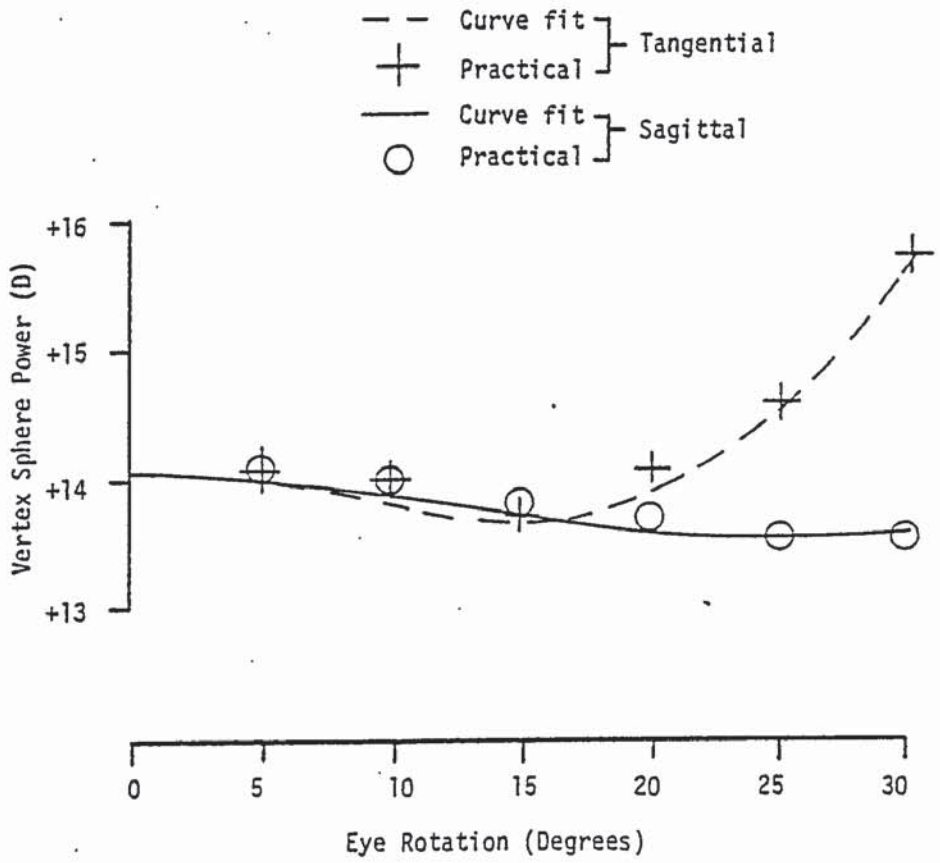

Figure 9.10

Theoretical performance of American Optical aspheric lenticular, determined by curve fitting coordinates given in patent (Davis and Fernald, 1965), then ray tracing, at centre of rotation distance of 27 mm. Other lens details as in Table 9.1.

Front surface aspheric coefficients:

p -1.366×10^{-3}

A 3.298×10^{-6}

B 2.339×10^{-9}

American Optical aspheric lenticular

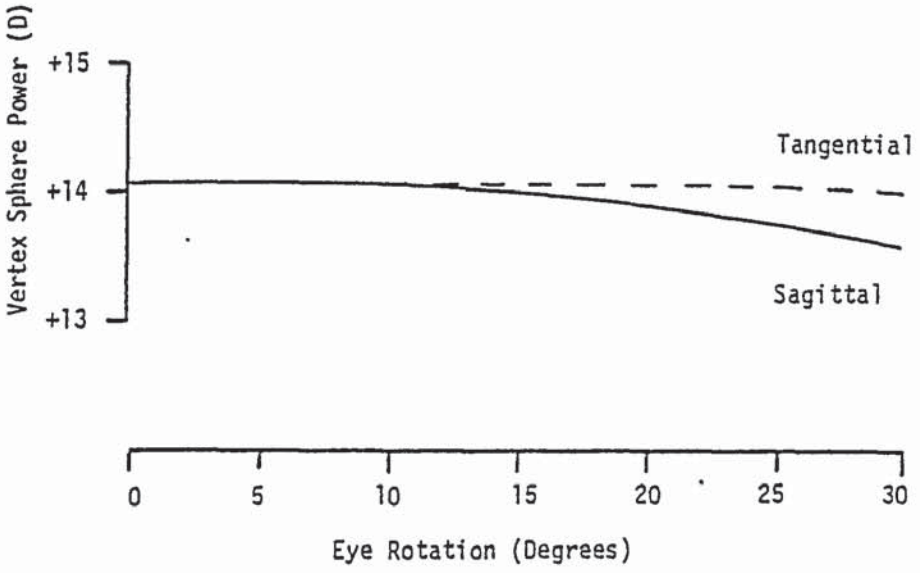

Figure 9.11

Distortion measurements of American Optical aspheric lenticular, from modified spectrometer, compared with theoretical ray trace of lens in patent, and ray trace of lens with front surface curve derived from curve fit of travelling microscope coordinates. Other lens parameters as in Table 9.1.

American Optical Aspheric Lenticular

BVP: +14.06 D F2: -3.74 D t: 7.5 mm n_d: 1.498 z: 27 mm

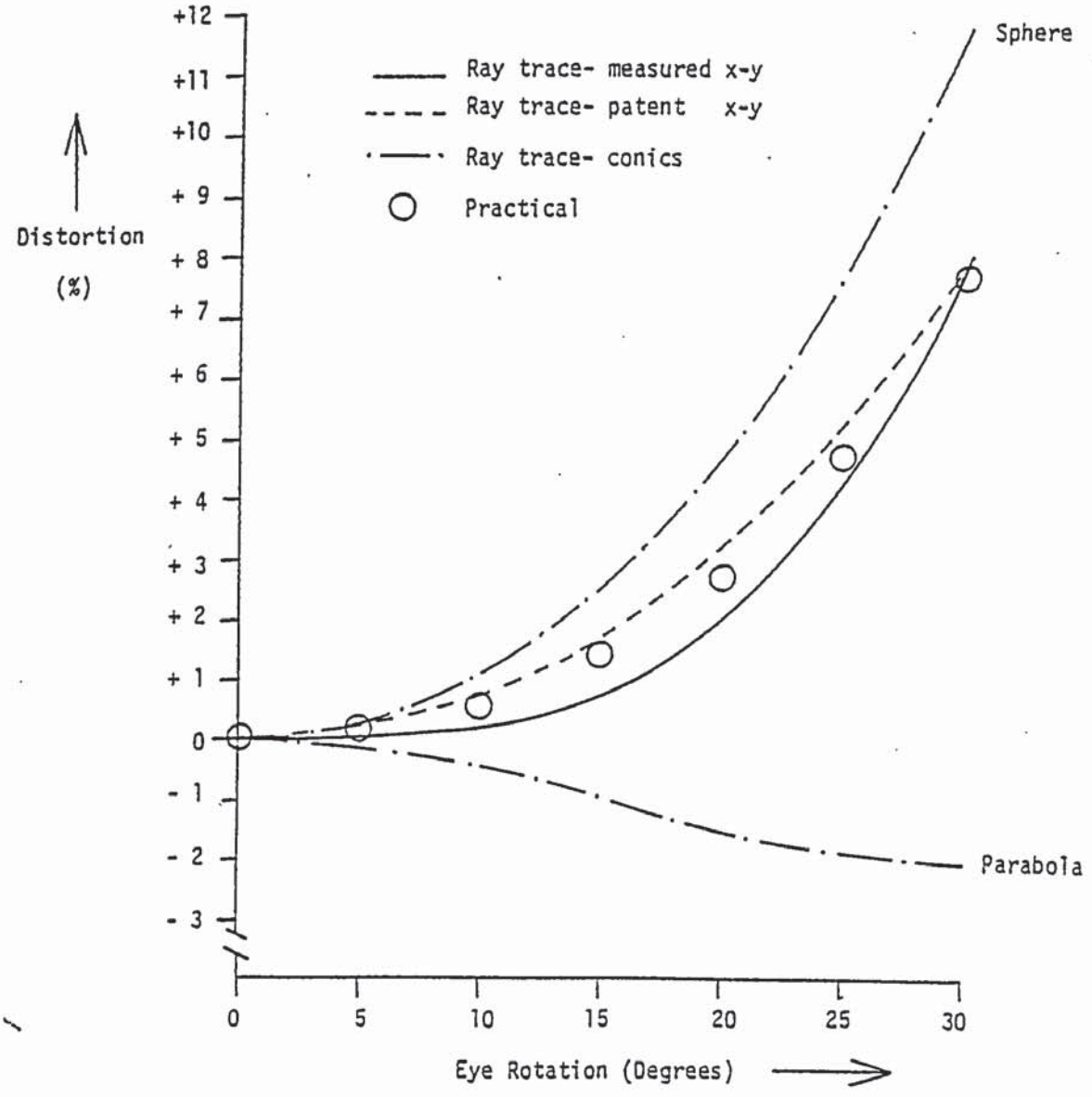

of the lens. However, a second example showed virtually identical results.

In Figure 9.11 the measured distortion of the lens is shown compared with some ray trace values. The results here indicated less of a discrepancy between the actual lens and its design value.

The measurements on this type of lens illustrate that no matter how good the design is, there is no guarantee that the finished lens will give a true representation of the wishes of the designer. It must be pointed out, however, that although the differences between the design and the reality of the lens appear large, they may well not be noticed by many wearers.

9.3 'DROP' TYPE LENSES

Lenses of four different designs were measured in this group, the Signet Hyperaspheric, Sola Hi-drop and Armorlite Multi-Drop in CR39 plastic, as well as the high refractive index glass Younger aspheric.

A single lens of each type was measured, except in the case of the Armorltie Multi-Drop, where lenses of two different base curves were used for the same power, and also a +12.00 D lens was obtained to compare practical measurements with the data of Renier (1977). The three CR39 designs gave very similar results for the nominal comparison power of +14.00 DS, thus these 3 lenses will be considered together.

9.3.1 CR39 'Drop' Lenses

From the basic lens parameters (Table 9.1), the radius of paraxial curvature of the Hyperaspheric was found to be 35.365 mm for the front surface. This is equivalent to a surface power of +14.082 (n = 1.498), and +14.987 (n = 1.530). As the front of the lens was engraved '15', the blanks are thus calibrated in crown tool power.

Similarly, Sola lens has a front surface radius of 35.128 mm, equivalent to a power (1.530) of +15.088 D. The Armorlite Multi-Drop has a radius of 32.614 mm, which gives +16.04 on an index of 1.523, thus being the No.16 in the known series of available lens blanks.

The similarity is most apparent if we compare the Mean Oblique Power measurements from the modified focimeter. These values are plotted for each lens in Figures 9.12 to 9.14. In each case, the measured powers are shown compared with the expected powers for various conic front surfaces, produced by ray tracing.

It is immediately apparent from these results that it would be inappropiate to describe the aspheric simply by giving the best fitting conic equivalent. All the lenses start out by being spherical in the central 10 degrees of so, the power then dropping rapidly towards the periphery.

One of the problems of assessing the power by the focimeter is that limitations in the instrument restricted the angle of

Figure 9.12, 9.13, 9.14

Mean Oblique Power measurements from the modified focimeter on the No.16 blank Armorlite Multi Drop (9.12), No.15 blank Signet Hyperaspheric (9.13), and No.15 blank Sola Hi Drop (9.14). Lens parameters as in Table 9.1

Armorlite Multi Drop

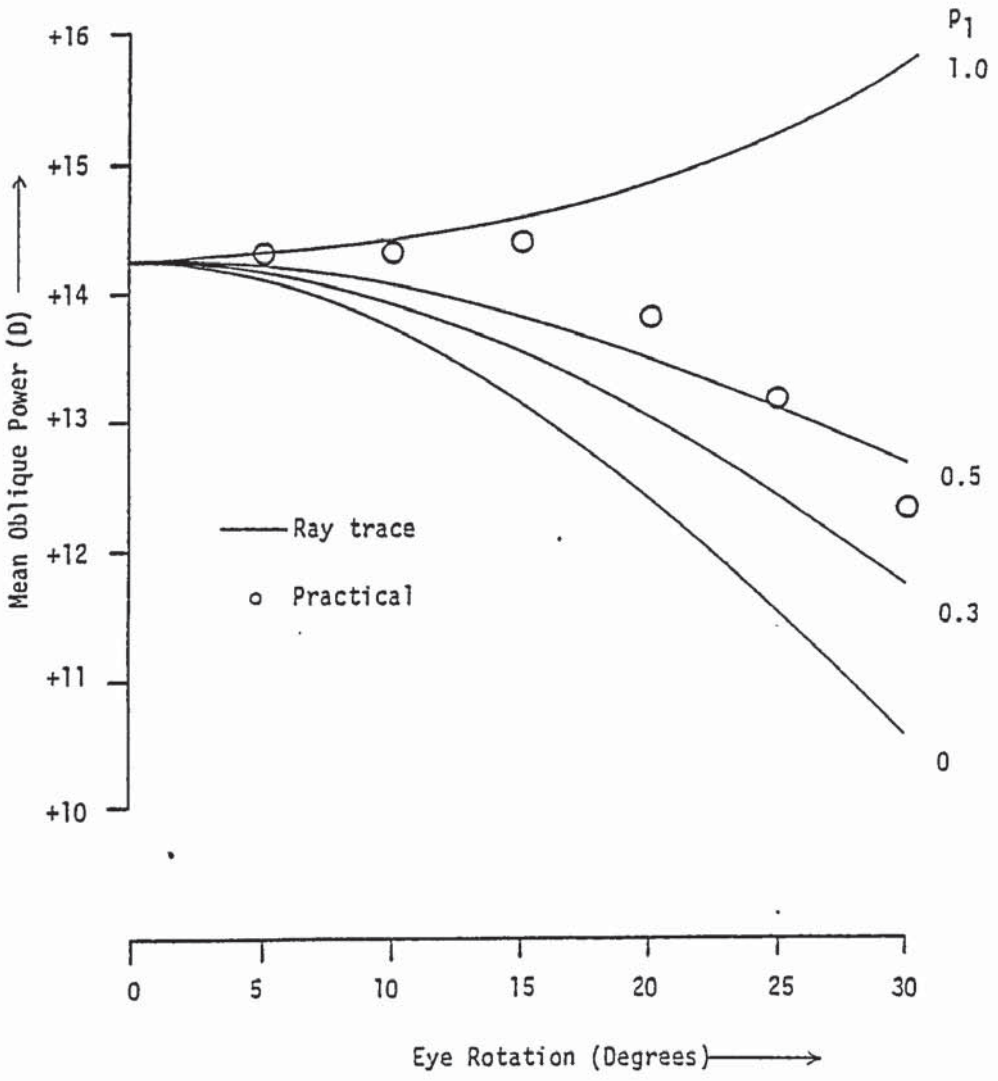

Signet Hyperaspheric

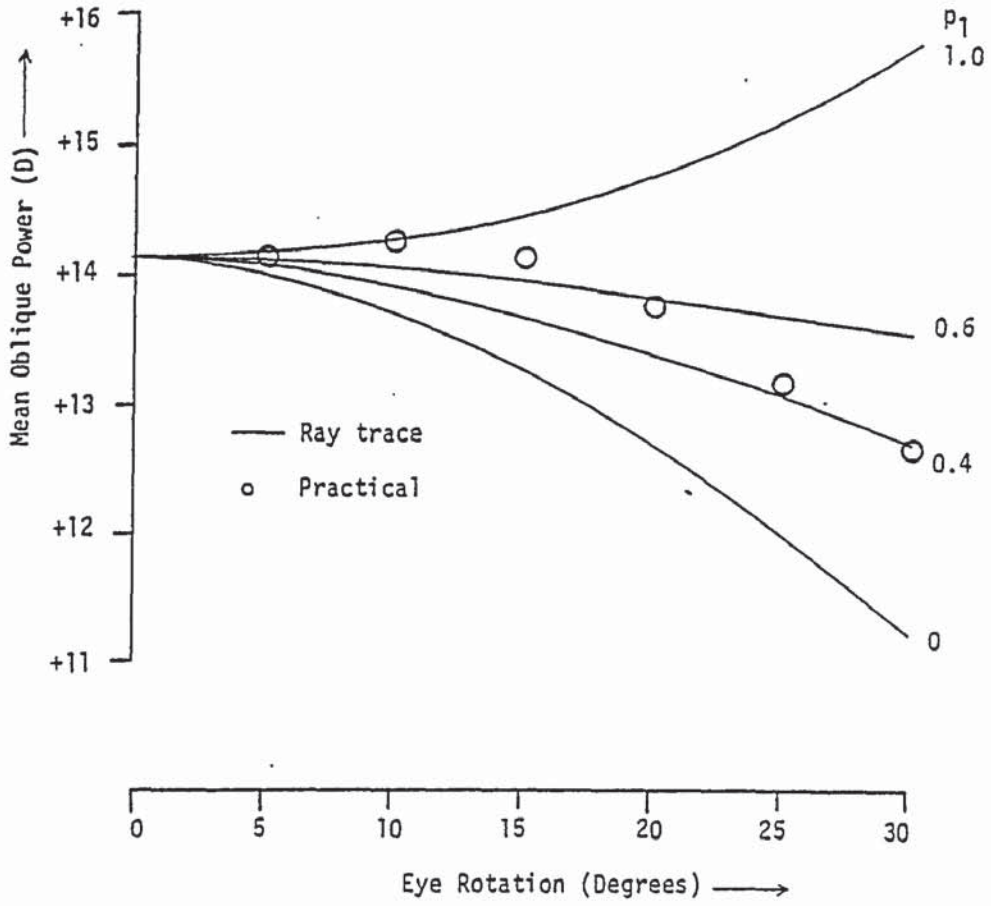

Sola Hi Drop

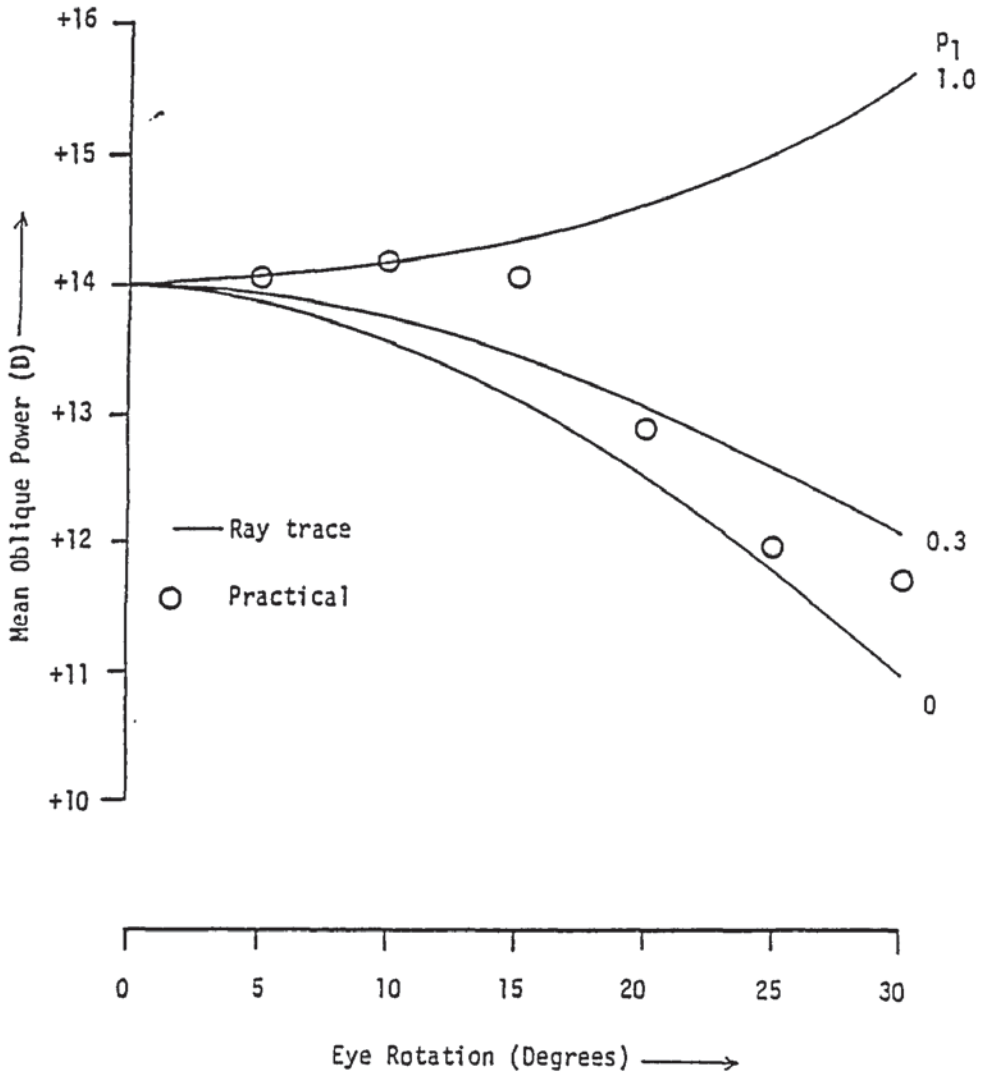
+16
+15
+14
+13
+12
+11
+10
Mean Oblique Power (D)
P1
1.0
0.3
0
Ray trace
Practical
0
5
10
15
20
25
30
Eye Rotation (Degrees)

rotation to 30 degrees. At this angle, the chief ray is passing through the front surface at a distance of 18.3 mm from the optical centre, in a lens with a diameter of 60 mm. However, the travelling microscope could assess the surface up to a distance of 24 mm from the optical centre.

The results from analysis of the front surface at each lens using the travelling microscope are shown in Table 9.2. The surface sags are shown at five distances from the optical centre. Also shown are the values of best fitting p_1, two figures being derived for each lens. The first of these (a) was produced by a curve fit through all given points. The second (b) was derived from POLYFIT3 and was biased towards the edge of the lens, the sag at 5 mm not being used.

Thus the differences between these designs can be described as follows: after the initial spherical zone, the power drops most rapidly in the Sola lens, but then fairly soon stabilises. The power drop in the Hyperaspheric is the most gradual. The Armorlite Multi Drop has the widest spherical zone, after which the power drops progressively towards the edge of the lens.

The figures given for the Mean Oblique Power give only part of the story, as they do not shown how the astigmatism changes in sign for various angles of view. Figure 9.15 gives the tangential and sagittal powers of the Sola lens, compared with the expected values for a p_1 of 0.30. Note that the oblique astigmatism starts off by being positive, as would be expected of a spherical surface of this power, then changes to negative for angles greater than 15 degrees.

Table 9.2

Parameters of 'Drop' type lenses

	Signet Hyperaspheric	Sola Hi-Drop	Armorlite Multi Drop	
y mm				
5	0.382	0.356	0.405	
10	1.485	1.476	1.599	
15	3.356	3.329	3.614	x mm
20	6.032	5.891	6.460	
24	8.812	8.498	9.360	
r_1	35.365	35.128	32.614	
Blank No.	15	15	16	
Curve fit (a) P_1	0.66	0.34	0.44	
Curve fit (b) P_1	0.38	0.30	0.27	

Figure 9.15

Sola Hi Drop No.15 blank sagittal and tangential power measurements from the modified focimeter compared with ray trace through equivalent lens having a conic front surface. Lens parameters as in Table 9.1

Sola Hi Drop oblique astigmatism

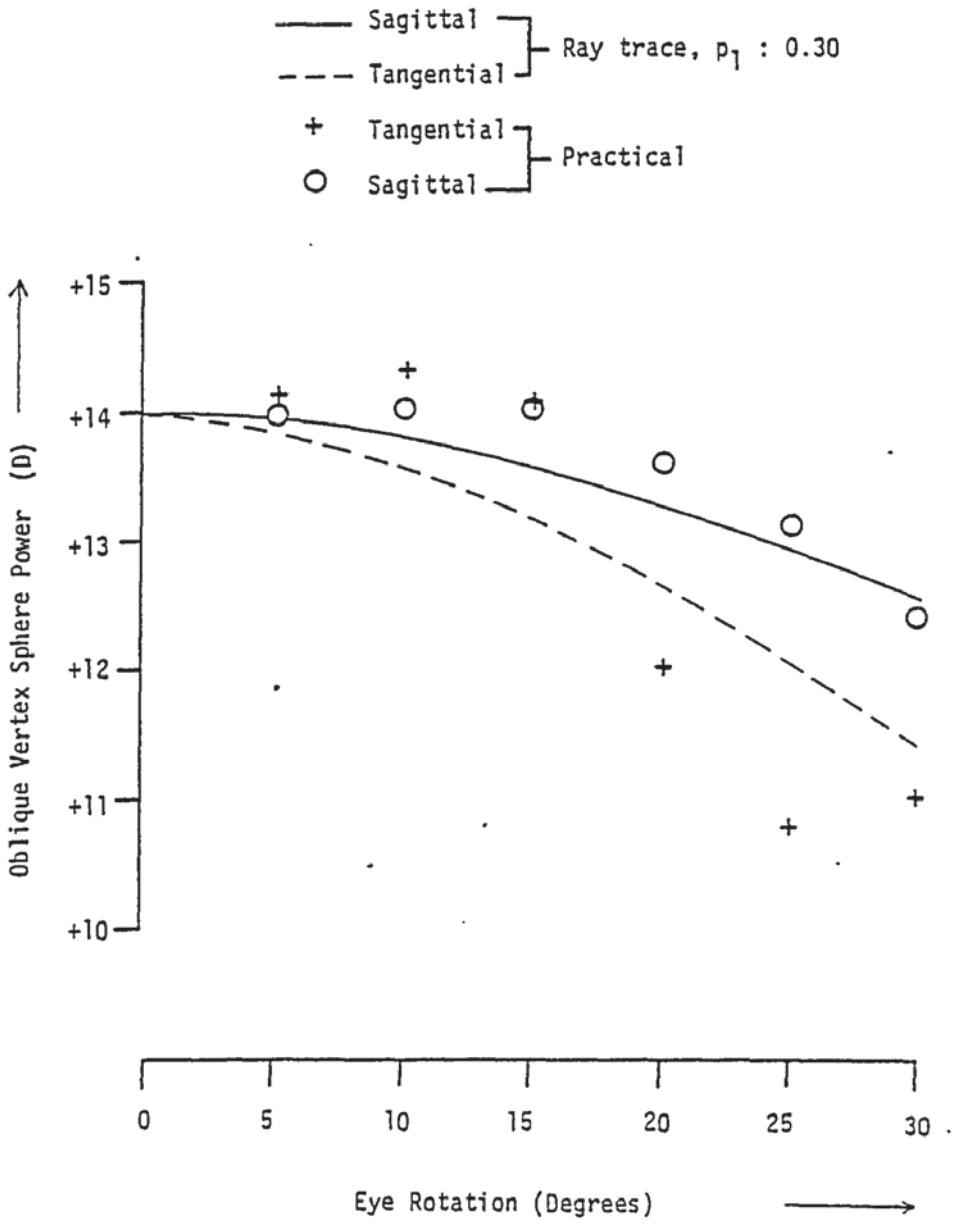

9.3.2 Distortion

One of the main design features of this group of lenses is the low amount of peripheral distortion compared with other types of aspherics. Using the apparatus described in Chapter 8, measurements of distortion were made on each lens. The results are summarised in Figure 9.16. From the discussion in Chapter 2 it will be apparent that although the configuration of the front surface has a marked effect on distortion, the curvature of the rear surface is also an important variable, particularly with the 'flatter' aspherics. Thus it will not be surprising that the Armorlite Multi Drop showed the least distortion at wide angles, as not only did it have the flattest front surface, but also the steepest rear surface of the lenses. The Signet lens shows the most distortion at wide angles, due to a combination of the steepest front surface and the flattest rear surface.

These findings on the properties of the three CR39 lenses are broadly in line with the results of Smith and Atchison (1983c). However, they do make one rather surprising statement:

> 'The asphericity of the Armorlite, Signet and Sola lenses is insufficient to provide much improvement in peripheral distortion characteristics relative to spherical lenses when these are ground with a flat back surface.'

In order to test this statement, an Armorlite lens was obtained manufactured from the No.14 blank, which naturally used a much shallower rear surface (-0.62) to give a power of +14.00 DS than

Figure 9.16

Distortion, as measured on the modified spectrometer, of the Sola Hi Drop (15 blank), Signet Hyperaspheric (15 blank) and Armorlite Multi Drop (16 blank). Lens parameters as in Table 9.1

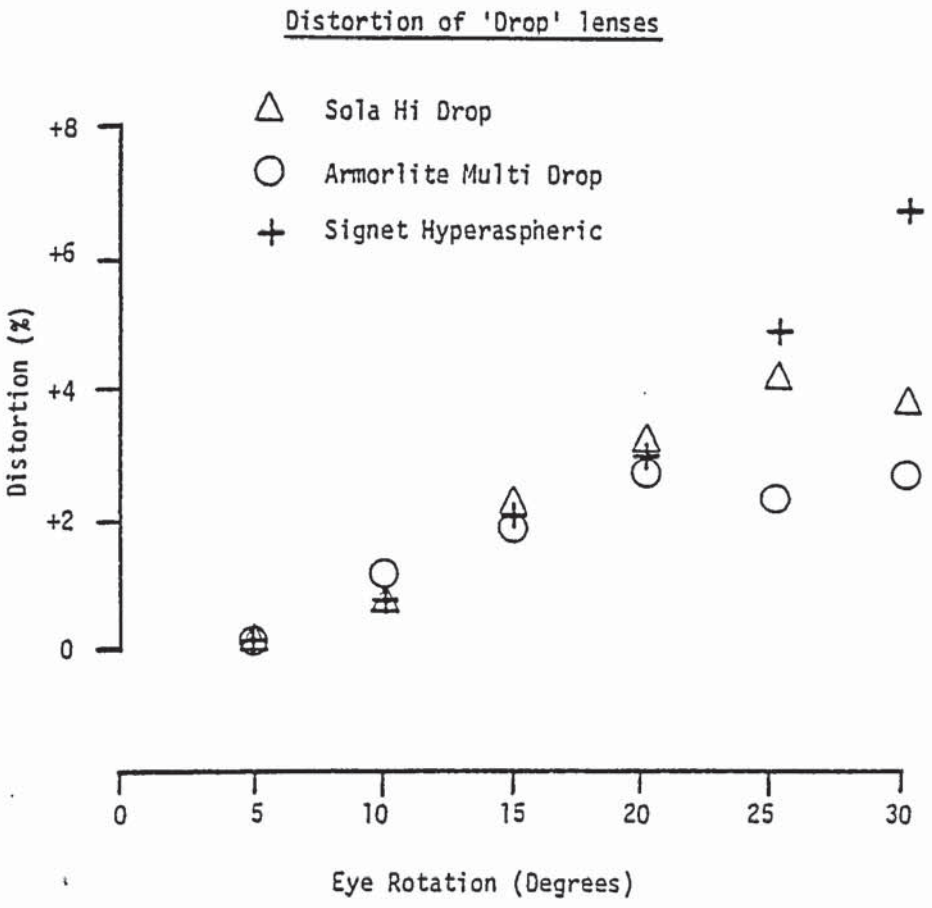
Distortion of 'Drop' lenses
Sola Hi Drop
Armorlite Multi Drop
Signet Hyperaspheric
Distortion (%)
+8
+6
+4
+2
0
0
5
10
15
20
25
30
Eye Rotation (Degrees)

the No. 16 blank measured initially. The oblique power errors and distortion of this lens are shown in Figures 9.17 and 9.18 respectively. It is immediately apparent that this blank has a flatter effective aspheric form than the No. 16 lens. This could be expected, as the original design philosophy of this lens was to have a four Dioptre power drop from the centre to the edge of the front surface, on each blank in the series. This means that the lower power blanks will have a greater percentage power drop.

From the results on this lens, it will be seen that the front surface is approximately parabolic (p_1=0) for eye rotations up to 30 degrees off axis. Despite the near plano rear surface, Figure 9.18 illustrates the considerable improvement in distortion performance achieved by this lens, compared with the equivalent spherical (P_1=1) front surface.

9.3.3 Investigation into the surface topography of the Armorlite Multi Drop

In a description of the various types of aspheric surface used for single vision spectacle lenses, Smith and Atchison (1983c) describe a lens surface made up of a series of different zones arranged in an annular pattern. In order that such a surface does not have any dividing lines on the surface, the tangents to the curves are arranged to coincide at the boundary. Such a surface is described as a 'zonal aspheric'. Smith and Atchison derive the optical properties of a lens with such a surface by means of curve fitting and ray tracing, but note that the calculated

Figure 9.17

Tangential and Sagittal powers of Armorlite Multi Drop (as measured on modified focimeter) compared with theoretical values calculated for lens with parabolic ($p_1 = 0$) front surface. No. 14 blank, lens parameters as in Table 9.1

Armorlite Multi Drop

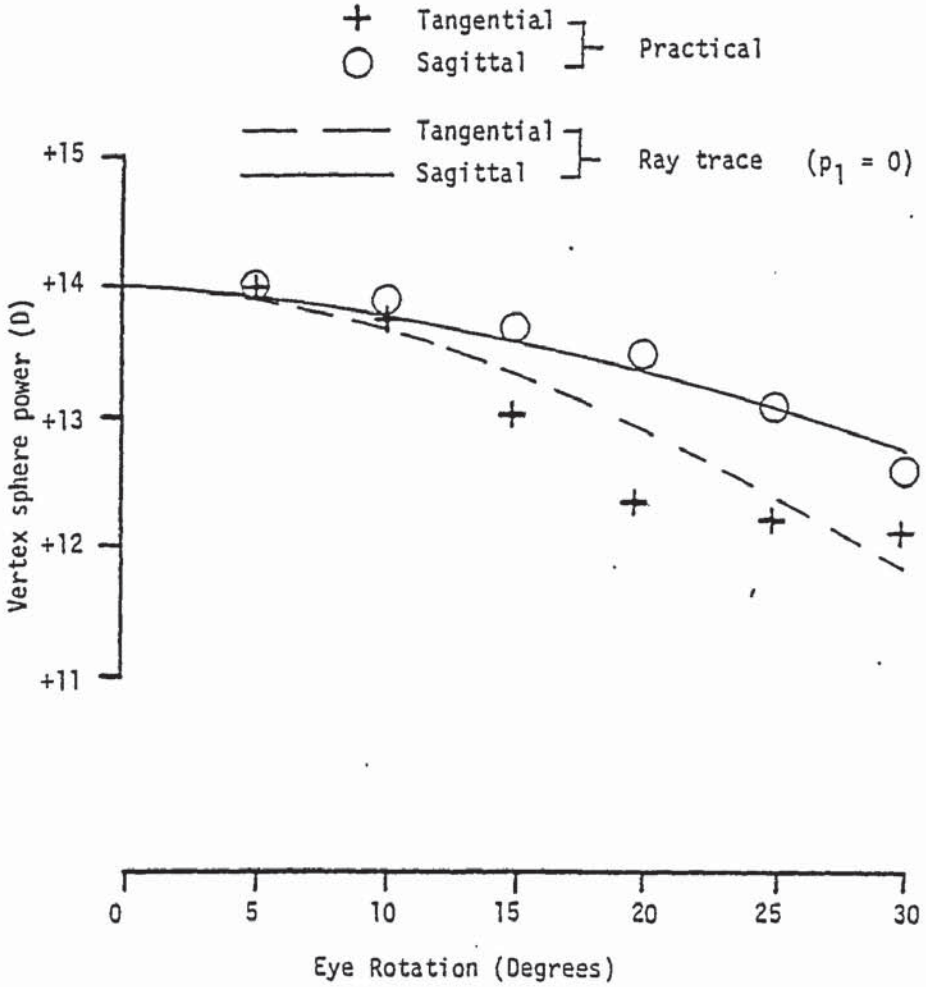

Figure 9.18

Distortion of Armorlite Multi Drop (as measured on the modified spectrometer) compared with theoretical values calculated for lenses with parabolic ($p_1 = 0$) and spherical ($p_1 = 1$) front surfaces. No.14 blank, lens parameters as in Table 9.1

Armorlite Multi Drop

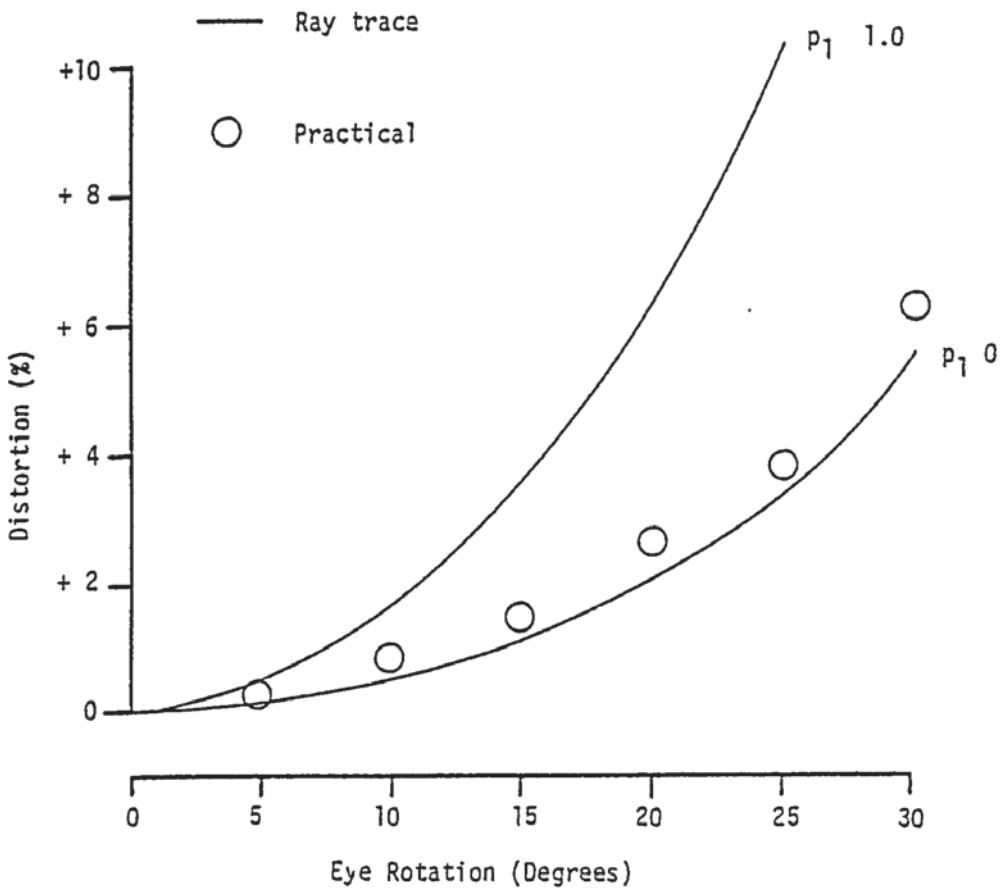

aberrations are somewhat different to commercially produced 'zonal aspheric' lenses. The comment is made by Smith and Atchison that 'the reason for this discrepancy is being investigated'.

9.3.3.1 THEORY

A schematic representation of a 'zonal aspheric' is shown in Figure 9.19. Here three intersecting curves are illustrated, with centres of curvature positioned at C_1, C_2 and C_3. Since it is required that there should be no discontinuity at the zone boundaries, C_1 and C_2 are on a common line with the point of intersecting of the zones at the surface, as are C_2 and C_3. The peripheral radii of a 'zonal aspheric' surface on the front of an aphakic power spectacle lens need to be progressively longer towards the periphery of the lens, in order to give acceptable optical properties. Combined with the previous requirement, this means that the centres of curvature are progressively offset to the opposite side of the axis of symmetry of the surface. For ray tracing purposes it is necessary to know the surface coordinates, in order that an equation may be fitted describing the surface. Thus from Figure 9.19, if the surface coordinates are required for any point inside the first zone, then these can be found quite simply from:

$$x = r_1 - (r_1 2 - y^2)^{\frac{1}{2}}$$

For the coordinates of any point outside the central zone (where 'i' is the zone number), then

Figure 9.19

Schematic diagram of an offset zonal aspheric, having three intersecting zones. The semi-diameter of each zone is given by y_1, y_2 and y_3

Offset Zonal Aspheric

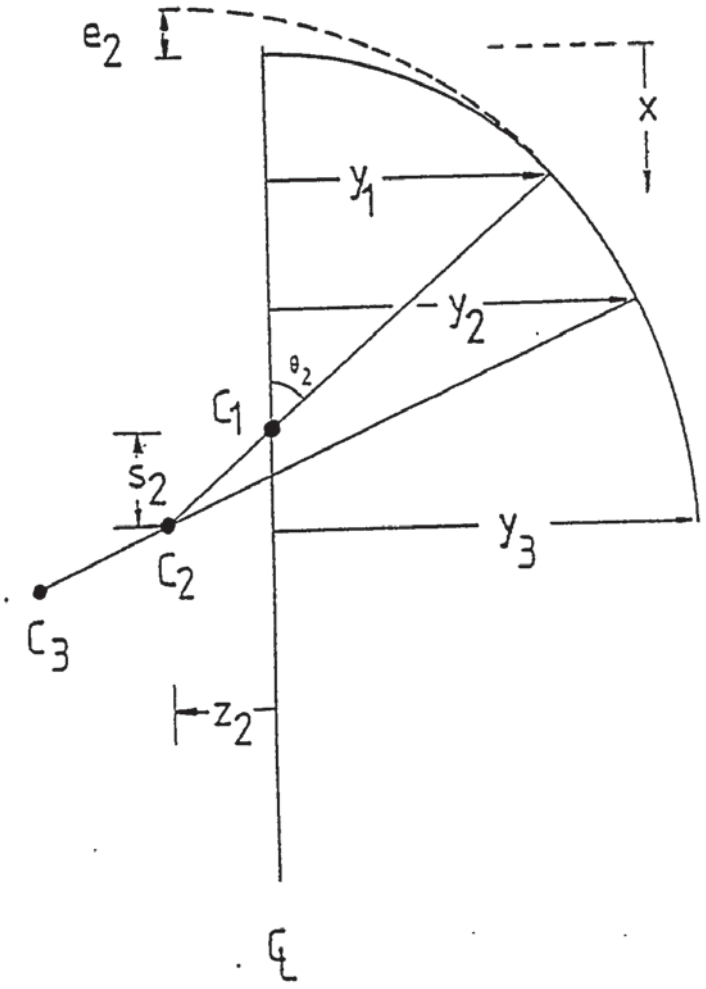

$$\text{Sin } \theta_i = \frac{y_{i-1} + z_{i-1}}{r_{i-1}}$$

$$z_i = (r_i - r_{i-1}).\text{Sin } \theta_i + z_{i-1}$$

$$s_i = (r_i - r_{i-1}).\text{Cos } \theta_i + s_{i-1}$$

$$e_i = r_i - (s_i + r_1)$$

then $$x = r_i - (r_i^2 - (y + z_i)^2)^{\frac{1}{2}} - e_i \qquad \text{- IX(2)}$$

(Note that $z_1 = e_1 = s_1 = 0$)

As Bennett (1978) pointed out, the peripheral zones are sections of a barrel torus, due to the offset of the centre of curvature from the axis of symmetry.

This mathematical model is one way of producing a 'zonal aspheric', but it is not the only method. Figure 9.20 shows a surface produced by a series of concentric coaxial curves with progressively longer radii towards the periphery. Obviously this will not produce a continuous smooth surface, as there will be a marked boundary to each zone, but this could be reduced during the smoothing and polishing process. As before the coordinates of any point within the central zone can be found from:

$$x = r_1 - (r_1^2 - y^2)^{\frac{1}{2}}$$

Figure 9.20

Schematic diagram of a coaxial zonal aspheric with three zones, having semi-diameters of y_1, y_2 and y_3

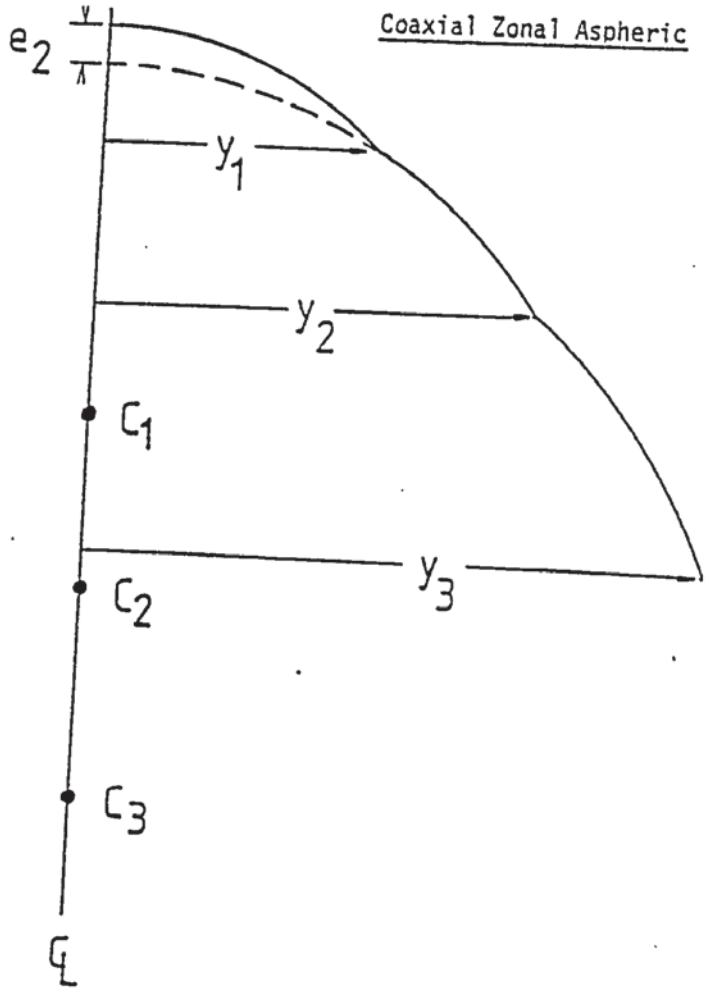
Coaxial Zonal Aspheric
e2
y1
y2
y3
C1
C2
C3
CL

Outside the central zone, to find the coordinates in zone 'i' then:

$$e_i = r_{i-1} - (r_{i-1}^2 - y_{i-1}^2)^{\frac{1}{2}} - (r_i - (r_i^2 - y_{i-1}^2)^{\frac{1}{2}}$$

thus

$$x = r_i - (r_i^2 - y^2) + \sum_i e_i \qquad \text{- IX(3)}$$

One type of commercially produced 'zonal aspheric' is the Armorlite Multi-Drop. Renier (1977) gives a detailed description of the surface of this lens, which is presumably correct as Welsh gives many editorial comments throughout the book. Although powers and diameters for the surface are given (Table 9.3), no indication is given as whether the constructon is offset or coaxial. It is also not apparent from Renier which is the most appropriate refractive index to use for converting the surface powers to radii of curvature. The obvious index would be 1.498 (CR39), corresponding to the lens material. However, inspection of a finished lens suggests that 1.523 (crown glass) gives values nearer to the mass produced product.

The coordinates of the front surface of a No. 12 blank Armorlite Multi-Drop, as calculated by the two methods described, are given in Table 9.4, based on the data of Renier. Also shown are the surface coordinates of a finished lens, measured using a travelling microscope. For ray tracing purposes, it is necessary to fit an equation to these coordinates, for example a polynomial of the

Table 9.3

Front surface zones of Armorlite Multi-Drop

Zone No.	Power (D)*	Diameter (mm)*	Radius (n=1.523)
1	12.37	24	42.28
2	12.00	30	43.58
3	10.50	40	49.81
4	9.00	50	58.11
5	8.00	58	65.38

*Data from Renier (1977)

Table 9.4

Surface coordinates, Armorlite Multi-Drop, No. 12 blank

y(mm)	Offset*	Coaxial(a)*	Coaxial(b)*	Practical
5			0.2967	
10	1.1996	1.1996	1.1996	1.1299
13.5			2.1977	
15	2.7465	2.7168		2.5307
17.5			3.5799	
18	3.9903	3.7706		3.6226
20	4.9512	4.5962		4.4493
	x values (mm)			

Curve fit

P	-0.063	0.275	-0.103	-0.700
A	2.391 E-6	-	-	-
B	-2.171 E-9	-	-	-
Error sum (mm)	0.01	0.346	0.102	0.010

*Derived from Renier (1977) data

form:

$$x = \frac{cy^2}{1 + (1 - pc^2y^2)^{\frac{1}{2}}} + Ay^4 + By^6 \qquad - IX(4)$$

For the curve fits shown in Table 9.4, each term of the equation was progressively applied to the data, and an error score derived. The form of the equation with the minimum error score was used to give the best fitting curve. In three out of the four cases shown, this consisted simply of the first term, and hence the curve fitted is a conic.

9.3.3.2 Results

It would perhaps be surprising if a lens surface of 'zonal aspheric' construction could be adequately fitted with an equation of the form described. However, in the central area of the lens, a reasonable fit (from the error scores) can be obtained using the 'offset' design philosophy, and also on the actual lens. The equivalent data points from the coaxial design 'coaxial (a)' in Table 9.4 yielded a poor error score. On inspection of the 'y' values used in relation to the zone margins, it will be apparent that these 'y' values are on or very close to zone margins in some instances. Thus it was decided to use 'y' values in the central part of each peripheral zone, as well as two points in the central zone. This is shown as 'coaxial (b)' in Table 9.4, where the reduction in error score is apparent.

The reasoning behind the choice of points in 'coaxial (b)' is shown in Figure 9.21. As the finished lens is moulded from glass moulds, the lens curves are ground in negative form. It is thus likely that the boundaries between zones would be reduced during the smoothing and polishing processes, so that the mid points of zones would be more representative of the finished lens.

9.3.3.3 Ray Tracing Results

The results of ray tracing through the various designs shown in Table 9.4 are shown in Figure 9.22. The lens thickness was taken to be 8.25 mm, refractive index 1.498, and distance of lens to centre of rotation 27 mm. The finished lens had a rear surface power -0.24 D, giving a front surface paraxial radius of 43.43 mm. The graphs of Mean Oblique Error (MOE) show that the 'offset' model gives a design quite close to a spherical surface, as shown by Smith and Atchison (1983c). 'Coaxial (b)' on the other hand is much more aspheric, and shows results that are closer to the finished lens. Besides ray tracing through coordinates derived from a travelling microscope, this lens was measured with a focimeter having a rotating lens support, simulating the rotation of the eye.

Figure 9.23 shows a comparison of distortion values for the various designs and the finished lens, measured using the modified prism spectrometer. Again, the near spherical values of the 'offset' model are shown, as well as the close relationship of the 'coaxial (b)' model to the finished lens.

Figure 9.21

Section through mould for coaxial (b) type surface showing possible effects of smoothing and polishing at points A and B in reducing the ridge between zones.

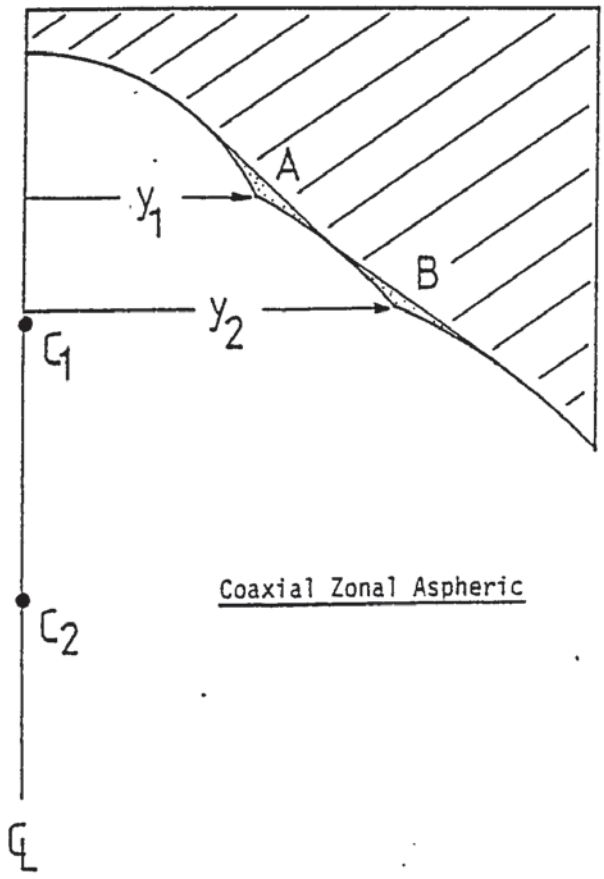

Coaxial Zonal Aspheric

Figure 9.22

Results of ray trace through various designs of lenses with front surfaces given by curve fitting through the coordinates of Table 9.4

A Spherical

B Offset zonal aspheric

C Coaxial (b) zonal aspheric

D Best fitting conic to Armorlite Multi Drop No. 12 blank

The circles represent practical measurements on the lens with a modified focimeter.

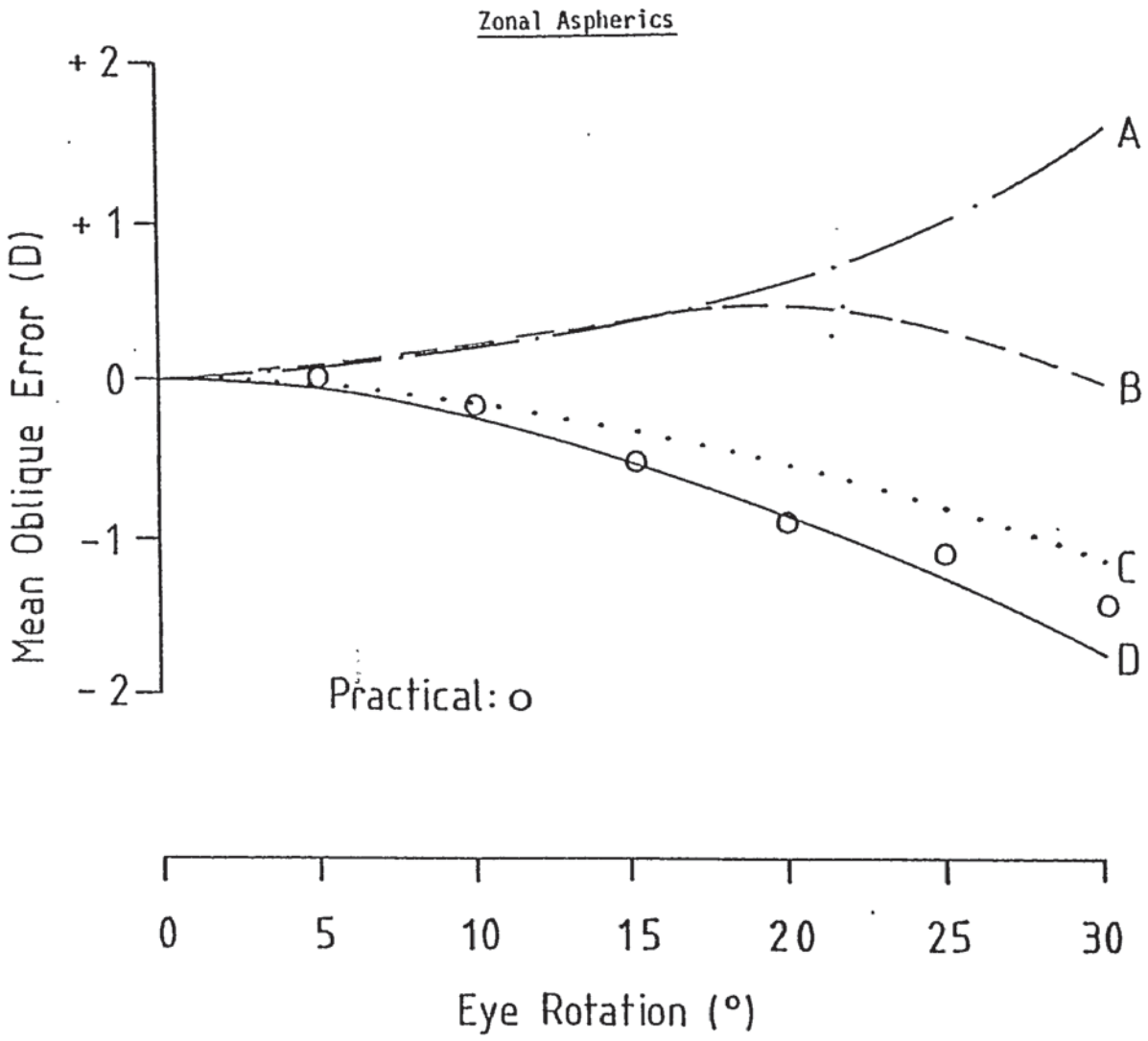
Zonal Aspherics
+ 2
+ 1
0
-1
- 2
Mean Oblique Error (D)
A
B
C
D
Practical: o
0
5
10
15
20
25
30
Eye Rotation (°)

Figure 9.23

Results of ray tracing through various designs of lenses with front surfaces given by curve fitting through the coordinates of Table 9.4

A Spherical

B Offset zonal aspheric

C Coaxial (b) zonal aspheric

D Best fitting conic to Armorlite Multi Drop No. 12 blank

The circles represent practical measurements on the lens with a modified spectrometer.

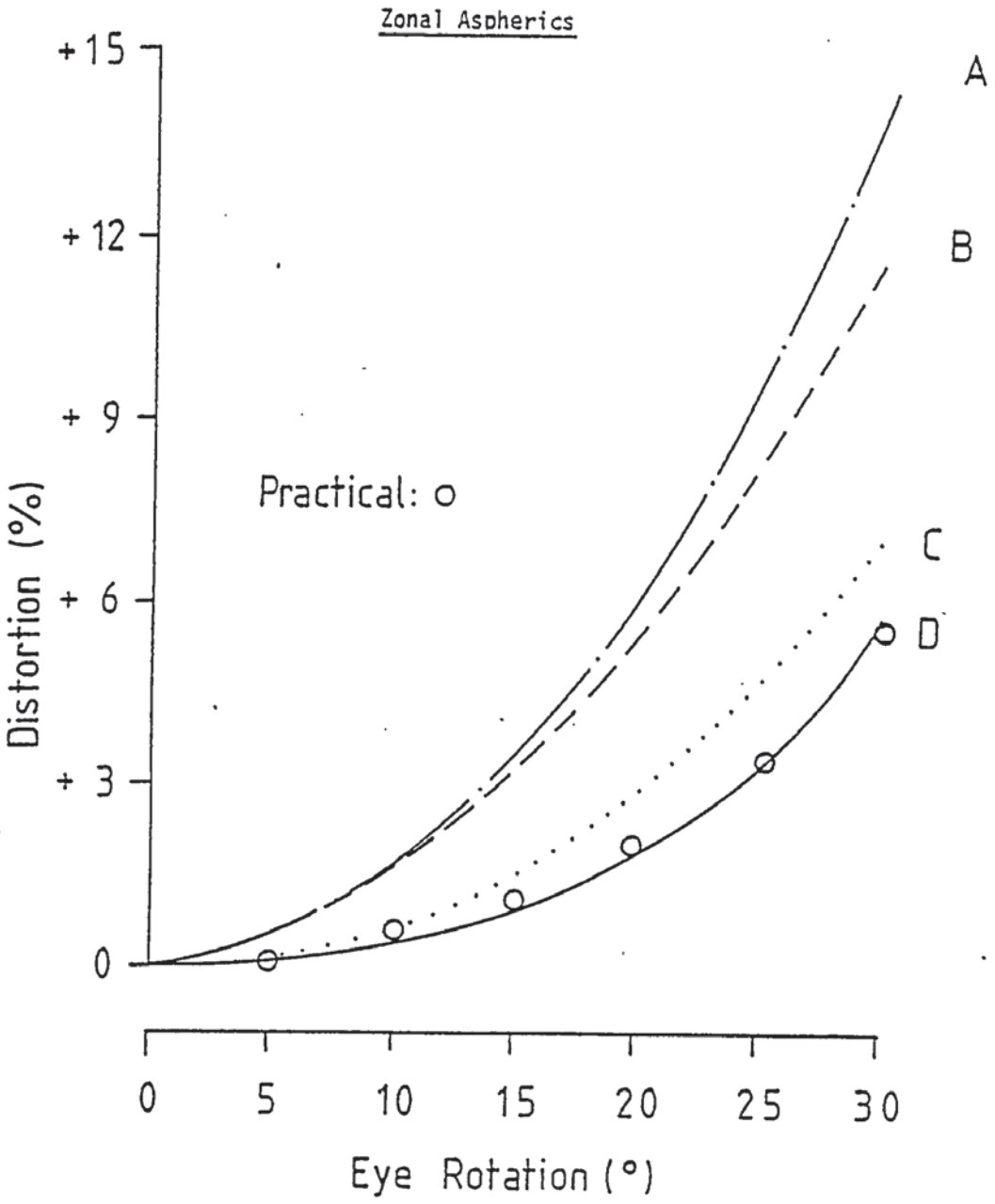
Zonal Aspherics
+15
+12
+9
+6
+3
0
Distortion (%)
Practical: o
A
B
C
D
0
5
10
15
20
25
30
Eye Rotation (°)

9.3.3.4 Conclusions

The above results would seem to show that the 'offset' curve model of a 'zonal aspheric' surface, as proposed by Smith and Atchison (1983c) does not apply to the surface form of the Armorlite Multi-Drop lens, and that some sort of smoothed coaxial surface gives a more realistic concept of an actual lens. It is possible, of course, that there is another answer: the lens surface may be ground as an offset curve, but the smoothing and polishing process may progressively flatten the lens periphery.

9.3.4 Younger high index glass aspheric

This lens is one of only two glass designs considered in this comparison. Unfortunately, not much is known of the design or the philosophy behind it. An enquiry to the manufacturer (Younger Manufacturing Company, Los Angeles, USA) gave only the fact that the aspheric surface was not a conic section, but had been designed to give the best acuity up to 30 degrees.

This lens is not readily obtainable in this country, but an example with a power of +12.25 DS was kindly donated by the Norville Optical Company Limited. As can be seen in Table 9.1, this lens is made of 1.701 index glass which gives the finished product a low centre thickness, but does make it heavy. In addition, the constringence of the glass is only 30, giving approximately double the transverse chromatic aberration of an equivalent CR39 lens.

Figure 9.24

Oblique astigmatism (measured on the modified focimeter) of Younger high index glass aspheric compared with ray trace values for equivalent lens with parabolic (p_1=0) front surface. Lens parameters as in Table 9.1

Younger glass aspheric

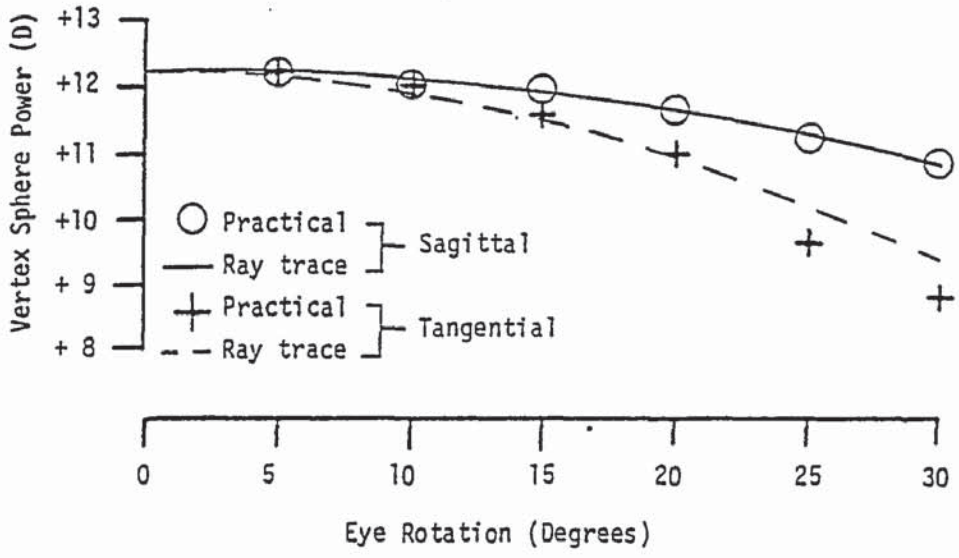

Figure 9.25

Distortion (measured with the modified spectrometer) of Younger high index glass aspheric compared with ray trace values for equivalent lenses with spherical (p_1=1) and parabolic (p_1=0) front surface. Lens parameters as in Table 9.1

Younger glass aspheric

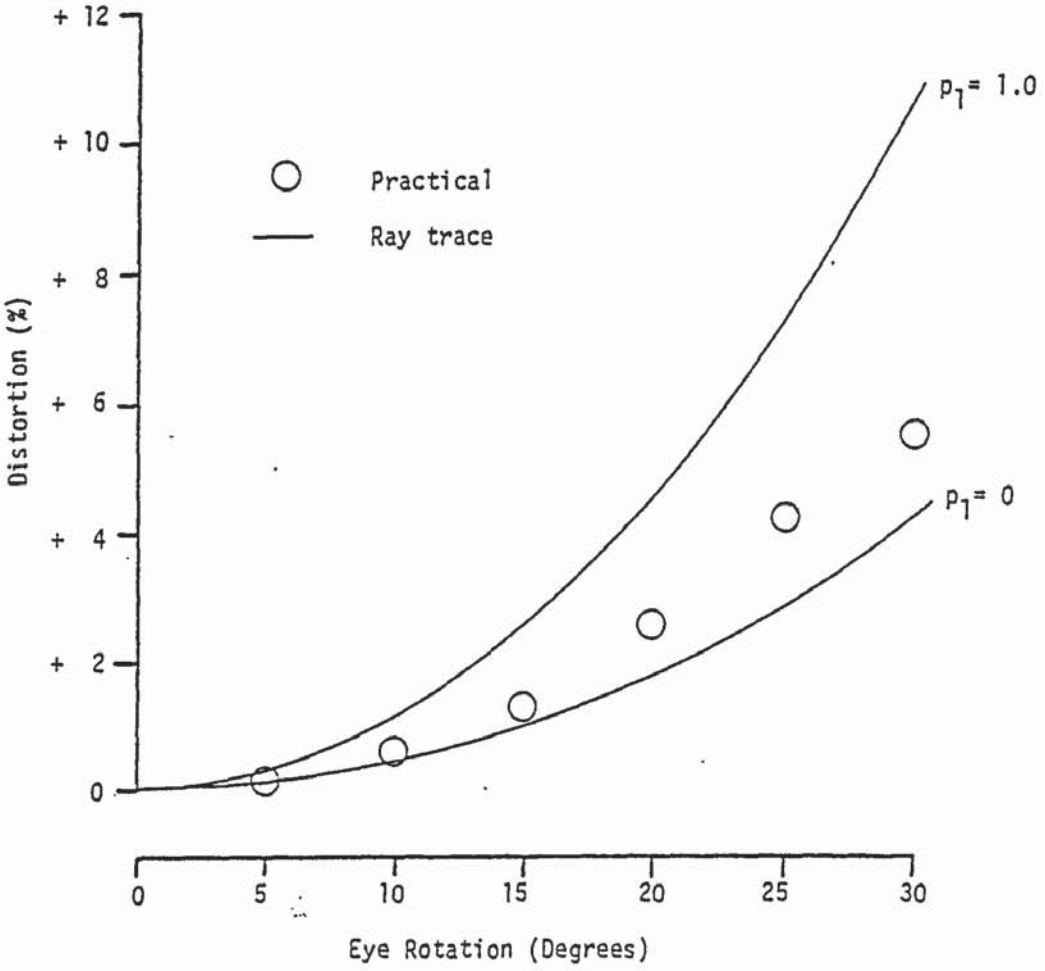

The measured values of oblique astigmatism and distortion are shown in Figures 9.24 and 9.25 respectively. These results illustrate that the central zone of the lens is fitted quite well by a front surface conic with a 'p_1' value of zero, which will certainly give low distortion, but the wearer will have peripheral blurred vision due to the power drop at the edge of the lens. A benefit of this reduction of power will be to reduce the effects of the transverse chromatic aberration.

9.4 BLENDED LENTICULAR LENSES

Four commercially produced designs were measured in this group, three made in CR39 plastic, and one in high refractive index glass. The three CR39 lenses have a very similar uncut diameter (66 or 67 mm), and a very similar appearance.

9.4.1 American Optical 'Ful-Vue'

From Figure 9.26 it can be seen that the example of this lens agreed very well with the theoretical values predicted by ray tracing for oblique power measurements. There is slightly greater tangential power at most angles sampled, but nowhere near the discrepancy, for example, found in the case of the same manufacturer's earlier lenticular design. One interesting feature of these measurements is the large amount of oblique astigmatism at 30° eye rotation, compared with the figures in the patent. This is due to the patent ray trace being carried out a centre of rotation to lens distance of 23 mm, whereas the measurements here were taken at 27 mm. This would be expected from the calculations made in Chapter 5.

The distortion measurements did not agree so well with the theory, as shown in Figure 9.27. This difference could be caused by the difference in mean power noted above.

9.4.2 Essilor 'Omega'

This lens is of unknown design, except that the central area of the

Figure 9.26

Oblique astigmatism, American Optical Ful-Vue

Ful-Vue

Comparison of aberration measurements from focimeter with ray trace of theoretical lens design from patent

BVP: + 14.50 DS F_2: - 1.767 D t: 10.75 mm n_d: 1.498 z: 27 mm

Aspheric coefficients of front surface (from AO patent US 4,181,409)

p 0	C 8.38095E-12
A 1.28124E-6	D -2.38066E-14
B 1.8212E -9	

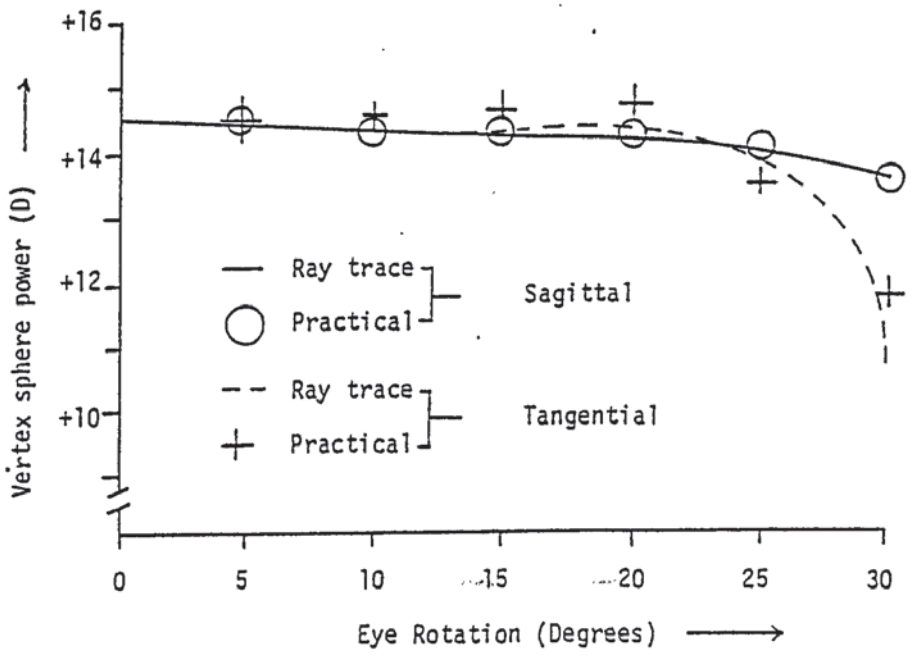

Figure 9.27

Distortion of American Optical Ful-Vue, as measured on the modified spectrometer, compared with theoretical values from ray trace. Lens parameters are as shown in Figure 9.26

American Optical Ful-Vue

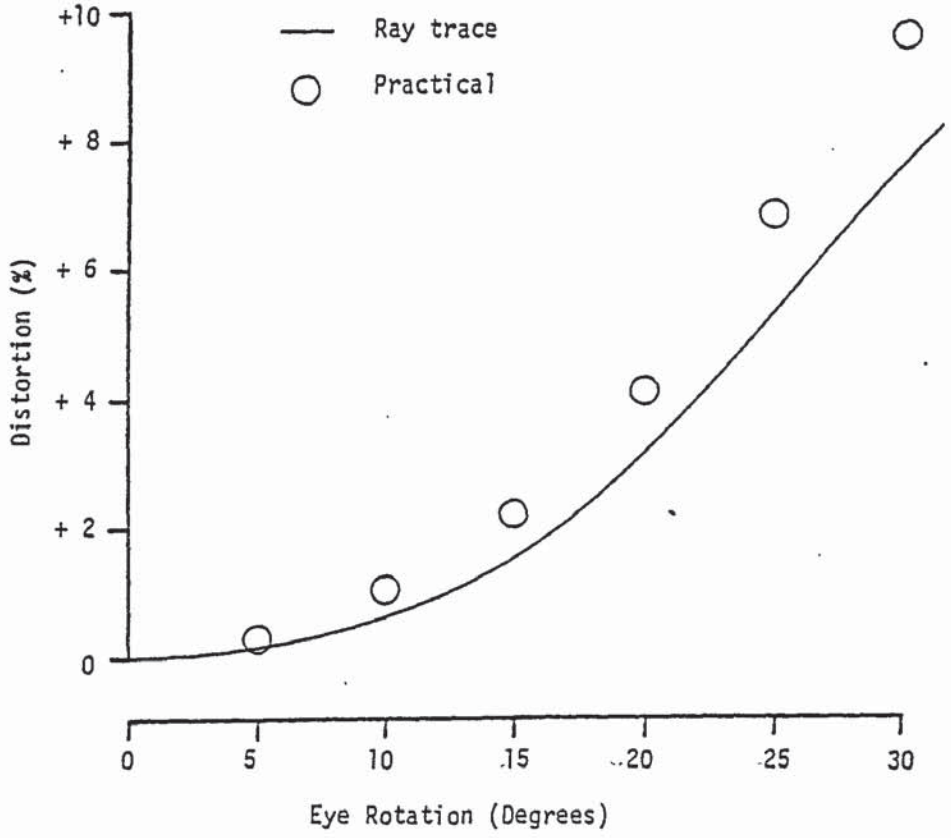

Figure 9.28

Essilor Omega, Mean Oblique Power, Lens parameters as in Table 9.1

Omega

Comparison of mean oblique power readings from the focimeter with a ray trace through lenses with various values for front surface conic asphericity

BVP: + 13.80 DS F_2 - 3.054 D t: 10.90 mm n_d: 1.498 z: 27 mm

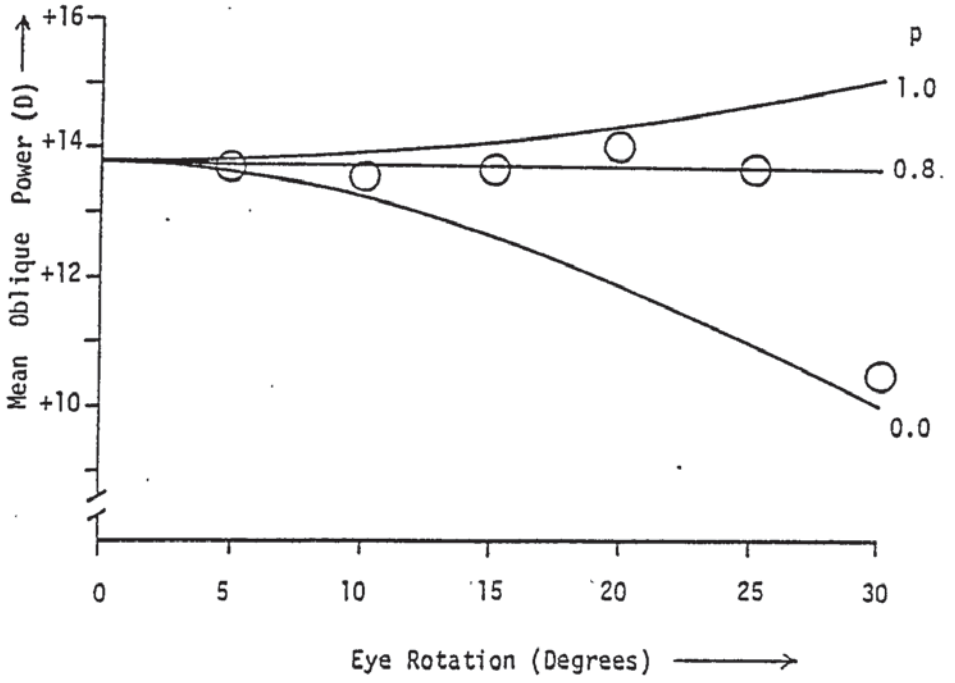

Figure 9.29

Distortion of Essilor Omega compared with expected values from ray trace. Lens parameters as in Table 9.1

Essilor Omega

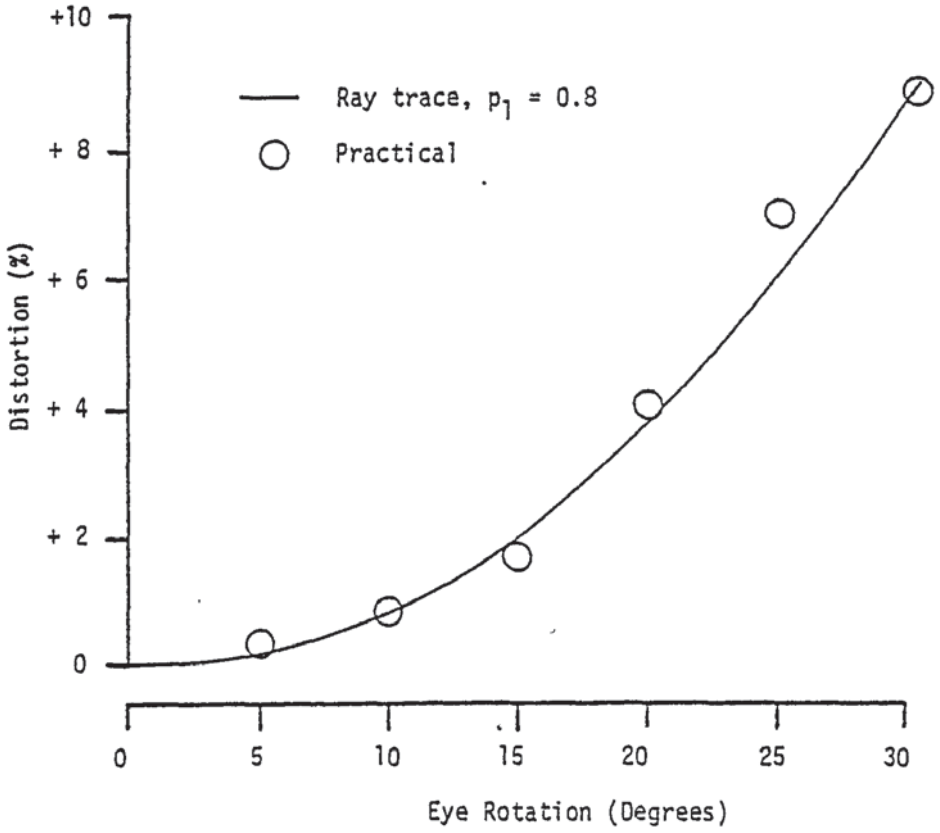

Figure 9.30

Essilor Omega oblique astigmatism, comparison with nearest Ful-Vue equivalent

Omega

Comparison of aberration measurements from focimeter with ray trace, assuming AO Ful-Vue aspheric coefficients

BVP: + 13.80 DS F_2:- 3.054 D t: 10.90 mm n_d: 1.498 z: 27 mm

Aspheric coefficients (from AO patent, US 4,181,409) of front surface:

p	0	C	9.01109E-12
A	1.39112E-6	D	-2.51844E-14
B	1.97901E-9		

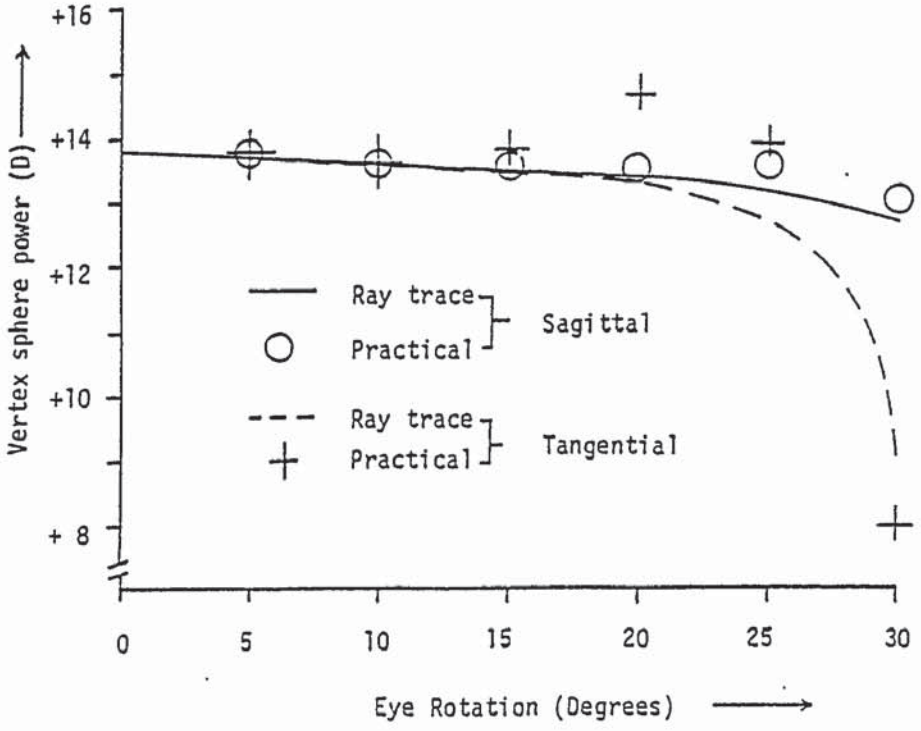

lens is ellipsoidal. Thus oblique power measurement were compared with calculated values for various ellipsoids, as shown in Figure 9.28. It is apparent that a p_1 of 0.8 gives a reasonable agreement with the experimental data, at least up to eye rotation of 25 degrees. This is confirmed by the distortion measurements. (Figure 9.29).

After the appearance of the 'Omega' on the market, Essilor were sued for patent infringement by American Optical. To see how close the two designs are, the practical measurements from the Omega were compared with the calculated values from the nearest Ful-Vue blank.

By calculation from the measured parameter, the Omega was found to have a paraxial radius of curvature of 33.17mm. The nearest Ful-Vue blank is the No. 15 with a paraxial radius of 33.23 mm. A comparison of the oblique power measurements is shown in Figure 9.30, where there is an obvious similarity between the practical Omega measurements and the Ful-Vue design. Whether this constitutes patent infringement is a matter of opinion, but the case was not proven in court.

9.4.3 Rodenstock Perfastar

As with the Ful-Vue, a detailed patent specification has been published for this lens, but as mentioned earlier, two designs are patented for a number of paraxial powers, thus it is not known which design of lens has been manufactured. Figure 9.31 illustrates the power measurements compared with a type 2 design.

Figure 9.31, 9.32

Mean Oblique Error (M.O.E) of Rodenstock Perfastar and astigmatism, as measured with the modified focimeter, compared with ray trace through lens, aspheric coefficients (Type 2) from patent (9.31).

Comparison of same lenses as Figure 9.31, but showing distortion (9.32). Measurements taken on modified spectrometer.

Lens parameters as in Table 9.1. Aspheric coefficients (from Guilino, Barth and Koeppen, 1983) of front surface:

K	-0.495
A	9.6 E-6
B	2.6 E-7
C	1.0 E-10
D	1.0 E-12

Rodenstock Perfastar

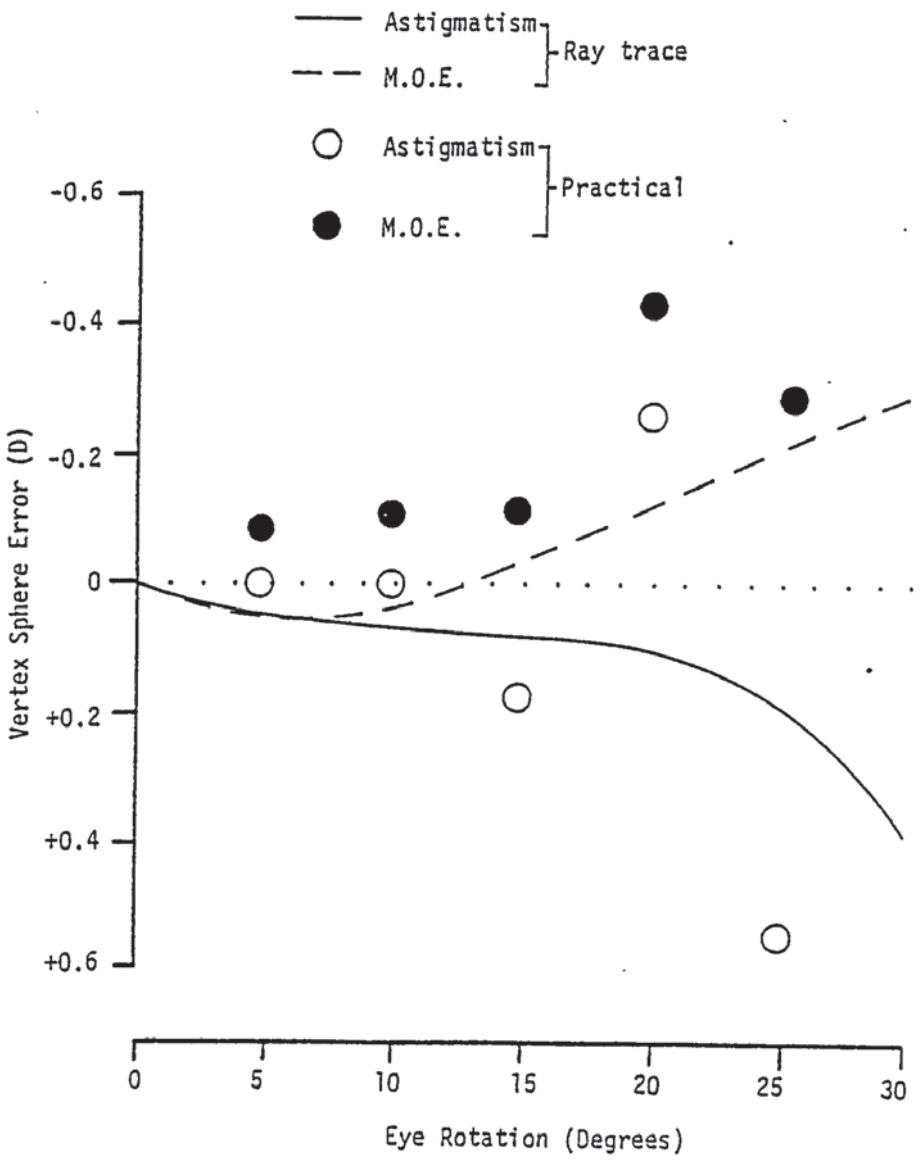

Rodenstock Perfastar

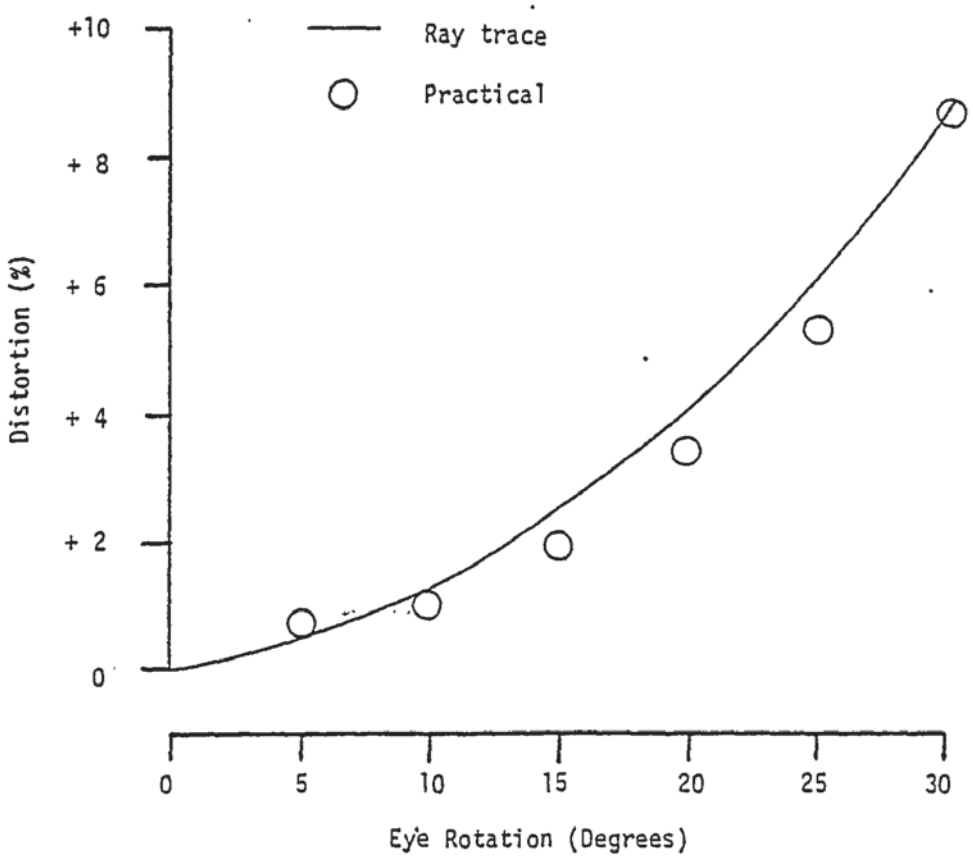

This type of diagram has been used to represent the data as it is the form in which the design is illustrated in the patent. This shows that the lens does not agree well with the patent specification, particularly at an eye rotation of 20 degrees. It should be noted that no measurements were possible at angles greater than 25 degrees as a clear focimeter image could not be obtained.

The distortion measurements, on the other hand, show a good correlation between the practical measurements and theoretical predictions. (Figure 9.32)

9.4.4 Hoya THI

This lens is manufactured in high index (n=1.806) glass, and is much smaller in diameter (55 mm) than the other lenses in this group. There is no known published information on the design of this lens.

Results of focimeter measurement on a +14.25D lens are shown in Figure 9.33, with ray trace values, for a front surface conic with a 'p' of 0.2 for comparison. This shows the rapid power reduction off axis, giving a mean power error of approximately -2D at 25 degrees. From the distortion results (Figure 9.34) it is apparent that this design gives a lens with very low peripheral distortion. The abrupt change in distortion between 25 and 30 degrees is due to the change from central powered zone to the blending area.

Figure 9.33, 9.34

Hoya THI oblique astigmatism, as measured on the modified focimeter (9.33) and distortion, as measured on the modified spectrometer (9.34) compared with ray trace through lens having conic front surface, $P_1 = 0.2$. Lens parameters as in Table 9.1

Hoya THI

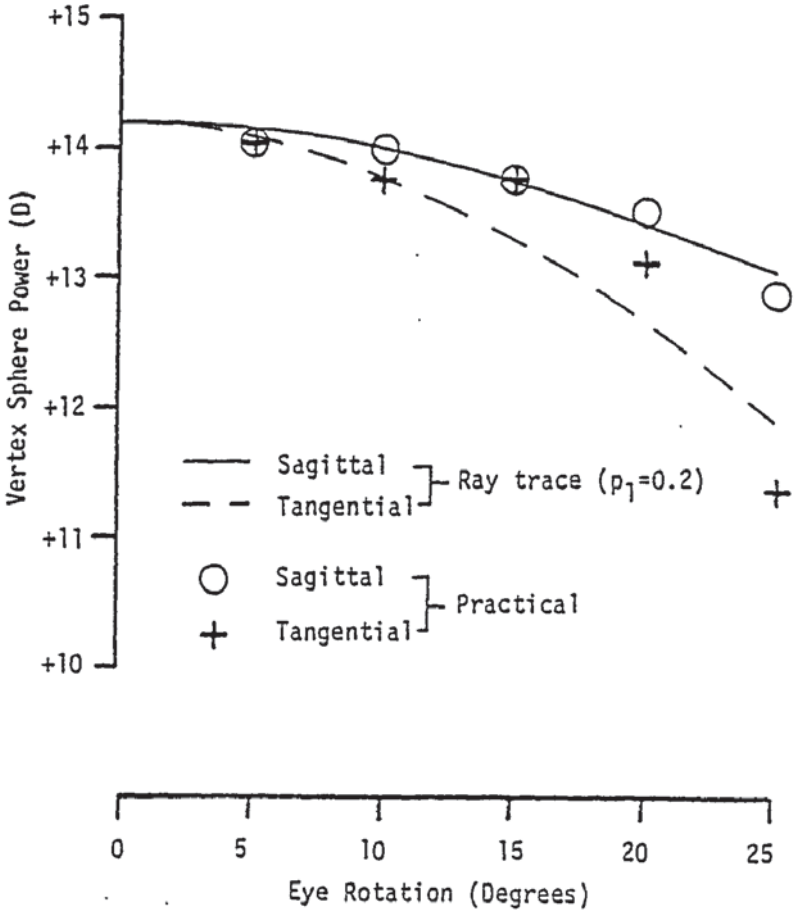
+15
+14
+13
+12
+11
+10
Vertex Sphere Power (D)
Sagittal
Tangential
Ray trace (p_1=0.2)
Sagittal
Tangential
Practical
0
5
10
15
20
25
Eye Rotation (Degrees)

Hoya THI

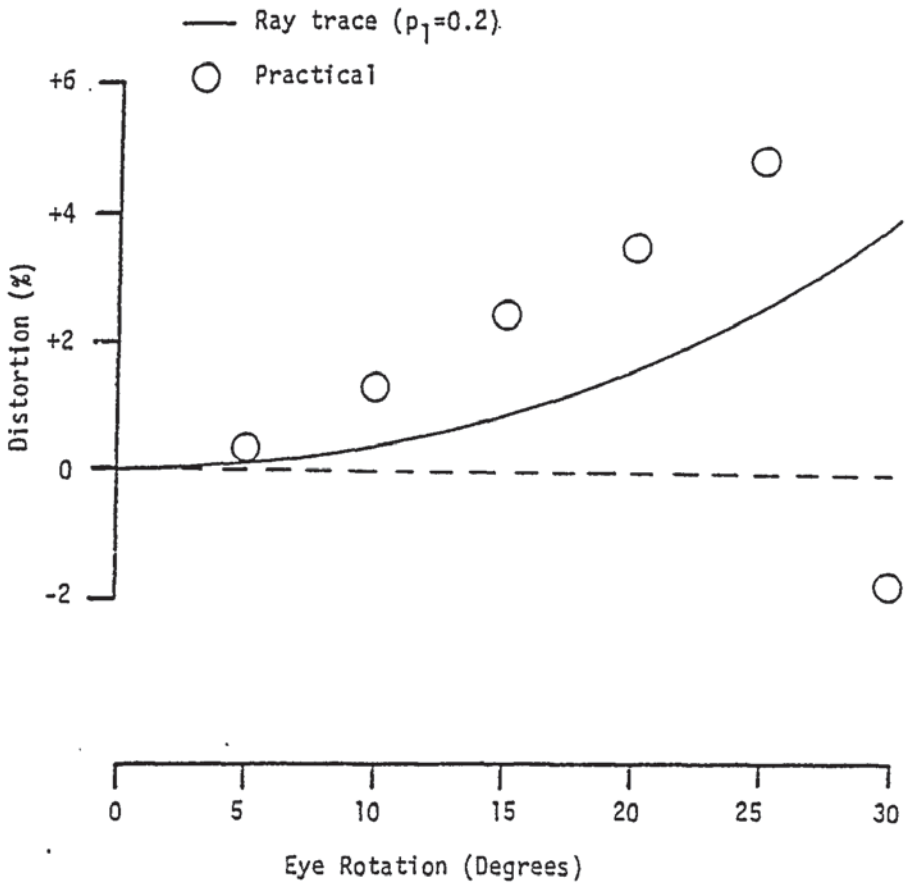
Ray trace (p_1=0.2)
Practical
+6
+4
+2
0
-2
Distortion (%)
0
5
10
15
20
25
30
Eye Rotation (Degrees)

PART 3

CHAPTER 10

Design and Construction of an Alternative Lens

From Parts 1 and 2, it will be apparent that aphakic lens designs currently being promoted fall into two main groups, the 'drop' type lenses and the blended lenticulars. Another feature of these lenses is that there is very little variation of design within each group. The most recent designs have all been in the blended lenticular group, no doubt because of the large uncut diameter obtainable. The question raised by this work was whether the blended lenticular format could be modified to give a more extreme lens which was still subjectively acceptable. Thus the purpose of the work described here was to see if the lens design in the blended lenticular category could be modified to give a lens with improved cosmetic appearance and reduced weight. As lens designs can only be evaluated effectively by practical tests, a method was evolved for the manufacture of this type of lens. Finally, the lenses were tested on a sample of aphakic patients.

10.1 Lens Design

There seems to be no end to the fashion for large aperture spectacle frames, and such frames are being glazed with lenses of higher power now that lens forms are available which render this possible without undue penalty in weight, appearance or optical properties. But how far can this trend continue? To illustrate the problems of large aperture, thin spectacle lenses of appreciable power, consider the lens shown in Figure 10.1.

Figure 10.1

Thoretical oblique astigmatism of flat form spherical lens

Flat Spherical Lens

B.V.P.: +14.00 F_2:Plano t: 12 mm

n_d: 1.498
z: 27mm

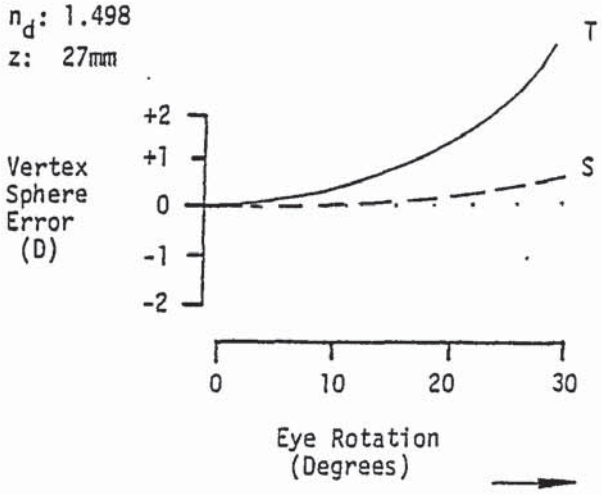

This is a flat +14.00 DS lens with centre thickness of 12 mm. The maximum diameter that such a lens could be manufactured, with a knife edge, is 57 mm. Having a spherical front surface, the optical properties on eye movement are less than optimum, as shown by the rapid increase in tangential power error (T) compared with sagittal (S) error.

However, it is known that such lenses are acceptable to some aphakics, so could the lens design be modified to give a thinner, better looking lens? Commercially available aspheric lenses of this power have a centre thickness in the order of 10 mm, so for an improved design we should aim for a further significant reduction in centre thickness, to around 7.5 mm. If we wish to make a lens with a 57 mm uncut diameter with this thickness, then a conic section front surface could be used, with a 'p' value calculated from:-

$$p = \frac{2rx - y^2}{x^2} \qquad \text{— X(1)}$$

of -4.2, a hyperboloid of revolation. The oblique astigmatism and curvature of this design are illustrated in Figure 10.2, and show the very rapid change in lens power with eye rotation from the axis of symmetry. Thus at 10 degrees off axis there is already -1.50 D of oblique astigmatism. It was felt that this change of power was too rapid, and that to be acceptable, an 'island' of central stablished power was required, in a similar manner to that employed in the commercial blended lenticular designs. But because the lens would be thinner than these designs, the central island would be inevitably smaller.

Figure 10.2

Theoretical oblique astigmatism of flat form lens with front hyperbolic surface

Hyperboloid Surface Lens

B.V.P.: +14.00 F_2 : Plano t: 7.5 mm

n_d: 1.498 z: 27 mm p_1: -4.2 p_2: 1.0

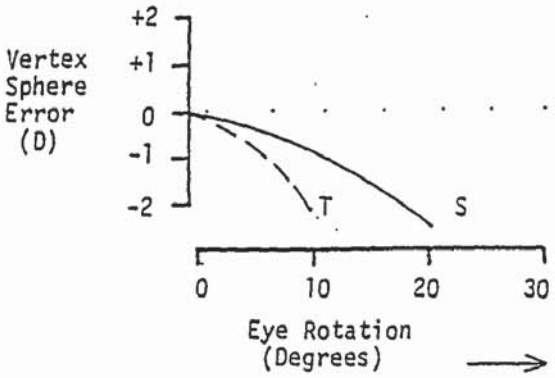

The choice of lens material was straightforward in that it was felt that a plastic material was desirable, both from the point of view of low weight and ease of fabrication. High refractive index (> 1.523) glass has the attraction of reduced curvature for a given surface power, but unfortunately this is gained at the expense of a material density of 2.99 or more, compared with 1.32 for CR39 plastic material. Undoubtedly, high refractive index plastic lenses will be increasingly used as these materials become available (Tarumi, Komiya and Sugimura, 1982).

10.2 Lens Production Method

Conventional methods for producing aspheric surface lenses included:-

1. Generating curve on lens or mould by the use of a numerically controlled meachine tool.

2. Generating curve with specialist aspheric curve generator. (Volk 1966a, 1966b, Twyman, 1952)

3. Grinding lens or mould with series of intersecting spherical curves, on conventional machinery, to give an approximation to an aspheric curve.

4. Sagging glass lens or glass mould for plastic lens by heat deformation.

None of these methods was readily available, so a different approach was taken, based on method 4.

Conventionally, CR39 plastic spectacle lenses are manufactured by polymerising the liquid monomer between glass moulds. After suitable heat treatment, the plastic hardens and the moulds can be removed, leaving a finished lens. An alternative procedure is to make a lens significantly thicker than ultimately required, after which one surface is cut on a prescription generator to the required curve, at the same time the lens being reduced to the required centre thickness. This latter method has the advantage of reducing the number of different moulds required to cover the wide range of possible rescription variations. CR39 has the advantage of being a thermosetting plastic, so that it is not deformed by heat during curve lapping, and can thus be processed on similar machinery to that used for the production of glass lenses.

The problem with producing glass moulds or lenses by sagging (Twyman, 1952) is that high temperatures are required for the deformation of the glass. It appeared more attractive to sag moulds in plastic materials, as this would require a much lower temperature, and should be easier to control. Additionally, the former used for producing all or part of the required curve need not be heat resistant to any great extent, and could be a glass or plastic spectacle lens. There is an inherent difference between the use of glass and plastic moulds, however. It is obviously essential to sag a mould from thermoplastic material, such as 'Perspex' (I.C.I. Ltd) acrylic sheet. It was found empirically that 'Perspex' forms a strong bond to CR39 during heat curing, and this if transparent sheet is used, a lens is produced where the thermoplastic mould ends up as an integral

part of the finished lens and is not reusable.

Deformation of sheet thermoplastic material is a well known method of scleral contact lens manufacture, using a replica of the anterior part of the eye as a former. Composite constuction of CR39 spectacle lenses has been suggested before (Bausch and Lomb, 1966), mainly in order to avoid the build up of stress in thick section CR39 lenses during polymerisation. The formation of thermoplastic reflectors by pressure deformation was suggested by Leach (1980) for the production of cheap reflectors.

One of the advantages in using 'Perspex' sheet and CR39 plastic for the bulk of the lens is that the dividing line between the two materials is virtually invisible, due to the small difference between their mean refractive indices, CR39 being 1.498 and 'Perspex' 1.491.

The procedure for mould production is illustrated schematically in Figure 10.3 'Perspex' transparent sheet, 1½ mm in thickness (1), is clamped in an annular brass support (2), which consists of two rings bolted together, having a free aperture of 65 mm in diameter. The plastic sheet is deformed by a former (3) after being heated from beneath by an electric radiant heat source (4). The depth of indentation is assessed by the use of a micrometer dial gauge (5) attached to the former support.

The former used consists of a glass or plastic spectacle lens mounted on a supporting rod coaxial with the axis of symmetry. CR39 spectacle lenses are quite suitable for this purpose, as

they are not affected by the relatively low temperatures (around 150 degrees C.) used for the deformation of the 'Perspex'.

10.2.1 Stages in mould production

1. The 'Perspex' sheet is clamped in the brass support and placed in the press. The former is placed against the sheet, and a zero micrometer reading taken. The former is then clamped in a position out of contact with the sheet.

2. The 'Perspex' sheet is heated from beneath for around 5 minutes, with the top surface being used as a reflector to view an electric light bulb. This makes visible the deformation of the sheet that occurs during the heating process. Initially, the sheet deforms considerably due to the heat being applied to one surface only. After a few minutes, these deformations mostly disappear, when the light bulb can be viewed undistorted.

3. The former is lowered to be in contact with the hot 'Perspex' sheet, and pressure is than applied so that the former deforms the sheet to the depth required. At this point, the former is clamped in position and the heat source removed.

4. The deformed sheet is allowed to cool down to room temperature, at which stage the brass support is dismantled. After inspection, the mould is trued to its finished size on a lathe.

Figure 10.3

Method for pressing front surface mould of blended lenticulars

Production of Front Surface Moulds

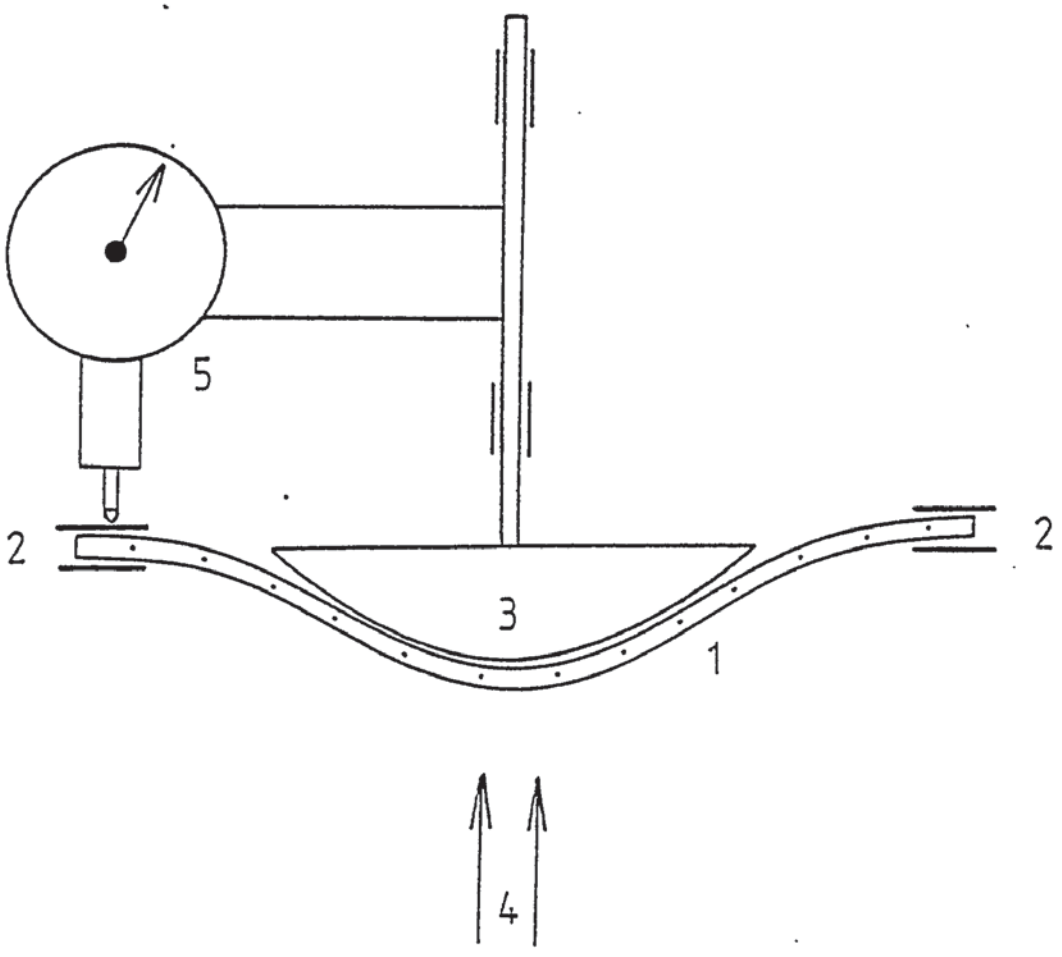

5. The heat deformation process causes a considerable build up of stress in the 'Perspex'. If this is not relieved, the considerable stress put on the moulds by the shrinkage of CR39 during curing will cause the 'Perspex' to crack. Thus moulds are annealed in a low temperature oven at 85 degrees C. for a minimum of two hours, and are then allowed to cool gradually to room temperature. This annealing is recommended by the manufacturers of 'Perspex' to reduce the stress build up in cementing the material in normal use (I.C.I., 1957).

10.2.2 Lens Production

Once the front surface moulds have been produced, lens production is virtually identical to that of conventional CR39 lenses with two glass moulds. The plastic mould is placed in flexible gasket with a rear glass spherical surface mould. Many different types of gasket were tried, but the most successful were those used by Sola Optical (UK) Ltd for the manufacture of semi - finished CR39 lenses. After assembly, the mould cavity is filled with liquid CR39, which is then cured at temperatures up to 45 degrees C. for 18 hours. The temperature cycle must be carefully controlled to avoid excessive build up of internal stress in the material.

As the front surface mould is retained in the finished lens, this must have its outer surface protected during the moulding process. Any seepage of excess material through the edge of gasket on to the front surface will cure to non - removable drips during polymerisaton. Thus many forms of protection were tried

before a material was found that was resistant to hot CR39 liquid monomer, and yet could be readily removed from the 'Perspex' at the end of the process. The eventual solution was to use 'Surface Saver' plastic lens protection film (3M Ltd), with the exposed edge sealed by 'Araldite' adhesive (Ciba - Geigy Ltd). Although 'Surface Saver' is self adhesive, this adhesive is dissolved by liquid CR39. After curing, the protective film can be peeled off, any remaining 'Araldite' being removed from the edge of the lens with a knife.

For the reasons mentioned earlier, lenses were made in semi - finished form, the rear surface being finished by grinding and polishing on conventional lens manufacturing machinery.

10.3 Optical Characteristics of Lenses

It is evident that the optics of the finished lens are going to be influenced first by the type of lens used as former, and secondly by the depth of indentation of the former during mould production. For formers, 40 mm aperture Sola aspheric lenticular semi - finished lenses were used. This type of lens surface gives a good correction for oblique astigmatism, which was required in the central 'island' of the finished blended lenticular.

To illustrate the relationship of optical properties to depth of pressing, a series of moulds were made using a Sola +14 D base lens as former. These were then cast as finished lenses, using flat glass plates as rear surface moulds, with a constant edge thickness. The parameters of the lenses produced are shown in

Figure 10.4

Stages in production of semi-finished blended lenticular

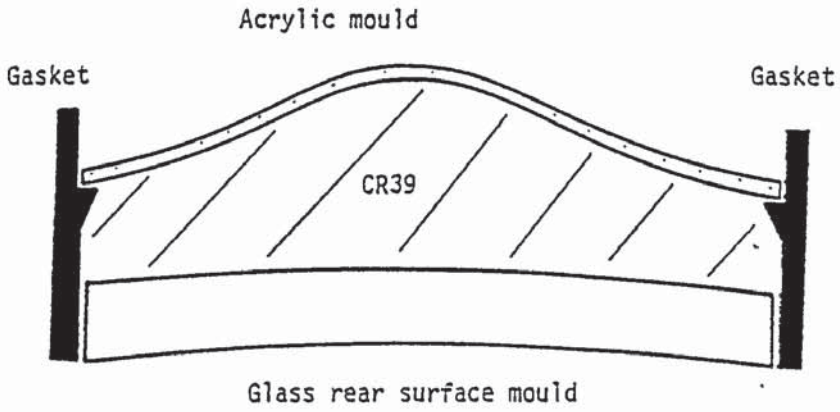

Section through lens during moulding

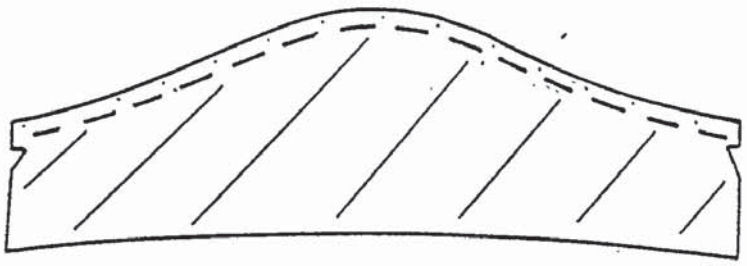

Semi-finished lens

Table 10.1

Variation of lens parameters to depth of pressing

Lens	Pressing Depth (mm)	Centre 't' (mm)	F (D) 2	B.V.P (D)
A	5.2	7.1	-0.71	+13.12
B	6.1	7.8	-0.59	+13.45
C	7.1	8.7	-0.59	+13.50
D	7.8	9.4	-0.59	+14.25
E	9.2	10.6	-0.59	+14.12

in Table 10.1 and as apparent from the values for the rear surface powers, the lenses flex on removal of the rear flat glass sheet. The variation in Back Vertex Power (B.V.P.) is due to the variation in the finished thickness of the lenses.

The further the former is indented, the nearer the alignment of the finished mould to the former contour. Thus if the oblique power error is measured at various angles of eye rotation (Figure 10.5) it will be appreciated that lens 'E', with the deepest indentation has very little Mean Oblique Error up to 25 degrees of eye rotation, as would be expected from the aspheric curve used for the former. Lens 'B' on the other hand, having a pressing depth of one third less only shows a flat M.O.E. up to 15 degrees, after which the mean power drops rapidly with increased angle.

In a similar manner, the distortion of the lenses in Table 10.1 was measured, using the modified spectrometer. Again the results are as expected, Figure 10.6 showing the measured values for two lenses from the series. Lens 'E' shows the distortion pattern expected from an ellipsoidal front surface, whereas lens 'A', which did not conform to the former contour over such a large area exhibits less distortion. This is particularly marked after 20 degrees, due to the rapid changes in power that occur in the blending zone between the central 'island' and the peripheral flange.

In view of the requirement previously mentioned for a centre thickness of approximately 7.5mm for a power of +14.00 DS,

Figure 10.5

Mean Oblique Power for two blended lenticulars, as measured on the modified focimeter. Lens details as in Table 10.1

Mean Oblique Power

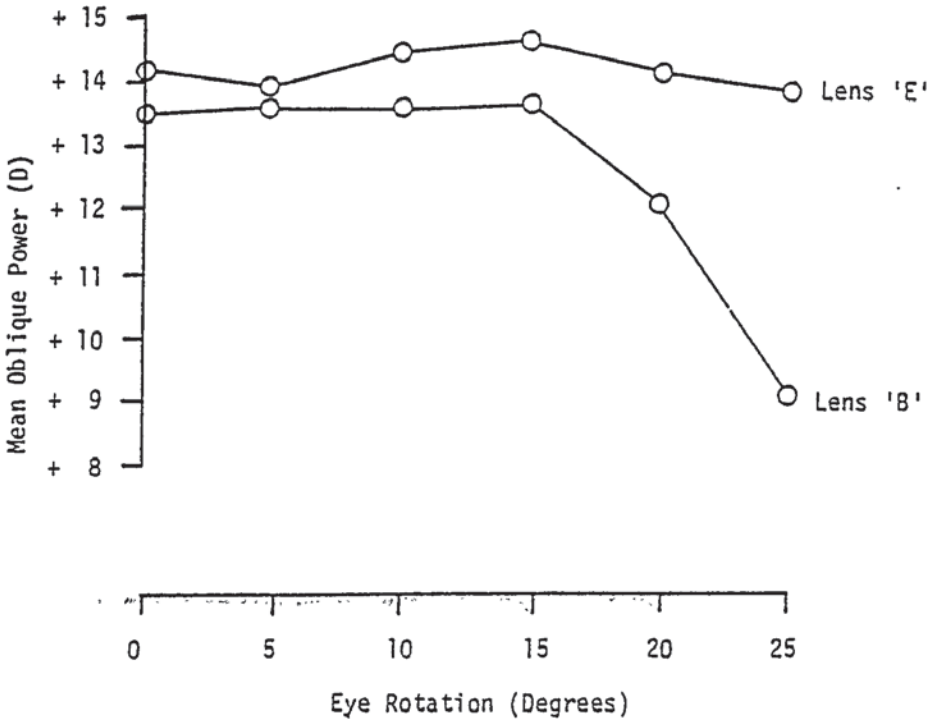

Figure 10.6

Distortion values, as measured with the modified spectometer, for two blended lenticulars. Lens details as in Table 10.1

Distortion

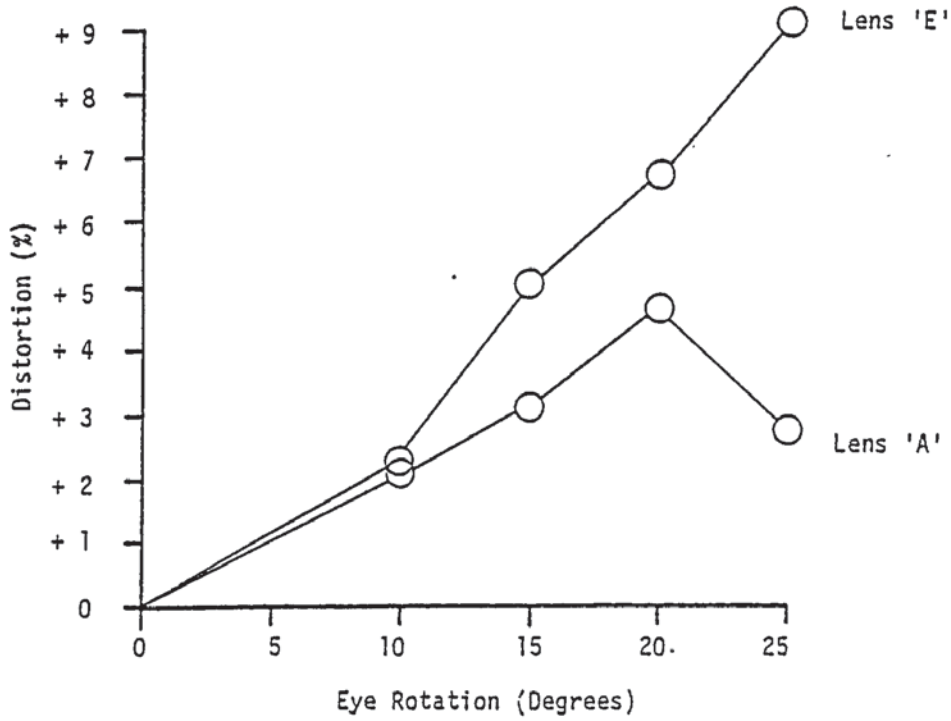
+ 9
+ 8
+ 7
+ 6
+ 5
+ 4
+ 3
+ 2
+ 1
0
Distortion (%)
0
5
10
15
20
25
Eye Rotation (Degrees)
Lens 'E'
Lens 'A'

lens 'B' is the nearest from Table 10.1 conforming to the chosen design.

10.4 Laboratory comparison with other lenses

Since the aim of this exercise is to produce a lens significantly different from existing commerical designs, for comparison purposes it was obviously essential to test this under laboratory conditions. Table 10.2 illustrates the lenses used in the comparison, which includes a spherical surface example for base line comparison. The blended lenticular used in this instance had a steeper rear surface (-1.25 D) than the lenses shown in Table 10.1, as it was felt that this would be more typical of the expected values for prescription lenses.

The results of the comparisons are shown in Figure 10.7 and 10.8, for Mean Oblique Power and Distortion respectively. The Mean Oblique Power was measured on the modified focimeter, and shows that the design of blended lenticular has a central island of 15 degrees eye rotation from the axis, as opposed to the spherical surface lens where the M.O.P. steadily increases with eye rotation. The Sola Hi - Drop also has a 15 degree central island, but beyond this value the M.O.P. drops at a slower rate than the blended lenticular. The Essilor Omega has a large 25 degree central stabilised zone, but the power drops very rapidly after this value.

The distortion results show a similar pattern to those of the M.O.P. Typically high plus lenses have pincushion distortion

Table 10.2

Parameters of lenses used in laboratory comparison

Type	B.V.P.(D)	F_2 (D)	t(mm)
Spherical	+14.00	-0.25	13.1
Essilor Omega	+13.80	-3.05	10.9
Sola Hi Drop	+14.00	-2.03	12.1
Blended lenticular	+14.75	-1.25	7.2

(positive), but as can be seen in Figure 10.8, the blended lenticular actually gives negative distortion at 25 degrees, as it has a much lower power at this angle than any other lens.

Thus although the design of blended lenticular illustrated here does not have very good control of M.O.P., this is compensated by very low distortion. But how much will this be appreciated by the wearer? The effect of the change in M.O.P. in peripheral vision will be to make vision through the edge of the lens blurred, and if it is too blurred, the benefits of low distortion will be masked. Thus the distortion was assessed subjectively through the various lenses. The results are shown in Figure 10.9, and are for one trained observer rendered artificially aphakic in spectacle refraction by the use of a contact lens. These results illustrate that the improved distortion of the blended lenticular can be appreciated, at least up to 20 degrees off axis. However, it was found that the lens with the theoretically known design, the spherical, had only about 50% of the distortion that would have been expected from theoretical calculations, presumably due to adaptation.

It is thus apparent that the proposed design of blended lenticular has some significant differences from commercial designs, but it is only by clinical experience that we can really tell if the features of the lens are appreciated by wearers, as the parameters of lens acceptability are largely unknown.

Figures 10.7 and 10.8

Mean Oblique Power (10.7) as measured on the modified focimeter, and distortion (10.8) as measured on the modified spectrometer for the four lenses shown in Table 10.2

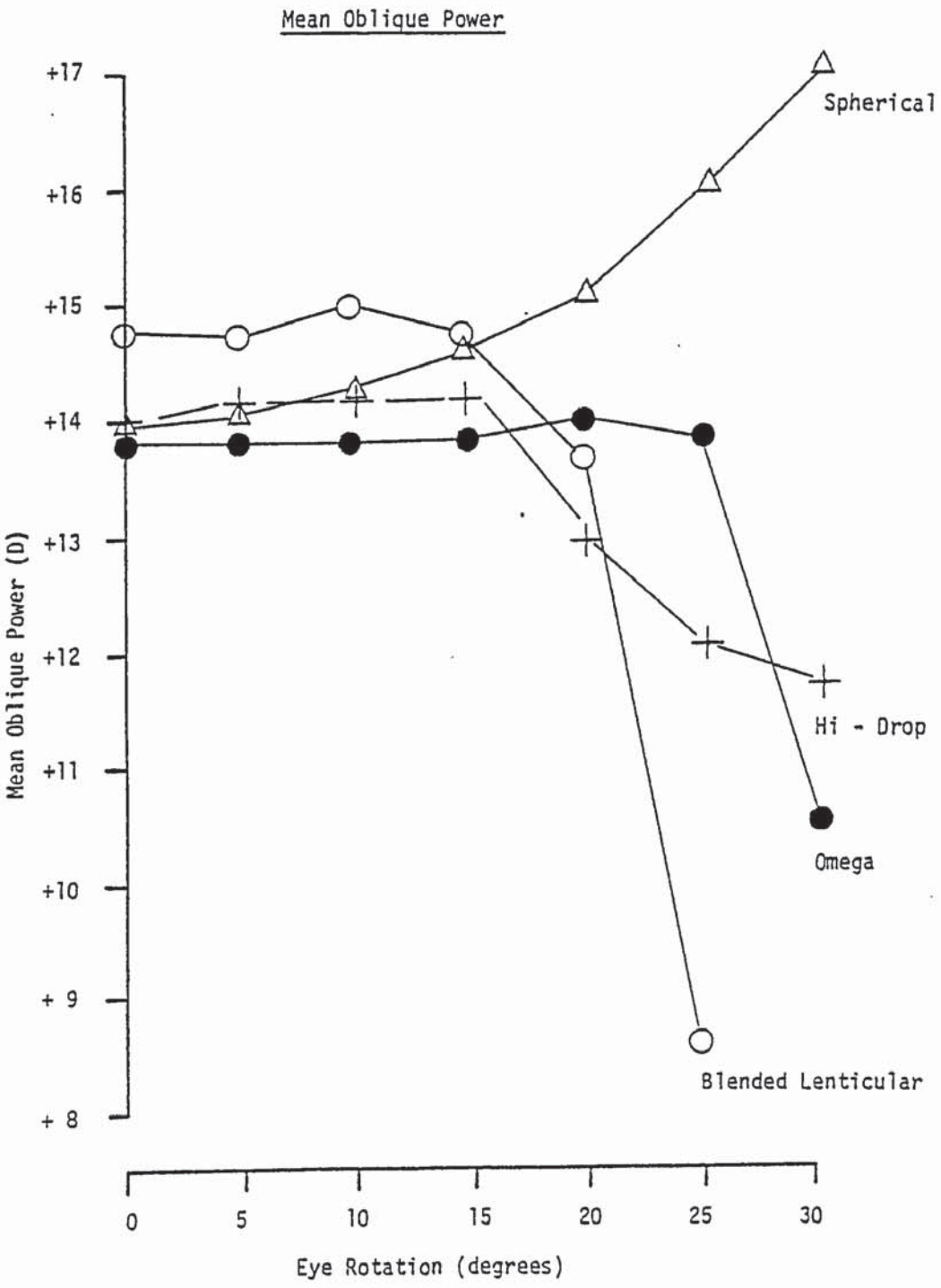
Mean Oblique Power
+17
+16
+15
+14
+13
+12
+11
+10
+ 9
+ 8
Mean Oblique Power (D)
Spherical
Hi - Drop
Omega
Blended Lenticular
0
5
10
15
20
25
30
Eye Rotation (degrees)

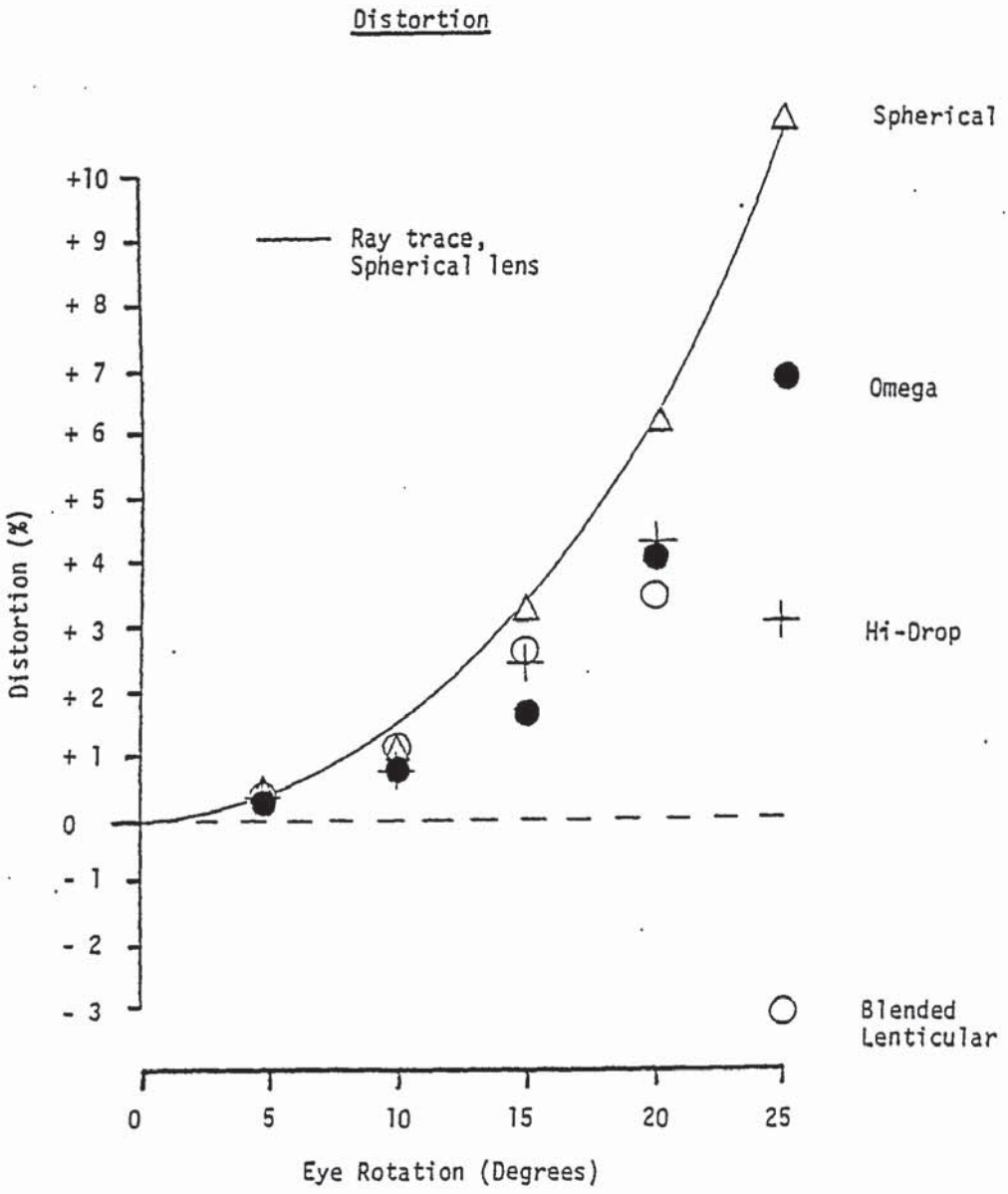
Distortion
Spherical
Ray trace,
Spherical lens
Omega
Hi-Drop
Blended
Lenticular
+10
+ 9
+ 8
+ 7
+ 6
+ 5
+ 4
+ 3
+ 2
+ 1
0
- 1
- 2
- 3
Distortion (%)
0
5
10
15
20
25
Eye Rotation (Degrees)

Figure 10.9

Subjective distortion of lenses shown in Table 10.2 by one subject (CWF). Apparatus as described in Chapter 8, used at a fixation distance of 5350 mm.

Subjective Distortion

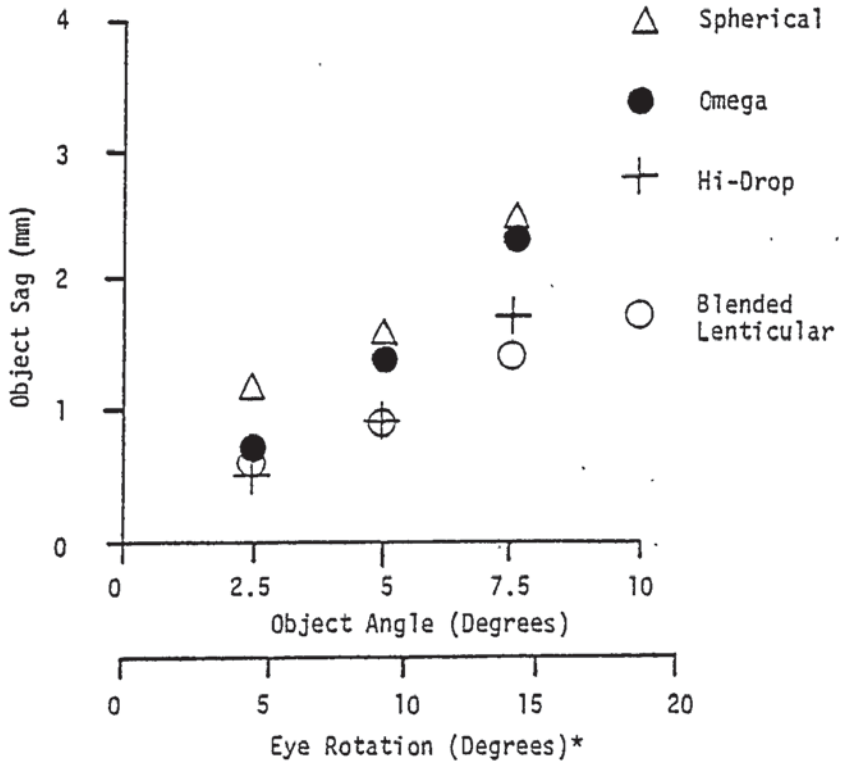

(*Calculated from raytrace through spherical Lens)

CHAPTER 11

Clinical Evaluation of Spectacle Lenses

Lenses were compared on a series of volunteer patients who were gathered from the University of Aston and the Birmingham and Midland Eye Hospital. The refraction details and acuities of the seven patients are shown in Table 11.1. The criteria for selection were that the individual had to be keen to cooperate in the trial, be active and mentally alert, and also be in close proximity to the University of Aston, as a number of visits were required. It had been hoped to use more patients, but this was not possible due to a lack of suitable individuals being located in the time available.

Each patient was tried with three different types of lens, a blended lenticular, Signet Hyperaspheric and Essilor Omega. the Signet lens is of similar construction to the Sola Hi Drop and Armorlite Multi Drop, and was used as it was readily available from the normal prescription supplier to the University, the Norville Optical Co. Ltd. Patients were assessed with both eyes corrected in the binocular state where appropriate, alternatively a cosmetically acceptable balance lens was used in front of the non - usable eye if monocular.

The patients were initially examined to see if their spectacle refraction was correct, and that there was no active abnormality of the eyes. Each was fitted with a suitable spectacle frame, all of which were chosen to have a minimum datum lens size of 50 mm.

Table 11.1

Details of patients

Name	Spectacle Prescription	V.A	Age	Sex
TW	R +12.50/+0.50x170	6/9	45	M
	L +11.50/+1.00x180	6/6		
MC	R +14.50 DS	6/9	43	F
	L +14.00/+2.00x5	6/6-		
PA	R +12.00 DS	6/18	30	M
	L Balance	H.M.s		
TP	R +10.00/+1.50 x170	6/9	38	M
	L +8.00/+3.50x45	6/9		
EH	R +13.50/+4.00x180	6/9-	73	F
	L +14.25/+2.00x175	6/6		
PY	R Balance	P of L	32	F
	L +12.00 DS	6/36		
JW*	R +12.00/+2.00x20	6/6	48	F
	L Balance	H.M.s		

* Note

Left eye had cataract removed during experiment, values shown here are as originally assessed.

Sizes beneath this value would not show the differences between the marginal performance of the various lens types.

The lenses were worn in sequence, the order being randomly set for each patient. It was unfortunate that two subjects had spectacle prescriptions outside the range of the Hyperaspheric and hence could not be fitted with this type of lens. Ideally, each lens type would have been worn by each person for exactly the same length of time, and any other type of spectacle correction removed. It was felt that this approach was unethical, since each of these lenses represented a completely different type of correction, and the blended lenticular was designed to be up to the expected limits of acceptability. Thus the subjects were not deprived of their normal spectacle correction, and were simply asked to wear the particular lenses under test as much as possible.

The response to each lens type was assessed in the following ways:-

1. Subjective response - visual comfort, weight etc

2. Peripheral visual field, monocular.

3. Field of view for good visual acuity, assessed as field for 50% of distance acuity, measured monocularly in the horizontal plane.

4. Subjective distortion.

11.1 Subjective response

The response to the different lenses can be summarised as follows:-

a) All the patients appreciated the light weight of the blended lenticular, but no differentiation was made between the weights of the two other lenses. Only one patient (EH) found the weight of the Hyperaspheric or Omega lenses to be a serious problem.

b) The reduced thickness, giving a less bulbous appearance, of the blended lenticular was apparent to all the patients. However none of this sample felt that the improved appearance relative to the other two designs was a significant feature - all the patients rated the optical qualities higher than the lens appearance.

c) The reduced visual field of clear acuity was noticed by all the wearers for the blended lenticular. It was this factor more than any other which governed the acceptance of the lens. Only one patient (PA) wore the blended lenticular for longer than a few days (total time: 6 weeks). One patient wore these lenses for a week (EH), and one for 3 days (TW). The remainder wore the lenses for a day or less.

d) All the patients remarked that the visual acuity through the blended lenticular was not quite so good as through the other types of lens, although this was not apparent on comparative measurement on a conventional letter chart. This could also be seen on less power measurement on the focimeter as a slight lack of crispness of the target image.

Figures 11.1 to 11.7

Visual field plots of the seven patients shown in Table 11.1, wearing different types of lens

△ Blended lenticular

□ Hyperaspheric

○ Omega

Field of view through aphakic spectacle lenses

Haag - Streit 330 mm bowl perimeter

Patient: TW

Target: 4 mm diameter

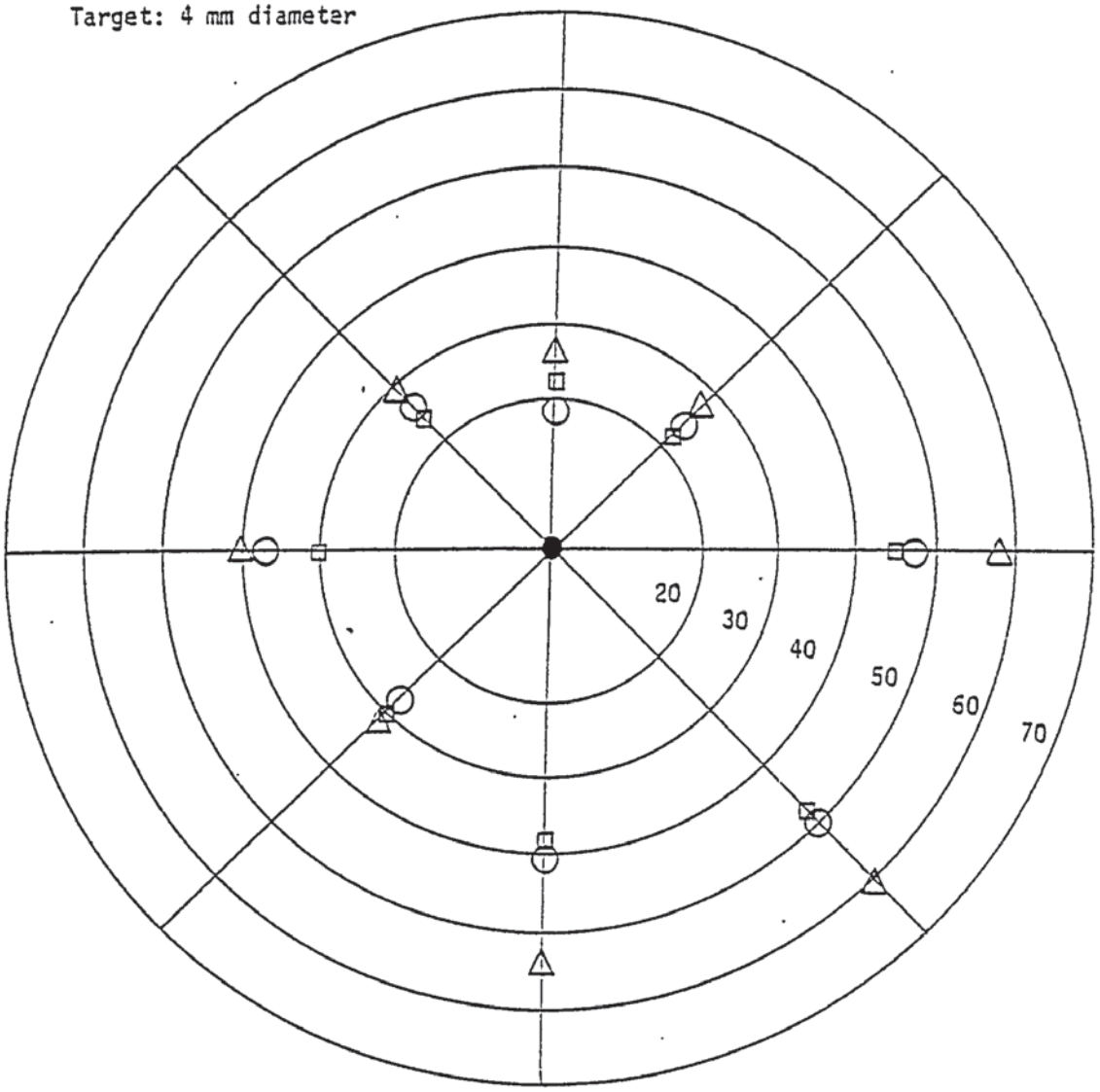

Field of view through aphakic spectacle lenses

Haag - Streit 330 mm bowl perimeter

Patient: MC

Target: 4 mm diameter

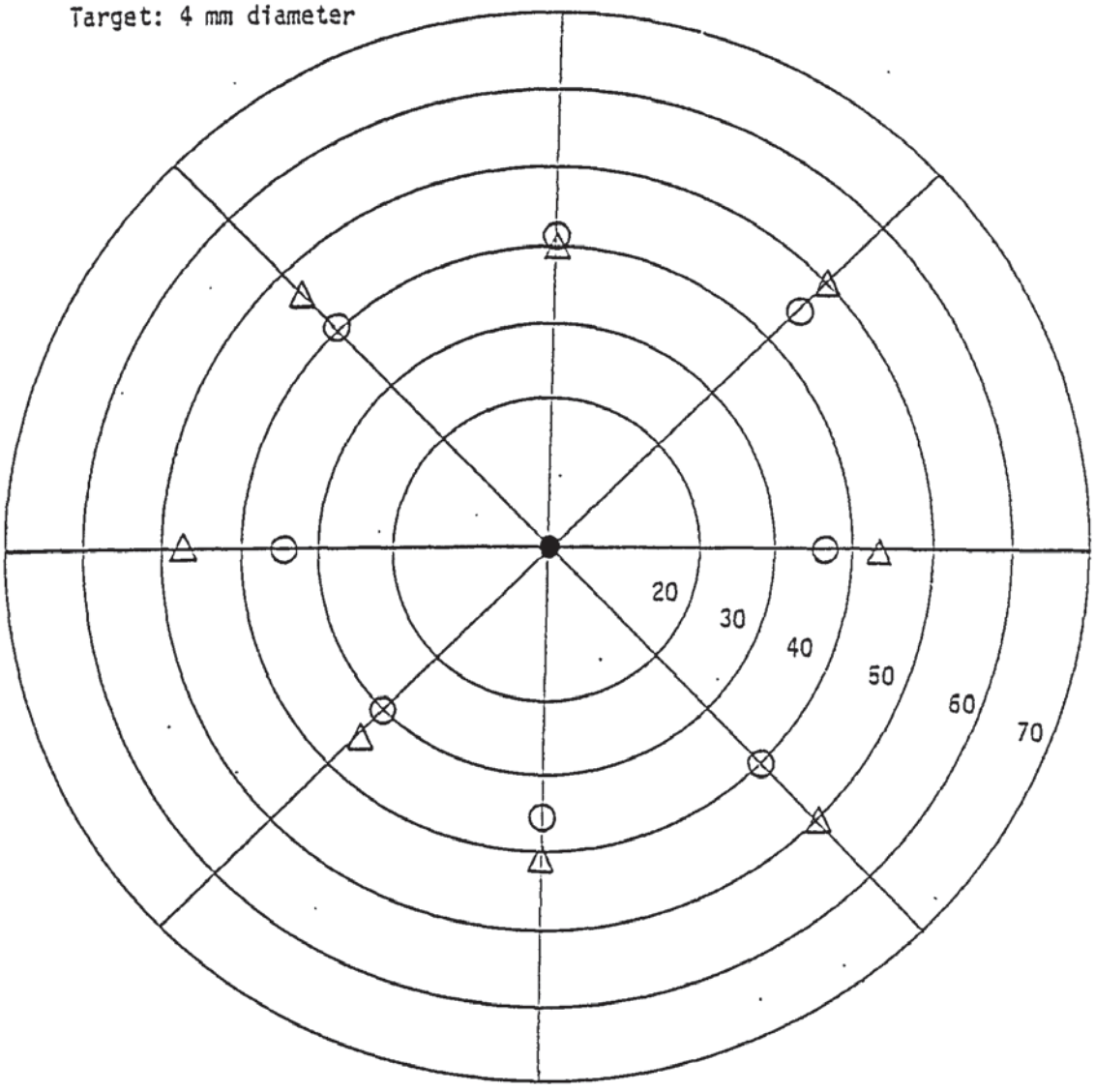

Field of view through aphakic spectacle lenses

Haag - Streit 330 mm bowl perimeter

Patient: PA

Target: 4 mm diameter

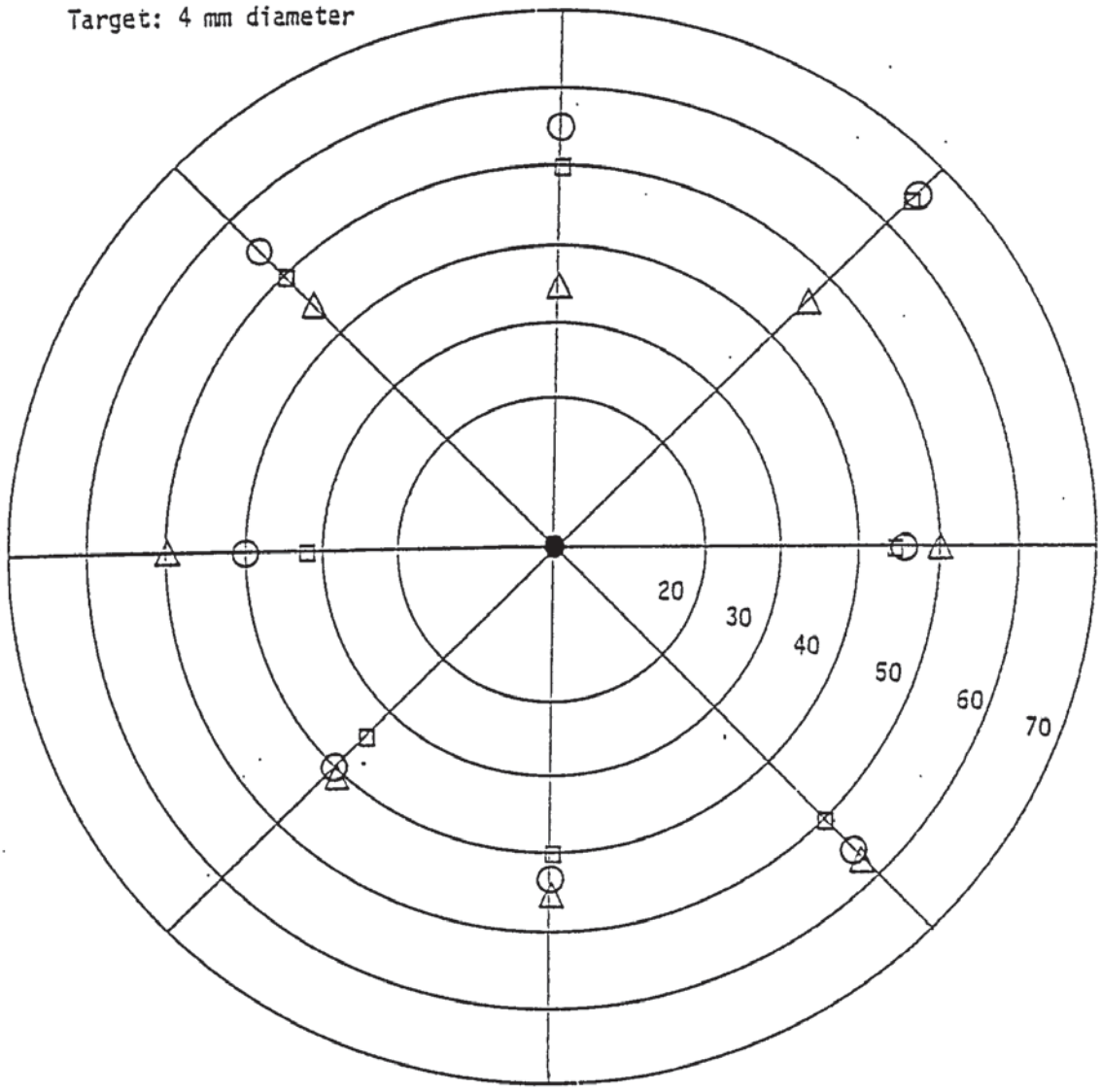

Field of view through aphakic spectacle lenses

Haag - Streit 330 mm bowl perimeter

Patient: TP

Target: 4 mm diameter

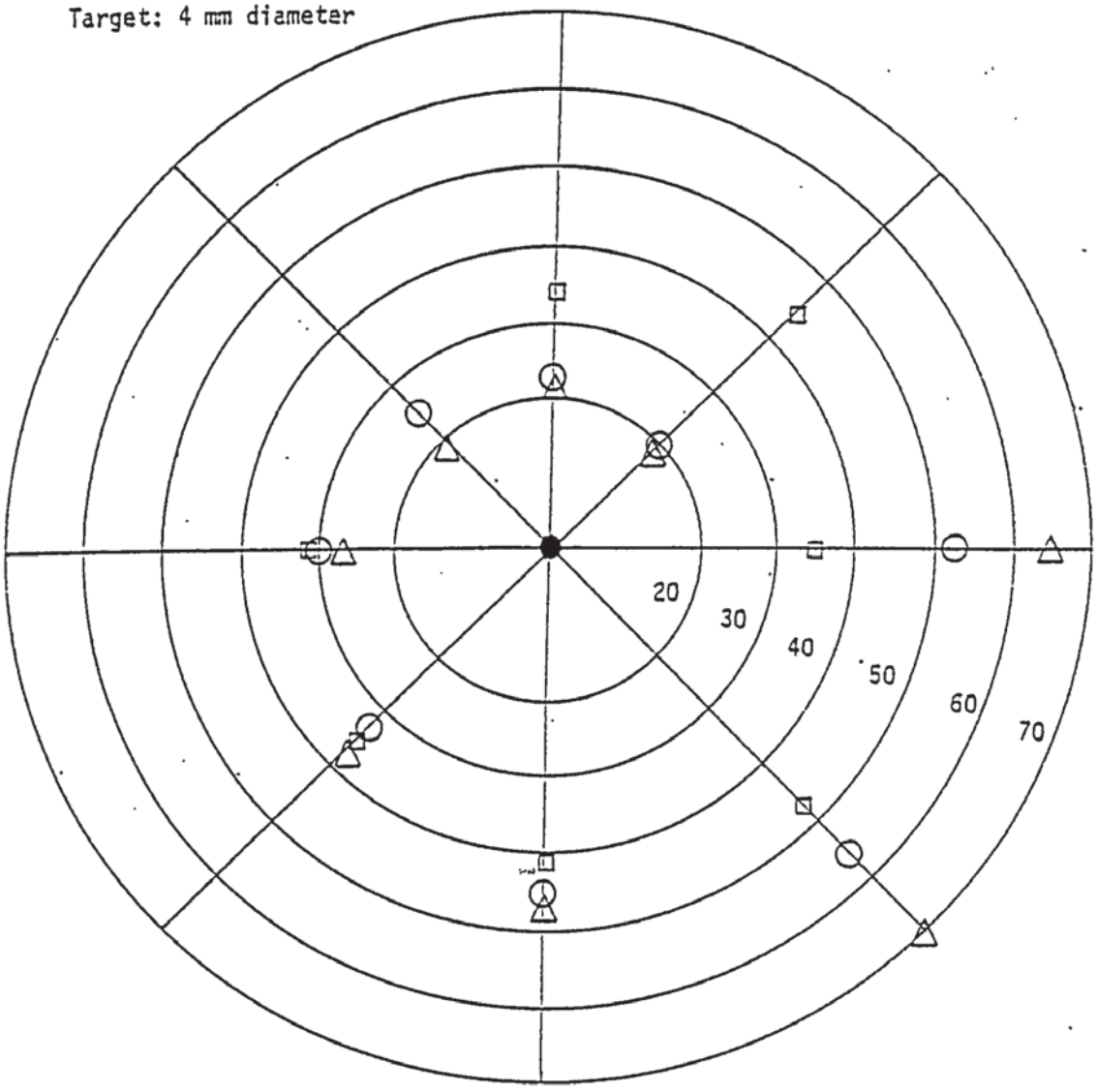

Field of view through aphakic spectacle lenses

Haag - Streit 330 mm bowl perimeter

Patient: EH

Target: 4 mm diameter

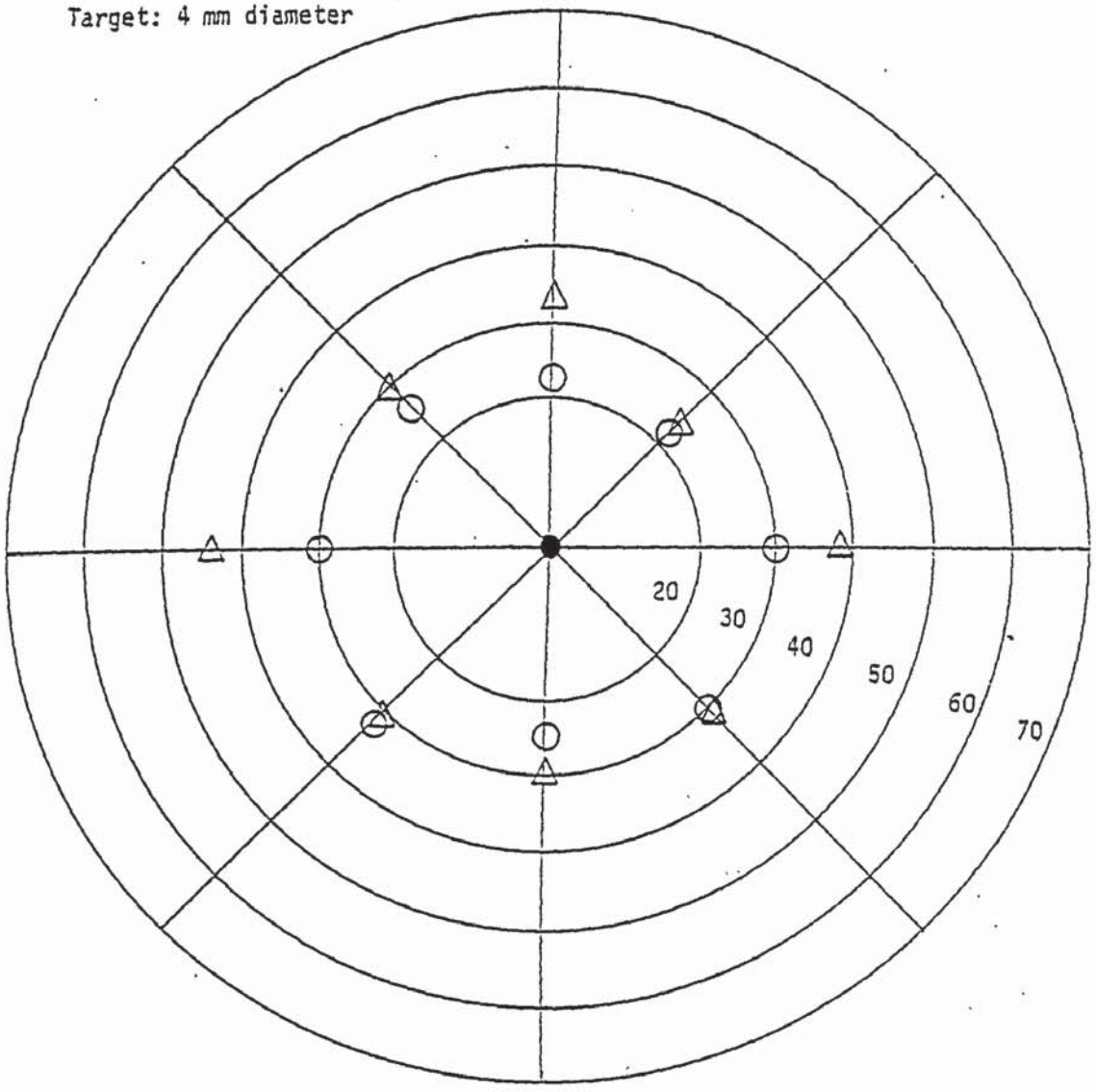

Field of view through aphakic spectacle lenses

Haag - Streit 330 mm bowl perimeter

Patient: PY

Target: 4 mm diameter

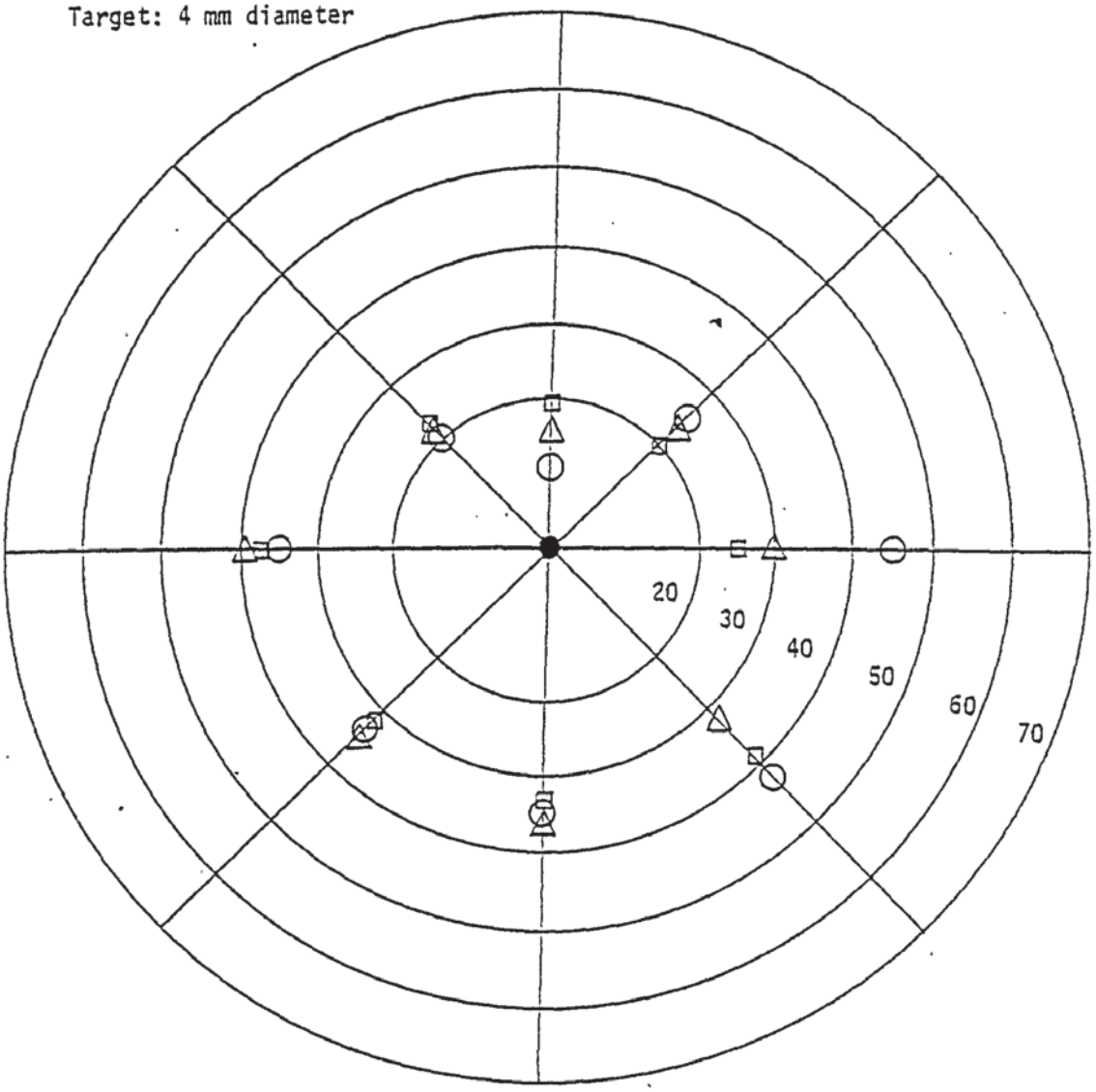

Field of view through aphakic spectacle lenses

Haag - Streit 330 mm bowl perimeter

Patient: JW

Target: 4 mm diameter

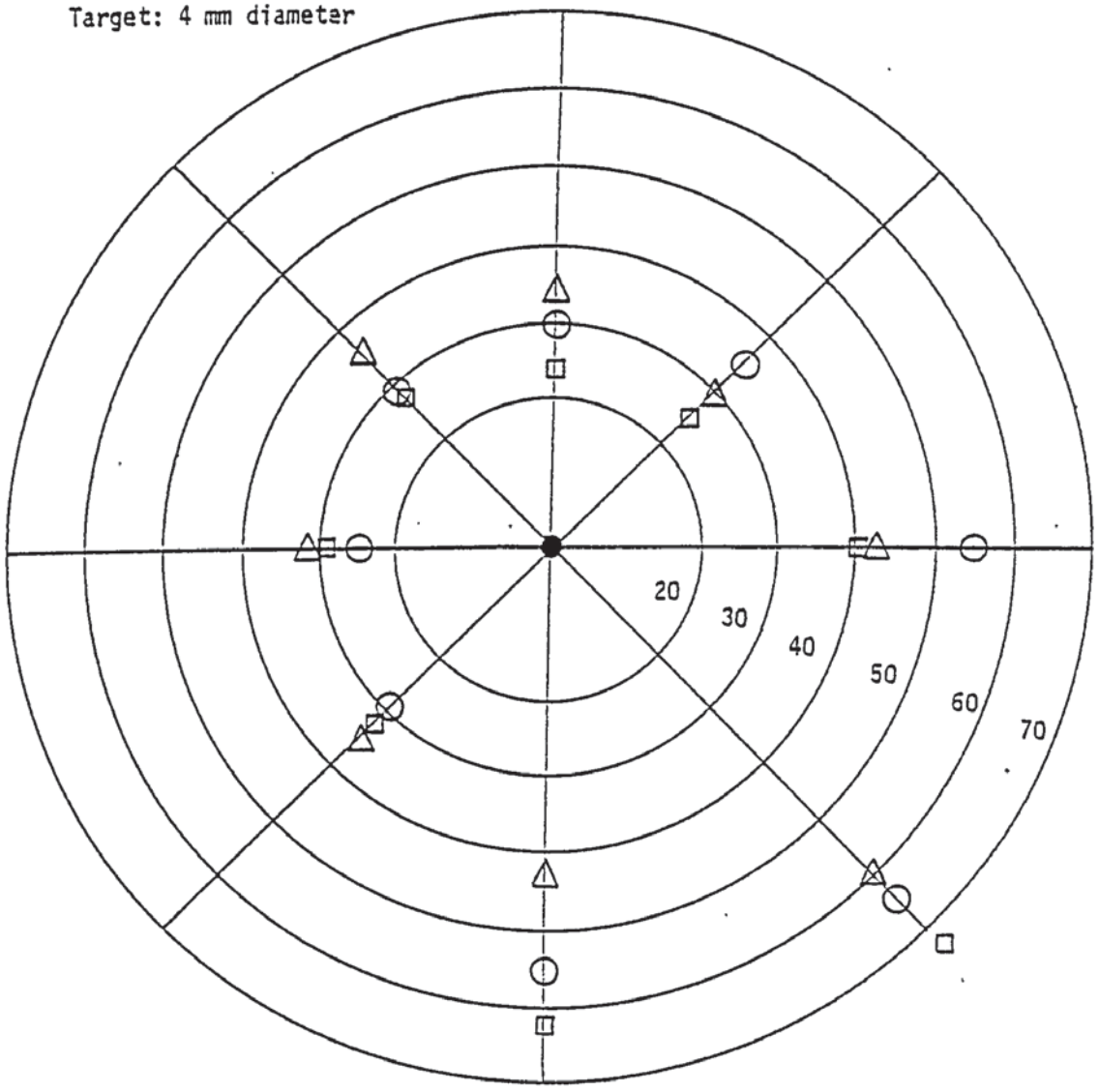

This is probably due to a combination of inexact replication of the aspheric former during mould production, and the effect of the mismatch between the refractive index of the front surface and the CR39.

e) The final preferred lenses were:-

Blended lenticular	1
Omega	4
Hyperaspheric	2

11.2 Peripheral visual field

The visual fields for each lens were measured on one eye of each subject, and are shown in Figures 11.1 to 11.7. These fields were measured on a Haag-Streit Goldmann bowl perimeter, which has a fixation distance of 1/3 metre. Target IV was used (4 mm diameter illuminated circulated patch) at maximum intensity, indicated on the instrument as intensity 4.

Visual fields can be interpreted in a number of different ways. Table 11.2 gives the average of the left and right fields for each lens worn by each observer. Also indicated are the ranked field sizes for each observer, and this shows that the Hyperaspheric always has the smallest field. Five wearers had bigger fields with the Blended Lenticular, and two with the Omega.

Table 11.2

Horizontal visual field

Subject	Blended Lenticular		Mean	Hyperaspheric		Mean	Omega		Mean
	L	R		L	R		L	R	
TW	40	58	49	30	45	38	37	47	42
MC	48	44	46	-	-	-	35	38	37
PA	50	50	50	32	45	38	40	45	43
TP	26	65	46	32	35	34	30	52	41
EH	45	38	42	-	-	-	30	30	30
PY	40	30	35	37	25	31	35	45	40
JW	32	43	38	30	40	35	25	55	40

(values in degrees)

Ranked mean size

TW BL > O > H

MC BL > O

PA BL > O > H

TP BL > O > H

EH BL > O

PY O > BL > H

JW O > BL > H

Drasdo and Peaston (1980) have argued that raw field data in degrees is misleading, due to the relative importance of central fields in carrying out visual tasks. They have produced grids for overlaying conventional field plots to give more meaningful interpretations, based on various criteria. One method is to assess the field in terms of percentage visual channel capacity (Figure 3c of Drasdo and Peaston). This is carried out by overlaying a dot pattern over the visual field, each dot representing 1% channel capacity. An indication of the relative importance given to the central field by this analysis is that 50% of the dots occur within the central 10 degrees. Such a grid was used to assess the data given in the field plots shown in Figures 11.1 to 11.7. The percentage channel capacity for each lens is shown in Table 11.3, and illustrates that in all cases the blended lenticular gave an equal or larger sized percentage channel capacity than the Omega, and the Omega always gave a bigger channel capacity than the Hyperaspheric.

In a recent study, Atchison and Smith (1984) compared the fields of Sola Hi Drop, Armorlite Multi Drop, and Signet Hyperaspheric with the American Optical Ful-Vue blended lenticular. The three 'drop' lenses exhibited similar fields as would be expected, whereas the Ful - Vue exhibited a larger field, in a similar manner to the Omega lens described here. The results are not comparable directly with this study, as Atchison and Smith used a mixture of III and V for the Goldman target sizes.

Table 11.3

Visual field data (Figures 11.1 to 11.7) expressed in terms of percentage channel capacity (Drasdo and Peaston, 1980)

Subject	Blended Lenticular	Omega	Hyperaspheric
TW	95	89	86
MC	96	93	-
PA	97	97	96
TP	93	92	91
EH	88	82	-
PY	87	85	83
JW	93	92	90

11.3 Subjective distortion

The experiment in Chapter 10 has shown differences in subjective distortion measurements for the different types of lens. These measurements were therefore taken on the lens wearers in the evaluation group. The results are shown in Table 11.4, and are given in terms of the measured sag and also the standard deviations. The standard deviations vary widely, the highest values (PY) being associated with the subject with the worst visual acuity. An additional factor is undoubtedly the alertness of the observer, TW and TP being particularly good in this respect.

The fixation distance used for the experiment was 5350 mm, six readings being taken for each lens (by the method of limits). The mean sag for each lens was, (at 10 degrees object angle)

Omega	+1.16 mm (n = 7)
Hyperaspheric	+1.84 mm (n = 5)
Blended lenticular	-0.16 mm (n = 7)

A plus sign indicates pincushion distortion, a negative sign barrel distortion.

The fact that the blended lenticular gave the lowest distortion was in line with the results shown in Chapter 10. However, using the Friedman two way analysis of variance on the five subjects who wore all the lenses, there was no significant difference between lenses (X^2_r 2.5, p = 0.367) or between observers (X^2_r 1.07, p = 0.90). Subjectively, none of the wearers complained of distortion as being a problem, which agrees with the findings

Table 11.4

Subjective Distortion

Patient	Omega		Hyperaspheric		Blended Lenticular	
	Sag	S.D	Sag	S.D	Sag	S.D
TW	+1.60	1.3	+3.0	1.7	-1.3	0.9
MC	+0.50	8.0	N.A		+0.4	6.4
PA	+1.00	5.1	+1.0	7.6	+1.3	7.4
TP	Zero	4.2	+2.2	3.3	Zero	2.6
EH	+2.00	6.5	N.A		+0.5	5.7
PY	+2.60	16.6	+1.9	14.9	-1.5	16.3
JW	+0.40	2.9	+1.1	8.5	-0.5	7.4

(Values for sags and standard deviations)

in millimetres

Figure 11.8

Subjective distortion data for the Omega lens, from Table 11.4, plotted against expected values calculated by ray tracing, assuming $p_1 = 0.8$

Subjective distortion (Omega)

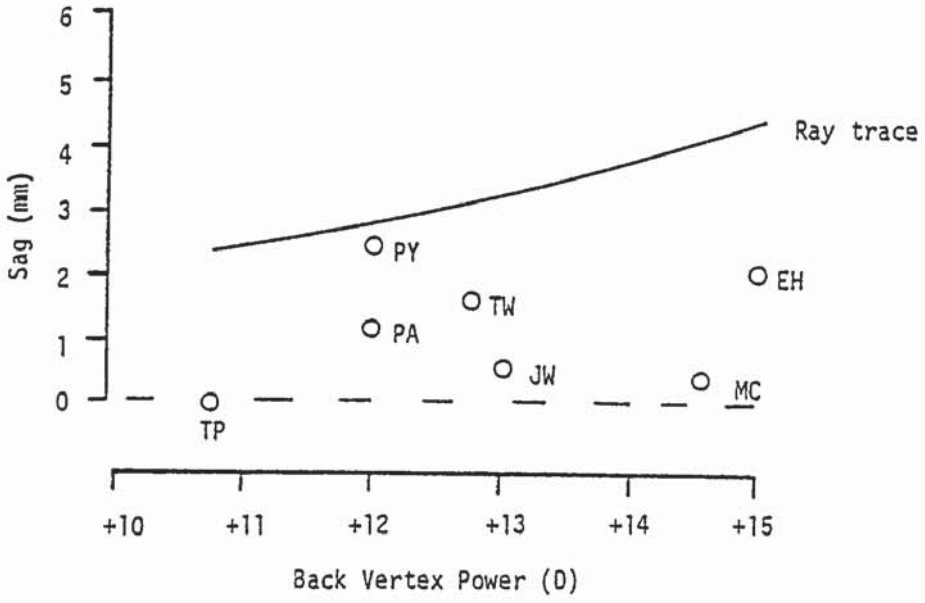

of Atchison and Smith (1984).

Perhaps the most interesting result is the small size of the measured sags in relation to the theoretical expectations from ray tracing. Figure 11.8 illustrates the results for the Omega lens, and shows that none of the subjects were experiencing as much distortion as would be anticipated from purely theoretical concepts. This would appear to show that some adaptation is taking place to distortion, which may explain the lack of subjective problems to this aberration.

11.4 Field of view for good visual acuity

In the previous section, the field of view was assessed assuming no eye movement, the target being viewed by peripheral vision. However, in natural viewing conditions, constant eye movements are taking place. Thus it was felt necessary to determine the horizontal visual field of good visual acuity, arbitrarily set at 50% of central visual acuity. This was measured using single optotypes introduced from the 'blind' area of the field, at a fixation distance of three metres.

The results (for monocular vision) are shown in Table 11.5. It is immediately apparent that the blended lenticular field was smaller for every subject, compared with the other lenses. In two of the five subjects that wore both Hyperaspheric and Omega,

Table 11.5

Patient	Hyperaspheric		Omega		Blended Lenticular	
	R	L	R	L	R	L
TW	15.2	16.1	11.7	14.8	6.8	10.0
MC	NA	NA	22.8	15.6	18.8	15.6
PA	19.6	19.0	18.6	14.6	11.3	6.8
TP	21.8	19.8	15.6	16.3	9.1	9.1
EH	NA	NA	10.4	12.2	9.5	9.3
PY	15.0	11.3	21.6	14.6	11.5	10.0
JW	25.6	20.8	32.6	17.7	12.8	14.1

Macular field of view for 50% distance acuity (degrees)

Total fields

	Hyperaspheric	Omega	Blended Lenticular
TW	31.3	26.5	16.8
MC	-	38.4	32.4
PA	38.6	33.2	18.1
TP	41.6	31.9	18.2
EH	-	22.6	18.8
PY	26.3	36.2	21.5
JW	46.4	50.3	26.9

the Omega field was larger than the Hyperaspheric, whereas in the other three cases the situation was reversed. It is interesting that it was the same two subjects who were found to have the largest horizontal field with the Omega on the perimeter, PY and JW.

Plate I and II

Side view of EH wearing a blended lenticular lens (top) and Essilor Omega (bottom). Note the reduced bulbousness of the blended lenticular.

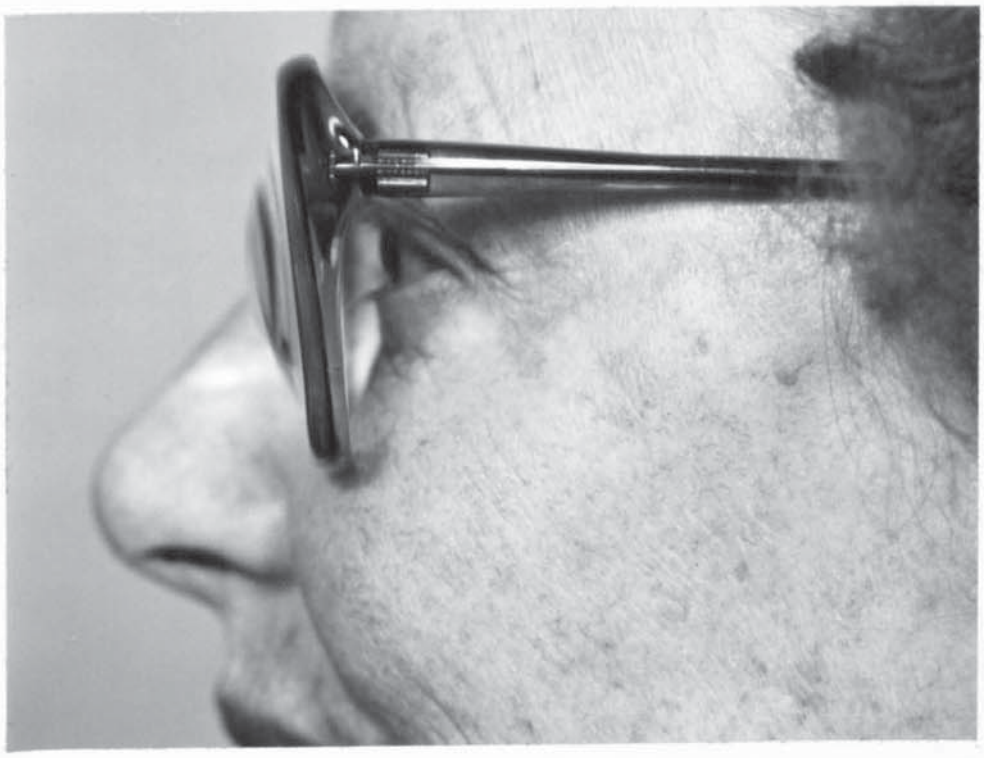

Plates III and IV

Three - quarter view of EH wearing blended lenticular lens (top) and Essilor Omega (bottom). Note the clearer view of the eye through the blended lens, due to the narrow area of high positive power.

Plate V

Stages in manufacture of blended lenticular by first making semi-finished lens. From left to right:

1. Flat Perspex sheet
2. Sheet moulded to shape over former
3. Gasket for casting
4. Front surface mould cut to fit gasket

Plate VI

(Continuation from Plate V)

5. Semi-finished lens on release from gasket. Note front surface protective tape.
6. Front surface protective tape removed
7. Lens after surfacing rear surface. Note reduction in thickness
8. Finished lens after edging

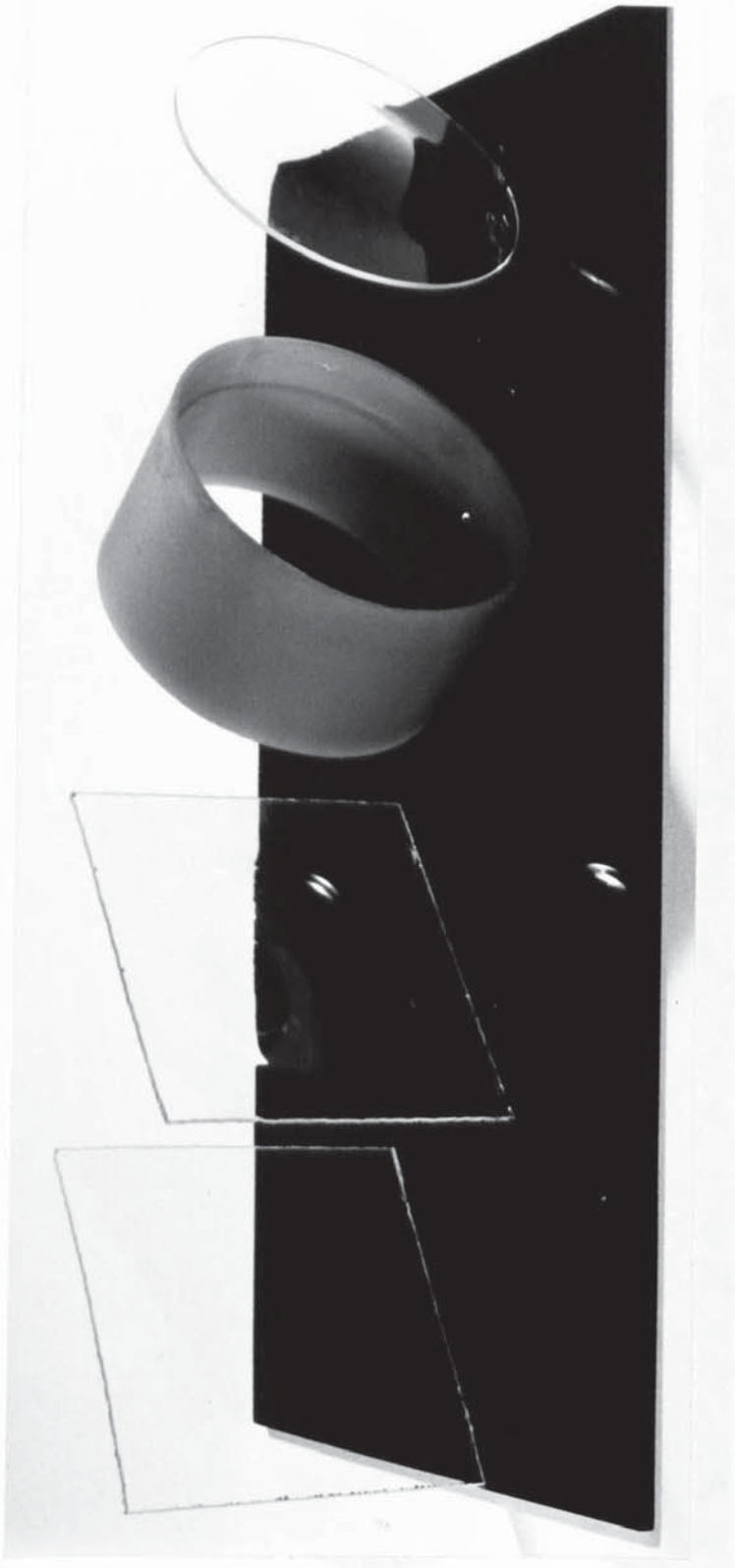

PART 4

CHAPTER 12

Summary, Conclusions - and the Future

12.1 Summary and Conclusions

Aspheric ophthalmic lens design has come a long way from the design of von Rohr (1909) - or has it? The use of aspheric curves with increasing numbers of polynomial terms could indicate an increased level of sophistication, or more cynically an attempt to overcome competitors' patents. It can be shown (Figure 12.1) that perhaps the major impetus in new lens design has been the requirement to provide lenses of ever increasing overall diameter in order to be able to glaze frames of ever increasing aperture, rather than trying to produce lenses of superior optical performance. Indeed, the attempts by Katz (1982) to use two aspheric surfaces to produce the 'perfect' lens illustrate that there are simply not the degrees of freedom available.

1. Lens designs can be grouped into four types, conic section lenses, polynomial surface lenses, 'drop' type lenses and blended lenticular, although the differences between the first two of these groupings can be minimal in some instances.

2. The measurement techniques used for the lenses all had their merits, but no one technique was universally superior. It had originally been hoped that the travelling microscope would be a 'universal' method of lens appraisal, but it is

Figure 12.1

Increase in maximum uncut diameter of aspheric lens designs with time

Uncut Diameter of Aspheric Lenses

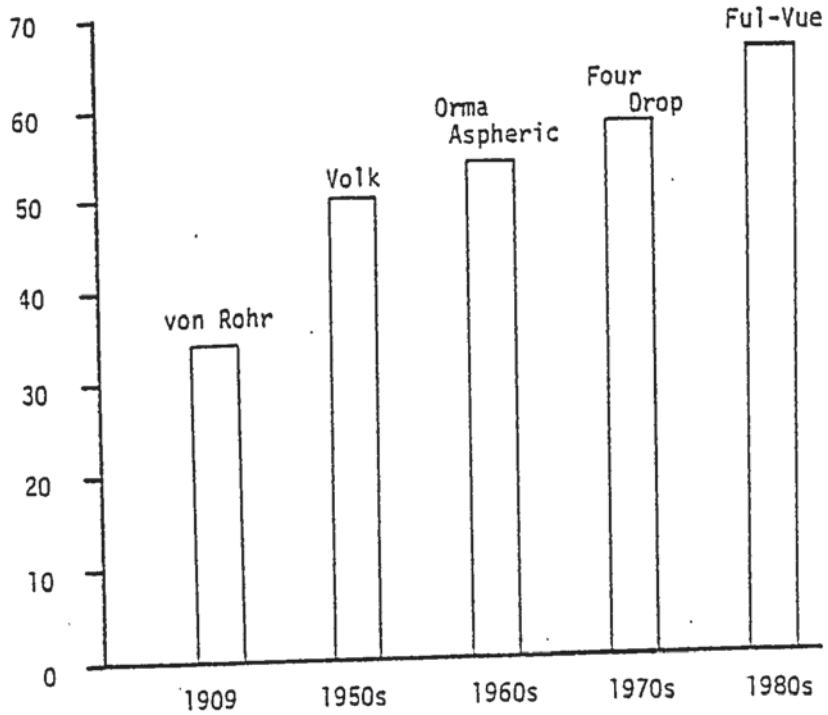

not as quick as the modified focimeter. This latter equipment, however, suffers from two problems for lens evaluation. It assumes that one surface is perfectly spherical, any asphericity being due only to one surface, and also there are potential problems due to the aberrations of the prism used to keep the image of the target within the field of view of the eyepiece. This latter problem is overcome by using the modified spectrometer for measuring distortion. Indeed the focimeter and spectrometer apparatus could be combined by calibrating the target movement on the spectrometer, so that the instrument could read power as well as angular deviations.

3. Lens measurements illustrate that where a design is known, lenses can vary in relation to the faithfulness of reproduction of the design. This is perhaps not surprising in view of the problems associated with the casting of lenses from CR39 and similar plastics, particularly the shrinkage that takes place during polymerisation. Also, of course due to the difficulty of verifying the design of an aspheric lens, quality control of manufacture is extremely difficult.

4. The manufacturing technique evolved for the blended lenticular was successful in that it enabled a more extreme design of lens to be tested against existing commercial designs, but refinement is still required. Protection of the front acrylic surface during polymerisation proved to be a major headache, and the present solution is not ideal, being

difficult to apply on a large scale. Although it had been originally hoped to cast the lenses to finished prescription, this was not found possible due to a lack of suitable rear surface glass moulds of shallow curvature.

5. The small scale clinical trial illustrated some clear results, even on a small sample. Although the blended lenticular was always the thinnest and lightest lens worn, its optical inadequacies in other directions made it unacceptable. In particular, width of field of good visual acuity proved an important requirement, as exhibited by the Signet Hyperaspheric and Essilor Omega lenses, even though the visual fields measured on the perimeter were larger on the whole with the blended lenticular. It is possible that this acceptability or otherwise is also governed by the rate of change of tangential power across the lens in relation to the point of fixation. Thus the blended lenticular might be more acceptable if the rate of blending was slower, as this would cut down the induced astigmatism (Charman, 1982).

The fact that one subject (PA) was able to wear the blended lenticular for an extended period of time shows that extreme lens designs can be worn, particularly when, as in this case, the wearer had no satisfactory alternative spectacle correction. It would have been very interesting to have removed all the subjects other spectacles during the wearing trial.

It is perhaps naive to expect any one lens design to be universally more acceptable than others. There are no doubt many aphakics who would appreciate the improved cosmetic appearance and lighter weight of the blended lenticular, even with its optical compromises.

6. One of the surprises of this investigation was the lack of problems caused by lens distortion. The subjective distortion apparatus enabled lens types to be ranked by good observers, but it did not give results that could be directly related to theoretical ray tracing. There is no doubt that some adaptation takes places, but the situation may also be complicated by the method of calculation. Katz (1983) has criticised the traditional methods of distortion calculation (as used here) because they do not take image curvature into account. However, it is likely that any differences would be very small at the 10 degree object angle used here for the subjective assessment.

In a questionnaire survey of aphakics, Atchison (1983) found only one out of 13 patients who complained of distortion, even though all but two were wearing spherical surface lenses. It is thus most likely that other lens problems associated with aphakia, such as poor field and magnification, are the overriding factors.

12.2 The Future

The first question to be addressed is this: will contact lenses and implants make spectacle lenses for aphakics obsolete? Undoubtedly these alternative forms of correction will be used increasingly in the future, but there are always those who react adversely to implanted or closely applied prosthetic devices.

To obtain lenses of reasonable centre thickness, but with large diameter, it is obvious that peripheral lenticularisation, or power reduction must take place, using conventional optics. The use of diffraction optical techniques (Freeman, 1984a) is an attractive possibility, as this would divorce lens power from lens thickness. There are problems with diffraction lenses, such as extremely poor constringence of the lens, but this can be turned to advantage, for the simultaneous correction of distance and near vision (Freeman, 1984b).

However, there is another possible technology that could be used, namely Fresnel lens surfaces. Flexible P.V.C. Fresnel lenses for ophthalmic purposes have been avaiable for some time (from the Optical Science Group, USA), which are designed to adhere to a conventional ophthalmic lens. Although widely used for temporary prism corrections, they do not appear to have gained wide acceptance for aphakic corrections, probably as a result of the poor resolving power of the lenses. It is suggested, however, that such lenses could be used to improve the peripheral optics of blended lenticulars, leaving the central area free for normal foveal vision. This would require the use of an aspheric Fresnel,

Figure 12.2

A) Blended lenticular with Fresnel multi zone annular corrector plate applied to the rear surface, seen in cross section.

B) Plan view of lens shown above. Radii of corecting Fresnel lenses, and powers:

	Radius (mm)	Power (D)	Zone width (mm)
ab	9	Plano	9
ac	12	+1.00	3
ad	19	+4.00	7
ae	24	+6.00	5
af	32	+10.00	8
ag	33	Plano	1

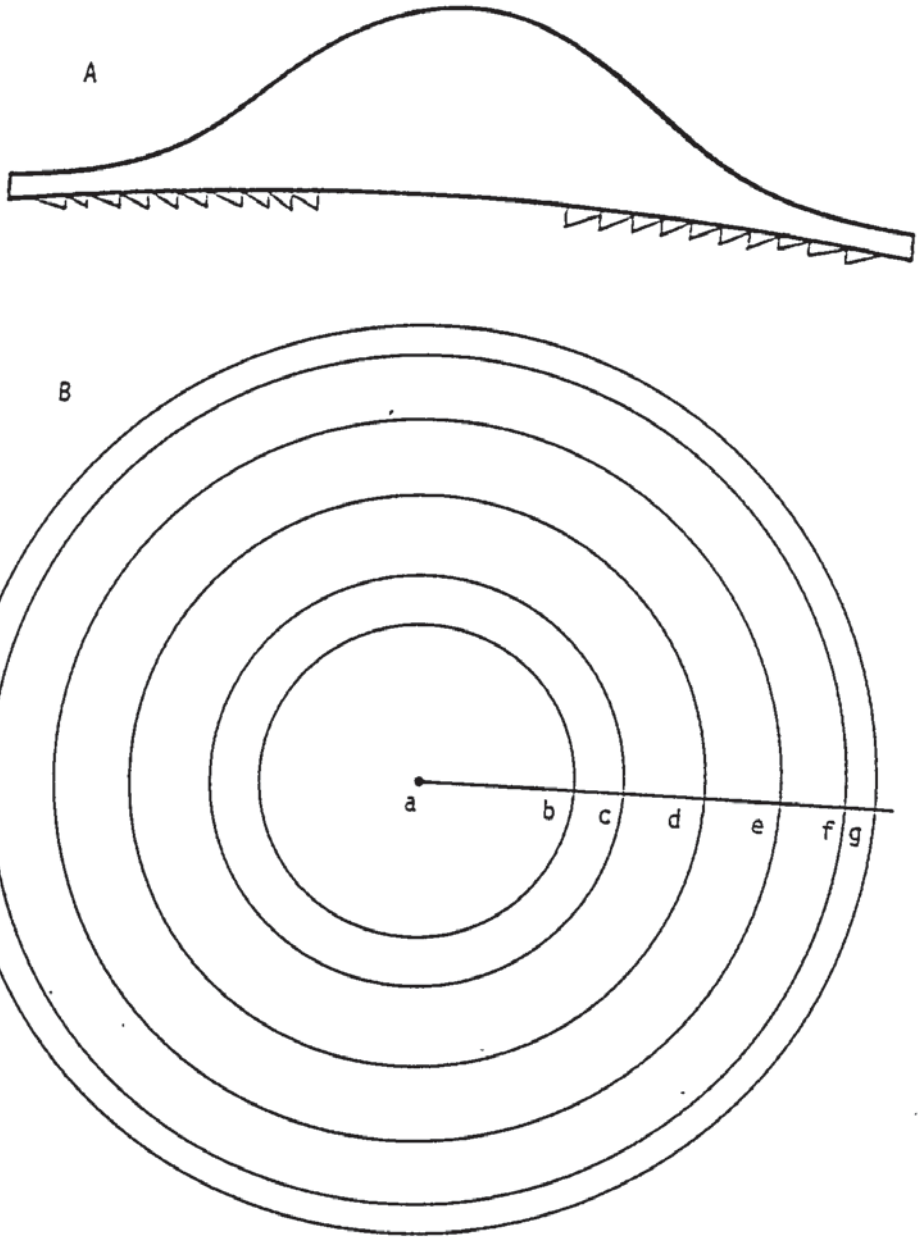
A
B
a
b
c
d
e
f
g

the use of which has been suggested for widening the field of biocular CRT magnifiers (Rogers, 1984).

In order to test this concept, a model was made consisting of a small field blended lenticular, with a rear surface Fresnel corrector, consisting of a series of concentric zones of spherical power (Figure 12.2). The oblique power errors of this lens are shown in Figure 12.3 both with and without the Fresnel corrector, lens in place. Hence the rear surface of the lens consists of a 'drop' type unblended aspheric surface. The sizes of the power zones were chosen to coincide with the 5 degree sampling interval used in lens measurements, hence reducing the discountinuities between zones. This modified lens is not a practical form, due to these discountinuities, but it does demonstrate the improvement that could be made if a continous aspheric Fresnel were used.

The problem with having two aspheric surfaces in a spectacle lens has always been the incorporation of a cylindrical correction. This is made easier, however, with the manufacturing method described earlier, as the mould for the front surface can consist of a toric convex surface, rather than a convex aspheric. This will however entail some loss of optical quality compared with an aspheric surface.

Perhaps the most interesting area in optics at the moment is the develpoment of materials for spectacle and other lenses (Tarumi, Komiya and Sugimura, 1982). In particular, satisfactory high refractive index plastics with low constringence would be welcomed by the lens designer. Very high refractive index glass is a

Figure 12.3

Mean Oblique Power and Astigmatism of blended lenticular, as measured on the modified focimeter.

○ Basic lens

• Lens with rear surface Fresnel corrector plate

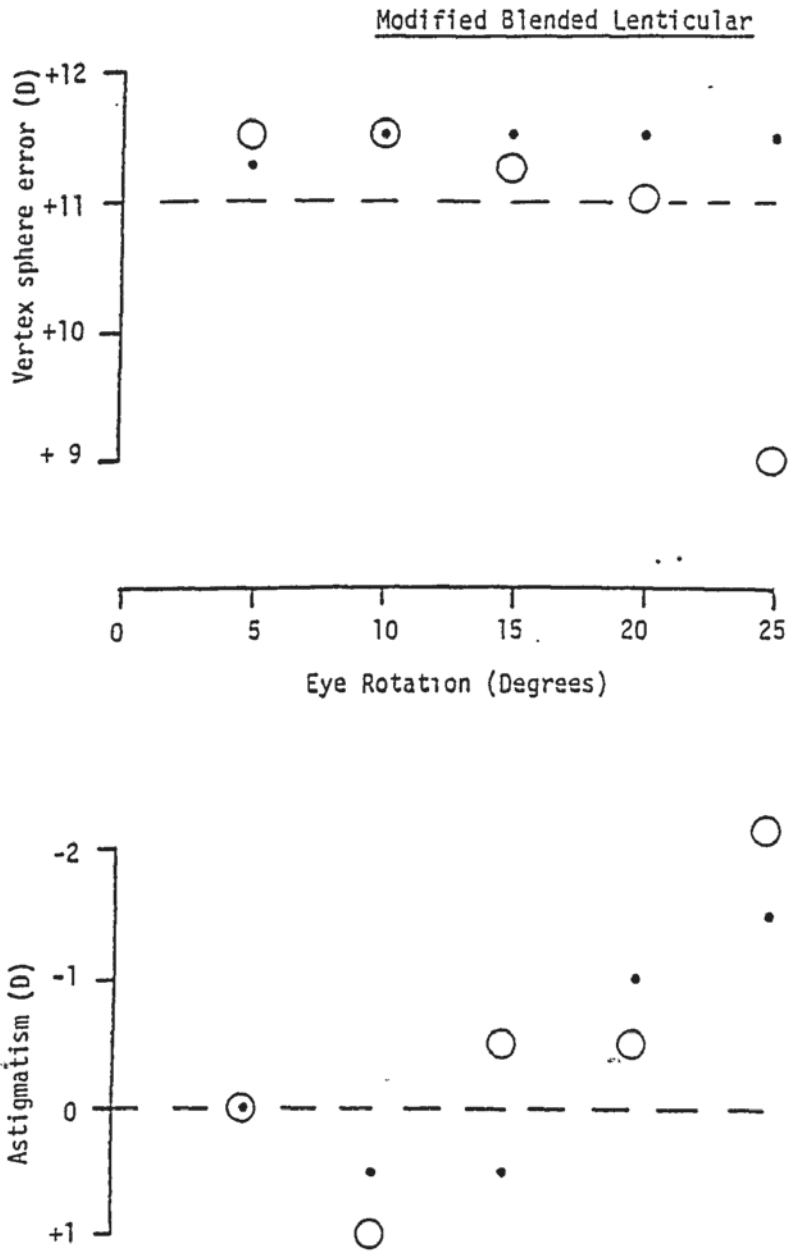
Modified Blended Lenticular
Vertex sphere error (D)
+12
+11
+10
+ 9
0
5
10
15
20
25
Eye Rotation (Degrees)
Astigmatism (D)
-2
-1
0
+1

possibility, which may revitalise interest in the fused lenticular for aphakia (Carl Zeiss Jena, 1961) in order to give a thin lens of acceptable weight. In addition, the transmission characteristics of lenses used for the correction of aphakia will undoubtedly become more important, as a result of concern about possible retinal damage caused by near visible Ultra Violet light, that is normally filtered out by the crystalline lens (Davis and Torgersen, 1983).

But whatever developments occur in the design of aspheric spectacle lensed for the correction of aphakia, it is certain that the aims of lens designers will be very much the same as when Smethwick (1666) wrote a patent claiming:

> 'A new and perfect way to grind opticke glasses in figures that are not sphericall, which will add much to the use of perspective glasses by sea and by land, as well as for the heavens, because his are all open and soe shew the object clearer as admitting more sight'

Appendix I

Ray tracing through conic section lenses

Although computing schemes for spherical surface lenses are common in the ophthalmic lens literature, the same is not true for those with aspheric surfaces. Emsley (1956) and Bennett (1968) have given equations useful for ray tracing through conic surfaces. Smith and Bailey (1981) have suggested modifications to the computing scheme for spherical lenses produced by Bennett and Edgar (1979, 1980) to make it suitable for conic surface lenses.

The program described here was written to calculate the oblique astigmatism and distortion in an ophthalmic lens which has one or both lens surfaces made from conic sections, for any fixation distance.

As described in Chapter 1, ray tracing through a spectacle lens conventionally starts at the centre of rotation of the eye. From Figure AI-1 it will be seen that a ray leaves the centre of rotation at an angle 'U' and is incident at the rear surface of the lens. The point of intersection of the ray and the rear surface is calculated from a quadratic equation derived from the expression of the ray:

$$y = \text{Tan } U\ (z - x) \qquad - - \text{AI(1)}$$

Figure AI.1

Beginning of ray trace sequence, light travelling from centre of rotation of the eye (C) to the rear surface of the lens at point (G).

Ray Trace

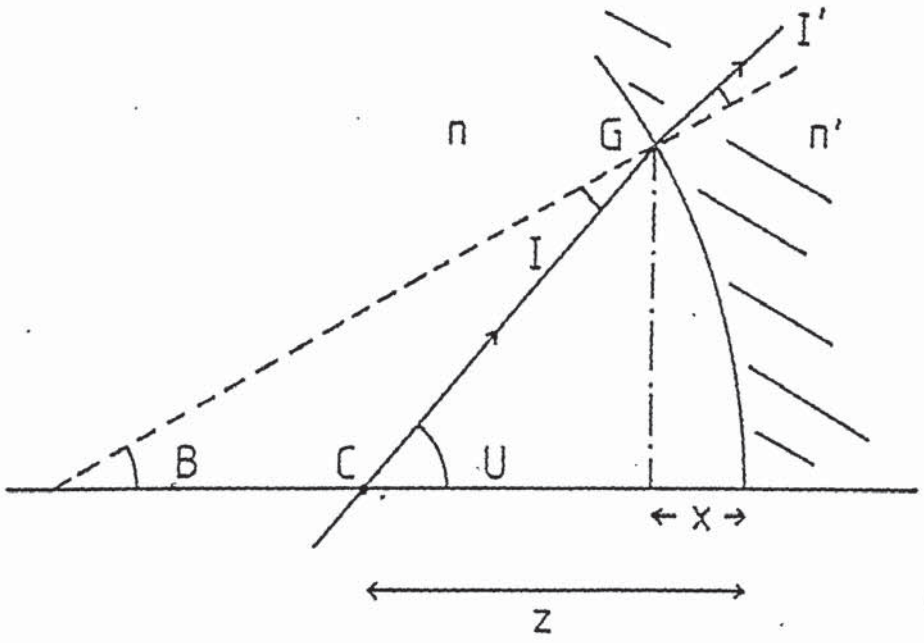

and the expression for the surface:

$$y^2 = 2rx - px^2 \qquad \text{-- AI(2)}$$

The origin of the coordinate system is considered to be at the rear vertex of the lens. The value 'r' is the paraxial radius of curvature of the surface. The angle of the normal to the axis, 'B', is calculated (Mandell and St Helen, 1971) from:

$$\text{Tan } B = \frac{y}{r - p\,x} \qquad \text{-- AI(3)}$$

From this, the angle of incidence can be readily calculated by:

$$I = B - U \qquad \text{-- AI(4)}$$

The angle of refraction is then given by Snell's law

$$n \text{ Sin } I = n' \text{ Sin } I' \qquad \text{-- AI(5)}$$

where n and n' are the refractive indices for air and the lens material respectively.

This process is repeated at the second surface, with the origin of the co-ordinate system being transferred to the vertex of the front surface.

Using this information, the astigmatism can be readily calculated using Coddington's equations, assuming that light is reversed and travels through the lens from front to back. The sign convention for angles and distances must also be carefully followed. The distortion is calculated in the manner described in Chapter 8.

Notes on program

Lines 1 - 110

Printer is switched on and formatting instruction given. Input variables are requested, from which the front (R1) and rear (R2) radii of curvature (in centimetres) are calculated. The headings are printed out, as well as the input variables for future reference.

Lines 111 - 115

Loops are set up to control range of p_1 and U'_2 (T0), and also set step intervals.

Lines 120 - 150

The value of U'_2 is converted to radians (then called T9), and in line 130 the variables are assigned for the subroutine contained in lines 1000 - 1050. This calculates the point of intersection of the ray with the rear surface, given by the co-ordinates (X2, Y2).

Lines 160 - 210

The angles of incidence (S9) and refraction (R9) are calculated, along with the angle of the refracted ray to the axis, U_2 (T7).

Lines 215 - 227

The distance of the point of intersection of the ray refracted ray from the front surface (Z1) is calculated. The subroutine starting at line 1000 is again used to calculate the point of intersection of the ray with the front surface (X1, Y1).

Lines 230 - 260

Angles of incidence (Q9) and refraction (P9) at the front surface are calculated, having first found the angle of the front surface normal to the axis (B1). Then the angle that the emerging ray from the lens makes with the axis is calculated (T5).

Lines 265 - 285

The distance travelled by the ray through the lens (G) is calculated. To calculate the oblique astigmatism, the radii of curvature in the tangential and sagittal meridians for both surfaces need to be known. Hence r_{1s} is R5, r_{1t} is R6, r_{2s} is R3, and r_{2t} is R4

Line 287 - 350

Using Coddington's equations, the oblique astigmatism is calculated at the front and rear surfaces of the lens. Line 287 converts an object distance measured along the axis into an object distance measured along the incident ray path. The sagittal and tangential powers at the rear surface of the lens are given by S3 and T3 respectively

Lines 360 - 440

It is conventional to give measurements of sagittal and tangential power relative to the vertex sphere. Hence V1 is the vertex sphere allowance, and V2 the sagittal power relative to the vertex sphere, and V3 the tangential. The value of the mean oblique power (M) is also found, as well as the astigmatism (A). In lines 395 - 430 the distortion in percentage (D2) is calculated. For a near object, the subroutine in lines 2000 - 2025 is used to calculate D2.

Lines 450 - 505

The results for a given range of input angles (U'_2) are printed out in line 504 the next value for front surface p_1 is selected.

- - - -

This is the end of the program proper, the rest of the listing comprising subroutines and instructions to turn off the printer.

Computer program

A listing is given of a computer program (for a Commodore 3032) to calculate the oblique astigmatism and distortion in a conic section surface lens. Because the BASIC language is restrictive on the names of variables, the nomenclature is non - standard.

The version of the program calculates the aberrations for a fixed value of p_2 and a value of p_1 that varies over stated limits. Thus the effects of an aspheric front surface of different amounts of flattening can be readily seen. In addition, the value of the eye rotation angle can be set to vary over a given range to simulate the eye looking across the lens.

```
1 PRINT"□
2 OPEN4,4
3 OPEN 2,4,2
4 OPEN 1,4,1
5 PRINT#2,"99.999-     "
10 PRINT"ASPHERIC RAY TRACE
20 PRINT"──────────────────"
30 PRINT
35 PRINT"F'V,F2,T(CM),N,Z(CM)"
40 INPUT V,F2,D,N,Z2
50 PRINT
55 F1=(V-F2)/(1+D/100/N*(V-F2))
56 R2=100*(1-N)/F2
57 R1=100*(N-1)/F1
60 PRINT"P(REAR)"
70 INPUT     P2
75 INPUT "FIXATION DISTANCE(METRES) ";L1
80 PRINT#4,"F'V          F2          T(CM)        N            Z(CM)
82 PRINT#1,V,F2 ,D,N,Z2
95 PRINT#4
100 PRINT#4," TAB";TAB(10);"AST";TAB(8);"MOP";TAB(8 );"DIST       S'         T'"
110 PRINT#4," ──";TAB(10);"──";TAB(8);"──";TAB(8 );"──────       ──         ──"
111 FOR P1=0   TO1.6 STEP 0.2
115 FOR T0=5TO 30 STEP 5
120 T9=0.0174533*T0
125 T8=TAN(T9)
130 T=T8:P=P2:R=R2:Z=Z2
140 GOSUB1000
150 X2=X:Y2=Y
160 B3=Y2/(R2-P2*X2)
180 S9=ATN(B3)-ATN(T8)
185 S8=SIN(S9)
190 R8=S8/N
195 R7=SQR(1-R8↑2)
200 R9=ATN(R8/R7)
```

```
205 T7=ATN(B3)-R9
210 T6=TAN(T7)
215 N=Y2/T6
220 Z1=N+X2+D
225 T=T6:P=P1:R=R1:Z=Z1
226 GOSUB 1000
227 X1=X:Y1=Y
230 B1=Y1/(R1-P1*X1)
235 Q9=ATN(B1)-ATN(T6)
240 Q8=SIN(Q9)
245 P8=N*Q8
250 P7=SQR(1-P8↑2)
255 P9=ATN(P8/P7)
260 T5=ATN(B1)-P9
265 G=SQR((X2+D-X1)↑2+(Y1-Y2)↑2)
270 R3=SQR(R1↑2+(1-P1)*Y1*Y1)
275 R4=R3↑3/R1↑2
280 R5=SQR(R2↑2+(1-P2)*Y2*Y2)
285 R6=R5↑3/R2↑2
287 IFL1<>0THENS1=100/((100/L1-X1)/COS(T5))
288 T1=S1 ;
290 F6=100*(N*COS(Q9)-COS(P9))/R3+S1
295 F7=(100*(N*COS(Q9)-COS(P9))/R4+COS(P9)↑2*T1)/COS(Q9)↑2
300 S2=100/(100/F6-G/N)
310 T2=100/(100/F7-G/N)
320 F8=100*(COS(S9)-N*COS(R9))/R5
330 F9=100*(COS(S9)-N*COS(R9))/R6/COS(S9)↑2
340 S3=S2+F8
350 T3=(COS(R9)/COS(S9))↑2*T2+F9
360 V1=Y2/SIN(T9)-Z2
370 V2=100/(100/S3-V1)
380 V3=100/(100/T3-V1)
385 T4=TAN(T5)
390 M=(V2+V3)/2
395 IFL1<>0 THEN 2000
```

```
400 L=1/((1-Z2/100*V)*(1-D/100/N*F1))
410 T4=TAN(T5)
420 B9=T8/T4
430 D2=100*(B9-L)/L
440 A2=V3-V2
450 PRINT#1,T0;TAB(10);.
460 PRINT#1,INT(A2*1000+.5)/1000;TAB(10);
470 PRINT#1,INT(M*1000+.5)/1000;TAB(10);
480 PRINT#1,INT(D2*1000+.5)/1000;
490 PRINT#1,INT(V2*1000+.5)/1000;TAB(8);INT(V3*1000+.5)/1000
500 NEXT T0
502 PRINT#4
503 PRINT#4,"'P'FRONT  ";P1;"  'P'REAR  ";P2:PRINT#4:PRINT#4
504 NEXT P1
505 GOTO1500
1000 A=(T*T+P)
1010 B=(-2*Z*T*T-2*R)
1020 C=(Z*Z*T*T)
1030 X=(-B-SQR(B*B-4*A*C))/(2*A)
1040 Y=(Z-X)*T
1050 RETURN
1500 END
2000 L3=L1+F1
2002 L2=L3/(1-D/100/N*L3)
2004 L5=L2+F2
2006 G1=1-Z2/100*L5
2010 H=1-X1/100*L1
2020 D2=(L3*G1*T8)/(L2*(-Y1*L1/100+H*T4))
2025 D2=100*(D2-1)
2030 GOTO440
2040 PRINT#4:PRINT#2:PRINT#1
2050 CLOSE4:CLOSE2:CLOSE1
READY.
```

Example of ray trace

Input values from Smith and Bailey (1981). Output values identical to those shown by Smith and Bailey for 30 degree eye rotation, to three decimal places.

F'V	F2	T(CM)	N	Z(CM)	
8.000	.000-	.660	1.523	2.700	
TH3	AST	MOP	DIST	S'	T'
5.000	.030	8.018	.234	8.003	8.034
10.000	.124	8.074	.947	8.012	8.136
15.000	.286	8.170	2.186	8.027	8.313
20.000	.529	8.312	4.039	8.048	8.577
25.000	.872	8.508	6.639	8.072	8.944
30.000	1.346	8.773	10.194	8.100	9.446

'P'FRONT .5 'P'REAR 1

Appendix II

Ray tracing through polynomial surface lenses

The computing scheme described here is based on a series of algorithms produced by Feder (1951), slightly modified by Smith (1966), that can be used for any rays, not just meridional rays as normally carried out for a Coddington trace. In the version of Smith, the algorithms can be used for a lens with surfaces of the form:

$$x = \frac{cs^2}{(1 + (1 - c^2s^2)^{\frac{1}{2}})} + A_2s^2 + A_4s^4 + \ldots A_js^j$$

-- AII(1)

where $s^2 = x^2 + y^2$, and 'c' is the paraxial curvature. Hence the first term is the equation of a spherical surface, with subsequent aspheric deformation terms. However, this is not quite the form as quoted in, for example, Whitney, Reilly and Young (1980). Also, it would be useful to be able to use the 'p' coefficient for conics. Thus in the program described here, a modified version of AII(1) was used, namely:

$$x = \frac{cs^2}{(1 + (1 - pc^2s^2)^{\frac{1}{2}})} + A_4s^4 + A_6s^6 + A_8s^8 + A_{10}s^{10}$$

-- AII(2)

The problem with this type of ray trace is in finding the co-ordinates of intersection of the ray with the lens surface. This is achieved here by a reiterative process. The first stage is to calculate the intersection co-ordinates of the ray (x_o, y_o, z_o) with the spherical surface having the same curvature value as the aspheric. Then the equivalent 'x' co-ordinate for the aspheric is found by substituting in AII(2), giving $\bar{x}_o$. The sequence of computations is then:

$$l_0 = (1 - pc^2 s_o^2)^{\frac{1}{2}} \qquad \text{-- AII(3)}$$

$$m_o = -y_o \left(c + l_o(4A_4 s_o^2 + 6A_6 S_o^4 + 8A_8 S_o^6 + 10A_{10} s_o^{10})\right) \qquad \text{-- AII(4)}$$

$$n_o = -z_o \left(c + l_o(4A_4 s_o^2 + 6A_6 S_o^4 + 8A_8 S_o^6 + 10A_{10} s_o^{10})\right) \qquad \text{-- AII(5)}$$

$$G_o = (l_o(\bar{x}_o - x_o))/(Xl_o + Ym_o + Zn_o) \qquad \text{-- AII(6)}$$

Note that X,Y,Z are the direction cosines of the ray. The above values are used to give a better approximation to the co-ordinates of the surface (x_1, y_1, z_1), using:

$$x_1 = G_o X + x_o \qquad \text{-- AII(7)}$$

$$y_1 = G_o Y + y_o \qquad \text{-- AII(8)}$$

$$z_1 = G_o Z + z_o \qquad \text{-- AII(9)}$$

The whole process is repeated until:

$$x_1 = \bar{x}_o \qquad \text{-- AII(10)}$$

with sufficient accuracy. This is usually achieved with very few iterations. Having now found the intersection co-ordinates, the next stage is to determine the refraction of the ray, and find the direction cosines of the ray after refraction, X_1,Y_1 and Z_1. This is carried out with the following equations:

$$P^2 = l_o^2 + m_o^2 + n_o^2 \qquad \text{-- AII (11)}$$

$$F = Xl_o + Ym_o + Zn_o \qquad \text{-- AII (12)}$$

$$F' = \frac{1}{N_1} (P^2(N_1^2 - N^2) + N^2F^2)^{\frac{1}{2}} \qquad \text{-- AII (13)}$$

$$g = \frac{1}{P^2} (F' - \frac{N}{N_1} F) \qquad \text{-- AII (14)}$$

Note that N is the refractive index in the incident medium, and N_1 the refractive index of the medium after refraction.

$$X_1 = \frac{N}{N_1} X + gl_o \qquad \text{-- AII (15)}$$

$$Y_1 = \frac{N}{N_1} Y + gm_o \qquad \text{-- AII (16)}$$

$$Z_1 = \frac{N}{N_1} Z + gn_o \qquad \text{-- AII (17)}$$

In the program described in Appendix I, oblique astigmatism was calculated by using Coddington's equations. Here a different approach was used. A ray was traced backwards through the centre of rotation and the lens, as described before. But in order to determine the tangential power, rays above and below this ray, and initially parallel to it, were traced back through the lens. The mean point of intersection of these rays with the central ray was taken as the tangential focus. Similarly, a ray displaced in the 'z' plane, at the same distance from the central ray as the

tangential, was traced through to find the sagittal focus (Figure AII-1). Only one sagittal ray was required as the lens is rotationally symmetrical.

Thus this program is used only for distant objects, with incident parallel light. It can be readily used for spherical surfaces by setting p = 1, and the rest of the aspheric coefficients to zero. Conic surfaces can also, of course, be used by setting 'p' to the appropriate value. The program was written for a Commodore 3032 Computer.

Figure AII.1

Ray trace through polynomial surface

Skew Ray Trace

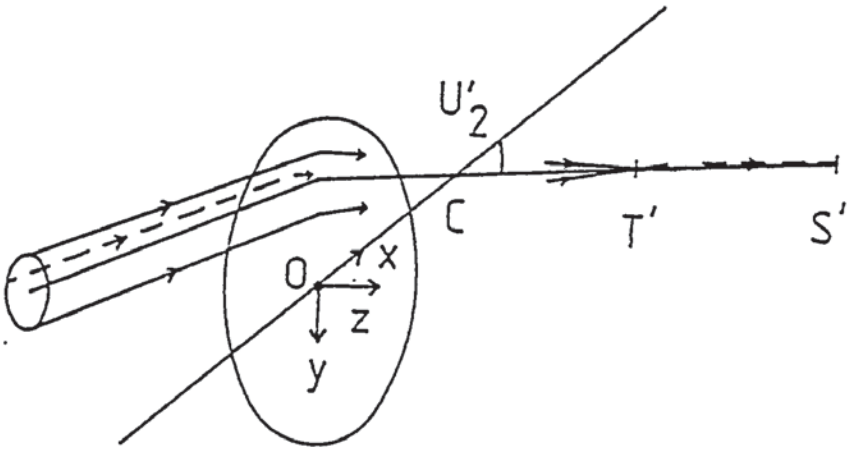

Notes on program

Lines 0 - 70

The printer is switched on and the input variables are requested. The diameter of the input parallel beam (W6) is set to the required value. The basic lens parameters and the rear surface aspheric coefficients are printed out, followed by the headings. A loop is set up for the value of U'_2 (TD), which is then coverted to radians (TR). The front surface power (FO) is calculated.

Lines 75 - 98

Having calculated the front and rear axial curvature (C1, C2), in millimetres, the opening of the ray trace starts at the centre of rotation. This is treated as the origin of the co-ordinate system, as a plane surface. The 'y' direction cosine (BY) is set to Sin U'_2, and the co-ordinates of the centre of rotation surface are set in line 95.

Lines 100 - 485

This is a sub-routine that calculated the intersection co-ordinates and new direction cosines, as described earlier. The co-ordinates required are (X1,Y1,X1) and the new cosines (CX,CY,CZ). The iterative loop is repeated until an error in 'x' of less than 1×10^{-9} mm occurs. The progress of this iteration can be checked, since intermediate values are shown on the display screen of the computer.

Lines 99, and 490 - 550

Having calculated the refraction at the rear surface, the origin of the co-ordinate system is transferred to the rear surface of the lens. Variables are assigned for use by the sub-routine to calculate the refraction at the front surface of the lens.

Lines 560 - 720

After refraction by the front surface, the point of intersection with an arbitrary reference surface is calculated, positioned 10 mm from the front surface, and normal to the axis. This surface is treated as a lens surface with all coefficients and curvature set to zero, with unit refractive index before and after the surface.

Lines 730 - 895

Having established the path of the chief ray through the lens, the first meridional ray, above the chief ray, is traced back through the lens, and the intersection co-ordinates in the centre of rotation plane determined. As this procedure will need to be carried out for other rays also, it is made into a sub-routine (lines 760 - 895).

Lines 896 - 1000

The second tangential ray, below the chief ray, is traced back through the lens, using the sub-routine. The mean tangential

vertex sphere power (FT) is calculated.

Lines 1010 - 1040

The sagittal vertex sphere power is calculated by tracing through a skew ray, then seeing where it cuts the chief ray.

Lines 1041 - 2000

Percentage distortion is calculated from variables already calculated, the aberration figures are printed out, as well as the front surface aspheric coefficients, once all the required values of U'_2 have been looped. Finally, the printer is switched off.

```
0 REM+++++++++TRACE4+++++++++++++++++
1 OPEN1,4
5 OPEN4,4,1
6 OPEN2,4,2
7 PRINT#2,"S99.9999   "
10 PRINT"□"
15 PRINT"SKEW RAYTRACE"
16 PRINT"──────────"
17 PRINT:PRINT:PRINT
18 INPUT "BVP,F2,T(MM),H,Z(MM)";FV,F2,TH,NG,CR
20 INPUT"P1,A1,B1,C1,D1";P1,A1,B1,G1,D1
25 INPUT"P2,A2,B2,C2,D2";P2,A2,B2,G2,D2
26 INPUT"RAY BUNDLE DIAMETER";W6
27 W=W6/2  :  PRINT#1,"TRACE4":PRINT#1
28 PRINT#1,"  F'V        F2          T(MM)         H         Z(MM)"
29 PRINT#4,FV,F2,TH,NG,CR:PRINT#1:PRINT#1,"RAY BUNDLE DIAMETER(MM) ";W6:PRINT#1
30 PRINT#1," P2 ";P2
31 PRINT#1," A2 ";A2                          :PRINT#1," B2 ";B2
32 PRINT#1," C2 ";G2                          :PRINT#1," D2 ";D2
35 PRINT#1
36 PRINT#1," ANGLE        S'V         T'V          AST      M.O.P.      DIST (%)"
41 FOR TD=5 TO30 STEP 5
45 H=1:H1=NG
50 F0=(FV-F2)/(1+TH/1000/NG*(FV-F2))
70 TR=π/180*TD
75 C1=F0/((NG-1)*1000)
80 C2=F2/((1-NG)*1000)
85 C=-C2:P=P2:A4=-A2:A6=-B2:A8=-G2:A0=-D2
90 BY=SIN(TR):BZ=0:BX=SQR(1-BZ↑2-BY↑2)
95 X=0:Y=0:Z=0:T=CR
98 GOSUB 100
99 GOTO490
```

```
100 REM++++++++++++++++++++++++++++++++++++++++++++++++CALCULATION SUBROUTINE
110 E=T*BX-(X*BX+Y*BY+Z*BZ)
120 MX=X+E*BX-T
130 M2=X12+Y12+Z12-E12+T12-2*T*X
160 E1=SQR(BX12-C+(C*M2-2*MX))
170 L=E+(C*M2-2*MX)/(BX+E1)
180 X0=X+L*BX-T
190 Y0=Y+L*BY
200 Z0=Z+L*BZ
210 S2=Y012+Z012
220 XI=C*S2/(1+SQR(1-C12*S2*P))+A4*S212+A6*S213+A8*S214+A0*S215
230 L0=SQR(1-C12*S2*P)
240 M0=-Y0*(C+L0*(4*A4*S2+6*A6*S212+8*A8*S213+10*A0*S214))
250 N0=-Z0*(C+L0*(4*A4*S2+6*A6*S212+8*A8*S213+10*A0*S214))
260 G0=L0*(XI-X0)/(BX*L0+BY*M0+BZ*N0)
270 X1=G0*BX+X0
280 Y1=G0*BY+Y0
290 Z1=G0*BZ+Z0
325 S2=Y112+Z112
330 XI=C*S2/(1+SQR(1-C12*S2*P))+A4*S212+A6*S213+A8*S214+A0*S215
335 IF ABS(X1-XI)<0.000000001THEN 350
340 X0=X1
345 Y0=Y1
346 Z0=Z1
347 GOTO 230
350 PRINT"X CO-ORD. ";X1
360 PRINT"Y CO-ORD. ";Y1
370 PRINT"Z CO-ORD. ";Z1
380 P7=L012+M012+N012
390 F=BX*L0+BY*M0+BZ*N0
420 F1=1/ABS(H1)*SQR(P7*(H112-H12)+H12*F12)
430 G=1/P7*(F1-H/H1*F)
440 CX =H/H1*BX+G*L0:PRINT"X DIR.COS. ";CX
450 CY =H/H1*BY+G*M0:PRINT"Y DIR.COS. ";CY
460 CZ =H/H1*BZ+G*N0:PRINT"Z DIR.COS. ";CZ
480 RETURN
485 REM++++++++++++++++++++++++++++++++++++++++++++++++++++++++++++++END SUBROUTINE
```

```
490 X(1)=X1:Y(1)=Y1:Z(1)=Z1
500 DX(1)=CX:DY(1)=CY:DZ(1)=CZ
510 T=TH:X=X1:Y=Y1:Z=Z1
520 BX=CX:BY=CY:BZ=CZ
530 H=HG:H1=1
540 C=-C1:P=P1:A4=-A1:A6=-B1:A8=-G1:A0=-D1
550 GOSUB 100
560 X(2)=X1:Y(2)=Y1:Z(2)=Z1
570 DX(2)=CX:DY(2)=CY:DZ(2)=CZ
680 T=10:X=X1:Y=Y1:Z=Z1
690 BX=CX:BY=CY:BZ=CZ
700 C=0:P=0:A4=0:A6=0:A8=0:A0=0
710 H=1:H1=1
720 GOSUB100
730 X(3)=X1:Y(3)=Y1:Z(3)=Z1
740 DX(3)=CX:DY(3)=CY:DZ(3)=CZ
750 X=0:Y=Y(3)+W/DX(3):Z=0:T=10
755 GOSUB 760
758 GOTO896
760 BX= DX(3):BY=-DY(3):BZ=CZ(3):REM********************************** SUBROUTINE
770 H=1:H1=HG
780 C=C1:P=P1:A4=A1:A6=B1:A8=G1:A0=D1
790 GOSUB100
800 BX=CX:BY=CY:BZ=CZ
810 T=TH:X=X1:Y=Y1:Z=Z1
820 C=C2:P=P2:A4=A2:A6=B2:A8=G2:A0=D2
830 H=HG:H1=1
840 GOSUB100
850 BX=CX:BY=CY:BZ=CZ
860 T=CR:X=X1:Y=Y1:Z=Z1
870 C=0:P=0:A4=0:A6=0:A8=0:A0=0
880 H=1:H1=1
890 GOSUB 100 :REM*****************************************************END SUBROUTINE
895 RETURN
```

```
 896 X(4)=X1:Y(4)=Y1:Z(4)=Z1
 897 DX(4)=CX:DY(4)=CY:DZ(4)=CZ
 951 X=0:Y=Y(3)-W/DX(3):Z=0:T=10
 952 GOSUB760
 953 X(5)=X1:Y(5)=Y1:Z(5)=Z1
 954 DX(5)=CX:DY(5)=CY:DZ(5)=CZ
 956 AL=ATN(DY(5)/DX(5))-ATN(DY(4)/DX(4))
 957 TF=DX(4)*(Y(4)-Y(5))/SIN(AL)
 958 CD=-Y(5)*SIN(TR)
 1000 FT=1000/(TF+CR+CD)
 1010 X=0:Y=Y(3):Z=W:T=10
 1020 GOSUB 760
 1030 XZ=-Z1/(CZ/SQR(1-CZ12))
 1040 FS=1000/(XZ+CR)
 1041 ZZ=CR-Y1/CY*CX
 1042 TB=SQR(1-DX(2)12)/DX(2)
 1043 LW=1/((1-ZZ/1000*FV)*(1-TH/HG/1000*F0))
 1044 TS=CY/CX
 1045 DI=100*(-TS/TB-LW)/LW
 1050 PRINT#4,TD,FS,FT,FT-FS,(FT+FS)/2,DI
 1090 NEXT TD
 1092 PRINT#1
 1093 PRINT#1," P1 ";P1
 1094 PRINT#1," A1 ";A1:PRINT#1," B1 ";B1
 1095 PRINT#1," C1 ";G1:PRINT#1," D1 ";D1
 1097 CLOSE1:CLOSE2:CLOSE4
 2000 END
READY.
```

Validation of program

Validation of this ray tracing program (version TRACE 4) consisted of comparing the output from the program with published ray trace examples.

a) Smith and Bailey (1981)

The example is of a conic section aspheric lens with a front surface 'p' of 0.5, with a plano rear surface. The output from TRACE 4 is identical with the aberration values given by Smith and Bailey, for a 30 degree eye rotation. The ray trace given in the paper was a Coddington trace, thus an arbitrary input ray diameter of one millimetre was used for comparison purposes.

b) Whitney, Reilly and Young (1980)

Figures are given in the patent for the 'Ful-Vue' lens for aberration figures of the various blanks. It is not known if these figures were derived from a Coddington trace, or by some other means. Thus the same one millimetre input ray was used as above. For the range of eye rotation figures given (10 to 40 degrees in five degree steps), the output from the program does not deviate by more than 0.01 D. It should be noted that the unusual rear surface power (-1.6344 D) is equivalent to a crown (1.53) tool power of -1.75 D on the stated lens matèrial, with index 1.495.

Example a)

```
TRACE4

   F'V          F2          T(MM)          N          Z(MM)
+ 8.0000    +  .0000    + 6.6000    + 1.5230    +27.0000

RAY BUNDLE DIAMETER(MM)  1

 F2  1
 A2  0
 B2  0
 C2  0
 D2  0

 ANGLE          S'V          T'V          AST        M.O.P.        DIST (%)
+ 5.0000    + 8.0031    + 8.0334    +  .0303    + 8.0183    +  .2323
+10.0000    + 8.0123    + 8.1358    +  .1234    + 8.0740    +  .9444
+15.0000    + 8.0273    + 8.3125    +  .2851    + 8.1699    + 2.1833
+20.0000    + 8.0474    + 8.5766    +  .5291    + 8.3120    + 4.0365
+25.0000    + 8.0719    + 8.9443    +  .8723    + 8.5081    + 6.6373
+30.0000    + 8.0998    + 9.4463    + 1.3464    + 8.7731    +10.1920

 P1  .5
 A1  0
 B1  0
 C1  0
 D1  0
```

Example b)

```
TRACE4
   F'V          F2          T(MM)          N          Z(MM)
+14.5000    - 1.6344    +10.2000    + 1.4950    +23.0000

RAY BUNDLE DIAMETER(MM)  1

 F2  1
 A2  0
 B2  0
 C2  0
 D2  0

 ANGLE          S'V          T'V          AST        M.O.P.          DIST (%)
+ 5.0000    +14.4724    +14.4625    -  .0099    +14.4674    +  .1658
+10.0000    +14.3950    +14.3738    -  .0212    +14.3844    +  .6965
+15.0000    +14.2836    +14.3226    +  .0390    +14.3031    + 1.6301
+20.0000    +14.1647    +14.4234    +  .2586    +14.2940    + 3.3102
+25.0000    +14.0556    +14.6409    +  .5853    +14.3482    + 5.7382
+30.0000    +13.9115    +14.2705    +  .3589    +14.0910    + 8.9193

 P1  0
 A1  1.28124E-06
 B1  1.8212E-09
 C1  8.38095E-12
 D1 -2.38066E-14
```

Appendix III

Curve fitting technique

The program used for calibrating the travelling microscope also fits the data to the nearest conic surface. However, many of the aspheric surfaces considered are not conic sections, thus it would seem reasonable to try and fit this data with a more complex equation. Thus a program was written to give a fit using the equation:

$$x = Ay^2 + By^4 + Cy^6 \qquad \text{-- AIII (1)}$$

This was solved by using sets of simultaneous equations on four pairs of data points, (x_1, y_1), (x_{11}, y_{11}), (x_2, y_2) and (x_{21}, y_{21}). Solving AIII(1) for 'A' gives us, using two pairs of points:

$$A = \frac{x_1 - By_1^4 - Cy_1^6}{y_1^2} \qquad \text{-- AIII (2)}$$

$$A = \frac{x_2 - By_2^4 - Cy_2^6}{y_2^2} \qquad \text{-- AIII (3)}$$

Cross multiplying and solving for 'B' gives us

$$B = \frac{x_2y_1^2 - x_1y_2^2 + C(y_2^2y_1^6 - y_1^2y_2^6)}{(y_1^2y_2^4 - y_1^4y_2^2} \qquad \text{-- AIII (4)}$$

A similar equation is derived for points (x_{11}, y_{11}) and (x_{21}, y_{21}).

Making the substitions:

$a = x_2 y_1^2$ and $e = x_{21} y_{11}^2$

$b = x_1 y_2^2$ and $f = x_{11} y_{21}^2$

$c = y_2^2 - y_1^2 y_2^6$ and $g = y_{21}^2 - y_{11}^2 y_{21}^6$

$d = y_1^2 y_2^4 - y_1^4 y_2^2$ and $h = y_{11}^2 y_{21}^4 - y_{11}^4 y_{21}^2$

we get:

$$ha - bh + Cch = ed - fd + Cgd$$

from which:

$$C = \frac{d(e - f) - h(a - b)}{ch - gd} \qquad \text{-- AIII (5)}$$

By solving similar sets of equations, the aspheric coefficients 'A' and 'B' can also be found.

For ray tracing purposes, we would wish to replace the term Ay^2 with:

$$\frac{cu.y^2}{1 + (1 - p.cu^2y^2)^{\frac{1}{2}}}$$

where 'cu' is the paraxial curvature of the surface, and 'p' the conic coefficent. Hence:

$$p = 1 - \frac{\frac{(cu - A)^2}{2}}{\frac{A}{cu^2 y^2}} \qquad \text{-- AIII (6)}$$

Other versions of this program set 'p' to a specific value.

Notes on program

0 - 150

Lines 0 - 150

The printer is switched on, and the output formatted. The axial radius of curvature is specified in this version (derived by calculation for BVP, thickness, refractive index and rear surface power). The four sets of co-ordinates are read.

Lines 151 - 230

The intermediate variables are assigned. Note that a small letter variable in the derivation given above is replaced in the program by a capital letter with the suffix '1'. Thus a = A1, b = B1, and so on.

Lines 231 - 270

The values of 'C', 'B', 'A' and 'p' are calculated.

Lines 275 - 410

The values of the calculated coefficients are printed out, together with the heading for an error table.

Lines 418 - 470

An error score is calculated for the differences between the calculated 'x' values and the data figures. The error total is taken as the absolute sum of the differences.

Lines 505 - 1010

Data statements and printer instructions.

```
9 REM        POLYFIT3
10 REM ENTER DATA AS X,Y DATA STATEMENTS IN LINES FROM 500
20 DIM X(30),Y(30)
25 OPEN1,4
40 OPEN3,4,2
45 OPEN2,4,1
50 PRINT#3,"999.999999    "
90 PRINT"POLYNOMIAL CURVE FIT"
95 PRINT"──────────────────────"
100 R=30.476
105 CU=1/R
140 READ X(1),Y(1)
145 READ X(2),Y(2)
148 READ X(11),Y(11)
150 READ X(21),Y(21)
151 L1=X(2)*Y(1)↑6
152 M1=X(1)*Y(2)↑6
153 N1=Y(2)↑2*Y(1)↑6-Y(1)↑2*Y(2)↑6
154 O1=Y(1)↑6*Y(2)↑4-Y(1)↑4*Y(2)↑6
155 T1=X(21)*Y(11)↑6
156 U1=X(11)*Y(21)↑6
157 V1=Y(21)↑2*Y(11)↑6-Y(11)↑2*Y(21)↑6
158 W1=Y(11)↑6*Y(21)↑4-Y(11)↑4*Y(21)↑6
160 A1=X(2)*Y(1)↑2
170 B1=X(1)*Y(2)↑2
180 C1=Y(2)↑2*Y(1)↑6-Y(1)↑2*Y(2)↑6
190 D1=Y(1)↑2*Y(2)↑4-Y(1)↑4*Y(2)↑2
200 E1=X(21)*Y(11)↑2
210 F1=X(11)*Y(21)↑2
220 G1=Y(21)↑2*Y(11)↑6-Y(11)↑2*Y(21)↑6
230 H1=Y(11)↑2*Y(21)↑4-Y(11)↑4*Y(21)↑2
231 FOR I=1TO 3
232 IFI=3THEN240
235 IF I=1 THEN C=0
236 IF I=2 THEN C=0
237 GOTO242
```

```
 240 C=(D1*(E1-F1)-H1*(A1-B1))/(C1*H1-G1*D1)
 242 IF I=1THEN B=0
 243 IF I=1 THEN 260
 250 B=(G1*(A1-B1)-C1*(E1-F1))/(G1*D1-H1*C1)
 260 A=(O1*(T1-U1)+W1*(M1-L1))/(V1*O1-N1*W1)
 270 P=(1-(CU-A)↑2/A↑2)/(CU↑2*Y(21)↑2)
 275 PRINT#1:PRINT#1
 280 PRINT#1," P   ";P
 290 PRINT#1," A   ";A
 300 PRINT#1," B   ";B
 310 PRINT#1," C   ";C
 370 PRINT#1," R   ";R
 400 PRINT#1
 410 PRINT#1,"       X              Y        ERROR"
 418 RESTORE
 419 Q=0
 420 FOR K=1 TO 4
 425 READ XX(K),YY(K)
 430 T=A*YY(K)↑2+B*YY(K)↑4+C*YY(K)↑6
 435 ER=T-XX(K)
 440 Q=Q+ABS(ER)
 450 PRINT#2,XX(K),YY(K),ER
 460 NEXTK
 465 PRINT#1,"ABSOLUTE ERROR SUM (MM) ";Q
 466 Q=0
 470 NEXT I
 505 DATA  1.710,10
 510 DATA  2.469,12
 515 DATA  3.889,15
 520 DATA  5.693,18
 1010 CLOSE1:CLOSE2:CLOSE3
READY.
```

Appendix IV

Publication from this thesis.

'Determination of the surface curves of aspheric single vision spectacle lenses'
The Optican Vol 181 No 4708 pp 21-30 (1981)

'Aspheric lenses'
The Optician Vol 184 No 4753 pp 14-15, 17-18, 23 (1982)

'The measurement of distortion in single vision ophthalmic lenses'
Transactions of the British College of Ophthalmic Opticians International Congress (Volume 1.) pp 148 - 157 (1984)

'Patent Review - Two spectacle lenses for aphakia'
Ophthalmic & Physiological Optics Vol 4 No 4 pp 369-373 (1984)

'Lens production'
UK Patent Applications No 2, 140, 344 A (1984)

'Aspheric spectacle lens designs for aphakia'
American Journal of Optometry and Physiological Optics Vol 61 No 12 pp 737-740 (1984)

'Some notes on the construction of zonal aspheric aphakic spectacle lenses'
Ophthalmic & Physiological Optics [In press - proof shown here]

References

Abbe, E (1900a) 'Improvements in the method of and means of producing spheroidal surfaces on lenses and reflectors' UK Patent No. 8,932 The Patent Office, London

Abbe, E (1900b) 'Improvements in lenses and reflector systems' UK Patent No. 8,933 The Patent Office, London

American Optical (1980) 'Comparison of performance of three non - lenticular aspheric cataract lenses' American Optical Corporation, Southbridge

Atchison, D A (1983) 'Problems of spectacle wearing aphakes' Australian Journal of Optometry Vol. 66 No. 6 pp 216-219

Atchison, D A (1984) 'Third-order theory and aspheric spectacle lens design' Ophthalmic & Physiological Optics Vol. 4 No.2 pp 179-186

Atchison, D A & Smith, G (1980) 'Assessment of aphakic spectacle lenses: high power flatback lenses for the correction of aphakia' Australian Journal of Optometry, Vol. 63 No. 6 pp 258-263

Atchison, D A & Smith, G (1983) 'Laboratory evaluation of commercial aspheric aphakic lenses' American Journal of Optometry and Physiological Optics Vol. 60 No. 7 pp 598-615

Atchison D A & Smith, G (1984) 'Clinical trial with commercial aspheric aphakic lenses' American Journal of Optometry and Physiological Optics Vol. 61 No. 9 pp 566-575

Baker, T Y (1943) 'Ray tracing through non - spherical surfaces' Proceedings of the Physical Society, Vol. LV pp 361-364

Bausch and Lomb (1966) 'Method of making lenses'
UK Patent No. 1,051,128
The Patent Office, London

Bechtold, E W (1973) 'Aspheric lens surface'
US Patent No. 3,781,097
The United States Patent Office

Bennett, A G (1968) 'Aspherical contact lens surfaces'
The Ophthalmic Optician
Published in three parts:
1) October 5th pp 1037-1040
2) November 30th pp 1297-1300
3) March 8th (1969) pp 222-224, 229-230

Bennett, A G (1969) 'The optics of contact lenses'
The Association of Dispensing Opticians, London

Bennett, A G (1973) 'A guide to ophthalmic lens design'
The Optician, Vol 167
Published in three parts:
1) January 4th pp 4-9
2) January 11th pp 4-12
3) January 18th pp 4-9

Bennett, A G & Edgar, D (1979, 1980) 'Spectacle lens design and performance'
The Optician
Series of articles:
1) Introduction and ray tracing scheme, July 27 (1979) pp 9-13
2) Distortion I, August 31, pp 9-13
3) Distortion II, September 28, pp22-26
4) Oblique power error, spherical lenses 1, October 26, pp 13-20
5) Oblique power error, spherical lenses 2, November 30, pp 9-17
6) Oblique power errors, spherical lenses 3, January 25 (1980) pp 20-30
7) Toric lenses 1, February 29, pp 13-23
8) Oblique power error, toric lenses 2, March 28, pp 10-18
9) Oblique power errors, toric lenses 3, April 25, pp 10-18
10) High powered plus lenses, June 27, pp 30-35
11) Lenses of high refractive index materials August 29, pp 18-25
12) Chromatic aberration 1, October 10, pp 25-28
13) Chromatic aberration 2, November 28, pp 28-31
14) Resume and summing up December 19/26 pp 14-22,42

BS 3062 (1970) 'Spectacle lens materials' (metric units) British Standards Institution, London

Carl Zeiss Jena (1961) 'Verre de lunettes a grand indice de refraction, notamment pour yeux sans cristallin' French Patent No.1, 281,019

Charman, W N (1982) 'Unwanted astigmatism in lenses with a concentric variation in sagittal power' American Journal of Optometry and Physiological Optics, Vol. 59 No. 12 pp 997-1001

Davis, J K (1959) 'Problems and compromises in the design of aspheric cataract lenses' American Journal of Optometry and Archives of the American Academy of Optometry, Vol. 36 No. 6, pp 279-288

Davis, J K (1973) 'Geometric optics in ophthalmic lens design' Proceedings of the Society of Photo - OPtical Instrumentation Engineers, Annual Technical Meeting, August 27-29

Davis, J K (1981) Personal communication

Davis, J K & Clotar, G (1956) 'An approach to the problem of a corrected curve achromatic cataract lens' American Journal of Optometry and Archives of the American Academy of Optometry, Vol 33 No. 12, pp 643 - 660

Davis, J K & Fernald, H G (1965) 'Ophthalmic aspheric lens series' US Patent No. 3, 169,247 The United States Patent Office

Davis, J K & Torgersen, D L (1983) 'The properties of lenses used for the correction of aphakia' Journal of the American Optometric Association Vol. 54 No. 8 pp 685-693

Drasdo, N & Peaston, W C (1980) 'Sampling systems for visual field assessment and computerised perimetry'
British Journal of Ophthalmology, Vol. 64 No. 9 pp 705-712

Emsley, H H (1956) 'Aberrations of thin lenses'
Constable, London

Essilor (1981) 'The Orma Omega'
Technical sales brochure

Feder, D (1951) 'Optical calculations with automatic computing machinery'
Journal of the Optical Society of America Vol. 41, pp 630-635

Fowler, C W (1978) 'The best form of high index spectacle lenses'
The Optician, Vol 175, No. 4518, p 9

Freeman, M H (1984a) 'Bifocal contact lens having diffractive power'
UK Patent Application No. 2,129,157
The Patent Office, London

Freeman, M H (1984b) 'Ophthalmic lens having negative diffractive power'
UK Patent Application No. 2,127, 988
The Patent Office, London

Frieder, P M (1980) 'Prosthetic aspheric spectacle lens for aphakia'
US Patent No. 4,185, 897
The United States Patent Office

Fry, G A (1977) 'Displaying distortion in ophthalmic lenses'
American Journal of Optometry and Physiological Optics, Vol. 54 No.5 pp 282-285

Guilino, G Barth, R & Koeppen, W (1983) 'Spectacle lens with high positive refractive power'
UK Patent Application No. 2,113,863
The Patent Office, London

Henker, O (1924) 'Introduction to the theory of spectacles' (Translated by R Kanthack) Jena School of Optics, Jena

I.C.I Ltd (1957) 'Perspex Acrylic Materials, Part 3 Cementing' Imperial Chemical Industries Ltd.

Jalie, M (1972) 'The Principles of Ophthalmic Lenses' Association of Dispensing Opticians, London

Jalie, M (1980) 'Ophthalmic spectacle lens' UK Patent Application No. 2,030,722

Jeffree, J H (1963) 'Improvements in lenses' UK Patent No. 930,219

Katz, M (1982) 'Aspherical surfaces used to minimize oblique astigmatic error, power error, and distortion of some high positive and negative power ophthalmic lenses' Applied Optics Vol. 21 No. 16 pp 2982-2991

Katz, M (1983) 'Distortion by ophthalmic lenses calculated at the farpoint sphere' American Journal of Optometry and Physiological Optics, Vol 60 No. 12 pp 944-959

Koeppen, W and Barth, R (1982) 'Die Entwicklung eines neuen aspharischen Starbrillenglases' Optometrie, No. 4 pp 215-222

Knoll, H A (1953) 'The measurement of oblique astigmatism in ophthalmic lenses' The American Journal of Optometry and Archives of the American Academy of Optometry Vol. 30 No. 4, pp 198-201

Leach, R J (1980) 'Producing reflectors' UK Patent Application No. 2,048,153 The Patent Office, London

Mandell, R & St Helen, R (1981) 'Mathematical model of the corneal contour' British Journal of Physiological Optics Vol. 26, No.3, pp 183-197

Michaels, D M (1978) 'Spectacle correction of aphakia: how aspheric do they have to be?' Ophthalmology (Journal of American Academy of Ophthalmology and Otolaryngology) Vol 85, January, pp 59-72

Morgan, M W (1961) 'The performance of ophthalmic lenses' Journal of the American Optometric Association Vol. 32, No. 10, pp 797-806

Renier, G L (1977) 'Clinical aphakia and its spectacle management' Professional Press, Chicago

Rogers, P J (1984) 'Biocular magnifying lens comprising positive Fresnel lens' UK Patent Application No. 2,126,747 The Patent Office, London

von Rohr, M (1909) 'Spectacle glass' UK Patent No. 15, 533 The Patent Office, London

von Rohr M, & Boegehold, H (1934) 'Das Brillenglass als optisches Instrument' Julius Springer, Berlin

Simonet, P, Papineau, Y & Gordon, D (1983) 'A scanning focimeter to measure peripheral lens powers' Ophthalmic & Physiological Optics, Vol. 3, No. 3, pp 305-310

Smethwick, F (1666) 'Grinding optical glasses' UK patent No. 149 (Published 1857) The Patent Office, London

Smith, W J (1966) 'Modern optical engineering' McGraw - Hill, New York

Smith, G & Atchison, D A (1983a) 'Effect of conoid asphericity on the Tscherning ellipses of ophthalmic spectacle lenses' Journal of the Optical Society of America Vol. 73 No.4 pp 441-445

Smith, G & Atchison, D A (1983b) 'Aspheric high positive power lenses and third order theory' American Journal of Optometry and Physiological Optics Vol. 60 No. 10 pp 843-845

Smith, G & Atchison, D A (1983c) 'Construction, specification and mathematical description of aspheric surfaces' American Journal of Optometry and Physiological Optics Vol. 60 No. 3 pp 216-223

Smith, G & Bailey, I L (1981) 'Aspheric spectacle lenses - design and performance' The Optician, Vol 181 Published in three parts:
a) Introduction, April 10th, pp 21-26
b) Conicoids: a ray tracing scheme, May 8th pp 25-27
c) Conicoids - distortion, curvature and oblique astigmatism, June 19th, pp 31-32

Societe des Lunetiers (1968) 'Improvements in or relating to ophthalmic astigmatic or toric lenses' UK Patent No. 1,239, 620 The Patent Office, London

Societe des Lunetiers (1970) 'Improvements in or relating to ophthalmic lenses' UK Patent No. 1,292,202 The Patent Office, London

Tarumi, N, Komiya, S & Sugimura, M (1982) 'A lens having high refractive index with a low dispersion made of copolymer' UK Patent Application No. 2,089,523 The Patent Office, London

Twyman, F (1952) 'Prism and lens making: a textbook for optical glassworkers' Second Edition Adam Hilger Ltd, London

Vernoy, M W & Luria, S M (1977) 'Perception of, and adaptation to, a three-dimensional curvature distortion' Perception and Psychophysics Vol. 23 No. 3 pp 245-248

Volk, D (1958) 'Conoid refracting surfaces and conoid lenses' American Journal of Ophthalmology, Vol. 46 No. 1 (part II) pp 86-95

Volk, D (1961) 'Conoid cataract lenses for the correction of aphakia'
American Journal of Ophthalmology, Vol 51 No. 4 pp 615-622

Volk, D (1966a) 'Lens surface generator'
UK Patent No. 1, 023,116
The Patent Office, London

Volk, D (1966b) 'Lens generating method and apparatus'
UK Patent No. 1,032,049
The Patent Office, London

Washer, F E (1955) Instrument for measuring the marginal power of spectacle lenses'
Journal of the Optical Society of America Vol. 45, No. 9 pp 719-726

Welsh, RC (1978) 'Spectacle lenses for aphakia patients'
US Patent No. 4,073,578
The United States Patent Office

Whitney, D B (1980) 'Technical report:'Ful-Vue' aspheric cataract lens'
American Optical Corporation, Southbridge

Whitney, D B, Reilly, J A, & Young, J M (1980) 'Aspheric lens series'
US Patent No. 4, 181,409
The United States Patent Office